AMD
AN OVERVIEW OF CLINICAL FORMS

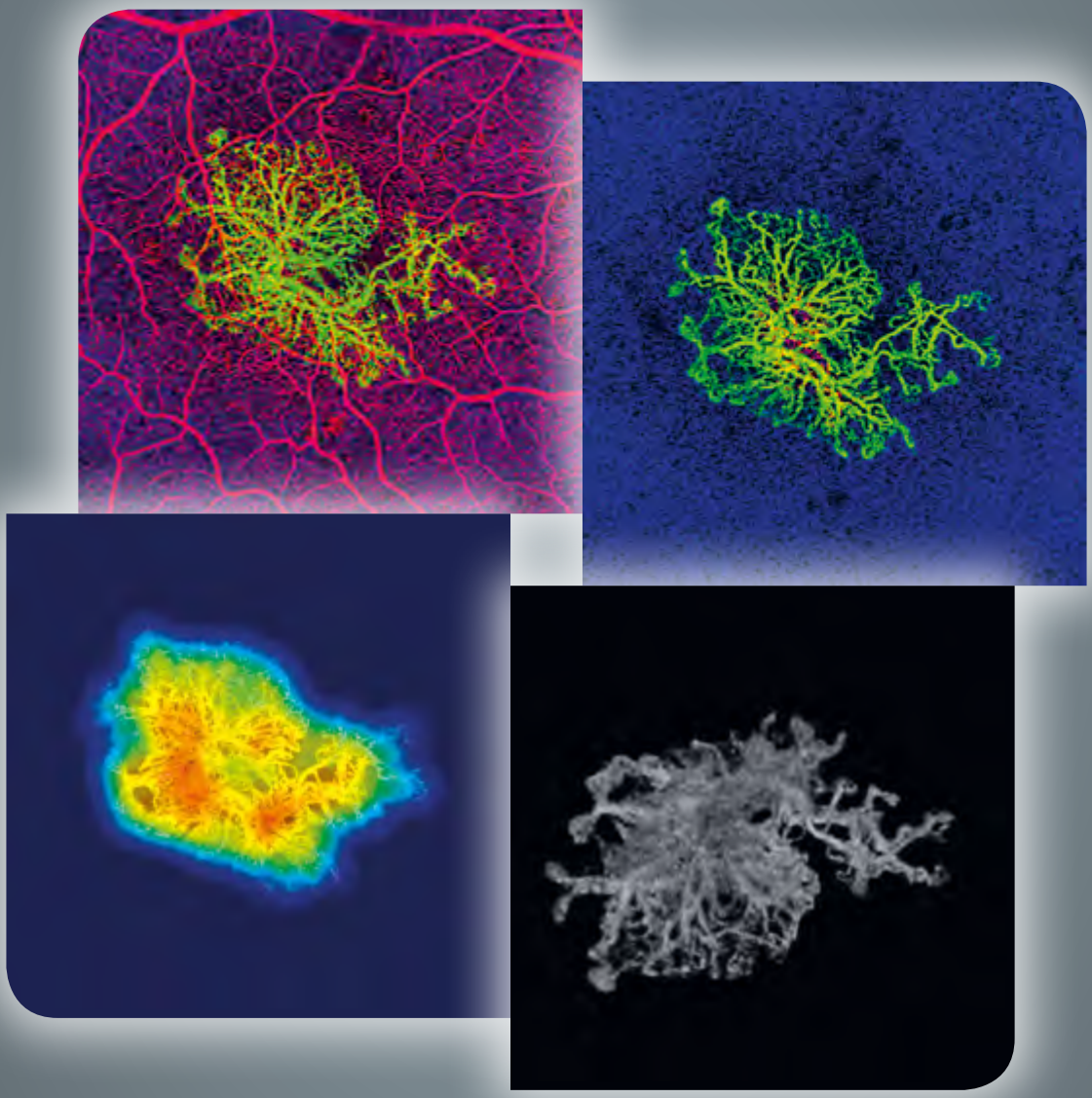

Oudy Semoun
Alexandra Miere
Mayer Srour
Eric Souied
and the Ophthalmology Créteil team

Théa PHARMA

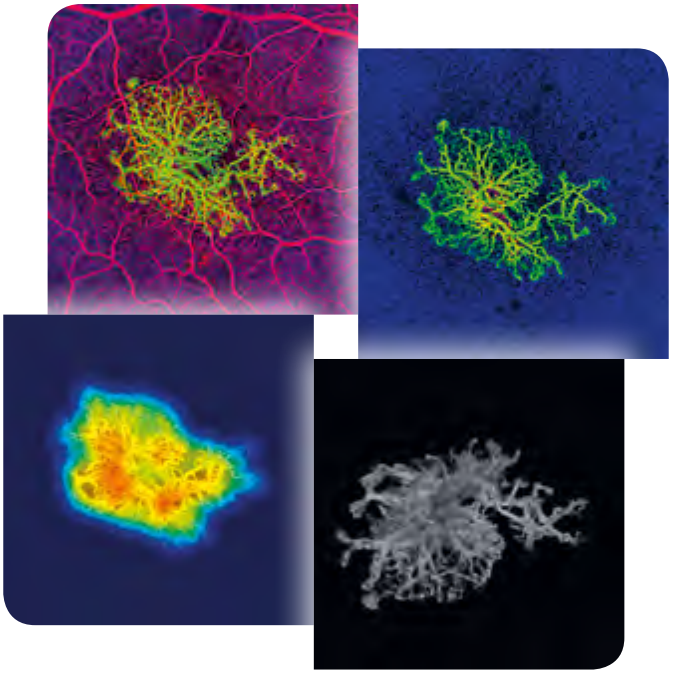

Dear readers,

This book presents the viewpoints of the authors and does not necessarily reflect the opinions of Laboratoires Théa.

All rights of translation, adaptation and reproduction by any means are reserved for all countries.

Any reproduction in whole or in part—by any means—of the pages of this book, without prior, written approval from the publisher, is prohibited, illegal and constitutes an infringement. Reproduction is allowed only where the copied material is strictly reserved for the private use of the copier and not for collective use, and in the case of brief analysis and quotations the use of which is justified by the scientific or educational nature of the work in which they are included (French Law of 11 March 1957 Art. 40 and 41 and French Criminal Code Art. 425).

© Reproduction prohibited

Foreword

This book has been written by the ophthalmology department team at Créteil Intercommunal Hospital. It aims to cover the full range of clinical knowledge on age-related macular degeneration.

Recent years have seen an increase in our understanding of the importance of the genetic origins of AMD, along with the impact of environmental and nutritional factors. Macular imaging has become multimodal, with colour and Multicolor® photographs, autofluorescence and infrared photographs, fluorescein angiography, indocyanine green angiography, OCTA, spectral-domain OCT, EDI-OCT, and wide-field and ultra-wide-field imaging.

The information obtained from these new forms of imaging has required us to revisit the group of diseases categorised as “age-related macular degeneration”, resulting in an even greater refinement of the associated clinical description and changes to the AMD classification system. Pigment epithelial detachment covers a spectrum of entities with different semiology and prognosis, including serous PED, fibrovascular PED, wrinkled PED and fibrous PED, among others. Fibrosis and atrophy underlying neovascularization are no longer **occult**, but better **described** and better **detected.** Finally, EDI-OCT has enabled us to differentiate between different pachychoroid diseases, including retinal pigment epitheliopathy, central serous chorioretinopathy, polypoidal vasculopathy and adult-onset foveomacular vitelliform dystrophy. Atrophic AMD is starting to appear in therapeutic considerations of the disease, and the clinical forms of the various entities included under this term are gradually being described.

The final piece of the puzzle is longitudinal patient monitoring, both prospective and retrospective. The technique of eye tracking has been hugely significant in optimising patient monitoring, both in terms of the natural history of the disease and after treatment, primarily via OCT.

Prof. Eric Souied
Head of Department of Ophthalmology,
Créteil Intercommunal Hospital Centre

Foreword

Coordinated by

Oudy Semoun

Alexandra Miere

Mayer Srour

Eric Souied

Acknowledgments

Department of Ophthalmology, Créteil Intercommunal Hospital Centre

Manar Addou

Francesca Amoroso

Polina Astroz

Jean-Louis Bacquet

Roxane Bunod

Vittorio Capuano

Ala El Ameen

Agnès Glacet

Gérard Mimoun

Alexandra Mouallem

Hassiba Oubraham

Sergio Piscitello

Giuseppe Querques

David Sayag

Daniel Seknazi

Pierre Sustronck

Julien Tilleul

Joel Uzzan

Setha Vo-kim

Olivia Zambrowski

Contents

1 **Age-related macular degeneration: epidemiology, environmental and genetic risk factors** 13
Alexandra Mouallem-Bézière, Jean-Louis Bacquet

2 **Multimodal imaging for age-related macular degeneration** 21

Part 1: Non-invasive imaging 22
Setha Vo Kim, Francesca Amoroso

Part 2: Optical coherence tomography angiography (OCTA) 34
Alexandra Miere, Roxane Bunod, Eric Souied

Part 3: Invasive imaging 40
Setha Vo Kim, Francesca Amoroso

3 **Age-related maculopathy** 47
Mayer Srour

4 **Type 1 neovascularization** 61

4.1 Type 1 - Jean-Louis Bacquet, Alexandra Mouallem-Bézière 62
4.2 Quiescent - Vittorio Capuano 70
4.3 Retinal pigment epithelial tears - Alexandra Mouallem-Bézière 78
4.4 Wrinkled pigment epithelial detachments - Gérard Mimoun 82
4.5 Peculiar pre-epithelial type 2 neovascularization healing mode following anti-VEGF treatment: “igloos” - Gérard Mimoun 90
4.6 Polypoidal choroidal vasculopathy (or aneurysmal type 1 choroidal neovascularization) - Mayer Srour, David Sayag 96
4.7 Fibrous choroidal neovascularization 104
Alexandra Miere, Manar Addou-Regnard, Eric Souied

5 **Type 2 choroidal neovascularization** 111
Al'a El Ameen

6 **Type 3 neovascularization** 119
Alexandra Miere, Giuseppe Querques, Roxane Bunod, Eric Souied

7 **Adult-onset foveomacular vitelliform dystrophy (AFVD)** 129
Jean-Louis Bacquet, Agnès Glacet-Bernard

8 **Geographic atrophy: a new classification** 141
Vittorio Capuano, Joel Uzzan

9 **Differential diagnoses for age-related macular degeneration** 151
Polina Astroz, Olivia Zambrowski

10 **Micronutrition and age-related macular degeneration** 169
Sergio Piscello, Pierre Sustronck

11 **Treatment protocols for exudative AMD** 179
Hassiba Oubraham

12 **Artificial intelligence and AMD** 189
Daniel Seknazi, Oudy Semoun

1

Age-related macular degeneration: epidemiology, environmental and genetic risk factors

Alexandra Mouallem-Bézière, Jean-Louis Bacquet

Age-related macular degeneration (AMD) is a common eye disease among older people, causing a severe visual impairment. The pathophysiology of AMD remains largely unknown: it is a complex, multi-factorial disease involving aging of the retina and a combination of environmental and genetic factors.

1. Epidemiology

The majority of the large epidemiological studies on age-related macular degeneration (AMD) have been conducted in the United States[1-3]. The Beaver Dam Eye Study[3] estimated the prevalence of advanced forms of the disease at 1.6% of the general population and 7.1% in people over 75 years old. In Europe, the data from the EUREYE Study[4] are consistent with the American data and indicate a prevalence of 1.2% for geographic atrophy and 2.3% for exudative forms. In France, the disease affects an estimated 1.5 million people[4]. It is estimated that by 2020, around 196 million people worldwide will be suffering from a form of AMD[5].

2. Constitutional and environmental risk factors

1) Constitutional factors

Several constitutional factors have been studied in order to identify their role in the onset of the disease. Age is obviously a factor, with prevalence increasing with age. In addition, the prevalence of the disease varies depending on the ethnic origin of the studied populations[6]. Advanced forms of AMD are more common in Caucasian populations than in dark-skinned populations[7]. In terms of sex, some meta-analyses have not found any differences in disease prevalence between men and women[7]. However, the Beaver Dam Study[3] found a higher incidence of age-related maculopathy in women over 75 compared to men of the same age.

Multiple studies have established correlations between certain cardiovascular risk factors and AMD. Klein *et al.*[8] found a correlation between patients with neovascular AMD and the presence of cardiovascular disease. Data from the AREDS study reveal increased cardiovascular mortality among patients with AMD[9]. However, other studies, such as AREDS Report No. 19, have not found any correlation between AMD and angina pectoris[10]. High blood pressure has been studied independently. The results are similarly divergent, with some studies finding an association[11] and others finding none[12].

Blood lipid level has also been considered independently in multiple studies. Lipid metabolism has been shown to be involved in the physiopathology of AMD, particularly via the role of apolipoprotein E, which has been suggested as a genetic susceptibility factor for AMD[13,14]. Here again, the results are contradictory when it comes to establishing a correlation between blood lipids and disease susceptibility.

2) Environmental factors

a) Smoking, alcohol, body mass index (BMI)

Smoking is the main identified environmental risk factor[15]. Alcohol consumption has also been reported as a major risk factor for age-related maculopathy (ARM)[16]. A more recent study found an increased incidence of atrophic AMD at 15 years with excessive alcohol consumption[17]. BMI is also a proven risk factor for AMD[18].

b) Omega-3 and vitamins

Omega-3s play a physiological role in the photoreceptor outer segments. Long-chain polyunsaturated fatty acids (DHA: docosahexaenoic acid and EPA: eicosapentaenoic acid) are synthesised from linoleic acid in food. A meta-analysis of omega-3 consumption found that it was associated with a reduced risk of developing AMD[19].

Lutein and zeaxanthin are the two beta-carotenes found in the retina, with maximum concentration in the macula. These pigments absorb at least 40% of blue light. Several studies have found that consuming lutein and zeaxanthin is beneficial in warding off the disease[20], but these results are contradicted by other studies[3,21].

Antioxidants have also been studied. AREDS Report No. 8[22] established a significant association between antioxidant (vitamins C and E and beta-carotene) and zinc intake and a reduced risk of exudative AMD, compared to placebo.

The NAT 2 study attempted to evaluate the efficacy of DHA and EPA supplementation in the prevention of choroidal neovascularization at three years in patients with age-related maculopathy (ARM)[23]. This study found a significant reduction (68%) in the risk of developing an exudative form of the disease in patients with the highest level of DHA and EPA. Genetic analysis of this cohort also demonstrated that the protective effect of the supplementation was maximum in patients who did not have the C-allele of the CFH Y402H polymorphism[24].

3. Genetic risk factors for AMD susceptibility and genetic factors impacting treatment response

Our understanding of the genetic factors behind AMD has developed alongside advances in genetic analysis methods, ranging from family-based analysis to association studies of large populations with AMD compared to control populations.

1) Genetics in family cases

Genetic susceptibility to early, intermediate and advanced AMD was first hypothesised by Gass in 1973[25]. Gass had observed several families with cases of AMD and hypothesised that the disease was an autosomal dominant disorder. Other studies of family aggregation have identified a higher frequency of the disease in the relatives of existing patients[26-28].

The existence of a genetic component has also been suggested in light of the high phenotypic concordance between monozygotic twins[29-31]. Monozygotic twin studies can also be used to assess the “heritability” of a disease, i.e. the proportion of the phenotype attributable to the genotype. The heritability of AMD is estimated to be between 45% and 70%, based on the studies conducted[32,33].

Genetic linkage studies conducted in the families of people suffering from the disease have identified various chromosomal loci of susceptibility. In 1998, Klein *et al.*[34] published the first linkage study, which mapped a locus of susceptibility to *1q*. Several years later, this locus was found to contain one of the major genes for susceptibility: *CFH*[35].

All of these family-based studies have clear limitations due to certain characteristics of AMD. The advanced age of patients makes it harder to find families for analysis, and non-Mendelian inheritance makes the disease difficult to analyse in a limited number of patients. Researchers therefore changed tack and began comparing populations with AMD to control populations, in order to study the distribution of genetic susceptibility markers.

2) Population genetics in AMD

a) Candidate gene approach

Certain genes, known as "candidate genes”, can be selected for analysis to determine their involvement in the physiology of a disease. For example, the lipid composition of soft drusen led researchers to study the genes involved in lipid metabolism, revealing an association with the 4 allele of the *apolipoprotein E* gene, which was found to play a protective role[36].

Candidate genes can also be genes already known to be involved in other types of retinal dystrophy or Mendelian-inherited maculopathy, such as the *ABCA4* gene, which is involved in Stargardt disease[37]; the *VDM2/BEST1* genes, involved in Best disease[38]; and the *RDS* gene, involved in numerous hereditary forms of retinal dystrophy[39].

These genes can also be identified by sequencing candidate regions highlighted in segregation studies or through positional cloning. The *HTRA1/ARMS2* region has been identified using this approach.

b) Genome-wide associations studies

More recently, genome-wide association studies (GWAS) and studies of candidate regions have enabled researchers to identify numerous other predisposing or protective variants involved in disease susceptibility. This approach has confirmed the results in the literature, as well as identifying new pathways potentially involved in the physiopathology of AMD. The most recent *GWAS*[40], published in 2015, summarises the full extent of our understanding of this field, identifying 52 variants associated with increased susceptibility to the disease in 34 loci.

c) Other types of variants causing susceptibility to AMD

Improvements in sequencing techniques have enabled researchers to study genetic variations other than single-nucleotide polymorphisms[41]. For example, chromosomal rearrangement, alternative splicing of certain isoforms, copy number variation (CNV), micro-ribonucleic acids (miRNA) and other non-coding RNAs, and epigenetics can all be investigated as potential factors involved in AMD susceptibility and physiopathology. Insertions and deletions in the *CFH* locus[42-44] have been identified in several studies, alongside CNVs in the same region[45,46]. Non-coding microRNAs have been implicated in the physiopathology of exudative AMD due to their supposed role in the regulation of both angiogenesis and inflammation[47]. Epigenetics also appears to play a role, with DNA methylation implicated in the onset of the disease[48].

3) Impact of genetics on treatment response

In terms of the severity of the disease, genotype-phenotype correlation studies have found an association with the single-nucleotide polymorphism rs10490924 in *ARMS2/HTRA1* in patients with advanced bilateral forms of AMD[49], as well as severe and early forms[50]. rs1061170 in *CFH*[51] is another polymorphism associated with bilateral forms. Additionally, a recent study identified a correlation between a polymorphism in C3 and large vascularised pigment epithelial detachments[52].

In terms of response to anti-VEGF treatment, several single-nucleotide polymorphisms in the *VEGF* A gene have been found to correlate with a better treatment response[53-56], as have certain polymorphisms in the gene coding for the *VEGF-R2* receptor [57]. Single-nucleotide polymorphisms in the *CFH*, *ARMS2* and *HTRA1* genes—which all play a key role in AMD—have also all been found to correlate with a better response to anti-VEGF treatment[58-61]. For each of these variants, some of the published studies did not find any association with treatment response[62].

These genetic data can be combined to calculate disease prediction scores that aim to take into account the various factors influencing the disease. For example, the score developed by Seddon *et al.*[63] combines 10 single-nucleotide polymorphisms in different loci *(ARMS2/HTRA1, CFB, C3, C2, COL8A1, RAD51B, C3*) with age, sex, education level, BMI, smoking history and clinical examination data (drusen, contralateral involvement) to assess the risk of AMD after 10 years. The score can be calculated at: https: //www.seddonamdriskscore.org/. The contribution of environmental and genetic factors has been assessed independently, and the authors conclude that combining both gives a better prediction.

Conclusion

The pathophysiology of AMD remains largely unknown and genetics is thought to be responsible for around 70%.

Ongoing progress in our understanding of susceptibility factors and factors influencing response to certain treatments offers hope that we will be able to develop personalized medicine for our patients in the near future, as well as new treatment approaches.

References

1. Leibowitz HM, Krueger DE, Maunder LR, *et al.* The Framingham Eye Study monograph: An ophthalmological and epidemiological study of cataract, glaucoma, diabetic retinopathy, macular degeneration, and visual acuity in a general population of 2631 adults, 1973-1975. Surv Ophthalmol. 1980;24 (Suppl): 335-610.
2. Bressler NM, Bressler SB, West SK, *et al.* The grading and prevalence of macular degeneration in Chesapeake Bay watermen. Arch Ophthalmol Chic Ill 1960. 1989;107(6):847-852.
3. Klein R, Klein BE, Linton KL. Prevalence of age-related maculopathy. The Beaver Dam Eye Study. Ophthalmology. 1992;99 (6): 933-943.
4. Augood CA, Vingerling JR, de Jong PTVM, *et al.* Prevalence of age-related maculopathy in older Europeans: the European Eye Study (EUREYE). Arch Ophthalmol Chic Ill 1960. 2006; 124(4):529-535.
5. Wong WL, Su X, Li X, *et al.* Global prevalence of age-related macular degeneration and disease burden projection for 2020 and 2040: a systematic review and meta-analysis. Lancet Glob Health. 2014;2 (2):e106-116. doi:10.1016/S2214-109X(13)70145-1.
6. Klein R, Peto T, Bird A, Vannewkirk MR. The epidemiology of age-related macular degeneration. Am J Ophthalmol. 2004;137(3):486-495.
7. Klein R, Klein BE, Jensen SC, *et al.* Age-related maculopathy in a multiracial United States population: the National Health and Nutrition Examination Survey III. Ophthalmology. 1999; 106(6):1056-1065.
8. Klein R, Klein BEK, Tomany SC, Cruickshanks KJ. The association of cardiovascular disease with the long-term incidence of age-related maculopathy: the Beaver Dam Eye Study. Ophthalmology. 2003;110(6):1273-1280.
9. Clemons TE, Kurinij N, Sperduto RD, AREDS Research Group. Associations of mortality with ocular disorders and an intervention of high-dose antioxidants and zinc in the Age-Related Eye Disease Study: AREDS Report No. 13. Arch Ophthalmol Chic Ill 1960. 2004;122(5):716-726.
10. Clemons TE, Milton RC, Klein R, *et al.* Age-Related Eye Disease Study Research Group. Risk factors for the incidence of Advanced Age-Related Macular Degeneration in the Age-Related Eye Disease Study. AREDS report no. 19. Ophthalmology. 2005;112(4):533-539.
11. Hogg RE, Woodside JV, Gilchrist SECM, *et al.* Cardiovascular disease and hypertension are strong risk factors for choroidal neovascularization. Ophthalmology. 2008;115(6):1046-1052.e2.
12. Tan JSL, Mitchell P, Smith W, Wang JJ. Cardiovascular risk factors and the long-term incidence of age-related macular degeneration: the Blue Mountains Eye Study. Ophthalmology. 2007;114(6):1143-1150.
13. Souied EH, Benlian P, Amouyel P, *et al.* The epsilon4 allele of the apolipoprotein E gene as a potential protective factor for exudative age-related macular degeneration. Am J Ophthalmol. 1998;125(3):353-359.
14. Klaver CC, Kliffen M, van Duijn CM, *et al.* Genetic association of apolipoprotein E with age-related macular degeneration. Am J Hum Genet. 1998;63(1):200-206.
15. Thornton J, Edwards R, Mitchell P, *et al.* Smoking and age-related macular degeneration: a review of association. Eye Lond Engl. 2005;19(9):935-944.
16. Chong EW-T, Kreis AJ, Wong TY, *et al.* Alcohol Consumption and the Risk of Age-Related Macular Degeneration: A Systematic Review and Meta-Analysis. Am J Ophthalmol. 2008; 145(4):707-715.e2.
17. Knudtson MD, Klein R, Klein BEK. Alcohol consumption and the 15-year cumulative incidence of age-related macular degeneration. Am J Ophthalmol. 2007;143(6):1026-1029.
18. Peeters A, Magliano DJ, Stevens J, *et al.* Changes in abdominal obesity and age-related macular degeneration: the Atherosclerosis Risk in Communities Study. Arch Ophthalmol Chic Ill 1960. 2008;126(11):1554-1560.
19. Chong EW-T, Kreis AJ, Wong TY, *et al.* Dietary omega-3 fatty acid and fish intake in the primary prevention of age-related macular degeneration: a systematic review and meta-analysis. Arch Ophthalmol Chic Ill 1960. 2008;126(6):826-833.

20. Seddon JM, Ajani UA, Sperduto RD, *et al.* Dietary carotenoids, vitamins A, C, and E, and advanced age-related macular degeneration. Eye Disease Case-Control Study Group. JAMA. 1994;272(18):1413-1420.
21. Mares-Perlman JA, Brady WE, Klein R, *et al.* Dietary fat and age-related maculopathy. Arch Ophthalmol Chic Ill 1960. 1995;113(6):743-748.
22. Age-Related Eye Disease Study Research Group. A randomized, placebo-controlled, clinical trial of high-dose supplementation with vitamins C and E, beta carotene, and zinc for age-related macular degeneration and vision loss: AREDS report no. 8. Arch Ophthalmol Chic Ill 1960. 2001;119(10):1417-1436.
23. Souied EH, Delcourt C, Querques G, *et al.* Oral docosahexaenoic acid in the prevention of exudative age-related macular degeneration: the Nutritional AMD Treatment 2 study. Ophthalmology. 2013;120(8):1619-1631.
24. Merle BMJ, Richard F, Benlian P, *et al.* CFH Y402H and ARMS2 A69S Polymorphisms and Oral Supplementation with Docosahexaenoic Acid in Neovascular Age-Related Macular Degeneration Patients: The NAT2 Study. PloS One. 2015;10(7): e0130816.
25. Gass JD. Drusen and disciform macular detachment and degeneration. Arch Ophthalmol Chic Ill 1960. 1973;90(3):206-217.
26. Seddon JM, Ajani UA, Mitchell BD. Familial aggregation of age-related maculopathy. Am J Ophthalmol. 1997;123(2):199-206.
27. Klaver CC, Wolfs RC, Assink JJ, *et al.* Genetic risk of age-related maculopathy. Population-based familial aggregation study. Arch Ophthalmol Chic Ill 1960. 1998;116(12):1646-1651.
28. Klein BE, Klein R, Lee KE, *et al.* Risk of incident age-related eye diseases in people with an affected sibling : The Beaver Dam Eye Study. Am J Epidemiol. 2001;154(3):207-211.
29. Klein ML, Mauldin WM, Stoumbos VD. Heredity and Age-Related Macular Degeneration. Observations in Monozygotic Twins. Arch Ophthalmol Chic Ill 1960. 1994;112(7):932-937.
30. Meyers SM. A twin study on age-related macular degeneration. Trans Am Ophthalmol Soc. 1994;92:775-843.
31. Grizzard SW, Arnett D, Haag SL. Twin study of age-related macular degeneration. Ophthalmic Epidemiol. 2003;10(5):315-322.
32. Fritsche LG, Chen W, Schu M, *et al.* Seven new loci associated with age-related macular degeneration. Nat Genet. 2013;45(4):433-439, 439-2.
33. Seddon JM, Cote J, Page WF, *et al.* The US twin study of age-related macular degeneration: relative roles of genetic and environmental influences. Arch Ophthalmol Chic Ill 1960. 2005;123(3):321-327.
34. Klein ML, Schultz DW, Edwards A, *et al.* Age-related macular degeneration. Clinical features in a large family and linkage to chromosome 1q. Arch Ophthalmol Chic Ill 1960. 1998;116 (8):1082-1088.
35. Maller J, George S, Purcell S, *et al.* Common variation in three genes, including a noncoding variant in CFH, strongly influences risk of age-related macular degeneration. Nat Genet. 2006;38 (9): 1055-1059.
36. Souied EH, Benlian P, Amouyel P, *et al.* The epsilon4 allele of the apolipoprotein E gene as a potential protective factor for exudative age-related macular degeneration. Am J Ophthalmol. 1998;125 (3): 353-359.
37. Souied EH, Ducroq D, Rozet JM, *et al.* ABCR gene analysis in familial exudative age-related macular degeneration. Invest Ophthalmol Vis Sci. 2000;41 (1): 244-247.
38. Allikmets R, Seddon JM, Bernstein PS, *et al.* Evaluation of the Best disease gene in patients with age-related macular degeneration and other maculopathies. Hum Genet. 1999;104 (6):449-453.
39. Baird PN, Richardson A, Islam A, *et al.* Analysis of the RDS/peripherin gene in age-related macular degeneration. Clin Experiment Ophthalmol. 2007;35 (2): 194-195.
40. Fritsche LG, Igl W, Bailey JNC, *et al.* A large genome-wide association study of age-related macular degeneration highlights contributions of rare and common variants. Nat Genet. 2016;48 (2):134-143.
41. Gorin MB. Genetic insights into age-related macular degeneration: controversies addressing risk, causality, and therapeutics. Mol Aspects Med. 2012;33 (4): 467-486.
42. Hughes AE, Orr N, Esfandiary H, Diaz-Torres M, *et al.* A common CFH haplotype, with deletion of CFHR1 and CFHR3, is associated with lower risk of age-related macular degeneration. Nat Genet. 2006;38(10):1173-1177.
43. Raychaudhuri S, Ripke S, Li M, *et al.* Associations of CFHR1-CFHR3 deletion and a CFH SNP to age-related macular degeneration are not independent. Nat Genet. 2010;42(7):553-555-556.
44. Spencer KL, Hauser MA, Olson LM, *et al.* Deletion of CFHR3 and CFHR1 genes in age-related macular degeneration. Hum Mol Genet. 2008;17(7): 971-977.
45. Kubista KE, Tosakulwong N, Wu Y, *et al.* Copy number variation in the complement factor H-related genes and age-related macular degeneration. Mol Vis. 2011;17:2080-2092.
46. Schmid-Kubista KE, Tosakulwong N, Wu Y, *et al.* Contribution of copy number variation in the regulation of complement activation locus to development of age-related macular degeneration. Invest Ophthalmol Vis Sci. 2009;50(11): 5070-5079.
47. Kutty RK, Nagineni CN, Samuel W, *et al.* Differential regulation of microRNA-146a and microRNA-146b-5p in human retinal pigment epithelial cells by interleukin-1β, tumor necrosis factor-α, and interferon-γ. Mol Vis. 2013;19:737-750.
48. Suuronen T, Nuutinen T, Ryhänen T, *et al.* Epigenetic regulation of clusterin/apolipoprotein J expression in retinal pigment epithelial cells. Biochem Biophys Res Commun. 2007;357(2):397-401.
49. Seddon JM, Francis PJ, George S, *et al.* Association of CFH Y402H and LOC387715 A69S with progression of age-related macular degeneration. JAMA. 2007;297(16):1793-1800.
50. Leveziel N, Puche N, Richard F, *et al.* Genotypic influences on severity of exudative age-related macular degeneration. Invest Ophthalmol Vis Sci. 2010;51(5):2620-2625.
51. Schick T, Altay L, Viehweger E, *et al.* Genetics of Unilateral and Bilateral Age-Related Macular Degeneration Severity Stages. PloS One. 2016;11(6):e0156778.doi:10.1371/journal.pone.0156778.
52. Mouallem-Bézière A, Blanco Garavito R, Richard F *et al.* Genetics of Genetics of large pigment epithelial detachments in neovascular age related macular degeneration. Retina 2019
53. Lazzeri S, Figus M, Orlandi P, *et al.* VEGF-A polymorphisms predict short-term functional response to intravitreal ranibizumab in exudative age-related macular degeneration. Pharmacogenomics. 2013;14(6):623-630.
54. McKibbin M, Ali M, Bansal S, *et al.* CFH, VEGF and HTRA1 promoter genotype may influence the response to intravitreal ranibizumab therapy for neovascular age-related macular degeneration. Br J Ophthalmol. 2012;9 (2):208-212.
55. Abedi F, Wickremasinghe S, Richardson AJ, *et al.* Variants in the VEGFA gene and treatment outcome after anti-VEGF treatment for neovascular age-related macular degeneration. Ophthalmology. 2013;120(1):115-121.
56. Nakata I, Yamashiro K, Nakanishi H, *et al.* VEGF gene polymorphism and response to intravitreal bevacizumab and triple therapy in age-related macular degeneration. Jpn J Ophthalmol. 2011;55(5):435-443.
57. Chang W, Noh DH, Sagong M, Kim IT. Pharmacogenetic association with early response to intravitreal ranibizumab for age-related macular degeneration in a Korean population. Mol Vis. 2013;19:702-709.
58. Menghini M, Kloeckener-Gruissem B, Fleischhauer J, *et al.* Impact of loading phase, initial response and CFH genotype on the long-term outcome of treatment for neovascular age-related macular degeneration. PloS One. 2012;7(7):e42014.
59. Francis PJ. The influence of genetics on response to treatment with ranibizumab (Lucentis) for age-related macular degeneration: the Lucentis Genotype Study (an American Ophthalmological Society thesis). Trans Am Ophthalmol Soc. 2011;109:115-156.
60. Park UC, Shin JY, Kim SJ, *et al.* Genetic factors associated with response to intravitreal ranibizumab in Korean patients with neovascular age-related macular degeneration. Retina Phila Pa. 2014;34(2):288-297.
61. Hagstrom SA, Ying G, Maguire MG, *et al.* VEGFR2 Gene Polymorphisms and Response to Anti-Vascular Endothelial Growth Factor Therapy in Age-Related Macular Degeneration. Ophthalmology. 2015;122(8):1563-1568.
62. Hagstrom SA, Ying G-S, Pauer GJT, *et al.* Pharmacogenetics for genes associated with age-related macular degeneration in the Comparison of AMD Treatments Trials (CATT). Ophthalmology. 2013;120(3):593-599.
63. Seddon JM, Silver RE, Kwong M, Rosner B. Risk Prediction for Progression of Macular Degeneration 10 Common and Rare Genetic Variants, Demographic, Environmental, and Macular Covariates. Invest Ophthalmol Vis Sci. 2015;56(4):2192-2202.

2

Multimodal imaging for AMD

Multimodal imaging of AMD

PART 1: Non-invasive imaging

Setha Vo Kim, Francesca Amoroso

1. Fundus photography

1) Conventional fundus cameras

a) Colour fundus photographs

Conventional fundus cameras acquire instant, high-resolution photographs of the fundus. They cover a 45-degree field of view, and some have an embedded digital zoom option allowing the acquisition of 30-degree fundus photographs of the macula or optic disc. The latest devices no longer always require pupil dilation before the procedure.

Colour fundus photographs are acquired using a white light fundus camera. Various monochrome filters can be used, highlighting particular structures in the fundus and therefore making it easier to assess them.

This procedure complements dilated fundus examination (Figure 1) and is a highly effective screening and diagnostic tool, particularly when combined with the remote transmission of digitised data. It can also be used to objectively monitor retinal diseases over time. Its efficacy in terms of screening for and monitoring AMD has been demonstrated in the literature[1,2] (Figures 2, 3 and 4).

Fig. 1: 45-degree colour fundus photograph centred on the posterior pole in a healthy subject.

Fig. 2: Soft drusen in the posterior pole.

Fig. 3: Adult-onset foveomacular vitelliform dystrophy: subfoveal material deposit associated with fine drusen.

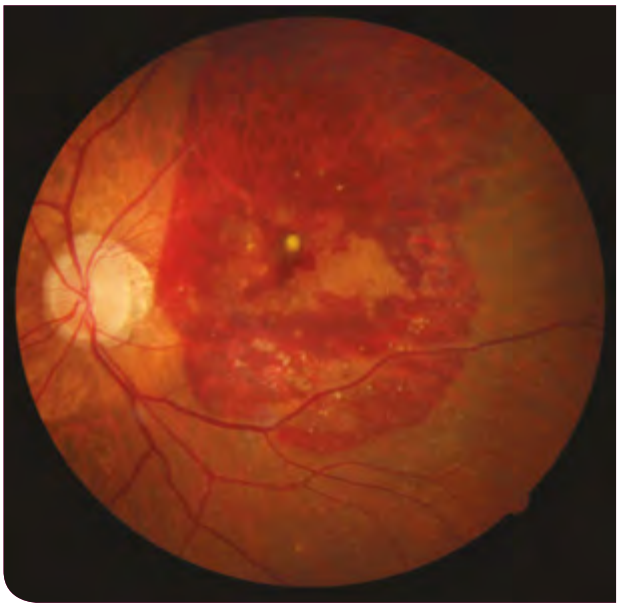

Fig. 4: Subretinal haemorrhage in AMD complicated by type 2 neovascularization accompanied by drusen.

b) Infrared fundus photographs

These photographs use aninfrared LED and highlight retinal folds secondary to epiretinal membranes (Figure 5), as well asthe presence of subretinal fluid, displayed as a darker area (Figure 6). The different phenotypes observed in AMD have been described in literature[3].

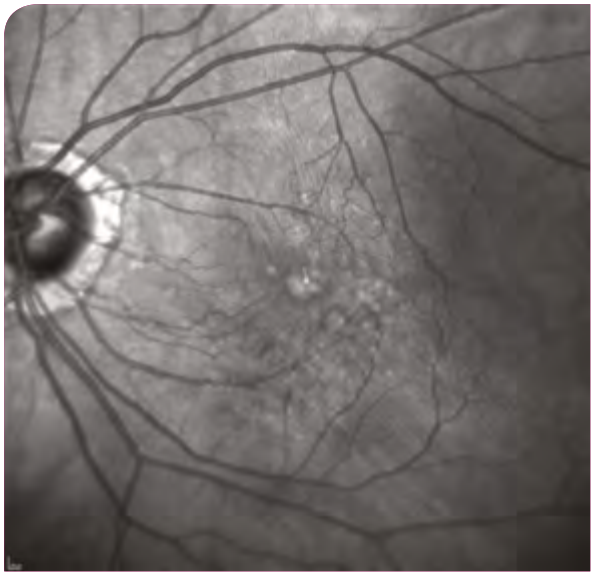

Fig. 5: Infrared photographs showing epiretinal membrane folds.

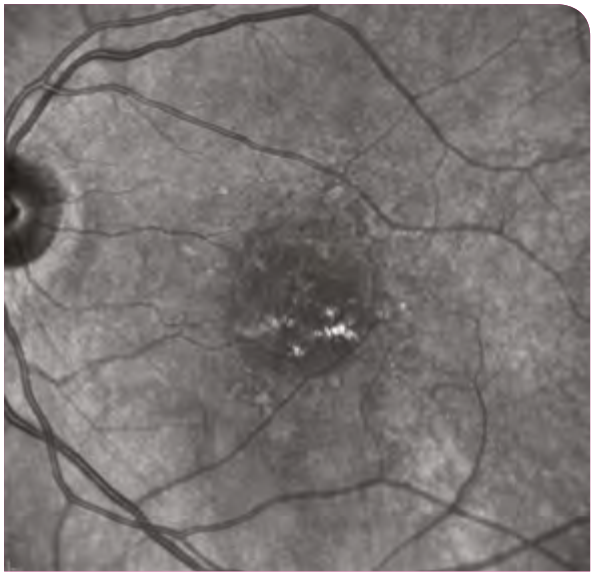

Fig. 6: Infrared photograph showing a pigment epithelial detachment.

c) Green or red-free fundus photographs

A 570 nm green filter highlights red structures, such as vascular structures and haemorrhages (Figures 7), and is therefore ideal for assessing vascular structures in the fundus.

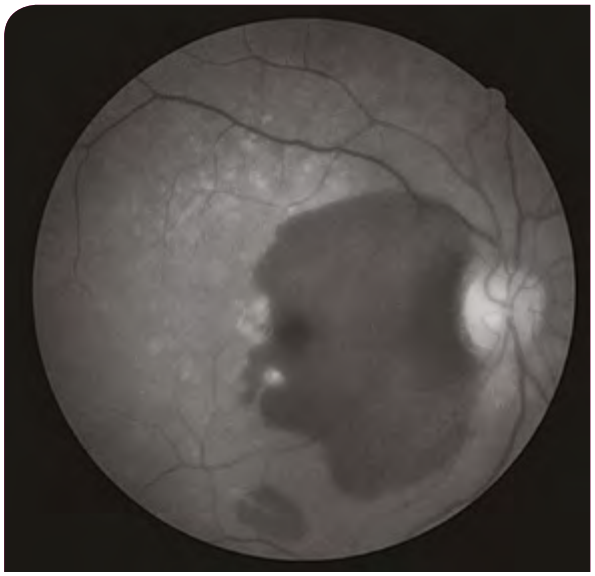

Fig. 7(A): Red free photograph showing a subretinal haemorrhage secondary to type 2 choroidal neovascularization.

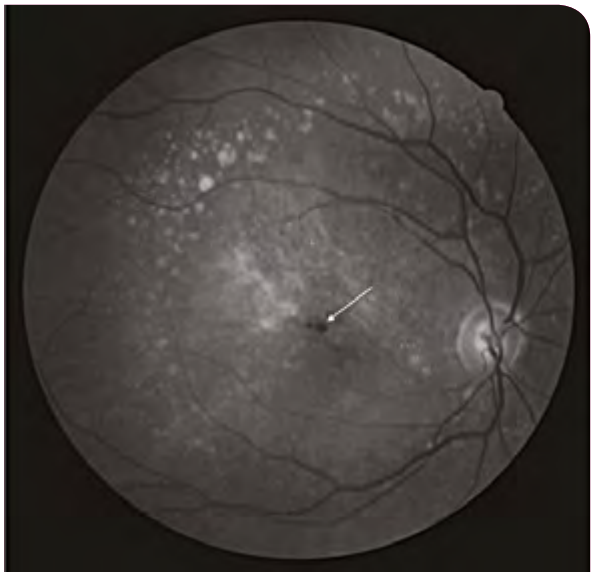

Fig. 7(B): Red free photograph of discrete intraretinal haemorrhage suggesting a type 3 neovascularization, associated with drusen.

d) Fundus photographs with blue illumination

A 500 nm blue filter highlights yellow structures, such as xanthophyll pigment in the macula, and refractive structures such as the optic fibres or an epiretinal membrane. These photographs can reveal certain types of drusen ("blue" drusen, known as reticular pseudodrusen or subretinal drusenoid deposits, first described by Créteil team[4] and associated with a risk of advanced ARMD[5]). They can also be used to detect vitelliform deposits (Figures 8). They cannot be used in the presence of significant lens opacity.

Fig. 8(A): Fundus photograph of adult-onset foveomacular vitelliform dystrophy associated with reticular pseudodrusen. The reticular pseudodrusen can be seen in the blue photograph.

Fig. 8(B): The vitelliform material disappears under blue light.

e) Fundus photographs with red illumination

A 645 nm red filter highlights pigment changes, which appear as darker areas in the image (Figures 9), and can be used to assess lesions located below the pigment epithelium, within the choroid.

Fig. 9(A): Fundus photograph showing retinal pigment epithelium changes.

Fig. 9(B): The pigment changes are highlighted in the red filter image.

2) Confocal scanning laser ophthalmoscopy (cSLO)

Unlike with conventional fundus cameras, the addition of a confocal filter prevents reflected rays from structures located in sections of the eye other than the posterior pole from reaching the sensor, resulting in a clear, reliable image even in the presence of media opacities. Images can be generated by associating monochrome laser sources (red, green and blue lasers), as with the "pseudocolour" MultiColor Imaging Spectralis® images (Heidelberg, Germany) (Figures 10 and 11), or using white light, as with the Eidon® system (Centrevue SpA, Padova, Italy).

Fig. 10: Posterior pole Drusen, Multicolor® mode.

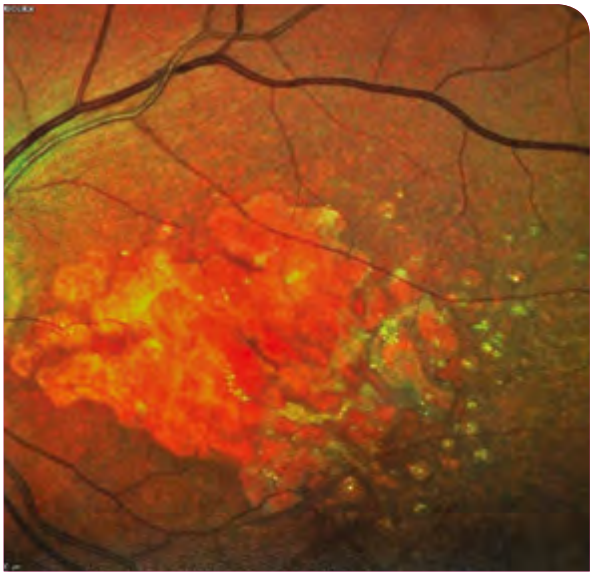

Fig. 11: Geographic atrophy of the posterior pole, Multicolor® mode: the choroidal vessels are visible.

2. Fundus autofluorescence imaging

Fundus autofluorescence imaging is based on the contrast resulting from the use of a specific wavelength to stimulate a fluorophore naturally present in the retina, the compound A2-E of lipofuscin generated by the break down of photoreceptors' outer segments. The photographs can be used to study pigment distribution, which provides information on the functioning of the retinal pigment epithelium.

The accumulation of lipofuscin and A2-E observed in AMD[6] causes pigment epithelium dysfunction[7]. Images can be acquired using a conventional fundus camera or a scanning laser ophthalmoscope (SLO)[8].

In healthy subjects, homogeneous coloration is observed, indicating homogeneous distribution of lipofuscin, with a daker area in the fovea due to xanthophyll pigment (Figure 12).

In the presence of retinal atrophy, the disappearance of the retinal pigment epithelium results in a dark, hypoautofluorescent area. As the disease progresses, a hyperautofluorescent outline can be seen, reflecting the accumulation of A2-E where the pigment epithelium is becoming damaged (Figure 13). This indicates that the atrophy is likely to spread in future[9].

An accumulation of lipofuscin is observed with adult-onset foveomacular vitelliform dystrophy and pattern dystrophy (Figure 14), both characterised by the accumulation of material in the posterior pole.

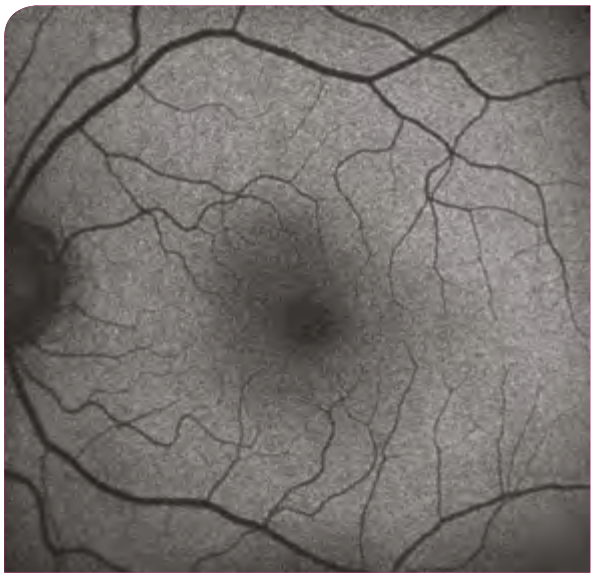

Fig. 12: Fundus autofluoresnce imaging of the posterior pole in a healthy subject.

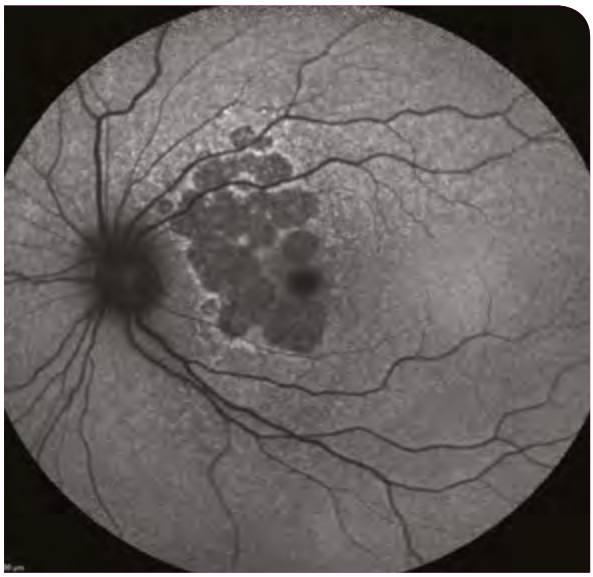

Fig. 13: Fundus autofluorescence imaging of progressive geographic atrophy (dry AMD): the hyperautofluorescent border around the atrophy reveals a ring of pigment epithelium alteration surrounding the atrophy.

Fig. 14: Fundus autofluorescence imaging of pattern dystrophy.

3. Optical coherence tomography (OCT)

This examination was first used in retinal investigations at the end of the 1990s[10-12] and soon became widespread. It involves emitting a beam of near-infrared light (840 nm) onto a semi-reflective mirror oriented to 45°, which splits the beam into two parts: one is projected onto a reference surface and the other is directed towards the investigated structure. The two reflected beams are then redirected into the slit of the spectrometer, where they are analysed.

1) Time-domain OCT (TD-OCT)[13]

At the end of the 1990s, the first devices were based on analysing the time between the emitted and reflected beams using a mobile reference mirror. The acquisition speed was 400 A-scan per second, with a resolution of 10-15 µm.

2) Spectral-domain OCT (SD-OCT)

Since 2007, OCT devices technology is based on the frequency of the refracted rays using the Fourier transform. This improves the acquisition speed (up to 85,000 A-scan per second) and the image definition. The axial resolution of SD-OCT is around 3–5 µm and its longitudinal resolution is 15–20 µm, enabling quasi-histological resolution of the retinal layers (Figure 15). AMD can be characterised by one or more retinal pigment epithelium (RPE) elevations (Figure 16), the appearance of intraretinal or subretinal exudative signs[14] (Figure 17) and/or areas of retinal atrophy[15] (Figure 18). From a qualitative perspective, treated pathological areas can be analysed and compared precisely over time, using the eye tracking system. Macular changes can be measured quantitatively: the volume or surface area of drusen[16] and neovascular membranes can be estimated, enabling more precise monitoring.

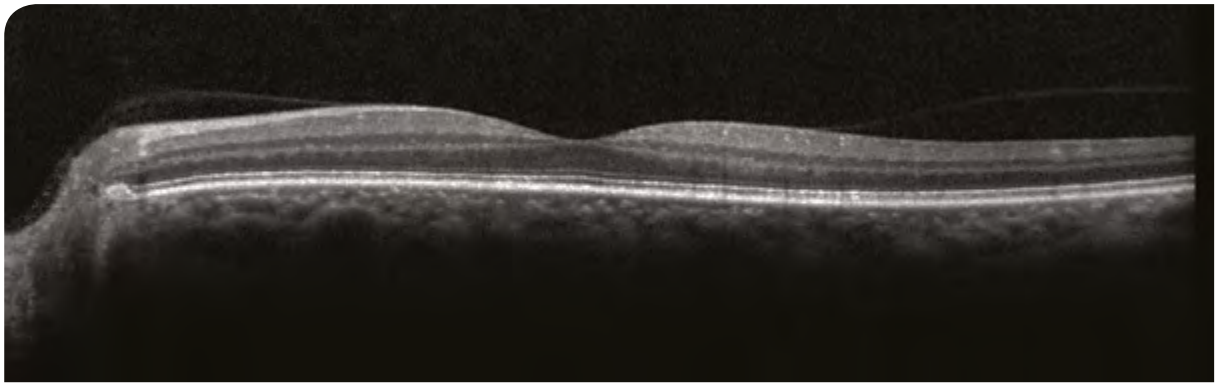

Fig. 15: SD-OCT scan in a healthy subject.

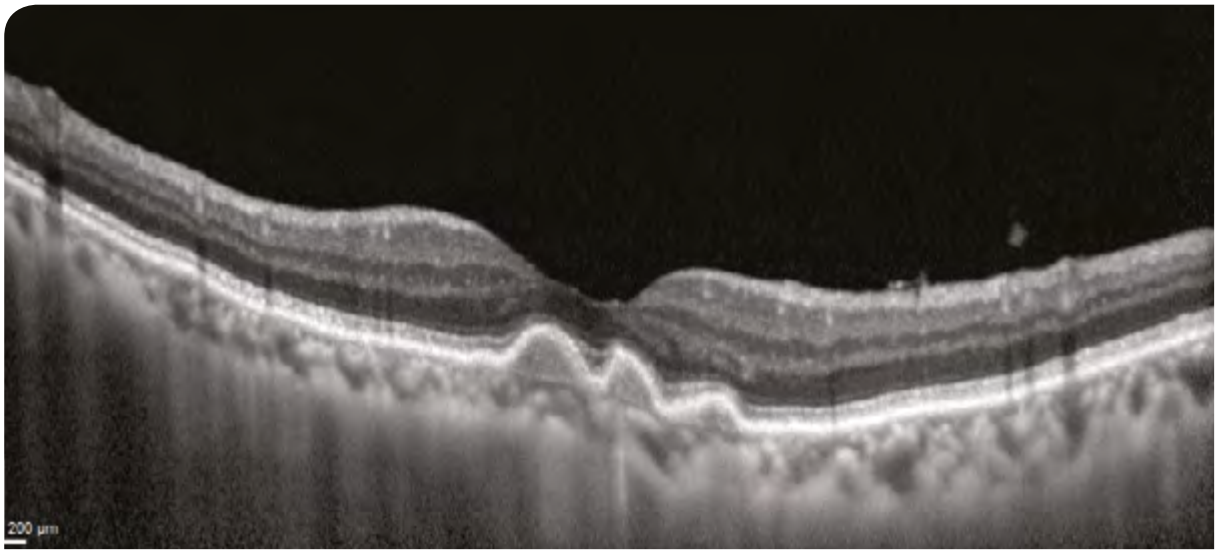

Fig. 16: Uncomplicated drusenoid PED in early AMD.

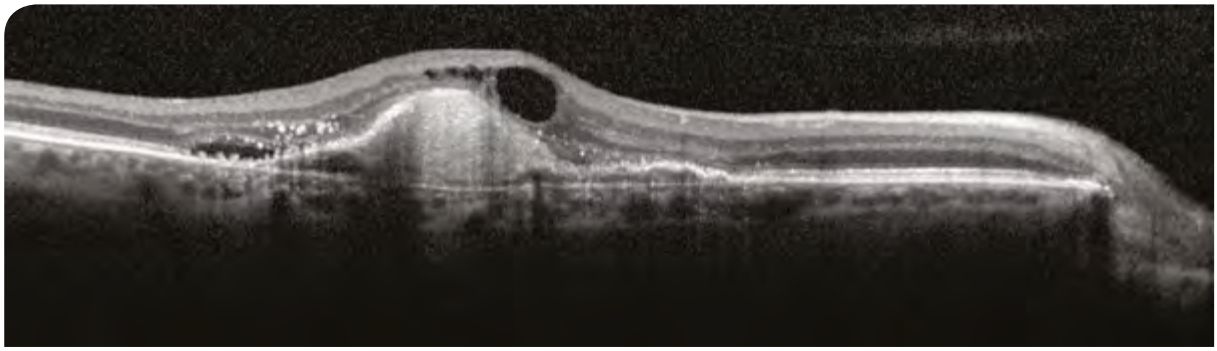

Fig. 17: Exudative AMD with type 1 neovascularization.

3) Enhanced depth imaging (EDI)-OCT

EDI-OCT is used for more precise assessment of the choroid[17].
The choroid becomes thinner with age, but also in hih myopia and in AMD. Conversly, thicker choroid is found in young people, emmetropic eyes and in pachychoroid spectrum diseases, such as polypoidal choroidal vasculopathy (Figures 18 and 19).

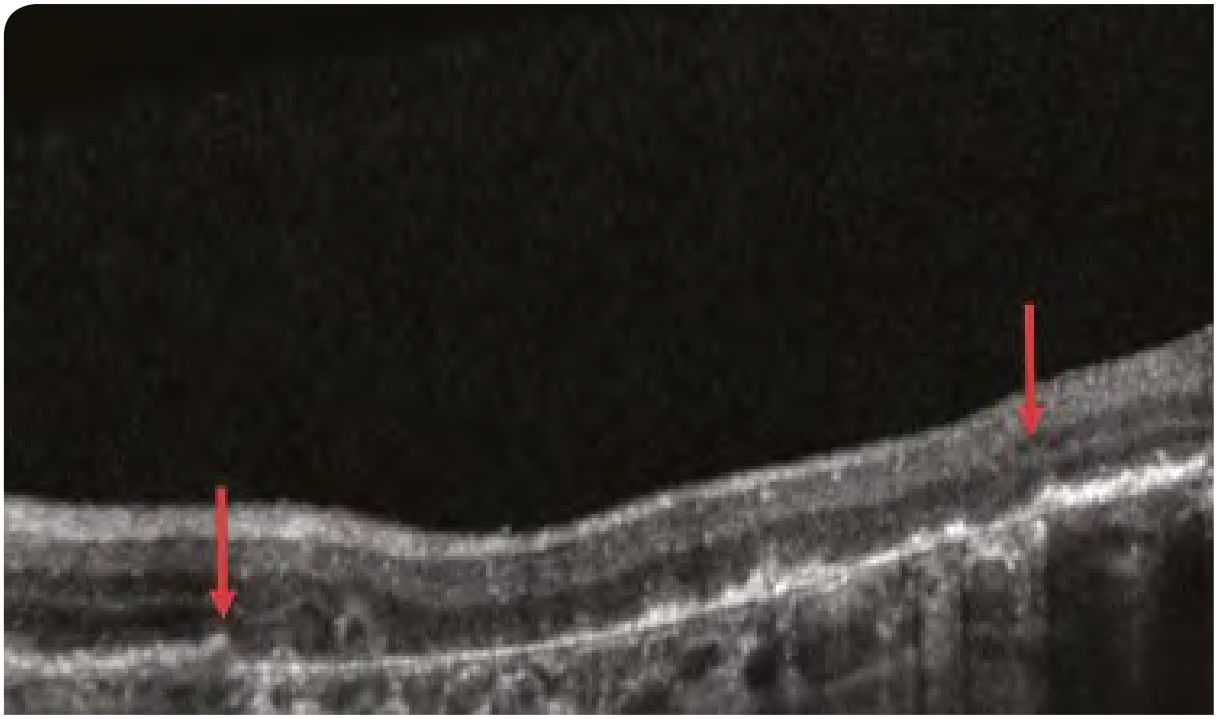

Fig. 18: Dry AMD. Atrophy of the RPE and outer layers (area between the arrows), with choroidal hyperreflectivity due to the window effect.

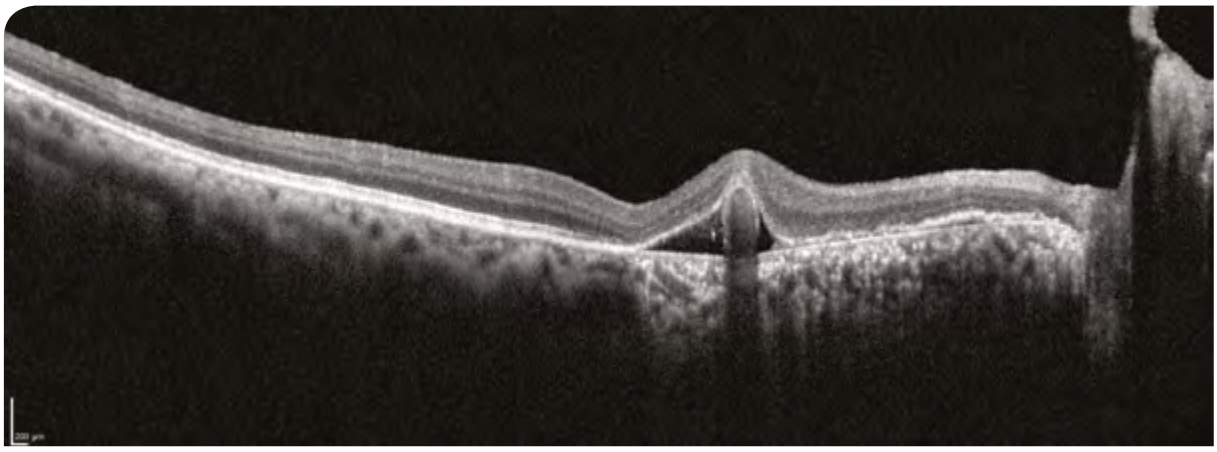

Fig. 19: Polyp located between the optic disc and the maculaassociated with pachychoroid.

References

1. Age-Related Eye Disease Study Research Group. The Age-Related Eye Disease Study System for Classifying Age-Related Macular Degeneration from Stereoscopic Color Fundus Photographs: The Age-Related Eye Disease Study Report Number 6. American Journal of Ophthalmology.2001;132(5):668-81.

2. A Pirbhai, T Sheidow, et P Hooper. Prospective Evaluation of Digital Non-Stereo Color Fundus Photography as a Screening Tool in Age-Related Macular Degeneration. American Journal of Ophthalmology.2005.139(3):455-61.

3. A Ly, L Nivison-Smith, N Assaad, et M Kalloniatis. Infrared reflectance imaging in age-related macular degeneration. Ophthalmic & Physiological Optics. 2016;36(3):303-16.

4. Mimoun, G., G. Soubrane, et G. Coscas. [Macular drusen]. Journal Francais D'ophtalmologie. 1990;13(10):511-30.

5. NM Pumariega, R. T Smith, MA Sohrab, *et al.* A PROSPECTIVE STUDY OF RETICULAR MACULAR DISEASE. Ophthalmology.2011(8):1619–1625.

6. RF Spaide. Fundus Autofluorescence and Age-Related Macular Degeneration. Ophthalmology. 2003;110(2):392-99.

7. F Schütt, S Davies, J Kopitz, *et al.* Photodamage to Human RPE Cells by A2-E, a Retinoid Component of Lipofuscin. Investigative Ophthalmology & Visual Science.2000;41(8):2303-8.

8. S Schmitz-Valckenberg, M Fleckenstein, AP Göbel, *et al.* Evaluation of Autofluorescence Imaging with the Scanning Laser Ophthalmoscope and the Fundus Camera in Age-Related Geographic Atrophy. American Journal of Ophthalmology.2008;146(2):183-92.

9. FG Holz, A Bindewald-Wittich, M Fleckenstein, *et al.* et FAM-Study Group. Progression of Geographic Atrophy and Impact of Fundus Autofluorescence Patterns in Age-Related Macular Degeneration. American Journal of Ophthalmology 2007;143(3):463-72.

10. MR Hee, JA Izatt, EA Swanson, *et al.* Optical Coherence Tomography of the Human Retina. Archives of Ophthalmology.1995;113(3):325-32

11. CA Puliafito, MR Hee, CP Lin, *et al.* Imaging of Macular Diseases with Optical Coherence Tomography. Ophthalmology.1995;102(2):217-29.

12. Hee, M. R., C. R. Baumal, C. A. Puliafito, J. S. Duker, E. Reichel, J. R. Wilkins, J. G. Coker, J. S. Schuman, E. A. Swanson, et J. G. Fujimoto. Optical Coherence Tomography of Age-Related Macular Degeneration and Choroidal Neovascularization. Ophthalmology. 1996;103(8): 1260-70.

13. D Huang, EA Swanson, CP Lin, J., *et al.* Optical Coherence Tomography. Science.1991;254(5035): 1178-81.

14. MM Castillo, G. Mowatt, N. Lois, *et al.* Optical Coherence Tomography for the Diagnosis of Neovascular Age-Related Macular Degeneration: A Systematic Review. Eye.2014;28(12):1399-1406.

15. K Sleiman, M Veerappan, KP. Winter, *et al.* Age-Related Eye Disease Study 2 Ancillary Spectral Domain Optical Coherence Tomography Study Group. Optical Coherence Tomography Predictors of Risk for Progression to Non-Neovascular Atrophic Age-Related Macular Degeneration. Ophthalmology. 2017;124(12): 1764-77.

16. G Gregori, F Wang, PJ Rosenfeld, Z Yehoshua, *et al.* Spectral Domain Optical Coherence Tomography Imaging of Drusen in Non-Exudative Age-Related Macular Degeneration. Ophthalmology.2011; 118(7): 1373-79.

17. RF Spaide, H Koizumi, MC Pozzoni. Enhanced Depth Imaging Spectral-Domain Optical Coherence Tomography. American Journal of Ophthalmology. 2008 146(4): 496-500.

AMD multimodal imaging

PART 2: Optical coherence tomography angiography (OCTA)

Alexandra Miere, Roxane Bunod, Eric Souied

1. Principle

OCTA is a new retinal imaging technique that generates images of the retinal and choroidal micro-vasculature using sequential B-scans of the same retinal scan, in order to detect motion contrast[1]. Unlike moving objects, stationary objects do not change from one image to the next and are therefore interpreted as having no flow. Blood circulating in the retinal microvasculature, however, creates fluctuations in reflectivity from one image to the next, which is interpreted as flow. The specific area in the retina can be assessed by repeating the analysis on several adjacent slices. A "split-spectrum amplitude decorrelation angiography" (SSADA) algorithm is used to calculate the difference in reflectivity between several sequential acquisitions from the same section of the retina[2].

2. OCTA images

OCTA data are viewed by creating segmented B-scan scans from different layers in the retina. The layers of the retina between two segmentation lines are then projected for en-face visualisation[1]. Most of the currently available OCTA devices offer several automatic segmentation options (Figures 1 and 2):

- Superficial capillary plexus
- Intermediate capillary plexus
- Deep capillary plexus
- Outer retina
- Choriocapillaris
- Custom segmentation

A structural B-scan is obtained simultaneously, providing real-time verification of the exact location and depth of the various structures. Figure 3 shows the multimodal imaging of an adult-onset foveomacular vitelliform dystrophy case complicated by choroidal neovascularization visualized on OCTA.

In addition to qualitative analysis based on the structural B-scan and en-face projections, quantitative markers for (neo)vascular disease have been developed, including vessel density, area of the foveal avascular zone, non-perfusion area and neovascular area.

Several OCTA devices using different algorithms and wavelengths are currently available. Swept-source OCTA devices have a wavelength of 1050 nm, which is higher than that of spectral-domain machines (840 nm). Devices that use swept-source technology therefore offer better penetration through the choroid than spectral-domain devices[3].

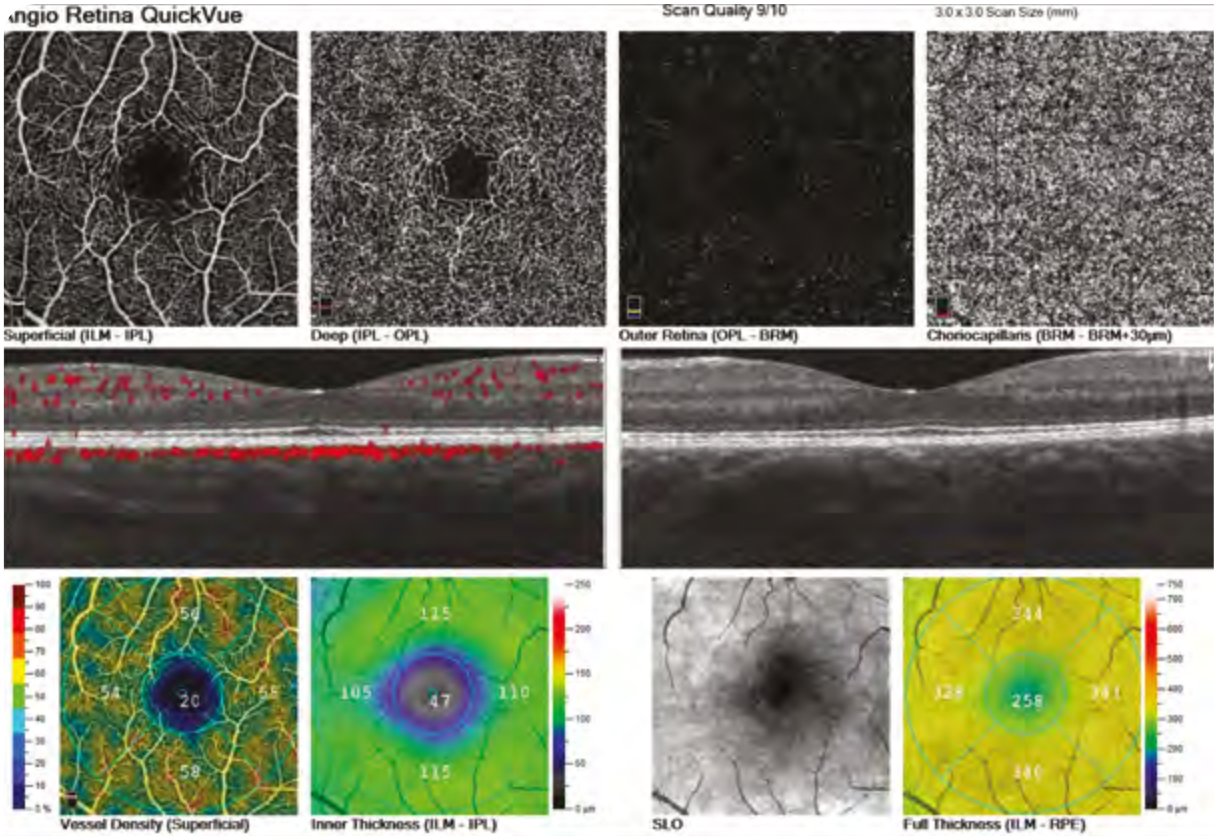

Fig. 1: Automatic segmentation available with AngioVue (Optovue).

Fig. 2: OCTA wide-field montage (PlexElite, Zeiss) from a male patient with proliferative diabetic retinopathy.
(A): Vitreoretinal interface slab. Multiple areas of pre-retinal neovascularization can be seen.
(B): Superficial capillary plexus slab. Areas of ischaemia are visible.
(C): Deep capillary plexus slab.

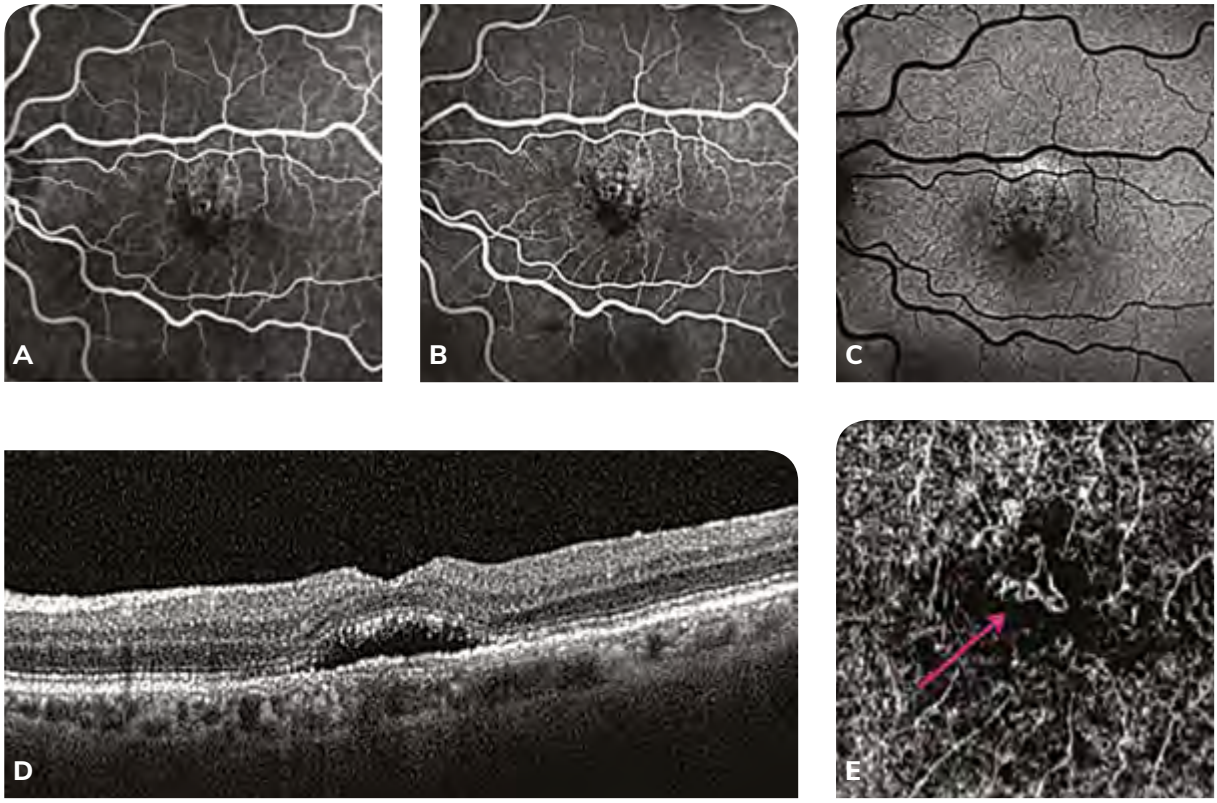

Fig. 3: Adult-onset foveomacular vitelliform dystrophy complicated by choroidal neovascularization.
Fluorescein angiography in the early (A) and late (B) frames reveals a typical aspect of staining of the vitelliform material with mild diffusion. There is no clearly identifiable neovascular network.
In fundus autofluorescence (C), the material appears hyperautofluorescent. The OCT B-scan shows serous retinal detachment (D) which can correspond to fragmented vitelliform material. Neovascularization cannot therefore be diagnosed with certainty. On OCTA , the presence of neovascularizsation within the choriocapillaris segmentation is clearly identifiable (arrow) (E).

3. Artefacts

There are several different kinds of artefact that can impact the OCTA signal, regardless of which device is used. The most common type of artefacts are projection artefacts. Projection artefacts aoriginates in the hyperreflective RPE; variations of the reflected light off the hyperreflective RPE would be interpreted as movement by the OCTA device, therefore generating the projection artefact[4]. Projection artefacts have been described in chorioretinal atrophy, drusen and drusenoid pigment epithelial detachment.

Other OCTA artefacts have been described, including artefacts linked to image acquisition, the intrinsic properties of the eye and eye disease (opacity of the media, vitreous haemorrhage), eye motion, as well as image processing and display strategies. The latter category includes automatic segmentation errors, thresholding and saturation artefacts.[4]

4. In practice

When using OCTA, it is therefore important to:

- **Carefully identify any false positives and false negatives generated by artefacts**
- **Acquire good quality images (> 5/10)**
- **Analyse en-face flow images with the corresponding B-scan.**

References

1. Spaide RF, Fujimoto JG, Waheed NK, *et al.* Optical coherence tomography angiography. Prog Retin Eye Res. 2018;64:1-55.

2. Huang D, Jia Y, Gao SS, Lumbroso B, Rispoli M. Optical coherence tomography angiography using the Optovue device. Dev Ophthalmol. 2016;56: 6-12.

3. Novais EA, Adhi M, Moult EM, Louzada RN, Cole ED, Husvogt L, Lee B, Dang S, Regatieri CV, Witkin AJ, Baumal CR, *et al.* Choroidal Neovascularization Analyzed on Ultrahigh-Speed Swept-Source Optical Coherence Tomography Angiography Compared to Spectral-Domain Optical Coherence Tomography Angiography. Am J Ophthalmol. 2016;164:80-8.

4. Spaide RF, Fujimoto JG, Waheed NK. Image artifacts in optical coherence tomography angiography. Retina 2015; 35: 2163-2180.

Multimodal imaging for AMD

PART 3: Invasive imaging

Setha Vo Kim, Francesca Amoroso

1. Fluorescein angiography

Although two students at the University of Indiana, Novotny and Alvis, had initially described the technique of fluorescein angiography (FA) in 1961[1], it was Donald Gass, in 1967, who really introduced it as a key retinal imaging technique[2]. As technology developed, the utility of the procedure was confirmed. Fluorescein angiography requires the use of a fundus camera equipped with excitation and barrier filters.

Fluorescein is injected intravenously, generally into the antecubital area. A blue excitation filter allows white light to pass through; the unbound fluorescein molecule then absorbs the blue light (465–490 nm) and emits light with a longer wavelength in the yellow-green spectrum (520–530 nm). A barrier filter blocks out any other reflected wavelengths to ensure that the images capture only the light emitted by the fluorescein.

The images are acquired immediately after the injection and over a total time of 6 to 15 minutes, depending on the disease. They are recorded digitally or on 35 mm film. The complications described after the injection are temporary nausea (3 to 15% of patients), vomiting (7%)[3] and pruritus. More severe reactions are rare and include urticaria, fever, thrombophlebitis and syncope. Local tissue necrosis can occur in the event of extravasation of the dye, but mild pain and redness are more common. Anaphylaxis, cardiac arrest and bronchospasm can occur, but are extremely rare.

a) Normal fluorescein angiography

After injecting the dye into an antecubital vein, fluorescein passes through the short posterior ciliary arteries and appears in the optic nerve and choroid within the next 8 to 12 seconds. Retinal circulation appears 1 to 3 seconds later (11 to 18 seconds after the injection), as the choroid fills. The early arteriovenous phase (filling of the retinal arteries, arterioles and capillaries) is followed by the late arteriovenous phase or laminar venous phase, as the dye fills the veins in a laminar pattern.

In a healthy macula, the foveal avascular zone (FAZ) appears dark, due to blockage of choroidal fluorescence by xanthophyll pigment and RPE cells. After 10 minutes, the fluorescein is no longer present in the retinal vessels, but the optic nerve head, Bruch's membrane and sclera remain stained with fluorescein[4].

b) Abnormal fluorescein angiography

Hypofluorescence is a reduction in normal fluorescence, and *hyperfluorescence* refers to increased or abnormal fluorescence[5].

Hypofluorescence can occur secondary to a blocking effect or due to a vascular filling defect. An opacity located anteriorly to the fluorescence (corneal scar, cataract, vitreous haemorrhage or nerve fibre haemorrhage) can block normal fluorescence, as can retinal haemorrhage, subretinal material or an abnormal accumulation of lipofuscin (as seen in Best disease, adult-onset foveomacular vitelliform dystrophy and drusenoid pigment epithelial detachment [PED]) (Figure 1).

Fig. 1: Example of hypofluorescence in fluorescein angiography: drusenoid PED. Multiple areas of hyperfluorescence around the macula in the early frame (A), increasing during the examination (B), with no late leakage(C). The central hypofluorescence is due to a blocking effect caused by the overlying drusenoid PED, and the focal inferonasal hyperfluorescence is linked to a window effect caused by retinal pigment epithelium atrophy.

Fig. 2: Example of leakage or diffusion: type 2 choroidal neovascularization secondary to exudative AMD. Fluorescein angiography typically clearly shows the neovascular membrane very clearly from the early frame. Here, it is accompanied by cystoid spaces. Note how the hyperfluorescent neovascular membrane contrasts with the surrounding hypofluorescent ring (A). The fluorescence increases over the course of the angiogram (B) and, in the late frame, intense leakage can be seen as the dye passes into the subretinal space (C).

Fig. 3: Example of pooling: serous PED. During the early phase, the PED appears hypofluorescent (A). Over the course of the angiogram, the fluorescence gradually increases (B), with hyperfluorescence in the late phase, due to gradual pooling of the PED. Note that the edges of the PED are well marked and the staining is uneven, due to blockage caused by the presence of the pattern disposition of vitteliform material (C).

Hyperfluorescence occurs as a result of ***leakage***, impregnation (or ***staining***), accumulation (or ***pooling***), or increased fluorescein transmission (***window effect***).

The phenomenon of fluorescein ***leakage*** is generally caused by immature blood vessels (type 2 choroidal neovascularisation secondary to AMD, pre-retinal neovascularization in the context of proliferative diabetic retinopathy) or in a retinal pigment epithelium tear. The areas of leakage are characterised by fluorescence that increases in intensity and size over the course of the examination, with blurred edges (Figure 2).

Staining is an increase in fluorescence over the course of the angiogram, with edges that remain sharp. Normal structures such as the optic nerve head and the sclera show physiological fluorescein staining.

Pooling occurs when the fluorescein gradually fills a fluid-filled space (umbrella shaped, leakage point in central serous chorioretinopathy, serous PED (Figure 3).

Transmission or a ***window effect*** occurs when the RPE is damaged and choroidal fluorescence is observed during the early frame of the examination. The intensity of the fluorescence does not change during the angiogram and the edges remain sharp (Figure 4).

Fig. 4: Window effect: atrophic AMD (Geographic atrophy).
(A): Fundus autofluorescence showing inferomacular hypoautofluorescence corresponding to the atrophic area.
(B): Fluorescein angiography shows early hyperfluorescence.
(C): The hyperfluorescence increases slightly in the late frame, with no diffusion of the dye, as a result of a window effect linked to the absence of the RPE/choriocapillaris complex (choroidal fluorescence can clearly be seen).

2. Indocyanine green angiography

Indocyanine green (ICG) is a water-soluble dye with a molecular weight of 775 daltons and near-infrared fluorescence (790–805 nm). After intravenous injection, ICG is almost completely protein-bound (98%), with limited diffusion through the small fenestrations of the choriocapillaris. This property makes ICG angiography the ideal tool for imaging choroidal circulation[6]. Its fluorescence can be detected only with infrared video angiography involving modified fundus cameras, a digital imaging system or a scanning laser ophthalmoscope (SLO).

ICG angiography uses a diode laser illumination system (805 nm) and barrier filters at 500 nm and 810 nm. Modern tools have enabled high-speed ICG angiography, which can generate up to 30 images per second with continuous recording of the angiogram. This system is very useful for visualising structures that appear only briefly, such as feeder vessels of choroidal neovascularization (Figure 5).

Due to its longer wavelength, ICG angiography can sometimes offer a better visualization compared to fluorescein angiography of the choroidal neovascularization associated with haemorrhage or hyperplasia of the RPE. It is also useful for pigment epithelial detachments and occult choroidal neovascularization (Figure 6).

In the differential diagnosis of neovascular AMD, early ICGA hyperfluorescence with a "hot spot" in the late frames of the angiogram is highly suggestive of chorioretinal anastomosis (type 3 neovascularization) (Figure 7)[8]. In contrast, early hyperfluorescence with a late "wash-out" of the neovascular lesion suggests the presence of polypoidal choroidal vasculopathy (Figure 8)[9].

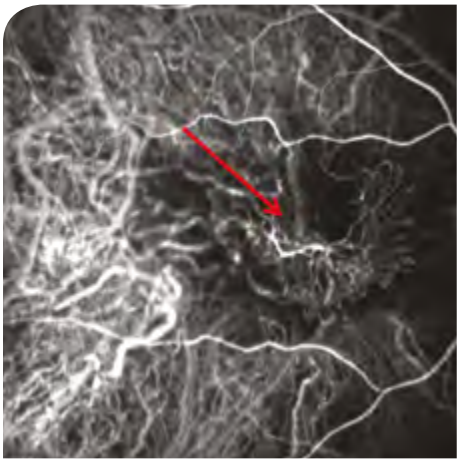

Fig. 5: Indocyanine green angiography of a female patient with exudative AMD.
The early frame of ICGA reveals the presence of a feeder vessel of the neovascular membrane (red arrow).

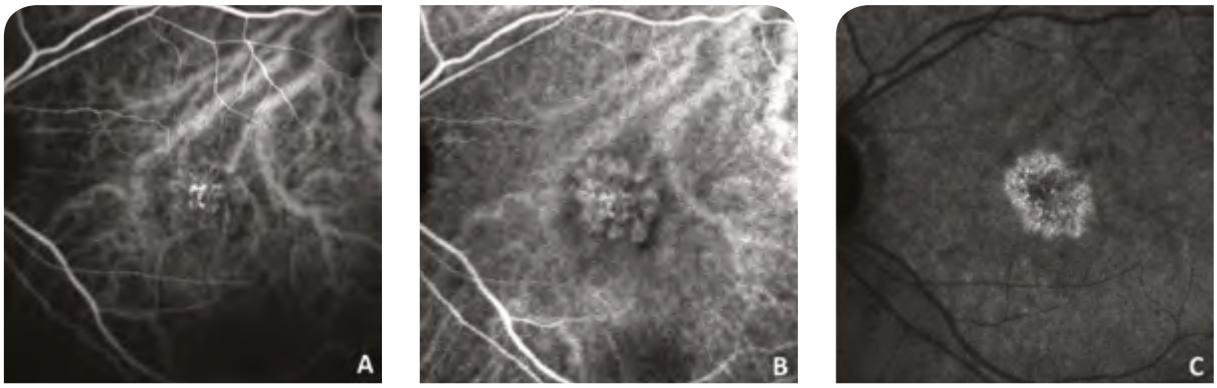

Fig. 6: Indocyanine green angiography of a male patient with type 1 choroidal neovascularization secondary to exudative AMD.
In the early frame, ICGA shows a hyperfluorescent neovascular membrane (A), which persists into the intermediate frame (B) and increases in fluorescence in the late frame, generating a typical "late plaque" appearance (C).

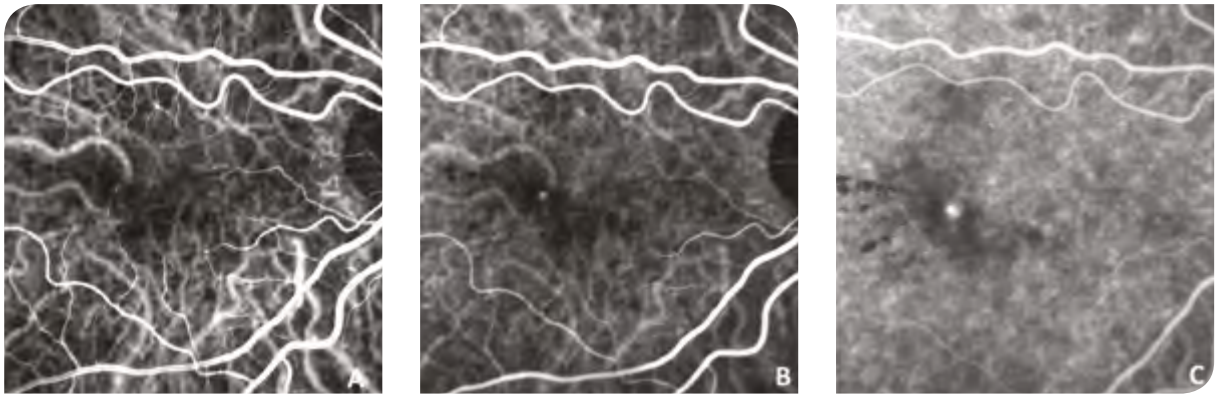

Fig. 7: Indocyanine green angiography of a female patient with type 3 neovascularization (retinal angiomatous proliferation, chorioretinal anastomosis). The early ICGA reveals a focal hyperfluorescence (A), its fluorescence increasing in the intermediate frame (B) and with a visible 'hot spot' in the late frame (C).

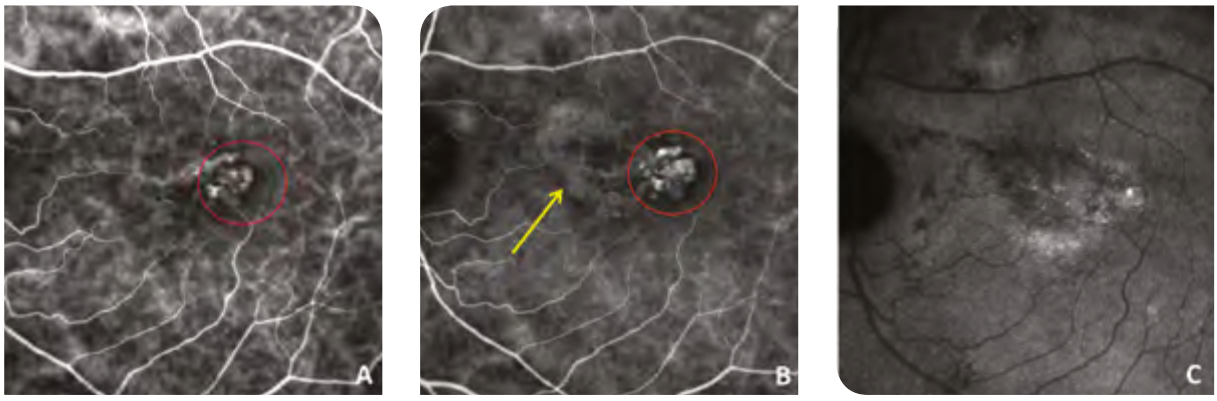

Fig. 8: Indocyanine green angiography of a male patient with polypoidal choroidal vasculopathy.
The ICGA shows early pooling of the polypoidal lesions (red circle) and the abnormal branching vascular network (yellow arrow) (A), persisting into the intermediate frame (B), with a wash-out in the late frames (C).

References

1. Novotny HR, Alvis DL. A method of photographing fluorescence in circulating blood in the human retina. Circulation. 1961;24:82-86.
2. Gass JDM, Sever, RJ, Sparks D, Goren J. A combined technique of fluorescein fundoscopy and angiography of the eye. Arch Ophthalmol. 1967;78:455-461.
3. Yannuzzi LA, Rohrer, MA, Tindel LJ, *et al.* Fluorescein angiography complication survey. Ophthalmology. 1986;93:611-7.
4. Schatz H, Burton TC, Yanuzzi LA, Rabb MF. Interpretation of fundus fluorescein angiography. St. Louis:Mosby-Year Book: 1978.
5. Gass JDM. Stereoscopic atlas of macular diseases: diagnosis and treatment, 4th edition. St. Louis:Mosby-Yearbook; 1997.
6. Gelisken F, Inhoffen W, Schneider U, *et al.* Indocyanine green angiography in classic choroidal neovascularization. Jpn J Ophthalmol 1998. 42:300-303.
7. Grossniklaus HE, Gass JD. Clinicopathologic correlations of surgically excised type 1 and type 2 submacular choroidal neovascular membranes. Am J Ophthalmol 1998. 126:59-69.
8. Kuhn D, Meunier I, Soubrane G, Coscas G. Imaging of chorioretinal anastomoses in vascularized retinal pigment epithelium detachments. Arch Ophthalmol. 1995. 113:1392-1398.
9. Spaide RF, Yannuzzi LA, Slakter JS, *et al.* Indocyanine green videoangiography of idiopathic polypoidal choroidal vasculopathy. 1995. Retina 15:100-10.

3

Early and intermediate AMD

Mayer Srour

1. Definition

"Age-related maculopathy" (ARM), also known as early and intermediate AMD, covers all age-related changes to the fundus preceding neovascular or atrophic AMD (i.e. late AMD). These changes generally occur from fifty years of age.

ARM manifests as changes to the retinal pigment epithelium (RPE): RPE depigmentation or hyperpigmentation (pigment clumps or migration). Drusen, including hard drusen, isolated or confluent soft drusen, reticular pseudodrusen, cuticular drusen, refractile drusen and ghost drusen are hallmarks of ARM. The presence of these lesions in the general population varies considerably by age[1] (25% after 52 years to 87% after 80 years).

While these lesions do not always progress to late AMD, their presence is a risk factor that merits careful analysis and precise monitoring. A score has been developed to predict exudative AMD based on an analysis of the fundus. Each eye is scored between 0 and 2 based on the presence or absence of drusen measuring over 125 microns or RPE changes, giving the patient a total score of between 0 and 4. Five-year and ten-year neovascular risk was assessed in this way in the AREDS study[2] (Tables 1 and 2).

Today, ARM is split into two entities: early AMD and intermediate AMD. Early AMD is characterised by the presence of numerous small drusen (< 63 microns, known as "hard" drusen) or intermediate drusen (≥ 63 microns but < 125 microns, known as "soft" drusen). Intermediate AMD is defined by the presence of extensive small or medium-sized drusen, or by large drusen (≥ 125 microns). Small drusen are commonly seen in people aged 50 years and over, and can be an epiphenomenon of ageing. Intermediate drusen are therefore more specific and more likely to be a marker of age-related macular degeneration than of normal ageing.

RIGHT EYE	**Drusen > 125 µm**	**No = 0**	**Yes = 1**
	Pigment migration	**No = 0**	**Yes = 1**
LEFT EYE	**Drusen > 125 µm**	**No = 0**	**Yes = 1**
	Pigment migration	**No = 0**	**Yes = 1**

Table 1: Scoring system described in AREDS Report No. 18. A score is given to each eye based on the presence or absence of pigment migration and drusen of over 125 microns in diameter. If one eye is more severely affected, its score is automatically 2 points, and the other is assessed based on the scale above. For intermediate drusen (63 µm to 125 µm), the score is 0.5, giving a score of 1 if both eyes are affected.

STAGE	Five-year risk of neovascularization	Ten-year risk of neovascularization
0	**0%**	**0.5%**
1	**3%**	**8%**
2	**12%**	**22%**
3	**25%**	**49%**
4	**50%**	**66%**

Table 2: Five-year and ten-year risk of AMD based on AREDS score. Scale to assess the risk of progression to late AMD (neovascular or atrophic in one or both eyes) for patients included in AREDS.

2. ARM classification

1) Retinal pigment epithelium changes

RPE changes are considered to be characteristic of early AMD and are defined as hyperpigmentation and/or hypopigmentation in the macular area, two disc diameters from the fovea, with or without drusen and with no other known retinal disease. Numerous studies[7,8] show that there is a high risk of these RPE changes progressing towards late AMD, therefore these RPE changes require a precise, regular monitoring in order to identifiy complications as early as possible (Figure 1).

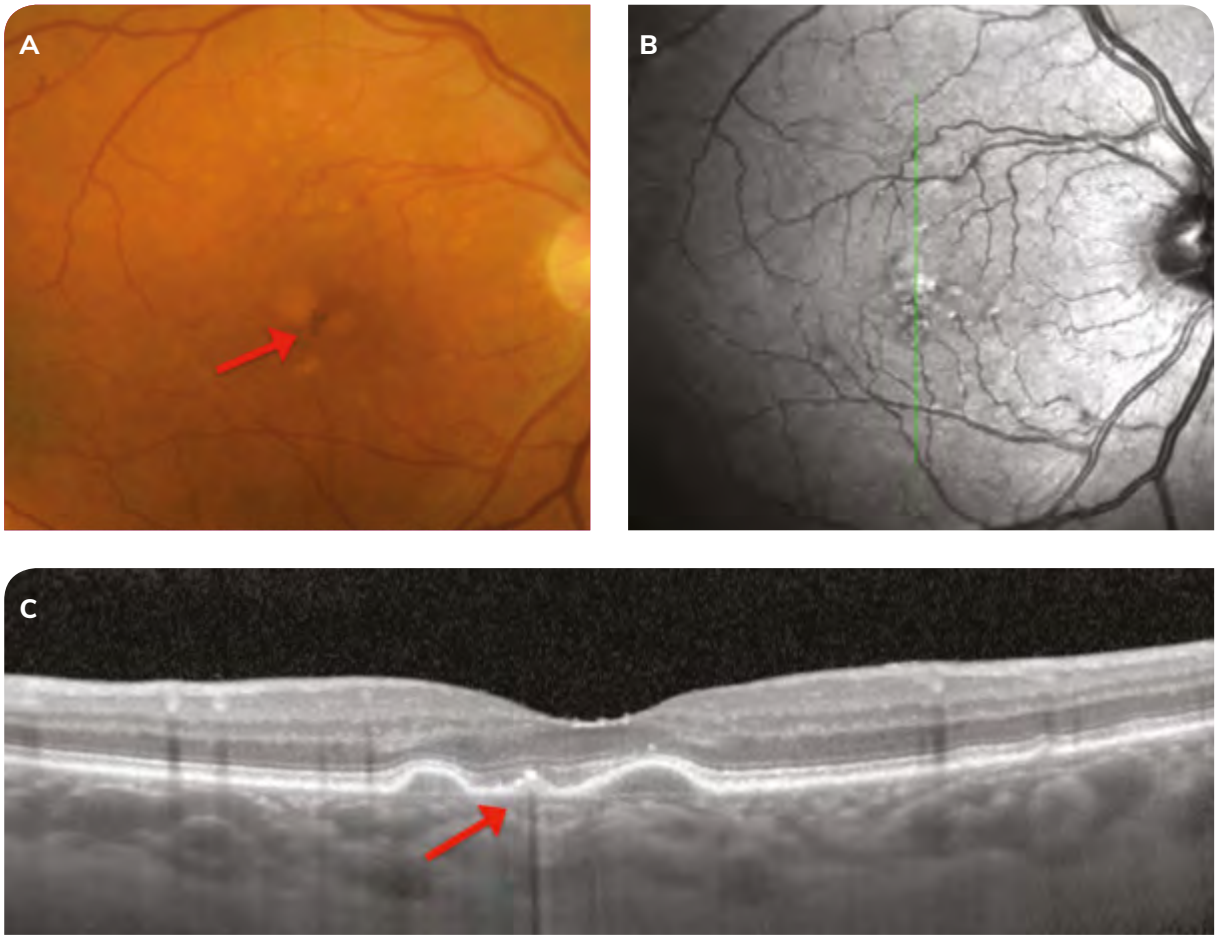

Fig. 1: Retinal pigment epithelium changes.

Colour photograph (A): pigment migration visible in the form of a pigmented lesion (RPE clumps) in the central area, associated with soft drusen. SD-OCT with corresponding infrared image, vertical B-scan (B, C), showing a focal hyperreflective visibility of the RPE, associated with a posterior shadowing corresponding to the hyperpigmentation area (red arrow). The B-scan also reveals dome-shaped elevations of the RPE corresponding to soft drusen.

2) Hard drusen

Hard drusen are found in 25 to 50% of people aged over 50. On fundus examination, these hard drusen are round, small (diameter < 63 µm) and yellowish, with distinct edges. There are often numerous and they are usually found in the temporal foveal area.

In fluorescein angiography they appear hyperfluorescent from the early frames of the angiogram, due to a window effect. In SD-OCT, they create very small elevations in the RPE (Figure 2). They can merge together and develop into larger drusen, and may be associated with soft drusen or reticular pseudodrusen. Complications within time are relatively rare and happen at a late stage[9] when the hard drusen are isolated; they are generally stable.

Fig. 2: Hard drusen.

Colour photograph (A) showing round, regular, small (< 63 µm), yellowish hard drusen (white arrow). Fluorescein angiography (B): the hard drusen appear hyperfluorescent from the beginning of the sequence and are easier to see than on the colour photograph (white arrow). SD-OCT (C): slight RPE elevations indicating hard drusen (white circle).

3) Soft drusen

Soft drusen are larger (diameter > 63 µm), with blurred edges and an irregular shape, and are paler than hard drusen. They are often associated with pigment migration.

In fluorescein angiography, they are hypofluorescent during the early phase, filling throughout the examination and becoming hyperfluorescent in the late frames. They remain hypofluorescent in all phases of ICG angiography. OCT reveals multiple dome-shaped elevations in the RPE. Soft drusen are moderately reflective and have a bumpy aspect. The external limiting membrane and the ellipsoid line often remain visible (Figure 3A).

Confluent sof drusen result in drusenoid pigment epithelial detachments (PED), with a hyperreflective content. Over several years, drusenoid PEDs can develop into extensive areas of atrophy, as the PED gradually subsides (Figure 3B).

Soft drusen eventually progress to late AMD in around 30% of cases[9]. In rare cases, soft drusen can regress or even calcify, resulting in ghost drusen associated with underlying atrophy.

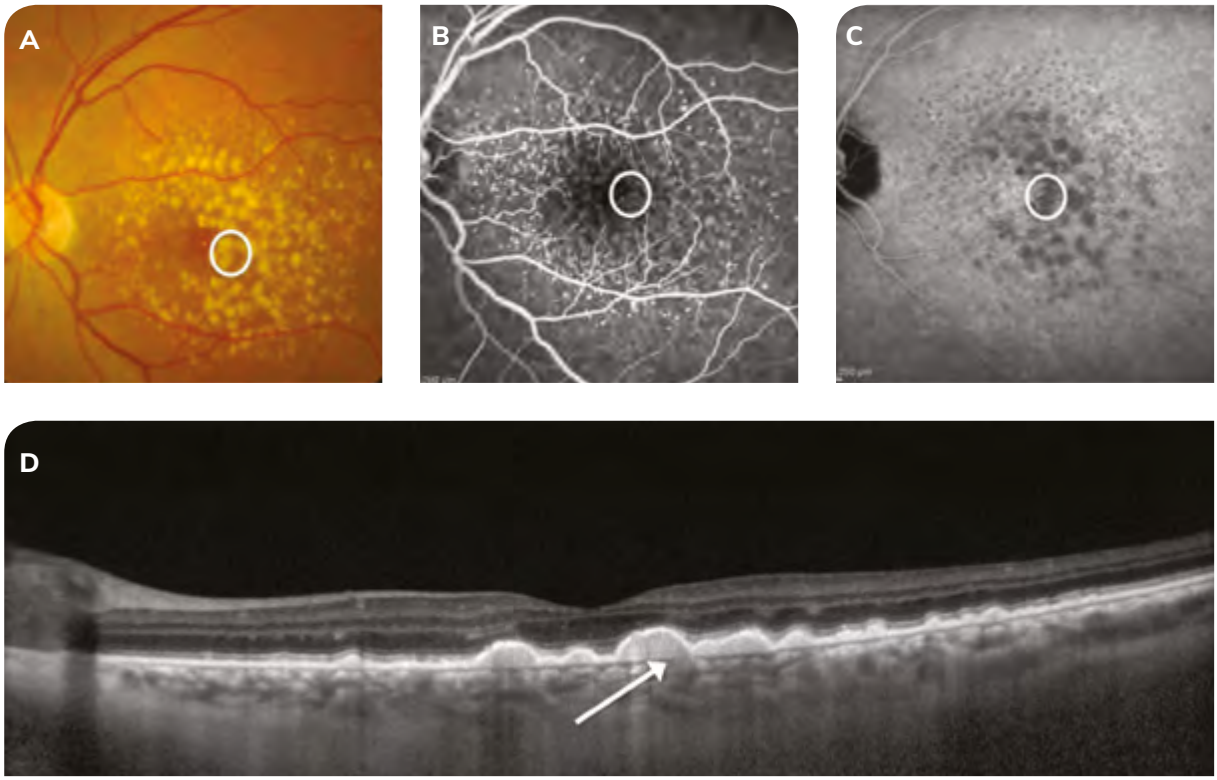

Fig. 3: Soft drusen.

Colour photograph (A) showing numerous lesions with blurred edges, paler than the hard drusen, measuring over 125 µm and located in the macular area, corresponding to soft drusen (white circle). Fluorescein angiography (B), intermediate frame, showing progressive and delayed staining of the soft drusen (white circle), with no leakage. Late frame of ICGA (C): the soft drusen remain hypofluorescent (white circle). SD-OCT scan through the soft drusen (D): multiple dome-shaped RPE elevations (white arrow) with homogeneous hyperreflective content. The external limiting membrane and ellipsoid line remain visible in this case, with no associated exudation.

4) Reticular pseudodrusen

Reticular pseudodrusen, or blue drusen, were first described by the Ophthalmology Créteil team[10]. These drusen are yellowish in colour and generally found on the superior temporal arcades. However, they may also appear in the macula and retinal periphery and are “cerebroid” in appearance (Figure 4).

They are referred to as “blue” drusen because they are easily visible on fundus photographs with blue illumination. In SD-OCT, they are hyperreflective. They can affect the ellipsoid zone and are associated with thinning of the choroid in EDI-OCT.

These deposits are found above the RPE, unlike soft drusen, which are located below it. In fluorescein angiography, they are either slightly visible or hypofluorescent. In the late phase of ICG angiography, they appear as a hypofluorescent network.

Four different stages have been described in SD-OCT[11]. During the early stages (stages 1 and 2), the hyperreflective material located above the RPE thickens over time, and during the advanced stages (stages 3 and 4), the material breaks up, resulting in discontinuity or total absence of the ellipsoid line. Several studies have found that reticular pseudodrusen were associated to a high risk of progression to atrophic or exudative AMD[12,13], and in particular to type 3 neovascularization.

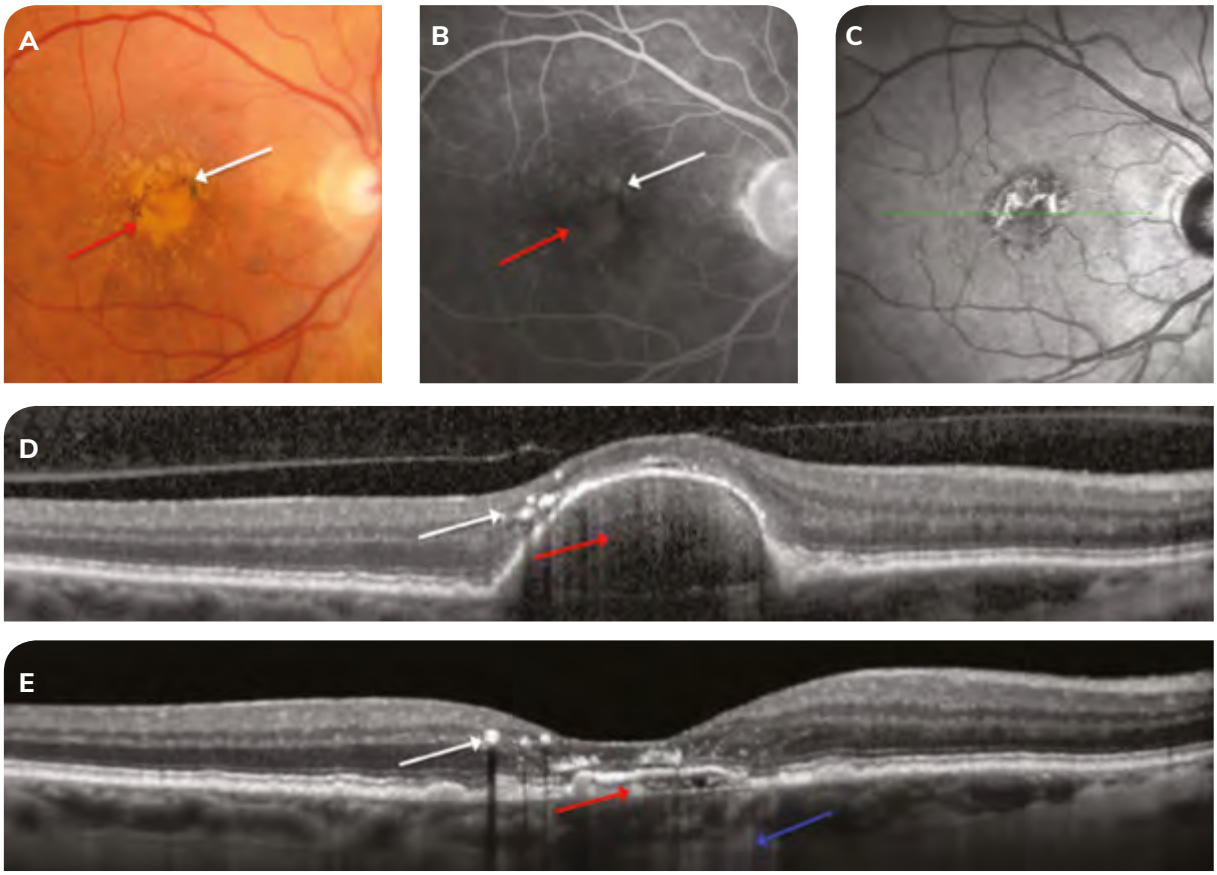

Fig. 4: Drusenoid pigment epithelial detachment and progression.

Colour photograph (A): Lesion measuring approximately one disc diameter causing a drusenoid PED (red arrow) due to confluent drusen, with pigment migration (white arrow). Intermediate frame of fluorescein angiography (B) showing a blocking effect caused by the pigment migration (white arrow), contrasting with the progressive hyperfluorescence of the drusenoid PED (red arrow). Infrared image and corresponding SD-OCT scan (C, D) showing considerable RPE elevation, resulting in a drusenoid PED (red arrow) with pigment migration (white arrow). Two years later (E), the drusenoid PED has subsided and atrophy is starting to develop (blue arrow), marked by the posterior hyperreflectivity.

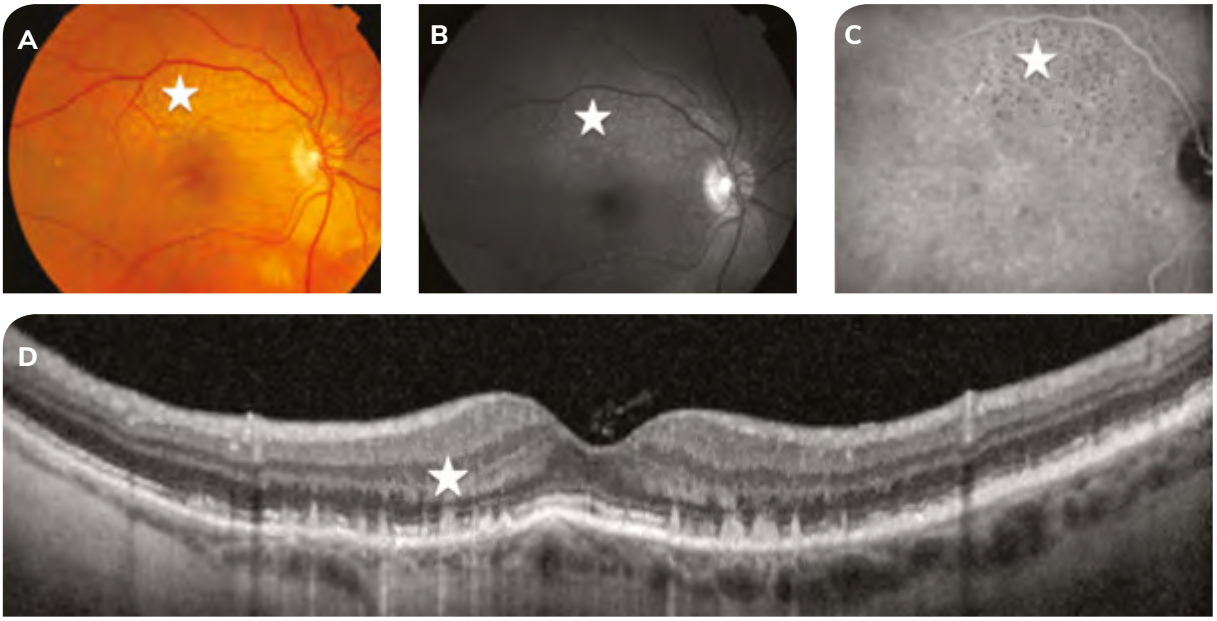

Fig. 5A: Reticular pseudodrusen.

The colour photograph (A) shows yellowish cerebroid pseudodrusen located on the superior temporal arcades (white star). The pseudodrusen are easier to see in the blue-light photograph (B) (white star). In ICGA (C), reticular pseudodrusen appear hypofluorescent during the late frame (white star). SD-OCT (D): the pseudodrusen are hyperreflective (white star), dense, irregular, fusiform in appearance and located above the RPE, meaning they could impact on the ellipsoid zone and the photoreceptors. Blue drusen are associated with thinning of the choroid in EDI-OCT.

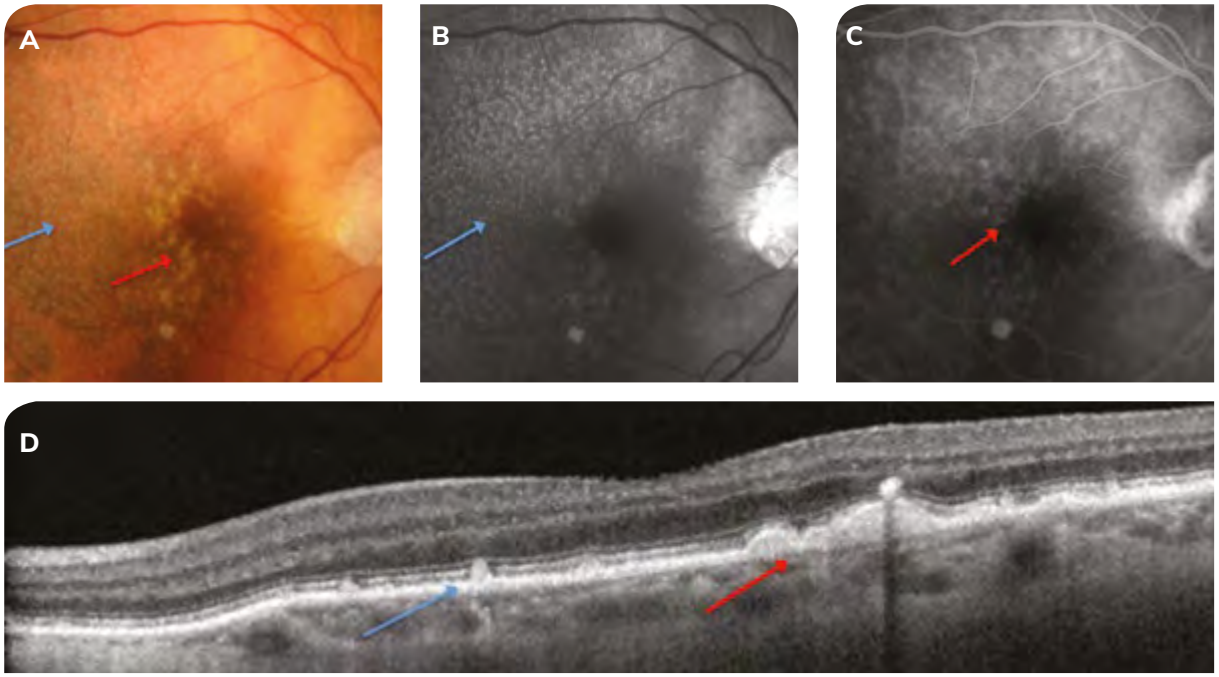

Fig. 5B: Soft drusen and reticular pseudodrusen.

The colour photograph (A) shows yellowish cerebroid reticular pseudodrusen, predominantly in the temporal region (blue arrow) of the macula, associated with larger, round, yellowish deposits corresponding to soft drusen (red arrow). The pseudodrusen are easier to see in the blue-light photo (B) (blue arrow). In the intermediate frame of fluorescein angiography (C), the soft drusen are hyperfluorescent while the reticular pseudodrusen drusen are hypofluorescent (red arrow). In SD-OCT (D), the pseudodrusen are dense, hyperreflective, irregular and fusiform in appearance, and located above the RPE (blue arrow), in contrast to the soft drusen that appear as dome-shaped RPE elevations with homogeneous hyperreflective content below the RPE (red arrow).

5) Cuticular drusen

Cuticular drusen were first described in 1977 by D. Gass (Figure 6). These drusen are round, numerous, small (25–75 microns) deposits concentrated primarily in the posterior pole, occasionally appearing in the retinal periphery. They appear in younger patients than those who have AMD, with an average age of 57 years. They carry a risk of developing into late AMD after the age of 70.

In angiography images, they have a characteristic "stars in the sky" appearance. Cuticular drusen are located between the RPE and Bruch's membrane. In OCT images, they have a very typical sawtooth appearance, with a slight or mound-shaped elevation. The choroid displays typical "bar code" reflectivity[14], with alternating areas of hyper- and hyporeflectivity corresponding to the drusen.

They may be associated to vitelliform material, deposits or choroidal neovascularization (usually type 1), as well as atrophy.

While their ultrastructural characteristics are similar to those of hard drusen, they are closer to soft drusen in terms of their life cycle and macular complications.

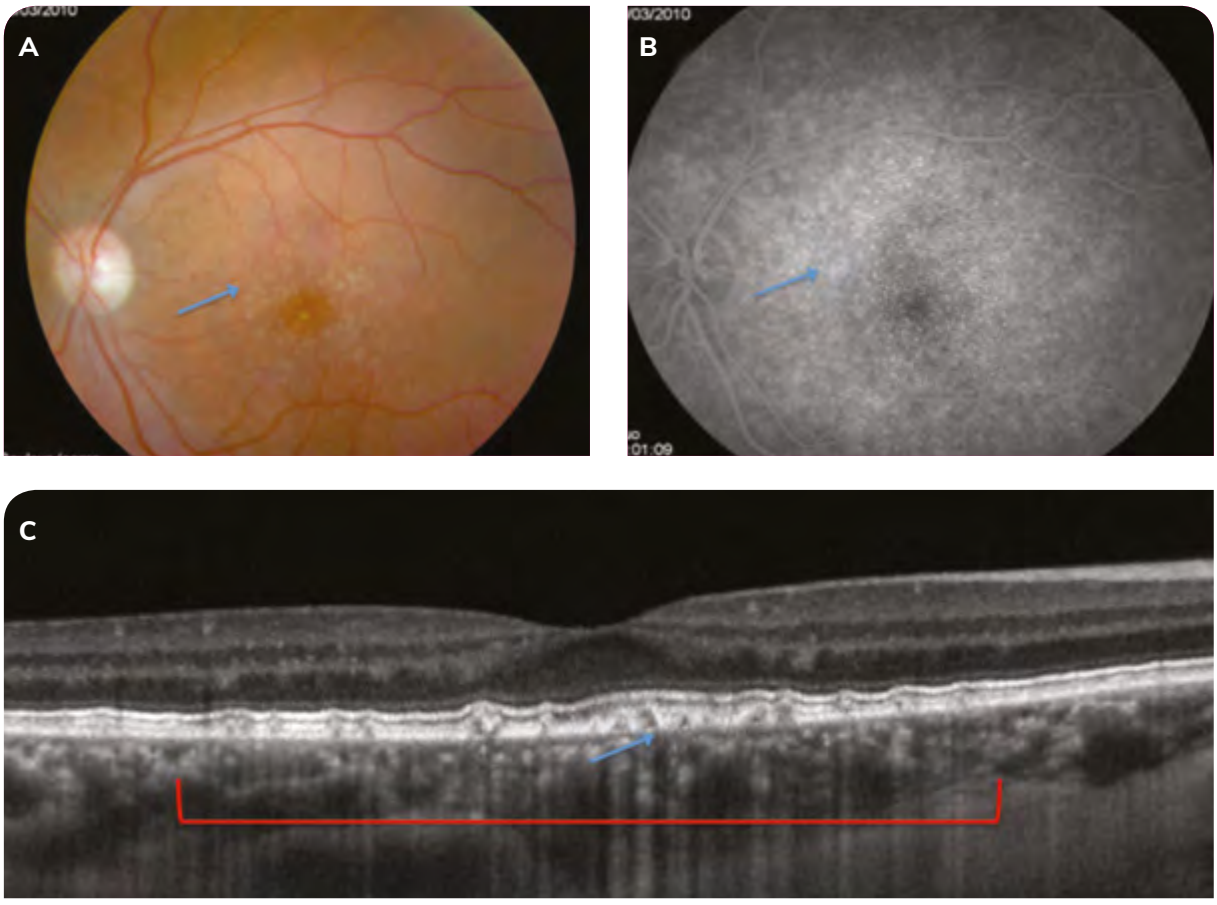

Fig. 6: Cuticular drusen.

Colour photograph (A): Numerous round, yellowish deposits (25–75 microns) concentrated in the macula, corresponding to cuticular drusen (blue arrow). Fluorescein angiography (B) shows the characteristic "stars in the sky" appearance, with a greater number of lesions than in the colour photograph (blue arrow). SD-OCT (C): saw-tooth pattern with slight or mound-shaped elevation (blue arrow) resulting in a "bar code" appearance (red parenthesis), with alternating areas of hyper- and hyporeflectivity corresponding to the drusen.

6) “Calcified”, “regressing” or “refractile” drusen

Calcified drusen were first described by Gass in 1973 and were initially called “refractile” due to their appearance in the fundus. More recently, the term “calcified drusen” has been replaced by “regressing drusen”[15].

Drusen are deposits of extracellular material rich in lipids (cholesterol) found between the basal membrane of the RPE and the internal layer of Bruch’s membrane. Several phagocytic processes have been observed, resulting in regression of the drusen in terms of size. Regressing drusen are deposits of calcified lipid material (cholesterol) that has not been ingested by macrophages, characterized by the presence of an intensely hyperreflective band in the choroid in SD-OCT images (Figure 7).

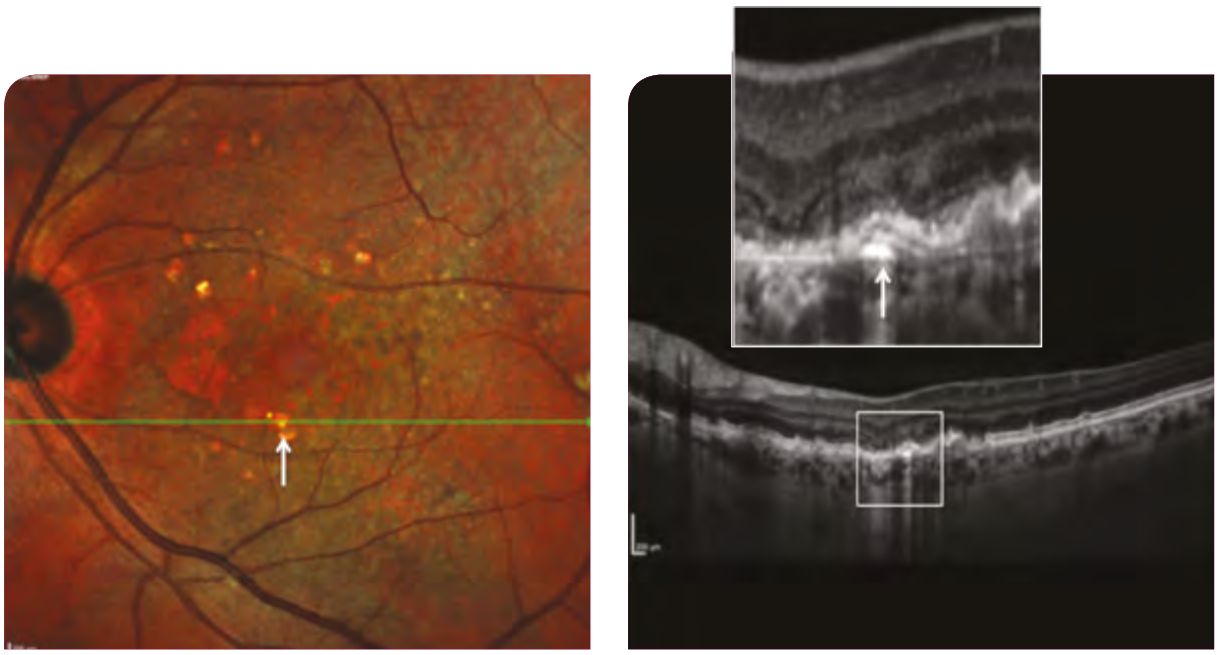

Fig. 7: Regressing calcified drusen.

Multicolor® photograph showing a calcified drusen (white arrow) with a refringent appearance, with the OCT B-scan through the lesion. The SD-OCT shows a band of intense hyperreflectivity corresponding to lipid material (cholesterol) that has not undergone phagocytosis (white arrow).

7) Ghost drusen

Ghost drusen[16] were first described by the Ophthalmology Créteil team and appear in OCT images as dense, hyperreflective pyramidal structures located above the RPE. They are associated with atrophic AMD (geographic atrophy). They are hard to visualize in fluorescein angiography and appear isofluorescent or hyperfluorescent on a background of atrophy (Figure 8). In a recent study[17] analysing the origins of ghost drusen, the authors found that soft drusen were initially present in a small number of cases.

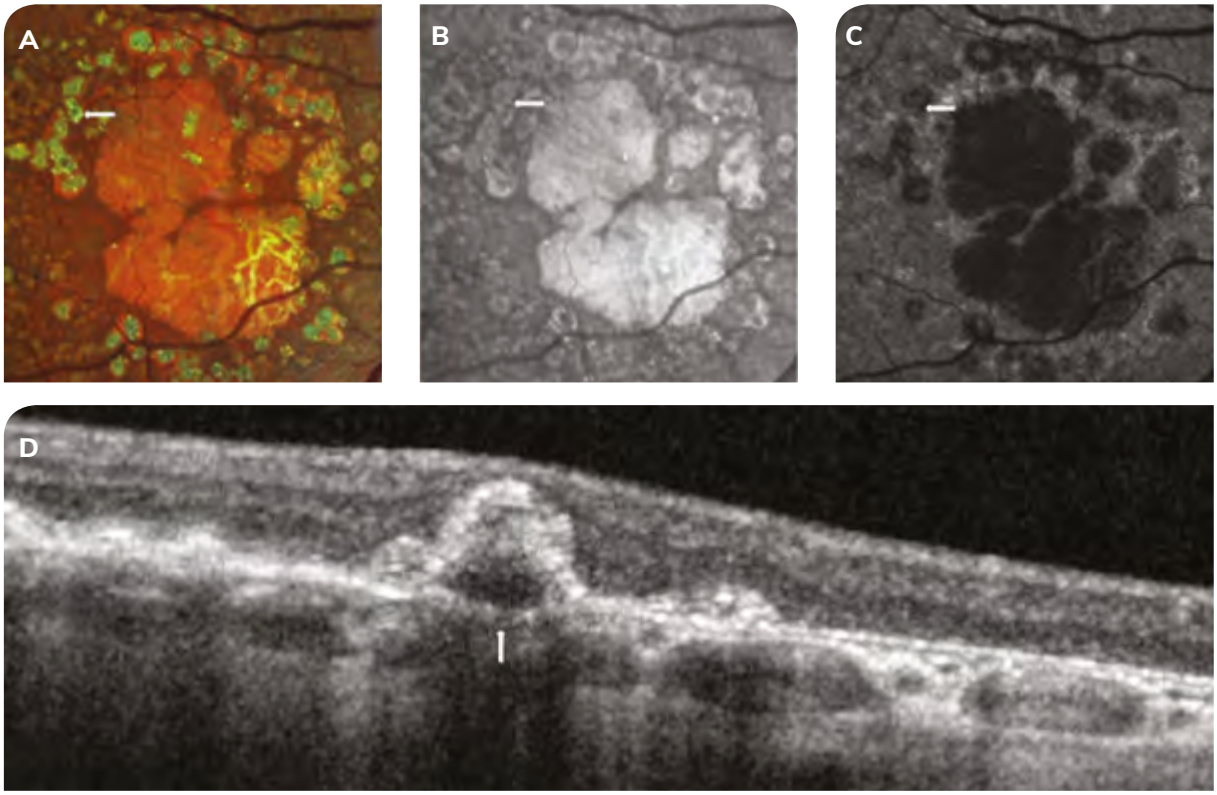

Fig. 8: Ghost drusen.

Multicolor® photograph (A): ghost drusen located primarily around the areas of atrophy (white arrow). Infrared photograph (B): hyporeflective lesion surrounded by a hyperreflective area with several small hyperreflective dots indicating the location of the ghost drusen (white arrow). Fundus autofluorescence image (C): the ghost drusen (white arrow) appear relatively hyperautofluorescent compared to the superior adjacent atrophy. SD-OCT (D): hyperreflective pyramid structure characterised by a hyporeflective centre (white arrow).

3. Age-related maculopathy and OCT-angiography

OCT-angiography (OCTA) is a non-invasive imaging technique that enables selective visualisation of the retinal and choroidal circulation. In most cases, soft drusen cause signal attenuation in the choriocapillaris and segmentation errors can occur, depending on the morphology of the drusen[18] (Figure 9). In terms of reticular pseudodrusen, Alten *et al.*[19] recently described a significant reduction in vascular density and the decorrelation signal index in the choriocapillaris, suggestive of functional impairment of the choriocapillaris, with statistically larger areas of non-perfusion than in the absence of pseudodrusen[20].

OCTA offers a new way of assessing ARM signs and symptoms, which can sometimes enable earlier detection of patients who are at risk of developing a late form of the disease. "Vascularised" drusen were described by Querques *et al.*[21], who hypothesized that they are a form of type 1 neovascularization mimiking soft drusen (Figure 9). A recent study by the Tufts team found this type of drusen in 9.4% of eyes with intermediate AMD[22], which raises questions about the frequency of monitoring for these patients, as well as their treatment. Although drusen and artefacts can have a blocking effect/signal attenuation on the choriocapillaris, OCTA can provide useful information on non-perfusion in the choriocapillaris and possible neovascularization of these lesions.

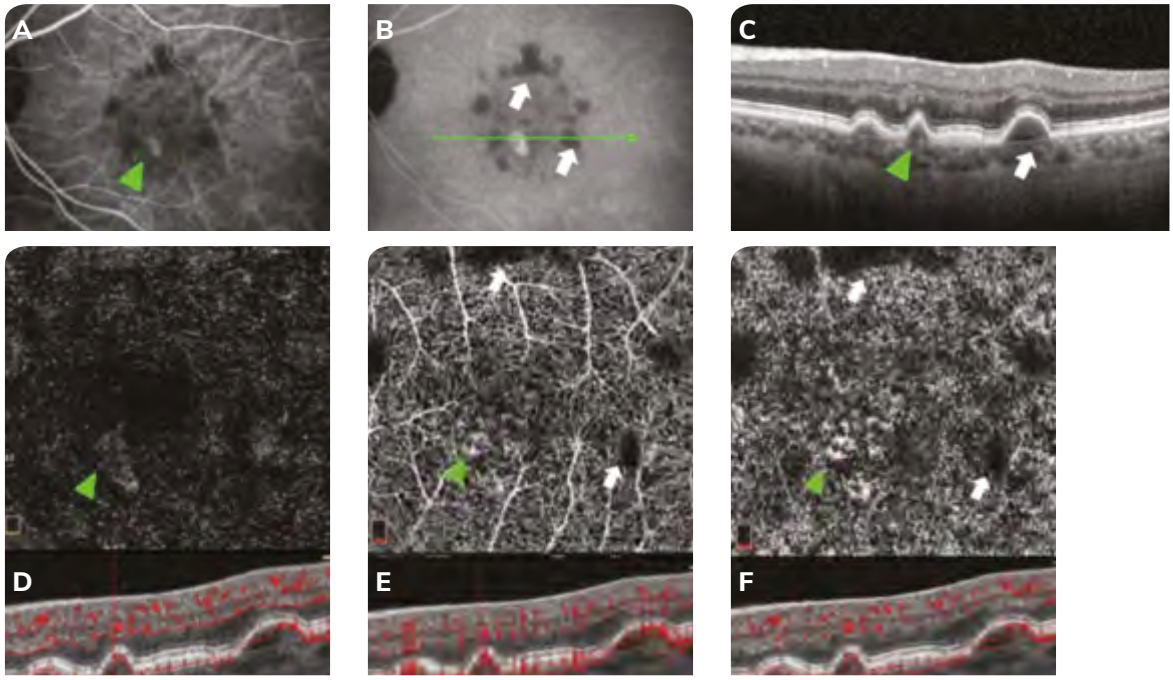

Fig. 9: Multimodal imaging of a male patient with soft drusen and a vascularised drusen.

ICG angiography, early frame (A) and late frame (B). A hyperfluorescent lesion can be seen in the early frame (green arrowhead), corresponding to a plaque in the late frame of the examination. Multiple soft drusen can be seen in the form of early and late hypofluorescence (white arrow). SD-OCT (C) shows drusenoid RPE elevations corresponding to the two observed lesions. OCTA (D) reveals a discrete high flow lesion in the outer retina slab (green arrowhead). In the choriocapillaris slab with projection artefacts (E) and without projection artefacts (F), the high flow lesion is visible and corresponds to a vascularised drusen. However, the choriocapillaris signal is attenuated by the presence of soft drusen (white arrow).

Conclusion

Screening for ARM is an essential part of any eye examination in patients aged 55 years and over, based on dilated fundus examination or color fundus photography.

There are several types of drusen that carry a risk of progression to late AMD. The risk of neovascular complication is very low with hard drusen. However, soft drusen are more likely to develop into choroidal neovascularization.

OCT is an essential examination for confirming a diagnosis of ARM and ruling out neovascular activity. If progression to exudative AMD is suspected, angiography becomes less useful, as OCTA can be carried out to provide valuable information on the whether neovascularization is present.

References

1. Klein R, Klein BEk, Linton KLP (1992). Prevalence of Age-related Maculopathy-The Beaver Dam Eye Study. Ophthalmology 99(6): 933-943.

2. Ferris FL, Davis MD, Clemons TE, *et al.* A simplified severity scale for age-related macular degeneration: AREDS Report No. 18. Arch Ophthalmol Chic Ill 1960. 2005;123(11):1570–4.

3. Li C-M, Clark ME, Chimento MF, Curcio CA. Apolipoprotein localization in isolated drusen and retinal apolipoprotein gene expression. Invest Ophthalmol Vis Sci. 2006;47(7):3119-3128.

4. Haimovici R, Gantz DL, Rumelt S, *et al.* The lipid composition of drusen, Bruch's membrane, and sclera by hot stage polarizing light microscopy. Invest Ophthalmol Vis Sci. 2001;42(7):1592-1599.

5. Dentchev T, Milam AH, Lee VM-Y, *et al.* Amyloid-beta is found in drusen from some age-related macular degeneration retinas, but not in drusen from normal retinas. Mol Vis. 2003;9:184-190.

6. Curcio CA, Messinger JD, Sloan KR, *et al.* Subretinal Drusenoid Deposits In Non-Neovascular Age-Related Macular Degeneration: Morphology, Prevalence, Topography, And Biogenesis Model. Retina. 2013;33(2) : 265-76.

7. Klein R, Klein BEk, Linton KLP. Prevalence of Age-related Maculopathy-The Beaver Dam Eye Study. Ophthalmology. 1992 ;99(6): 933-943.

8. A Randomized, Placebo-Controlled, Clinical Trial of High-Dose Supplementation With Vitamins C and E, Beta Carotene, and Zinc for Age-Related Macular Degeneration and Vision Loss. Arch Ophthalmol. 2001;119(10):1417-1436.

9. Klein R, Klein BEK, Knudtson MD, *et al.* Fifteen-year cumulative incidence of age-related macular degeneration: the Beaver Dam Eye Study. Ophthalmology. 2007;114(2):253-262.

10. Mimoun G, Soubrane G, Coscas G. Macular drusen. J Fr Ophtalmol. 1990;13(10):511 30.

11. Querques G, Canouï-Poitrine F, Coscas F, *et al.* Analysis of progression of reticular pseudo-drusen by spectral domain-optical coherence tomography. Invest Ophthalmol Vis Sci. 2012;53(3):1264-1270.

12. Zweifel SA, Imamura Y, Spaide TC, *et al.* Prevalence and significance of subretinal drusenoid deposits (reticular pseudo-drusen) in age-related macular degeneration. Ophthalmol. 2010;117(9):1775-1781.

13. Klein R, Meuer SM, Knudtson MD, *et al.* The epidemiology of retinal reticular drusen. Am J Ophthalmol. 2008;145(2):317-326.

14. Balaratnasingam C, Cherepanoff S, Dolz-Marco R, *et al.* Cuticular Drusen: Clinical Phenotypes and Natural History Defined Using Multimodal Imaging. Ophthalmology. 2018;125(1):100-118.

15. Querques G, Georges A, Ben Moussa N, *et al.* Appearance of regressing drusen on optical coherence tomography in age-related macular degeneration. Ophthalmol. 2014;121(1):173-179.

16. Bonnet C, Querques G, Zerbib J, *et al.* Hyperreflective pyramidal structures on optical coherence tomography in geographic atrophy areas. Retina. 2014;34(8):1524-30.

17. Bottin C., Zambrowski O., Querques G, *et al.* Origins of Ghost Drusen: A follow-up Analysis. Ophthalmology @ Point of Care.

18. Alten F, Lauermann JL, Clemens CR, *et al.* Signal reduction in choriocapillaris and segmentation errors in spectral domain OCT angiography caused by soft drusen. Graefes Arch Clin Exp Ophthalmol. 2017;255(12):2347-2355.

19. Alten F, Heiduschka P, Clemens CR, Eter N. Exploring choriocapillaris under reticular pseudo-drusen using OCT-Angiography. Graefes Arch Clin Exp Ophthalmol. 2016;254(11):2165-2173.

20. Nesper PL, Soetikno BT, Fawzi AA. Choriocapillaris Nonperfusion is Associated With Poor Visual Acuity in Eyes With Reticular Pseudo-drusen. Am J Ophthalmol. 2017;174:42-55.

21. Querques G, Souied EH. Vascularized Drusen: Slowly Progressive Type 1 Neovascularization Mimicking Drusenoid Retinal Pigment Epithelium Elevation. Retina. 2015;35(12):2433-9.

22. Chris Or, Jeffrey Heier, Namrata Saroj, A. Yasin Alibhai, Nadia Waheed. Incidence of Vascularized Drusen in Non-Exudative Age-related Macular Degeneration using Spectral Domain Optical Coherence Tomography (OCT) Angiography. Poster B0328 ARVO 2018.

4

Type 1 neovascularization

Type 1 neovascularization

PART 1:

Type 1 choroidal neovascularization

Jean-Louis Bacquet, Alexandra Mouallem-Bézière

1. Definition

Type 1 or sub-RPE neovascularization is by far the most prevalent subtype in exudative AMD, ranging from 60% to 85% at diagnosis depending on the series. It is defined as neovascular growth below the retinal pigment epithelium (RPE). First described in 1987 and classified by Gass in 1994, it differs from type 2 neovascularization, which occurs above the RPE ("visible" neovascularization), and from type 3 neovascularization, which occurs in the retina itself (from the deep retinal capillary plexus), meaning the natural history and origin of type 3 is highly debated as to its occurence through chorioretinal anastomosis, retinochoroidal anastomosis or intraretinal proliferation.

Some authors add to type 1 neovascularization the polypoidal choroidal vasculopathy (PCV) class, under the term "aneurysmal type 1 CNV" (Freund *et al.*). Since type 1 neovascularization was first defined based on its appearance in angiography images, the term "occult neovascularization" is sometimes used instead, in contrast to "visible" or "classic" neovascularization located above the RPE (type 2).

Type 1 neovascularization, given its aspect in fluorescein angiography, is also frequently referred to in the literature as "ill-defined".

2. Epidemiology

According to a study conducted on a US population by Jung *et al.*, involving 374 patients (two thirds of whom 2/3 were female, 95% Caucasian), type 1 neovascularization accounts for 50% of all clinical forms of exudative AMD, compared to 12% for type 2 (visible) neovascularization and 28% type 3 intraretinal neovascularization. The remaining 10% comprises mixed forms that combine several subtypes. This was the first time an epidemiological study found such a low frequency of type 1 CNV and such a high proportion of type 3.

3. Clinical presentation

Type 1 neovascularization should be the first diagnosis considered when an older patient presents with an acute or subacute macular syndrome. The signs and symptoms may include:

- Reduced visual acuity, primarily relating to near vision
- Metamorphopsia
- Scotoma/microscotoma
- Micropsia
- Dyschromatopsia
- Reduced contrast sensitivity.

These signs may be present to varying degrees and some may be absent. The patient may have very few symptoms or be asymptomatic. Compared to type 2 (visible) neovascularization, the functional impact is more insidious, developing gradually, and the patient may be unable to pinpoint when it started.

It is possible to observe signs of neovascularization in the fundus, including retinal oedema, serous retinal detachment, macular haemorrhage and exudates. These are more common than with type 2 (visible) neovascularization. However, these signs are often inconspicuous, and nonspecific. Cystoid macular oedema or white retinal oedema is unusual in the early stages, but may be found if the diagnosis is made later on.

Precursors to all forms of AMD, such as drusen and/or reticular pseudodrusen, will of course need to be monitored for, along with retinal pigment epithelium defects (migrations or changes).

4. Symptomatology: different type 1 CNV phenotypes

With high-resolution diagnostic tools at our disposal, we can characterise several phenotypes of sub-RPE choroidal neovascularization based on imaging.

It should be noted that in France, we tend to separate “vascularised pigment epithelial detachment” (v-PED) from other forms of neovascularization. This is not generally the case in English-language publications, since “vascularised PED” simply refers to a vascularised elevation of the RPE. However, vascularised PED and type 1 CNV can have a different prognosis and therapeutic response: v-PED responds somewhat unpredictably to anti-VEGF treatment, particularly in terms of the risk of RPE tears.

Under biomicroscopy, vascularised PED appears in relief as a yellow-orange lesion. This lesion is typically hyperfluorescent in fluorescein angiography, while OCT displays heterogeneous reflectivity below the RPE, which can be associated with hyporeflective subretinal fluid.

These images enable us to identify multiple subtypes of type 1 CNV, which will be described in the next few chapters (Figure 1).

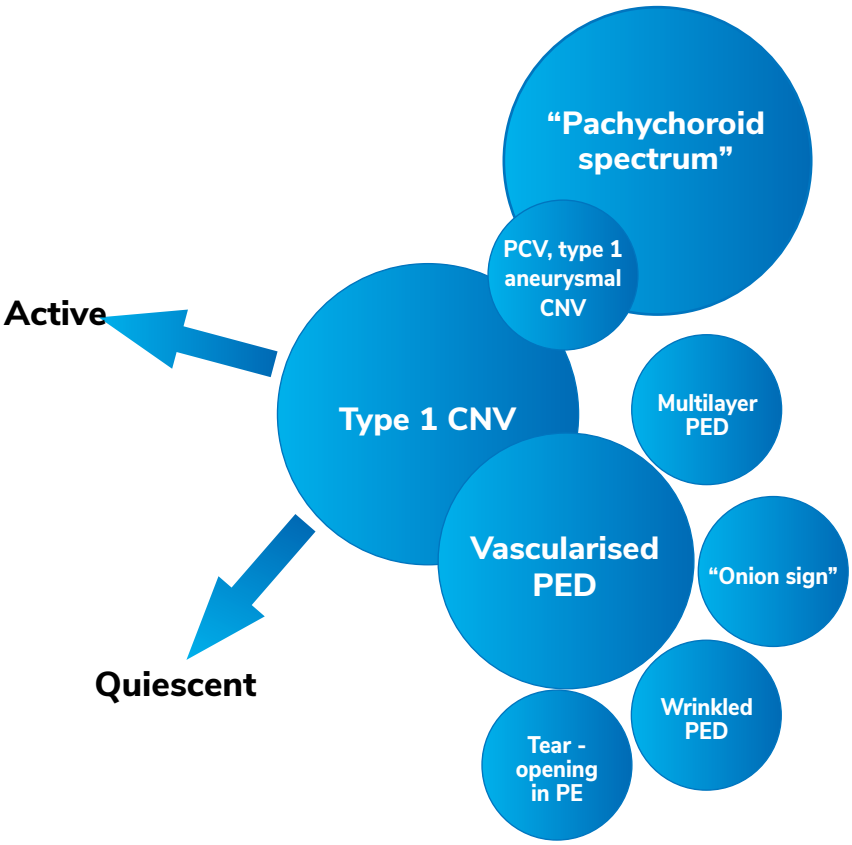

Fig. 1: Type 1 choroidal neovascularisation presentation and subtypes

5. Physiopathology

This form of neovascularization is **choroidal** in origin. The currently accepted theory is that vascular proliferation (angiogenesis) causes the Bruch's membrane to break in a patient who has drusen and is genetically predisposed.

The role of intraretinal inflammation (potentially visible in images as hyperreflective dots) and macrophages is increasingly being demonstrated, particularly by Sennlaub *et al.* The strong genetic association with mutations in certain complement factors reinforces this hypothesis.

6. Imaging

First described using angiography and histology, and later by OCT B-scans and, most recently, by OCTA, the various clinical forms and types of neovascularization now play a crucial role in characterizing patients suffering from exudative AMD ("neovascular phenotype").

The main imaging characteristics of type 1 choroidal neovascularization are summarised below. Since it is important to know where the CNV is located in order to interpret imaging examinations, note that the biological substrate in the images is the location of the neovascularization: the new vessels **emerge from the choroid and extend under the RPE**, detaching the RPE and the overlying neurosensory retina (PED, SRD) (Figure 2).

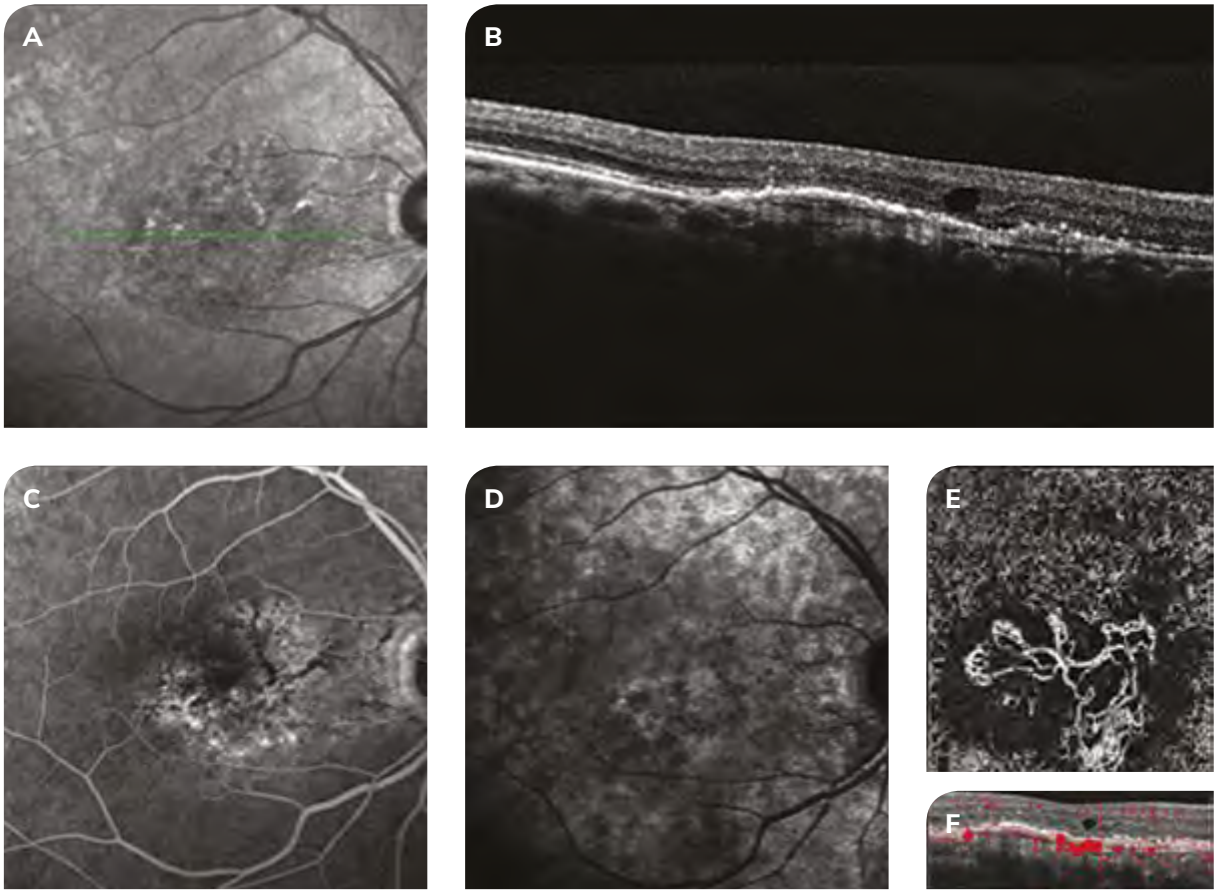

Fig. 2: Multimodal imaging of type 1 choroidal neovascularisation.
A: Heterogeneous granular hyper- and hyporeflectivities in an infrared photograph.
B: OCT-SD showing subretinal and intraretinal fluid, associated with double-bump PED and intraretinal hyperreflective dots. An area of subsidence can be seen in the external limiting membrane, indicative of focal atrophy of the photoreceptors.
C: Intermediate-phase fluorescein angiography: heterogeneous perifoveal hyperfluorescence ("pinpoints") associated with linear hypofluorescence caused by pigment migration and a subsequent blocking effect.
D: Late-phase indocyanine green angiography: discrete hyperfluorescence in the macular zone (plaque).
E: OCT-angiography showing the neovascular network and its ramifications.
F: Vascular flow within the PED next to the intraretinal space.

1) Fluorescein and indocyanine green angiography

In **fluorescein angiography**, type 1 neovascularization is ill-defined, inhomogeneous with early staining of the lesion, resulting in hyperfluorescent pinpoints. In the late frames of FA, the lesion increases in size and fluorescence, with blurred edges caused by leakage of the dye. This is known as late frame angiographic leakage.

This clinical form most commonly appears as a hyperfluorescent late plaque in late frame of **ICG angiography**.

2) SD-OCT

Depending on which stage of neovascularisation the patient is experiencing, OCT-SD shows RPE elevation or detachment in 98% of cases. This elevation is initially moderate, separated from Bruch's membrane by a hyporeflective space.

However, the PED can become very significant. Occult neovascularisation should be suspected if the RPE appears irregular, scalloped, fragmented or thickened.

This type of neovascularisation is often associated with signs of exudative activity, including:

- Subretinal fluid (or serous retinal detachment, SRD)
- Hyperreflective intraretinal dots (according to certain authors)
- Pre-epithelial hyperreflectivity
- Cystoid spaces in the neurosensory retina
- Diffuse or localised increase in retinal thickness.

3) OCT-angiography

OCTA now plays a major role in characterising type 1 CNV. Numerous studies evidence its sensitivity and call into question the pre-eminence of systematic angiography. The COFT-1 study found a sensitivity level of 85.7% for OCTA combined with structural B-mode OCT compared to the gold standard (angiography). OCTA alone was insufficiently sensitive (66.7%). The leading cause of false negatives is the neovascular signal being blocked by a PED, which can disrupt the automatic segmentation (Figure 3). OCTA therefore has a place within multimodal imaging, but is insufficient on its own to form a reliable diagnosis.

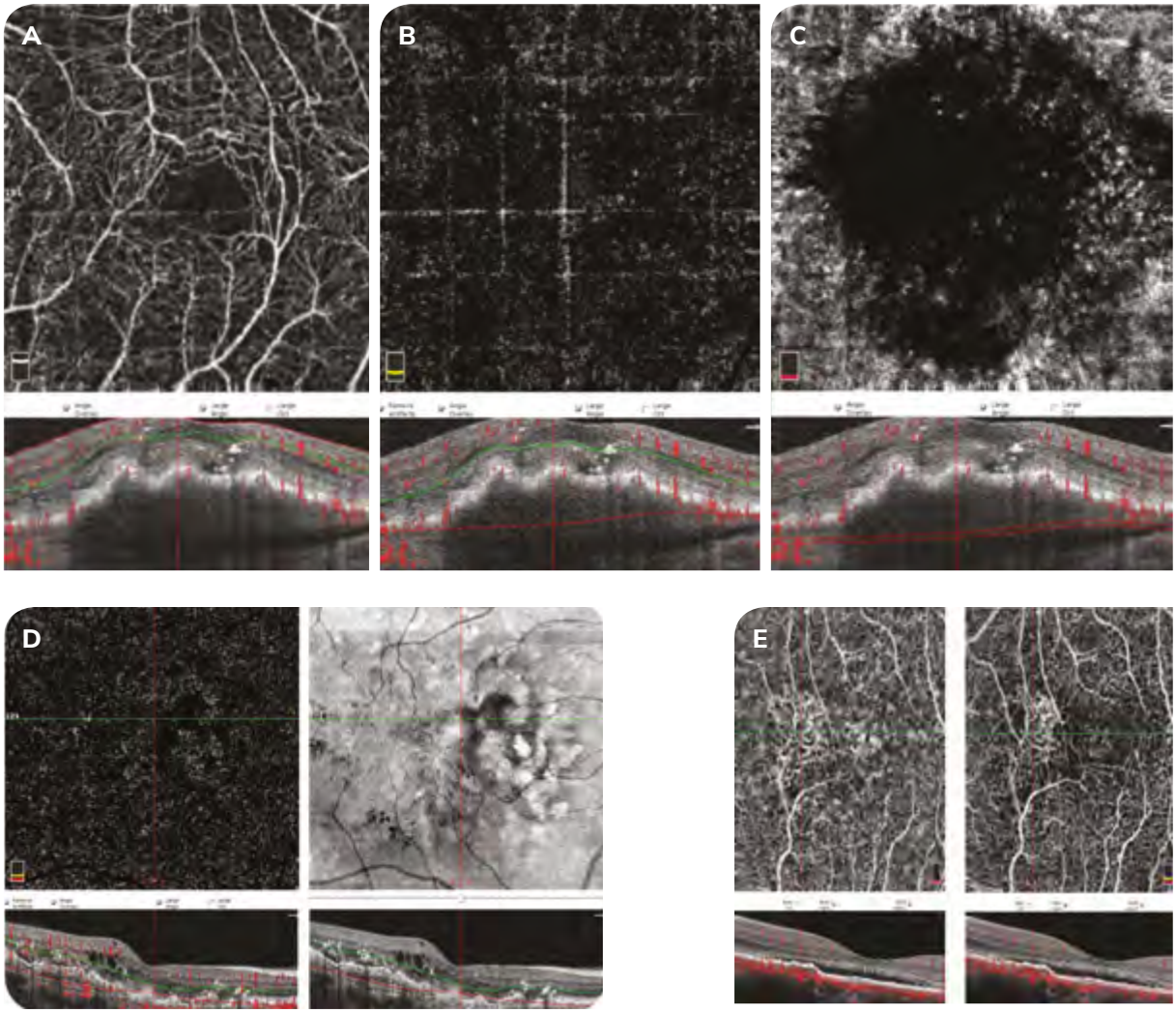

Fig. 3: A, B, C: Attempt to visualise a neovascular network within a very high v-PED using manual segmentation. The neovascularisation remains invisible.
D: Signs of exudative activity evident in structural OCT (intraretinal spaces, exudates, retinal thickening) with no neovascularisation visible in OCTA.
E: Part of the neovascular network is unblocked and the image becomes clearer following manual correction of the segmentation (left: automatic, right: manual).

7. Treatment

Patients with neovascular AMD and type 1 neovascularisation are today treated with intravitreal injections of angiogenesis inhibitors, preferably using the "Initiation – Observation – Individualisation" strategy recommended in the Fédération France Macula guidelines.

Comparative studies are still being conducted into the different treatment protocols ("pro re nata" or "PRN", "treat and extend", "observe and plan") and drugs used (anti-VEGF therapy). There is consensus around the use of three anti-VEGF injections at one-month intervals to initiate treatment for type 1 CNV, as per the French Society of Ophthalmology guidelines.

The prognosis for type 1 neovascularisation appears to be good, with a positive response to anti-VEGF therapy in general and less atrophy at follow-up compared to type 3 neovascularisation. Only a minority of patients (around 5%) require very few IVIs to maintain a "dry" retina (no exudative relapse). A larger proportion, with more severe forms, require monthly injections, sometimes for several years (around 10% of cases). Between these two extremes, the majority of patients with type 1 CNV require between six and eight IVIs on average, administered to an individualised schedule.

Dietary supplements rich in antioxidants, lutein, zeaxanthin and omega-3 have proven effective in terms of prevention (see dedicated chapter), particularly with regard to the contralateral eye.

8. Future developments

The treatment of type 1 CNV will certainly develop in the future, with:

- Ever more precise characterisation of each patient's neovascular phenotype
- Quantitative imaging analysis (in particular of the isolated neovascular network) to determine therapeutic response anatomically within the neovessels and not solely based on the retina
- The establishment of phenotype/genotype correlations
- Therapies adapted to the genetic profile and vascular phenotype of each patient.

References

Dansingani KK, Gal-Or O, Sadda SR, *et al.* Understanding aneurysmal Type 1 neovascularization (polypoidal choroidal vasculopathy): a lesson in the taxonomy of 'expanded spectra' - a review. Clin Exp Ophthalmol. 2017;46(2):189-200.

Jung J., Chen C., Mrejen S., *et al.* The Incidence of Neovascular Subtypes in Newly Diagnosed Neovascular Age-Related Macular Degeneration. American Journal of Ophthalmology, 2014, Pages 769-779.e2

Coscas G, De Benedetto U, Coscas F, *et al.* (2013) Hyperreflective dots: a new spectral-domain optical coherence tomography entity for follow-up and prognosis in exudative age-related macular degeneration. Int J Ophthalmol 229:32–7.

Ores R, Puche N, Querques G, *et al.* (2014) Gray hyper-reflective subretinal exudative lesions in exudative age-related macular degeneration. Am J Ophthalmol 158:354–61.

Kuehlewein L, Bansal M, Lenis LT, *et al.* (2015) Optical Coherence Tomography Angiography of Type 1 Neovascularization in Age-Related Macular Degeneration Am J Ophthalmol 160: 739–748.

Mrejen S, Sarraf D, Mukkamala SK, Freund KB (2013). Multimodal imaging of pigment epithelial detachment: a guide to evaluation. Retina 33:1735–1762.

Pang CE, Messinger JD, Zanzottera EC *et al.* (2015). The Onion Sign in Neovascular Age-Related Macular Degeneration Represents Cholesterol Crystals. Ophthalmology 122:2316-26.

Querques G, Capuano V, Costanzo E, *et al.* 2016. Retinal pigment epithelium aperture : A Previously Unreported Finding in the Evolution of Avascular Pigment Epithelium Detachment. Retina 36 Suppl 1:S65-S72.

Lam D, Semoun O, Blanco-Garavito R, *et al.* 2017, Wrinkled vascularized retinal pigment epithelium detachment prognosis after intravitreal anti-VEGF therapy. [Epub ahead of print]

Querques G, Srour M, Massmaba N, *et al.* 2013, Functional characterization and multimodal imaging of treatment-naïve quiescent choroidal neovascularization. Invest Ophthalmol Vis Sci 21;54:6886-92.

Semoun O, Cohen SY, Srour M, *et al.* Comité scientifique de la Fédération France Macula. Individualized management of patients with exudative AMD, IOI protocol: Injection-observational-individualization. J Fr Ophtalmol. 2017;40(3):169-176.

Inoue M, Jung JJ, Balaratnasingam C, *et al.* COFT-1 Study Group, 2016. A comparison between optical coherence tomography angiography and fluorescein angiography for the imaging of Type 1 neovascularization. Investig. Opthalmology Vis. Sci. 2016 ;57,314-323.

Type 1 neovascularisation

PART 2: *Quiescent* type 1 choroidal neovascularisation

Vittorio Capuano

1. Diagnosis

In 2013, Giuseppe Querques and the Ophthalmology Créteil team[1] described the functional and imaging characteristics and natural progression of *quiescent* type 1 choroidal neovascularisation (CNV) in the context of intermediate age-related macular degeneration (AMD) (Figure 1).

The imaging characteristics are as follows:

1. In **fluorescein angiography** (FA), *quiescent* CNV appears as hyperfluorescent lesions with distinct edges and no late-phase leakage

2. In **indocyanine green angiography** (ICG), *quiescent* CNV is characterised by a hyperfluorescent network in the early and intermediate phases, and a hypercyanescent plaque in the late phases (like the type 1 CNV described by D. Gass)[2]

3. In **optical coherence tomography** (OCT), *quiescent* CNV appears as a slight pigment epithelial detachment (PED) with a horizontal main axis, with no signs of subretinal or intraretinal exudation. This PED displays moderate reflectivity, allowing Bruch's membrane to be seen.

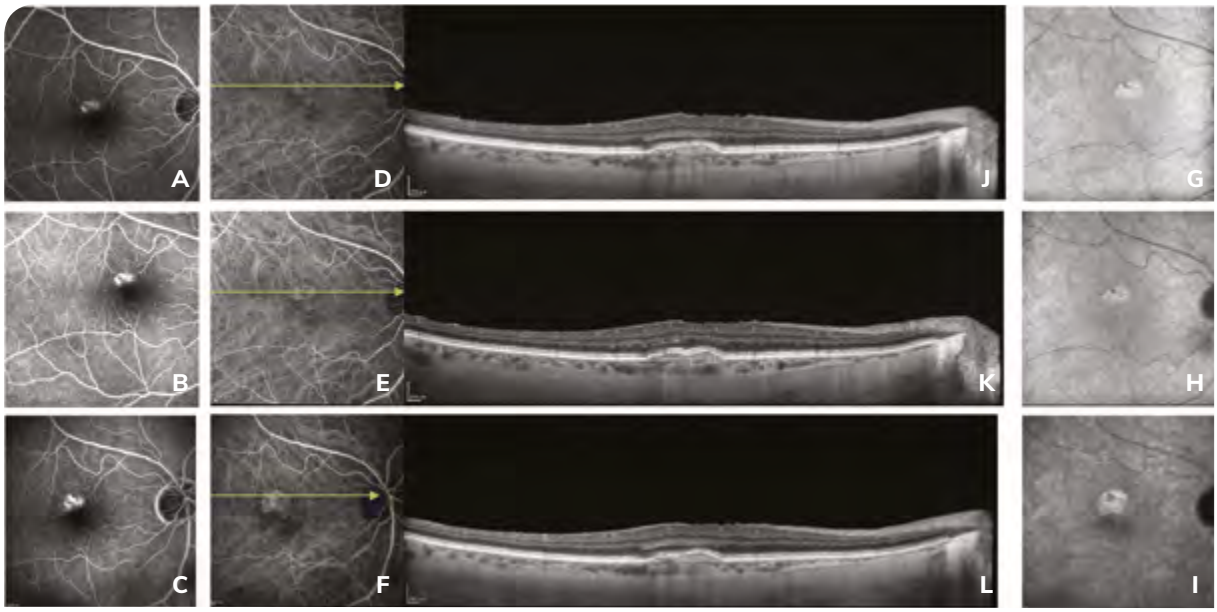

Fig. 1: Multimodal imaging of *quiescent* type 1 choroidal neovascularisation and progression over time.

In fluorescein angiography (A, F), the *quiescent* CNV appears as hyperfluorescent lesions with distinct edges and no late-phase leakage (A, B, C). In indocyanine green angiography (ICG), the *quiescent* CNV is characterised by a hyperfluorescent network in the early and intermediate phases (D, E, F), and a hyperfluorescent plaque in the late phases (G, H, I). In optical coherence tomography (OCT), the *quiescent* CNV appears as a slight pigment epithelial detachment (PED) with a horizontal main axis, with no signs of subretinal or intraretinal exudation. This PED displays moderate reflectivity, allowing Bruch's membrane to be seen (J, K, L) (HRA, Heidelberg Engineering).

Quiescent neovascularisation therefore has the following main functional characteristics:

1. No patient symptomatology

2. No changes revealed by microperimetry.

It has the following secondary characteristics:

1. No exudative signs for at least six months. However, certain authors[3] refer to *quiescent* CNV from the first observation, without waiting for this time to elapse

2. No history of eye treatments (anti-VEGF intravitreal injections, PDT, Argon laser).

Three years later, Palejwala et al.[4] published the first OCTA image of *quiescent* CNV. This non-invasive examination quickly became the *gold standard* for diagnosing and monitoring *quiescent* CNV. In 2016, Carnevali[5] calculated the sensitivity and specificity of OCTA (*non-invasive* examination) *versus* standard imaging techniques (FA, ICG, OCT) *(invasive* examination) used during the initial diagnosis, finding a detection rate of 81.8% and 100%, respectively. *Quiescent* CNV typically appears in **OCTA** as regular lesions with well defined edges and no peripheral arcades. A feeder vessel is a common finding (Figure 2).

Quiescent CNV is not exclusive to "intermediate" AMD; it has also been described with the late atrophic form[6] (Figures 3 and 4) and with pachychoroid diseases[7]. More recently, a case was reported with angioid streaks[8]. In these cases, the main and secondary characteristics are similar to those defined for AMD, but with certain peculiarities. In particular, with atrophic AMD, OCTA is less sensitive than with intermediate AMD (68% *versus* 81%), but has the same specificity (100%).

In the only longitudinal study[6] conducted on patients with *quiescent* CNV and atrophic AMD, the patients retained their visual acuity longer than patients without foveal involvement. The hypothesis here is that *quiescent* CNV could be a protective factor against atrophic progression, due to the blood flow feeding the choriocapillaris and photoreceptors.

In patients with a pachychoroid and *quiescent* CNV, the most common characteristic in OCTA is a hypersignal with distinct edges and a fairly irregular shape within a PED. In late-phase ICG angiography, hypofluorescence due to wash-out of the lesion has also been described[7].

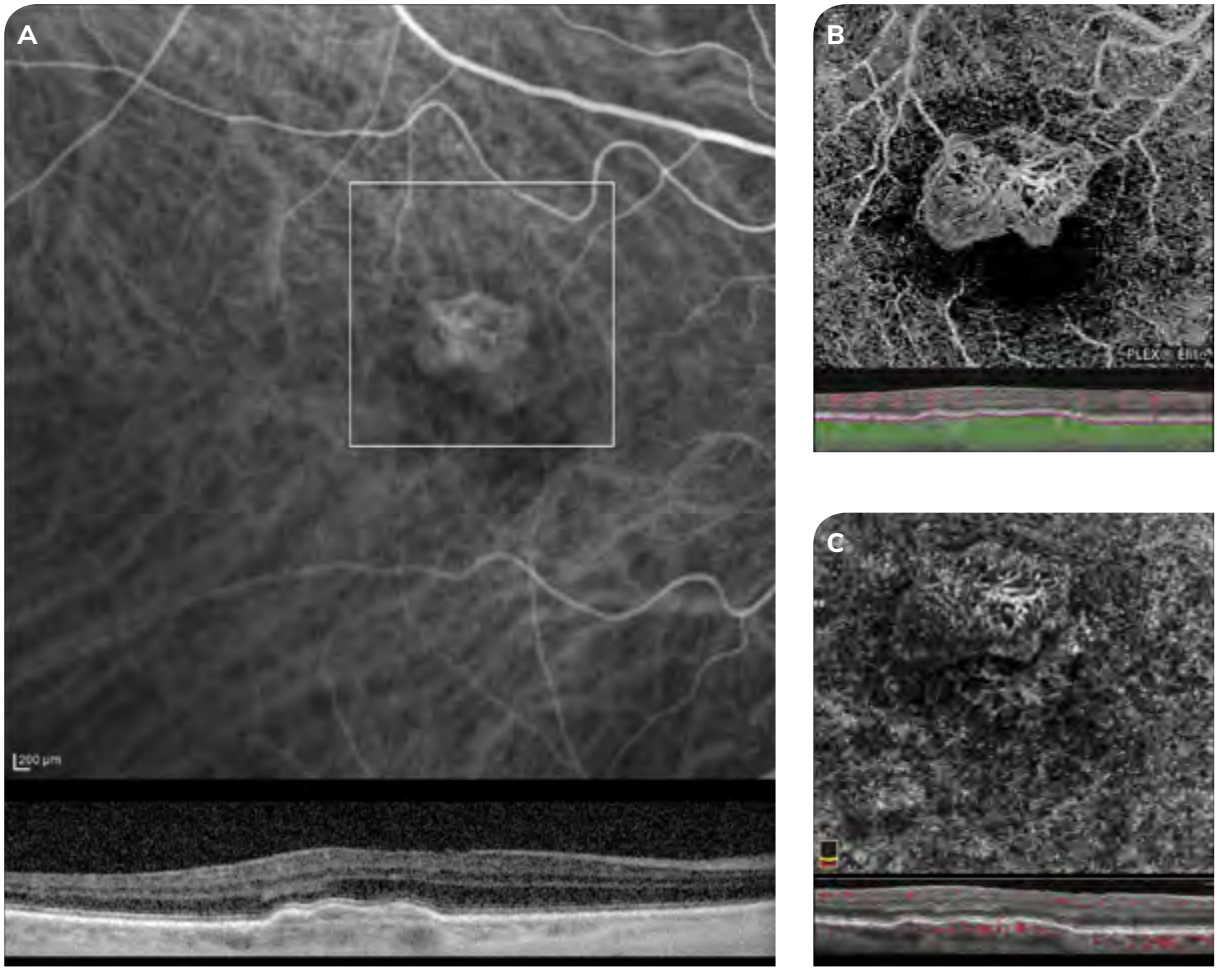

Fig. 2: Intermediate-phase indocyanine green angiography (ICG) and optical coherence tomography angiography (OCTA) of *quiescent* type 1 choroidal neovascularisation (CNV) (multimodal imaging of the patient in Figure 1).

In ICG angiography, the *quiescent* type 1 CNV is characterised by a hyperfluorescent network in the early and intermediate phases (A: HRA, Heidelberg Engineering). In OCTA, the same lesion is characterised by a regular shape with well defined edges and a feeder vessel, with no peripheral arcades (B: PLEXelite, Carl Zeiss) (C: rtvue, Optovue).

2. Monitoring

Bimonthly monitoring from the first visit onwards and for at least six months is strongly recommended. If exudative signs appear during this monitoring period, "early detection of CNV" is the preferred term. From the sixth month onwards, the diagnostic criteria for *quiescent* CNV have been fulfilled. *Quiescent* CNV typically remains stable (with no exudation over the long term), while the size of the neovascular membrane increases. Quarterly monitoring is nevertheless indicated. The complication rate varies from 6.6% for exudation associated with intermediate AMD to 26% with atrophic AMD. If exudation occurs after the sixth month, the preferred term is "conversion of *quiescent* CNV to active (or exudative)".

However, this nomenclature is not accepted by certain authors[3].

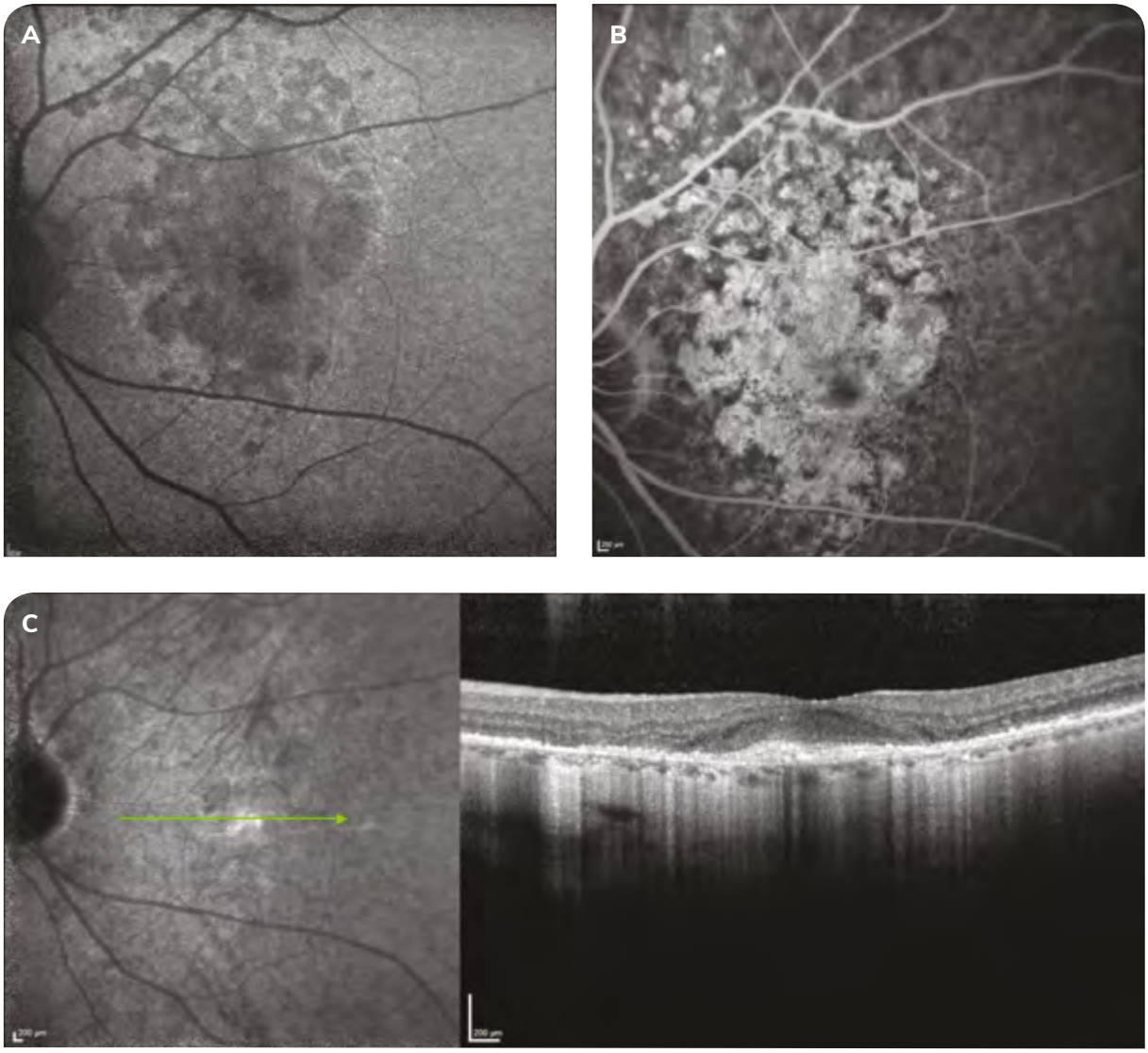

Fig. 3: Multimodal imaging of *quiescent* type 1 choroidal neovascularisation (CNV) associated with atrophic age-related macular degeneration.

In autofluorescence, the *quiescent* type 1 CNV is not visible (A). In fluorescein angiography (FA), the *quiescent* CNV appears as hyperfluorescent lesions with distinct edges and no late-phase leakage. Hyperfluorescence caused by atrophy of the retinal pigment epithelium can also be seen (B). In indocyanine green angiography (ICG), the *quiescent* CNV is characterised by a hypercyanescent plaque in the late phases (C). In optical coherence tomography (OCT), the *quiescent* CNV appears as a slight pigment epithelial detachment (PED) with a horizontal main axis, with no signs of subretinal or intraretinal exudation. This PED displays moderate reflectivity, allowing Bruch's membrane to be seen. Around the membrane, the retina has thinned and light transmission has increased due to atrophy of the retinal pigment epithelium (HRA, Heidelberg Engineering).

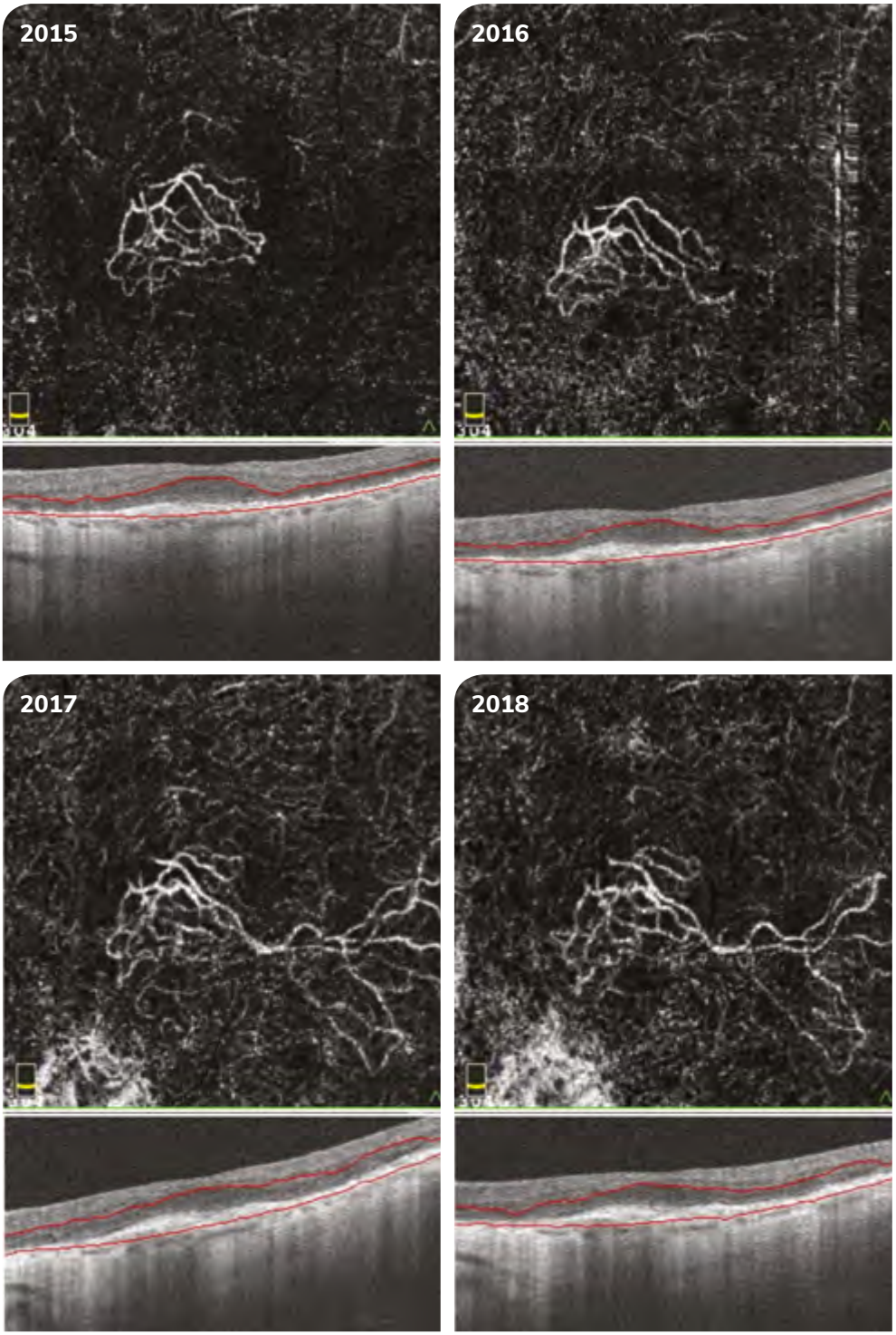

Fig. 4: Optical coherence tomography angiography (OCTA) of *quiescent* type 1 choroidal neovascularisation (CNV) associated with atrophic age-related macular degeneration (AMD) (multimodal imaging of the patient in Figure 3).

In OCTA, the *quiescent* type 1 CNV associated with AMD is characterised by a fairly irregular shape with well defined edges and no feeder vessel or peripheral arcades. Its flow appears "filiform". This lesion will grow over time without changing in appearance (C: Rtvue, Optovue).

3. Treatment

The gold standard treatment for "activated" *quiescent* CNV is a series of anti-VEGF intravitreal injections, which has been shown to be effective in reducing intraretinal and subretinal signs of exudation[1,6,7].

Conclusion

***Quiescent* CNV is a new entity described in conjunction with intermediate and late AMD, as well as with pachychoroid diseases and angioid streaks. It refers to treatment-naive CNV (visible in ICG angiography and OCTA) that shows no signs of exudation in OCT or leakage in FA.**

Regular monitoring is recommended.

Conversion to exudation is uncommon but possible. In these cases, a series of anti-VEGF injections is indicated[1,8].

References

1. Querques G *et al.* Functional characterization and multimodal imaging of treatment-naive «quiescent» choroidal neovascularization. Invest Ophthalmol Vis Sci 2013; 54(10):6886-6892.

2. Gass JDM. Stereoscopic Atlas of Macular Diseases. Diagnosis and Treatment. Mosby, St Louis; 1997.

3. de Oliveira Dias JR. *et al.* Natural History of Subclinical Neovascularization in Nonexudative Age-Related Macular Degeneration Using Swept-Source OCT Angiography. Ophthalmology. 2018 Feb;125(2):255-266.

4. Palejwala NW *et al.* Detection of non exudative choroidal neovascularization in age-related macular degeneration with optical coherence tomography angiography. Retina. 2015;35(11):2204-11.

5. Carnevali A *et al.* Optical Coherence Tomography Angiography: A Useful Tool for Diagnosis of Treatment-Naïve Quiescent Choroidal Neovascularization. Am J Ophthalmol. 2016;169:189-198.

6. Capuano V. *et al.* Treatment-Naïve Quiescent Choroidal Neovascularization in Geographic Atrophy Secondary to Nonexudative Age-Related Macular Degeneration. Am J Ophthalmol. 2017;182:45-55.

7. Carnevali, A. *et al.* OCT Angiography of Treatment-Naïve Quiescent Choroidal Neovascularization in Pachychoroid Neovasculopathy. Ophthalmology Retina, 1(4), 328–332.

8. Mentes J, *et al.* Multimodal imaging characteristics of quiescent Type 1 neovascularization in an eye with angioid streaks. Am J Ophthalmol Case Rep. 2018 24;10:132-136.

Type 1 neovascularisation

PART 3: Retinal pigment epithelial tears

Alexandra Mouallem-Bézière

1. Clinical description and physiopathology

In 1981, Hoskin *et al.*[1] were the first to describe retinal pigment epithelium (RPE) tears caused by irregular separation of the RPE from its basement membrane. Three years later, Gass[2] used fluorescein angiography to propose a series of physiopathological stages to explain why RPE tears occur in AMD, starting with a vascularised retinal pigment epithelial detachment (PED) accompanied by signs of exudation (stage one). This serous detachment is generally slightly wider and more elevated than the area of PED (stage 2). As the pressure of the escaping serous fluid detaches the RPE from the opposite side, a point is reached where the pigment epithelial cells cannot withstand this pressure, and a tear occurs at the junction of Bruch's membrane and the attached and detached RPE (stage 3). The serous fluid moves under the RPE into the subretinal space as the free edge of the tear retracts like an accordion and the RPE rolls under into an organised mound (stage 4) (Figure 1).

Gass also describes the typical ophthalmoscopy results, in which an RPE tear appears as a single, clearly defined area of absent RPE associated with a pigmented mound corresponding to the retracted RPE. The tear can progress and become larger, with significant loss of vision.

In 1990, Coscas *et al.*[3] identified the clinical characteristics that precede the appearance of a tear. Before a tear appears, the PED was found to increase in size and change shape. The authors also described the angiographic characteristics: a hyperfluorescent area appearing on the edges of the PED in the early phase, spreading gradually over time (Figure 1). They concluded that laser treatment should be considered carefully in the presence of these characteristics, given the high risk of a tear as a result of thermal contraction of the neovascular lesion. In addition to laser photocoagulation, several treatments have been reported as possible causes of RPE tears secondary to AMD, including photodynamic therapy[4,5] and the injection of various anti-VEGF drugs[6,7]. Anti-VEGF injections can cause contraction and fibrosis of the neovascular lesion, associated with fibrovascular PED, which correlates directly with breaks in the RPE[8].

Recently, Nagiel *et al.*[9] used spectral-domain optical coherence tomography (SD-OCT) to identify contractile neovascular tissue on the undersurface of the PED as a causal mechanism of RPE tears following anti-VEGF injections for AMD.

In 2016, Mouallem *et al.*[10] described a case series with double tears of the RPE. These double tears on either side of the neovascularised PED can occur simultaneously or sequentially. The advanced physiopathology is the development of choroidal neovascularisation in the centre of the PED, exerting tangential pressure on both sides, which leads to the tear[10,14].

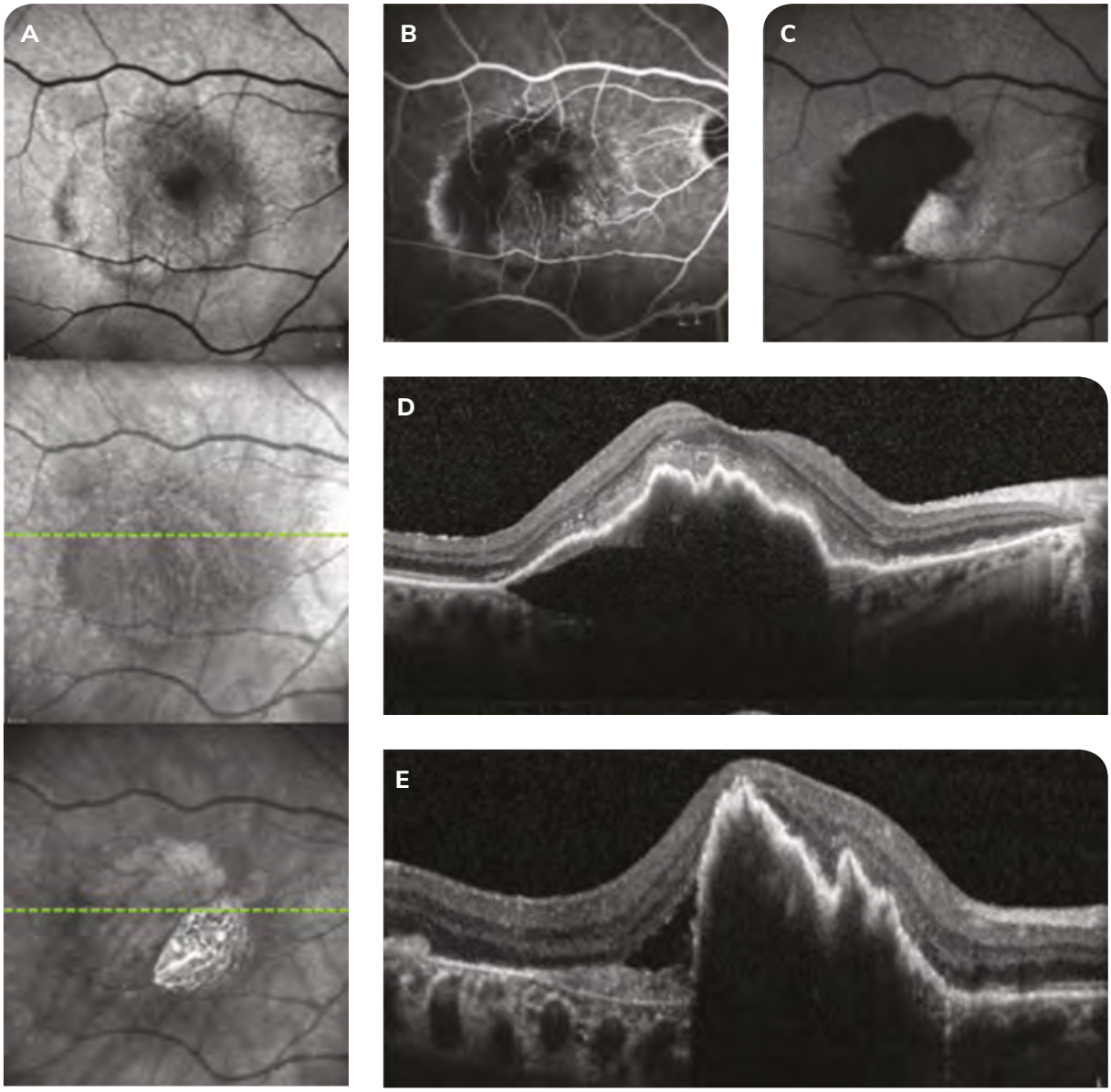

Fig. 1: Multimodal imaging (autofluorescence photograph, fluorescein angiography and SD-OCT) of an 83-year-old treatment-naive female patient who presented with an RPE tear in her right eye at the initiation of anti-VEGF treatment for exudative AMD.

(A): Autofluorescence photo of the posterior pole prior to the RPE tear.
(B): Fluorescein angiography image (intermediate phase, 3 minutes) showing hyperfluorescence along the edge of the PED corresponding to a fragile area of the RPE.
(C): Autofluorescence photograph of the posterior pole revealing a large, grade-4, hypoautofluorescent tear in the geographic edge of the RPE. The RPE appears hyperautofluorescent where it has rolled up at the edge of the tear.
(D): Pre-tear SD-OCT image revealing bridge-shaped choroidal neovascularisation under the entire RPE, which appears wrinkled due to the horizontal pressure exerted by the neovascularisation.
(E): Post-tear SD-OCT image showing an increase in the size of the PED, with accordion-like retraction of the RPE at the edge of the detachment.

2. Classification of RPE tears

In 2010, David Sarraf *et al.*[11] proposed a new four-level grading system for RPE tears:

- Grade 1: RPE tear of less than 200 µm
- Grade 2: Tear of between 200 µm and 1 disc diameter
- Grade 3: Tear greater than 1 disc diameter
- Grade 4: Grade 3 involving the fovea.

3. Treatment and visual prognosis

Gutfleish *et al.*[12] studied a series of 37 single RPE tears and found that visual acuity deteriorated considerably after the RPE tear, as well as during the follow-up period, with 53.2% of eyes classed as legally blind at 12 months. More recently, Durkin *et al.*[13] examined 14 single tears and found significant loss of one or more lines of vision compared to baseline, irrespective of the size of the tear. It should be noted that after an RPE tear appeared, an improvement in visual acuity was found in 5 patients (35.7%) who had received anti-VEGF therapy, and that all the patients retained their best corrected visual acuity after the tear thanks to anti-VEGF treatment. According to the grading system developed by Sarraf *et al.*[11], the prognosis for RPE tears is linked to the biggest linear diameter of the tear and to the presence or absence of foveal involvement.

Conclusion

Retinal pigment epithelium tears are complications of neovascularised PED. The prognosis for these tears is directly linked to their severity grade, and their appearance has no impact on the usual retreatment criteria for exudative AMD.

References

1. Hoskin A, Bird AC, Sehmi K. Tears of detached retinal pigment epithelium. Br J Ophthalmol 1981; 65:417–422.
2. Gass JD. Pathogenesis of tears of the retinal pigment epithelium. Br J Ophthamol 1984; 68:513-519
3. G. Coscas, F. Koenig, G. Soubrane. The pretear characteristics of pigment epithelial detachments. A study of 40 eyes. Arch Ophthalmol 1990;108:1687–1693
4. Gelisken F, Indhofen W, Partsch M, *et al.* Retinal pigment epithelial tear after photodynamic therapy for choroidal neovascularization. Am J Ophthalmol 2001;131:518–520.
5. Pece A, Introini U, Bottoni F, *et al.* Acute retinal pigment epithelial tear after photodynamic therapy. Retina 2001;21:661–665.
6. Dhalla MD, Blinder KJ, Tewari A, *et al.* Retinal epithelial pigment tear following intravitreal pegaptanib sodium. Am J Ophthalmol 2006;141:751–753.
7. Bakri SJ, Kitzmann AS. Retinal pigment epithelial tear after intravitreal ranibizumab. Am J Ophthalmol 2007;143:505–507.
8. Spaide RF. Enhanced depth imaging optical coherence tomography of retinal pigment epithelial detachment in age-related macular degeneration. Am J Ophthalmol 2009; 147:644–652.
9. Nagiel A, Freund KB, Spaide RF *et al.* Mechanism of retinal pigment epithelium tear formation following intravitreal anti-vascular endothelial growth factor therapy revealed by spectral-domain optical coherence tomography. Am J Ophthalmol 2013; 156:981-988.
10. Mouallem A, Sarraf D, Chen X *et al.* Double retinal pigment epithelium tears in neo vascular age related macular degeneration. Retina 2016;36(11):2197-2204
11. Sarraf D, Reddy S, Chiang A *et al.* A new grading system for retinal pigment epithelial tears. Retina 2010;30:1039-45.
12. Gutfleisch M, Heimes B, Schumacher M *et al.* Long-term visual outcome of pigment epithelial tears in association with anti-VEGF therapy of pigment epithelial detachment in AMD. Eye (Lond). 2011;25:1181-6.
13. Durkin SR, Farmer LD, Kulasekara S, Gilhotra J. Change in vision after retinal pigment epithelium tear following the use of anti-VEGF therapy for age-related macular degeneration Graefes Arch Clin Exp Ophthalmol. 2015 Mar 8.
14. Mukai R, Sato T, Kishi S. Repair mechanism of retinal pigment epithelial tears in age-related macular degeneration. Retina. 2015;35:473-80.

Type 1 neovascularisation

PART 4: Wrinkled pigment epithelial detachment

Gérard Mimoun

Vascularised pigment epithelial detachment (PED) associated with AMD is still considered to be a factor in poor visual prognosis, with a gradual or sometimes sudden reduction in visual acuity linked to macular haemorrhage or a retinal pigment epithelium tear.

However, we have observed a unique form of vascularised PED, characterised by small, jagged folds of the retinal pigment epithelium (RPE) in spectral-domain OCT that we refer to as "wrinkled PED", which could be a characteristic of good visual prognosis, with fewer anti-VEGF intravitreal injections and a long relapse-free period.

1. Definition

Wrinkled pigment epithelial detachment is defined as a neovascularised pigment epithelial detachment (nPED) with a height in SD-OCT of over 200 µm and generally less than 500 µm, with at least four small, jagged folds of the retinal pigment epithelium (Figure 1).

Its appearance differs from that of unwrinkled neovascularised pigment epithelial detachment, where the RPE is raised or bulging but stretched out and smooth.

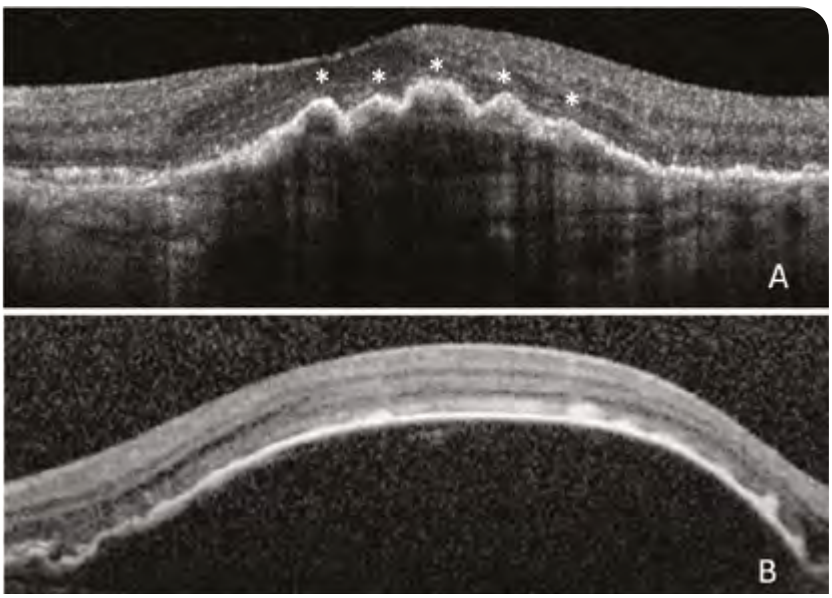

Fig. 1: Wrinkled and unwrinkled pigment epithelial detachment in OCT.
A: Wrinkled neovascularised PED is defined as a PED with a height of over 200 µm in SD-OCT and at least four small, jagged folds of the retinal pigment epithelium.
B: This contrasts with unwrinkled PED, in which the RPE bulges out but remains smooth.

2. Description

1) Fundus examination

The macula appears raised and slightly blurry, sometimes with several visible folds, giving it a scalloped appearance. This is much more visible in en-face OCT imaging.

2) Red monochrome photograph

The retinal pigment epithelium appears raised and is often inhomogeneous.

3) Fluorescein angiography

Wrinkled pigment epithelial detachment can be observed in the initial phase prior to treatment (Figure 2).

- In early-phase fluorescein angiography, progressive, inhomogeneous staining is visible, with in this particular case (Figure 2) a hyperfluorescent lesion located nasal to the macula and pinpoints in the temporal section of the macula.
- In late-phase fluorescein angiography, leakage from the lesion can be seen in the nasal section of the macula, with an increase in pinpoints temporal to the macula.

4) Indocyanine green angiography (ICG)

In the early phase, a round, fairly extensive hypercyanescent lesion can be seen, with small folds already visible. These hypercyanescent folds grow over time and by the late phase are even more visible, associated with a plaque in the centre of the pigment epithelial detachment.

In Figure 3, the patient has PED complicated by choroidal neovascularisation in the context of exudative age-related macular degeneration, but OCT is required in order to characterise it.

5) Optical coherence tomography (OCT)

A slightly bulging, heterogeneous elevation of the retinal pigment epithelium can be seen. In the slice focused on the section nasal to the lesion that was hyperfluorescent in FA, an irregular, hyperreflective structure can be seen on the undersurface of the RPE. Above the RPE, the subretinal area is grey and hyperreflective, with blurred edges (grey SRD), suggestive of exudative choroidal neovascularisation (Figure 4).

OCTA shows a neovascular flow hypersignal within the pigment epithelial detachment. Moderate arborisation is present, usually without any bordering arcades.

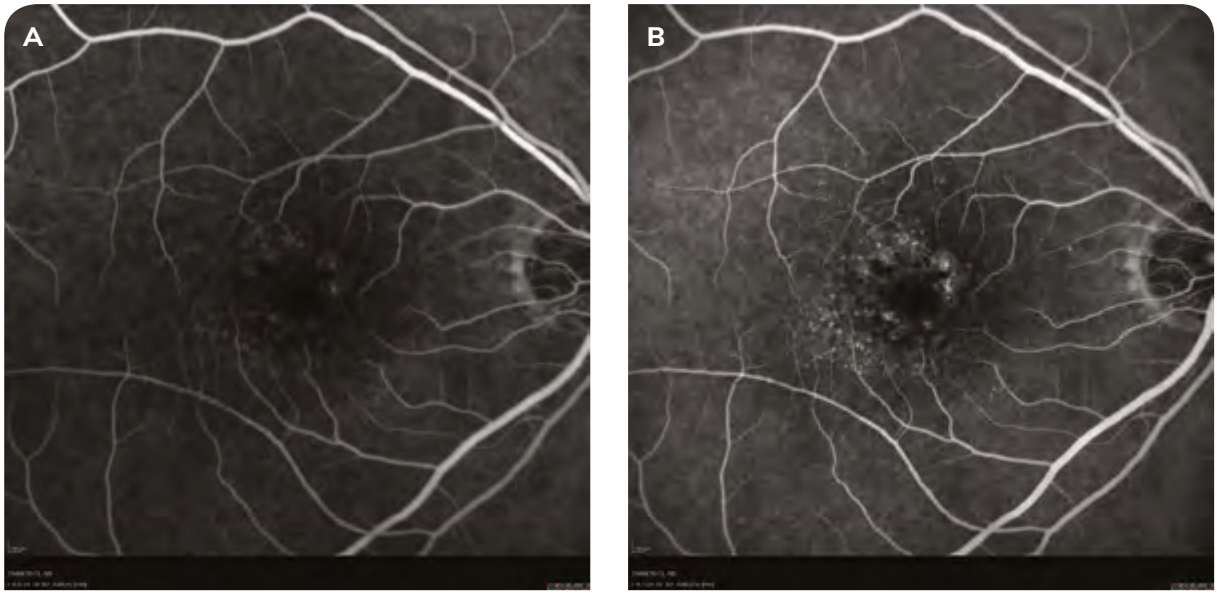

Fig. 2: Fluorescein angiography.
Early-phase A: progressive, inhomogeneous staining, with a hyperfluorescent lesion located nasal to the macula and pinpoints in the temporal area.
Late-phase B: leakage from the lesion nasal to the macula, with an increase in pinpoints in the temporal area.

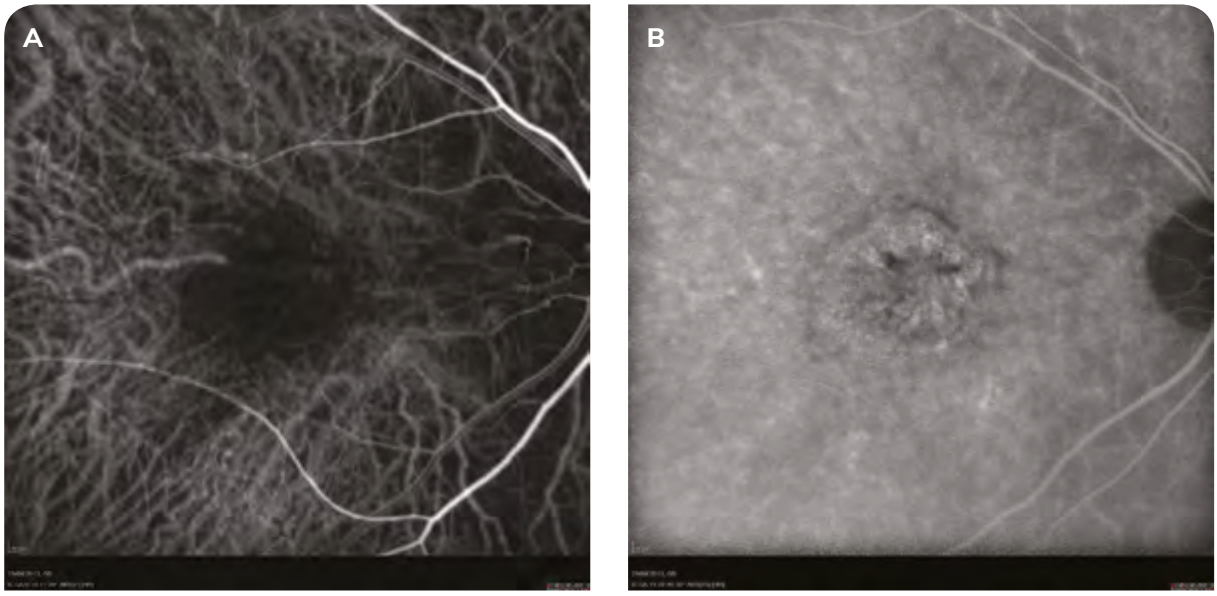

Fig. 3: Indocyanine green angiography.
Early-phase A: round, hypercyanescent lesion with small folds already visible.
Late-phase B: hypercyanescent plaque within the PED with hypercyanescent folds becoming more and more visible.

3. Morphological changes and appearance of jagged folds in the RPE after treatment with intravitreal injections (IVI)

Wrinkled pigment epithelial detachment is a progression of neovascularised PED that appears when it is treated with anti-VEGF intravitreal injections (Figures 5 and 6).

The following is observed after intravitreal injections for neovascularised PED:

- In **fluorescein** angiography (Figure 6): the localised hyperfluorescence nasal to the macula and the pinpoints in the temporal area get smaller
- In **indocyanine green** angiography (ICG): the late hypercyanescence of the round central lesion becomes stronger and the folds become thicker and more visible
- In **optical coherence tomography** (OCT): very early after treatment for neovascularised PED (from the first month after the first anti-VEGF IVI), small jagged folds appear on the temporal section of the lesion in the centre of the dome formed by the raised retinal pigment epithelium. The thickness of the central retina decreases, the grey SRD starts to disappear and the signs of exudation and intraretinal or subretinal fluid disappear (Figures 5, 6 and 7).

4. Wrinkled PED progression and prognosis

In a retrospective, case-control study conducted on 52 eyes with a 3-year follow-up comparing two groups—one with wrinkled PED and one with unwrinkled PED—we found significantly better corrected visual acuity in the wrinkled PED group following IVI treatment. Visual acuity remained stable at around 20/40 for the wrinkled group throughout the entire 3-year observation period, while average visual acuity in the unwrinkled group fell to 20/63 at 1 year and 2 years and to 20/80 at 3 years ($p = 0.002$).

The number of anti-VEGF IVIs was much lower in the wrinkled PED group, to a statistically significant extent ($p = 0.0011$), at 2.93 the first year, 1.93 the second year and 1.88 the third year. In the unwrinkled PED group, the number of IVIs was much higher, at 5.87, 4.44 and 6.21 respectively.

The average maximum time without relapse for wrinkled PED was significantly longer, at 7.87 months at 1 year, 13.5 months at 2 years and 14.8 months at 3 years. The times for the unwrinkled PED group were shorter, at 4.59, 7.83 and 8.57 months respectively.

Wrinkled PED is associated with a statistically significant better visual prognosis at 3 years, a lower number of IVIs and a long-term reduction in relapse frequency.

The presence of small, jagged folds in the RPE during treatment could therefore be a phenotypic characteristic and a valuable predictive factor, making their identification important when treating patients with vascularised PED associated with AMD.

The physiopathology of wrinkled PED remains unknown. However, we know that as the neovascularised PED is formed and increases in size under the effects of subretinal pigment epithelial exudation linked to occult choroidal neovascularisation, the RPE itself distends and increases in length.

There are several possible explanations: under the effect of IVIs, the hydrostatic pressure within the PED decreases, weakening the PED, and the now-distended and lengthened RPE is forced to roll up, since it has become too long for the surface it covers. This would explain the folds in the RPE and its wrinkled appearance. Alternatively, it could be a specific characteristic of less active or less exudative neovascularisation, or linked to the retinal pigment epithelium being less capable of distension in certain patients.

Fig. 4: Initial OCT before treatment: slightly bulging, heterogeneous elevation of the retinal pigment epithelium with grey SRD above the RPE.

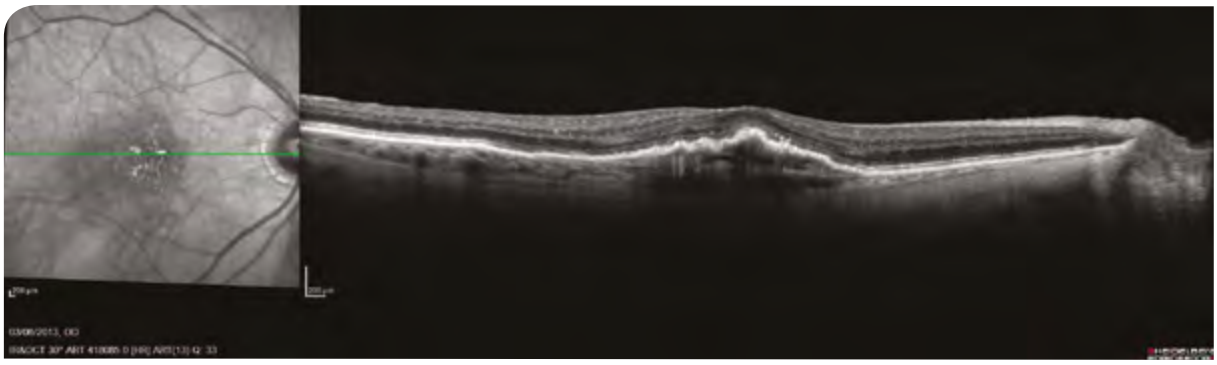

Fig. 5: OCT one month after IVI: small, jagged folds appear in the RPE and the PED flattens out. The grey SRD has started to disappear, as have the signs of exudation.

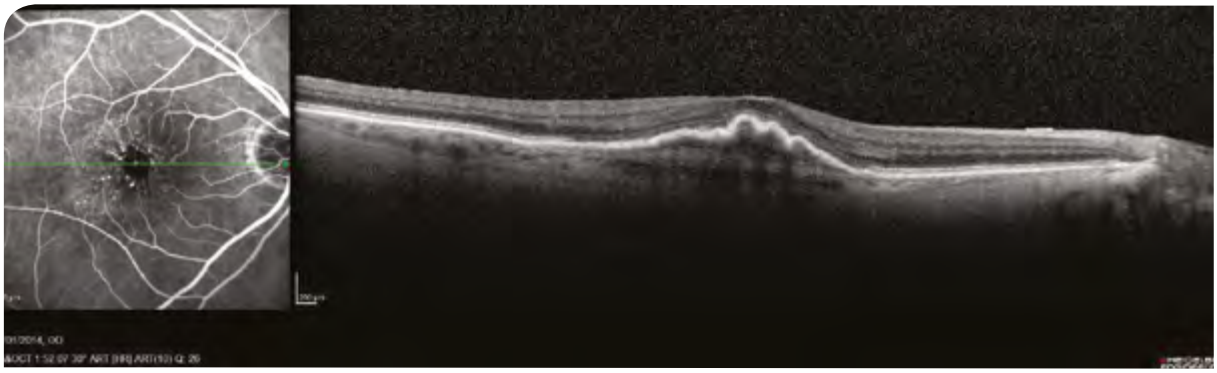

Fig. 6: OCT one month after six IVIs: small, jagged folds in the RPE, the PED has flattened out, no grey SRD or signs of exudation.

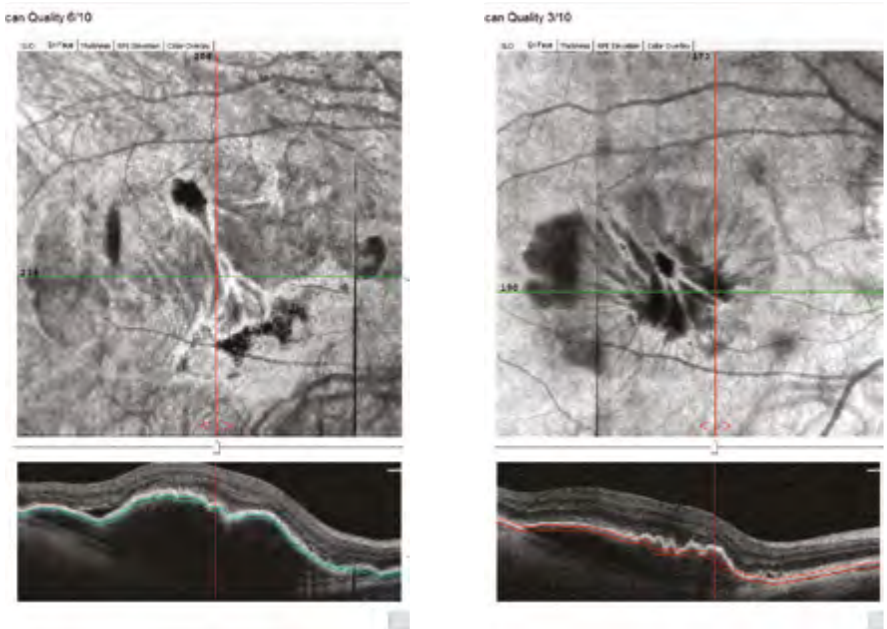

Fig. 7: En-face OCT before and after treatment. En-face OCT provides a clearer image of the RPE folds.

Conclusion

Wrinkled PED is a progressive form of neovascularised PED that occurs during treatment for AMD. It is characterised by small, jagged folds in the RPE and is associated with a better visual prognosis, fewer IVIs and a long-term reduction in relapse frequency—to a statistically significant extent.

The presence of small folds in the RPE could therefore be a valuable predictive factor, and their identification in clinical practice important for patient treatment.

References

1. Mrejen S, Sarraf D, Mukkamala SK, Freund KB. Multimodal imaging of pigment epithelial detachment: a guide to evaluation. Retina Phila Pa. 2013;33(9):1735-1762. doi:10.1097/IAE.0b013e3182993f66.

2. Hoerster R, Muether PS, Sitnilska V, *et al.* Fibrovascular pigment epithelial detachment is a risk factor for long-term visual decay in neovascular age-related macular degeneretion. Retina Phila Pa. 2014;34(9):1767-1773.

3. Poliner LS, Olk RJ, Burgess D, Gordon ME. Natural history of retinal pigment epithelial detachments in age-related macular degeneration. Ophthalmology. 1986;93(5):543-551.

4. Rofagha S, Bhisitkul RB, Boyer DS, *et al.* SEVEN-UP Study Group. Seven-year outcomes in ranibizumab-treated patients in ANCHOR, MARINA, and HORIZON: a multicenter cohort study (SEVEN-UP). Ophthalmology. 2013;120(11):2292-2299.

5. Solomon SD, Lindsley K, Vedula SS, *et al.* Anti-vascular endothelial growth factor for neovascular age-related macular degeneration. Cochrane Database Syst Rev. 2014;(8):CD005139.

6. Chan CK, Abraham P, Meyer CH, *et al.* Optical coherence tomography-measured pigment epithelial detachment height as a predictor for retinal pigment epithelial tears associated with intravitreal bevacizumab injections. Retina Phila Pa. 2010; 30(2):203-211. doi:10.1097/IAE.0b013e3181babda5.

7. Lam D, Semoun O, Blanco-Garavito R, *et al.* WRINKLED VASCULARIZED RETINAL PIGMENT EPITHELIUM DETACHMENT PROGNOSIS AFTER INTRAVITREAL ANTI-VASCULAR ENDOTHELIAL GROWTH FACTOR THERAPY. Retina. 2018. Jun;38(6):1100-1109.

Type 1 neovascularisation

PART 5: Unique pre-epithelial type 2 neovascularisation healing style following anti-VEGF treatment: “igloos”

Gérard Mimoun

Choroidal neovascularisation (CNV) is very often responsible for a severe reduction in visual acuity, due to bleeding, exudation or fibrous scarring. CNV was initially categorised using fluorescein angiography, into classic neovascularisation (well defined) and occult neovascularisation (poorly defined). With the introduction of spectral-domain OCT (SD-OCT), it began to be categorised into pre-epithelial type 2 neovascularisation, located above the RPE, and “occult” type 1 neovascularisation, located below the RPE.

In high myopia and angioid streaks, pre-epithelial type 2 CNV is the most common form of CNV, but it is rare in AMD, occurring in just 9 to 17% of cases. Subepithelial type 1 or occult CNV is the most common form found in AMD.

Thanks to anti-VEGF therapy—particularly when administered in the early stages of the disease—visual acuity after IVI in high myopia, angioid streaks and certain cases of AMD is currently well controlled and remains acceptable.

However, we have observed a specific progressive sign of healing arising after pre-epithelial type 2 CNV is treated with anti-VEGF IVI: a dense, relatively homogeneous, localised subretinal elevation with a characteristic hyperreflective dome appearance in SD-OCT, which we refer to as an “igloo” (Figure 1).

When pre-epithelial type 2 CNV heals in this way, the prognosis is generally favourable, with fairly good visual acuity, fewer intravitreal injections and a long period without relapse.

1. Description

The igloo is a way in which pre-epithelial type 2 CNV heals after IVI treatment. In the initial pre-treatment stage, the signs are therefore the same as with visible type 2 CNV.

1) Fundus examination

The macula is raised and retinal haemorrhage may be visible. The CNV itself can sometimes be detected.

2) Fluorescein angiography

In early-phase fluorescein angiography, a vascular network with a feathered appearance is clearly visible, exhibiting early hyperfluorescence, with a highly hyperfluorescent wreath and a slightly darker centre. In the late phase, there is extensive leakage from the lesion: the hyperfluorescence increases in intensity and size, and its edges become blurred (Figure 2).

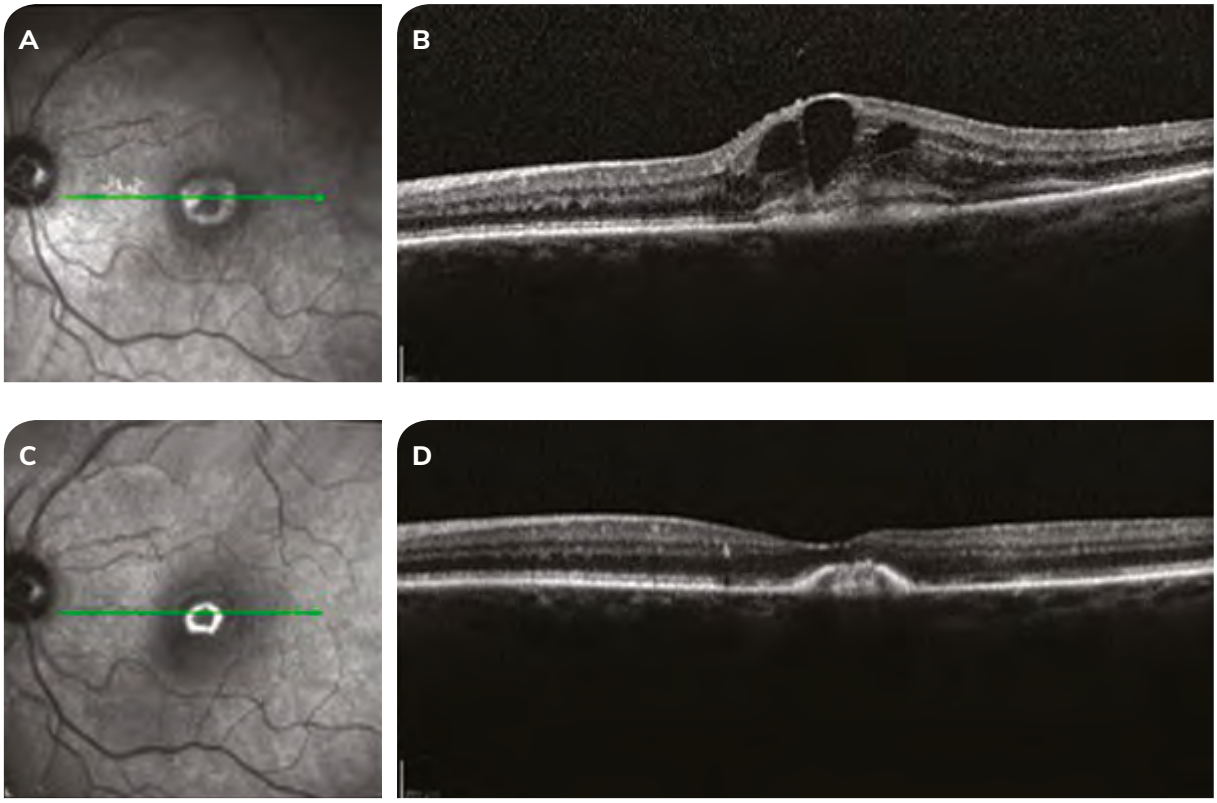

Fig. 1: SD-OCT of a 79-year-old woman with exudative AMD, before treatment and three months after IVI.

A: Infrared photograph showing a hyperreflective perifoveal ring prior to treatment.
B: SD-OCT before treatment, showing pre-epithelial (type 2) CNV with grey SRD and intraretinal spaces.
C: Infrared photo three months after treatment. The ring is now highly hyperreflective, dense and well defined.
D: SD-OCT after treatment, showing a hyperreflective subretinal lesion with the characteristic igloo appearance and a hyperreflective PED.

3) Indocyanine green angiography (ICG)

In the early phase, there is distinct hypercyanescence, which sometimes remains into the late phase but often lessens due to wash-out, the neovessels fading into the grey of the fundus (Figure 2).

4) Optical coherence tomography (OCT)

OCT confirms the retinal elevation: the fovea no longer appears funnel-shaped and the macula bulges out. This is accompanied by serous retinal detachment (SRD) and, in rare cases, intraretinal spaces. Grey SRD is often present, with a fairly dense, hyperreflective subretinal structure with blurred edges above the RPE, which is specific to type 2 CNV (Figure 3).

OCT-angiography reveals a pathological neovascular flow hypersignal, often with a characteristic image of perfused CNV with a clearly visible surrounding arcade, a dark halo of vascular steal and extensive arborisation with numerous fine connected networks.

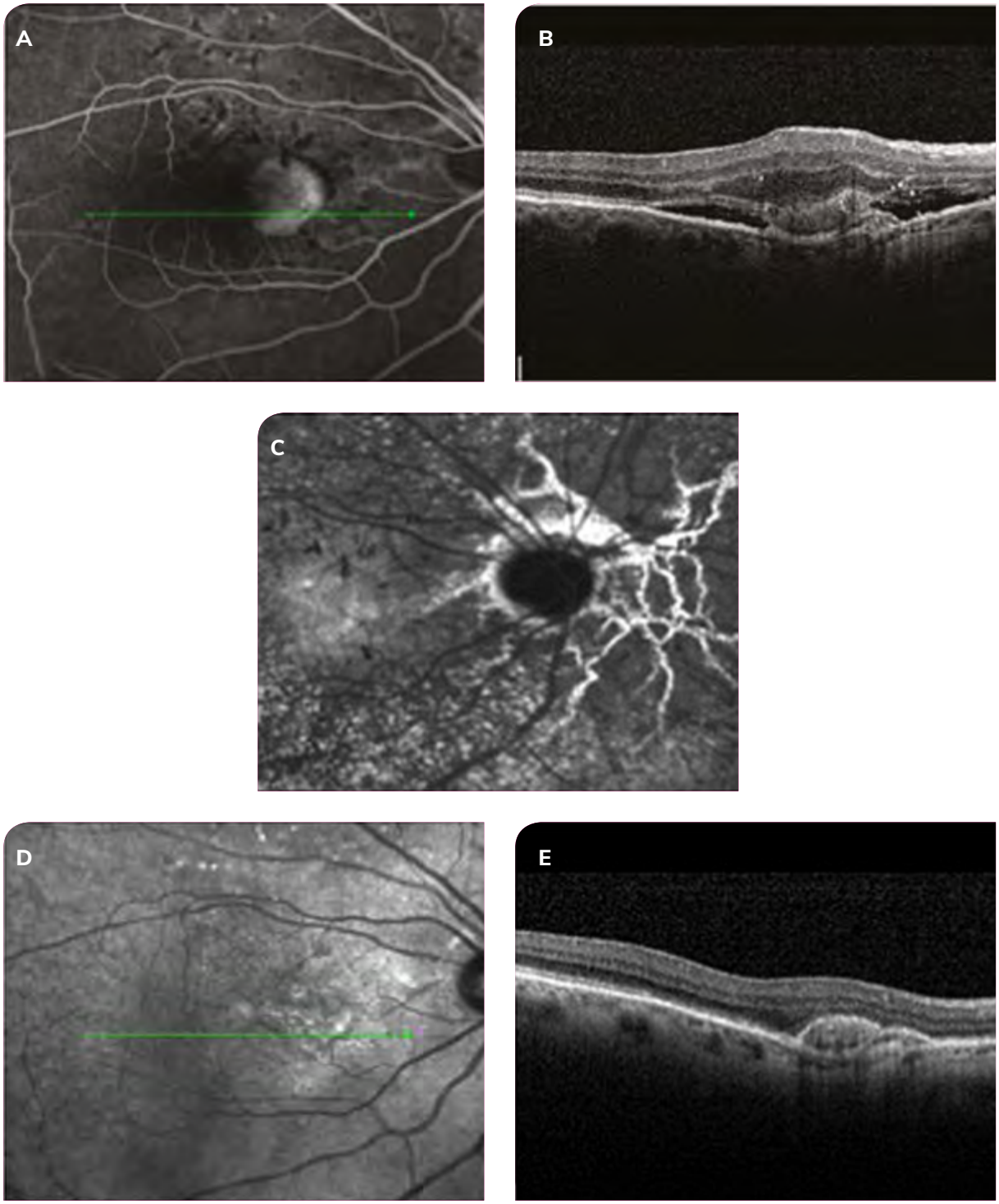

Fig. 2: Angioid streaks complicated by CNV before and four months after IVI.

• Before treatment:
A: Fluorescein angiography (FA) showing visible CNV with leakage.
B: OCT: Pre-epithelial (type 2) CNV with grey SRD and SRD.
C: ICG image showing streaks becoming stained in the late phases and subfoveal CNV.

• Four months after treatment:
D: IR: Lesion barely visible.
E: OCT: Hyperreflective subretinal igloo that appears to be resting on the RPE.

2. Morphological changes and appearance of igloos in the RPE after treatment with intravitreal injections (IVI)

Igloos are a stage in the progression of type 2 CNV that appear when it is treated with anti-VEGF IVI. The following is observed after treatment for type 2 CNV:

- In **fluorescein angiography**: the hyperfluorescent structure of the CNV reduces in size and intensity, with almost no leakage, although it may remain stained.
- In **ICG angiography**: the late hypercyanescence completely or almost completely disappears.
- In **optical coherence tomography (OCT)** (Figure 3): the igloo can be seen from the first month onwards (i.e. very soon after the first anti-VEGF IVI). It appears as a dense, hyperreflective subretinal lesion with distinct edges that forms a localised dome-shaped elevation with a posterior shadow, exactly where the CNV used to be. The lesion comprises a hyperreflective strip with a very similar tone to the RPE itself, although its content is slightly less hyperreflective.

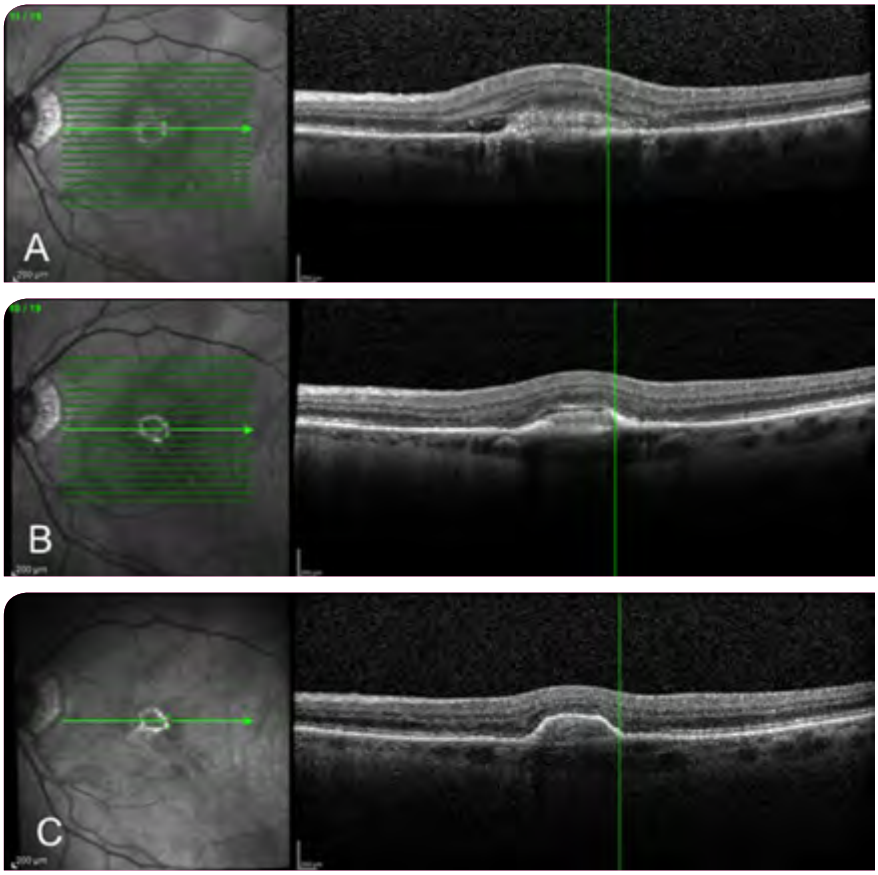

Fig. 3: OCT showing the progression of type 2 choroidal neovascularisation towards an igloo.

A: Before treatment. Fusiform hyperreflectivity can be seen above the RPE corresponding to the neovascularisation, associated with a SRD.
B: After treatment with three anti-VEGF IVIs. The signs of exudation decrease and the neovascular lesion becomes dense and more reflective.
C: After six months, the lesion is dense and free of exudation.

Locating the igloo against the outline of the RPE is not easy, since the OCT tone along the edges of the igloo is the same as the RPE, making it hard to precisely follow the line of the RPE. The igloo often appears as a smooth hyperreflective subretinal elevation above the RPE that seems to correspond to CNV scarring above the RPE. More rarely, the igloo looks like a PED and is therefore located below the RPE, indicative of CNV scarring below the RPE that can only be explained by the RPE expanding over and enveloping the CNV.

3. Igloo progression and prognosis

Igloos appear very soon after treatment and are found in 100% of type 2 CNV cases one month after IVI therapy. The igloo may appear heterogeneous to begin with, but over time becomes more and more hyperreflective. Relapse is possible, evidenced by the reappearance of grey SRD or signs of exudation.

In a retrospective study assessing post-IVI progression in 29 eyes with type 2 CNV (AMD: 14, myopia: 10, angioid streaks: 5) with an average follow-up of 3.6 years, we found a significant improvement in visual acuity from the first IVI: 20/80 with $p < 0.001$, confirmed at 1 year at 20/40 with a significant p of 0.004. The average number of IVIs during the first year was 4.3 injections.

Conclusion

The igloo is a specific progressive sign of healing following anti-VEGF IVI treatment for pre-epithelial type 2 CNV, appearing in OCT as a dense, fairly homogeneous, hyperreflective, dome-shaped, localised subretinal elevation. It is found in particular in cases of high myopia and angioid streaks—occurring rarely in AMD—and is associated with a good visual prognosis.

References

Dolz-Marco R, Phasukkijwatana N, Sarraf D *et al.* Regression of Type 2 Neovascularization into a Type 1 Pattern after Intravitreal Anti-Vascular Endothelial Growth Factor Therapy for Neovascular Age-Related Macular Degeneration. Retina 2016.

Hoang Mai Le, Gérard Mimoun, Salomon Y. Cohen *et al.* Regression of Type 2 neovascularization in Age-related Macular Degeneration, Myopia and Angioid Streaks: the “Igloo” pattern. (sous presse).

PART 6: Polypoidal choroidal vasculopathy (aneurysmal type 1 choroidal neovascularisation)

Mayer Srour, David Sayag

Polypoidal choroidal vasculopathy (PCV) was first described by Yannuzzi in 1982[1]. The condition involves abnormal branching vascularisation within the choroid, associated with aneurysmal vascular dilations that can lead to serous detachment of the retinal pigment epithelium (RPE) and, in some cases, extensive haemorrhage. PCV is more prevalent in Asian populations than in Caucasian populations. Age at diagnosis is lower than in AMD.

PCV is usually idiopathic, but can also be secondary to exudative AMD, myopic staphyloma, CSCR/DRPE (central serous chorioretinopathy/diffuse retinal pigment epitheliopathy) or a naevus[2]. More recently, Freund placed PCV on the pachychoroid spectrum (Figure 1) and renamed it "aneurysmal type 1 neovascularisation"[3].

	NON-NEOVASCULAR PACHYCHOROID			NEOVASCULAR PACHYCHOROID	
	Pachychoroid Pigment Epitheliopathy (PPE)	Peripapillary Pachychoroid SD (PPS)	Acute/K CSCR	Pachychoroid neovasculopathy	Polypoidal choroidal vasculopathy (PCV)
Clinic	Localised RPEC	Inter-PM RPEC + IR spaces +/- SRD	Serous PED/ SRD bleb	Type 1 CNV	Polyps
Fluo A	Non-specific	Non-specific	Serous PED/ Leakage point	V-PED	Polyps
AutoFluo	Localised RPEC	Localised RPEC	+/- Gravitational tracks	Non-specific	Non-specific
ICG	Hyperpermeability			CNV plaque	Polyps
EDI-OCT	Pachychoroid with pachyvessels				
OCTA	No flow			Type 1 CNV	BVN +/- polyps

Fig. 1: Pachychoroid clinical spectrum.
K: chronic. RPEC: retinal pigment epithelium changes. PM: papillomacular. SRD: serous retinal detachment. CNV: choroidal neovascularisation. A: angio. PED: pigment epithelial detachment. V: vascularised. ICG: indocyanine green angiography. BVN: branching vascular network.

1. Diagnosis

1) Fundus

In the fundus, PCV may be suspected in the presence of PED with lipid exudates, often associated with subretinal haemorrhage. One or more round, red-orange lesions may also be observed under the RPE, varying in size and prominence (Figure 2).

Drusen, RPE changes and areas of geographic atrophy are absent or rare. The location of the PCV can be subfoveal, juxtafoveal, extrafoveal, peripapillary or even peripheral, and varies from population to population. In Caucasians, the lesions are often extrafoveal, with high levels of peripapillary involvement (23 to 68%). In Asian populations, polyp location is variable, with the central subfoveal area affected

in almost 30% of certain Chinese populations. In rare cases, polypoidal dilations may be found on the retinal periphery and can be classified as exudative haemorrhagic chorioretinopathy. Patients are often asymptomatic and lesions may be discovered by chance. The condition often improves spontaneously. If extensive haemorrhage is present, a differential diagnosis may be required to rule out a tumour.

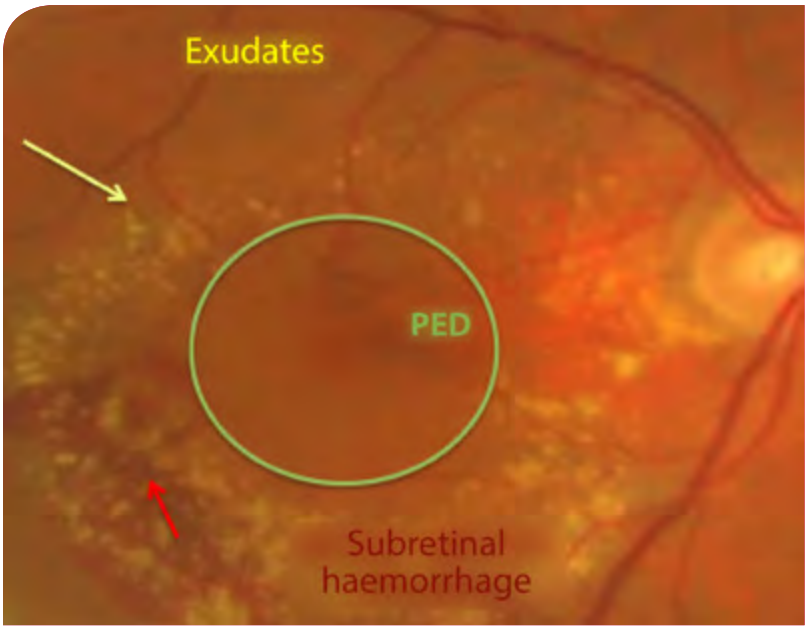

Fig. 2: Polypoidal vasculopathy within the fundus.

Pigment epithelial detachment (PED) is present (green circle), often associated with exudates (yellow arrow) and subretinal haemorrhage (red arrow).

2) Fluorescein angiography (FA) and indocyanine green angiography (ICG)

Fluorescein angiography has low specificity for PCV. It shows progressive staining of aneurysmal dilations, with little diffusion during the late phase and, very often, associated hyperfluorescence of the branching vascular network (BVN), which is difficult to differentiate from polyps (Figure 3). Polypoid lesions are often masked by bleeding and merged into the PED hyperfluorescence.

ICG is the key examination for diagnosing PCV. Polyps are displayed as round, hyperfluorescent lesions in the early phases and can remain into the late phase or undergo “wash-out” (Figure 4). The BVN is visible in the early phases, with polyps located within the network or on its edge, resulting in a late “hyperfluorescent lesion”. Choroidal hyperpermeability is also evident when using ICG. ICG is essential when monitoring PCV, since it can show whether the polyp hyperfluorescence has lessened or disappeared following treatment. Pulsatile filling of polyps can sometimes be seen and is thought to be a risk factor for rupture and haemorrhage.

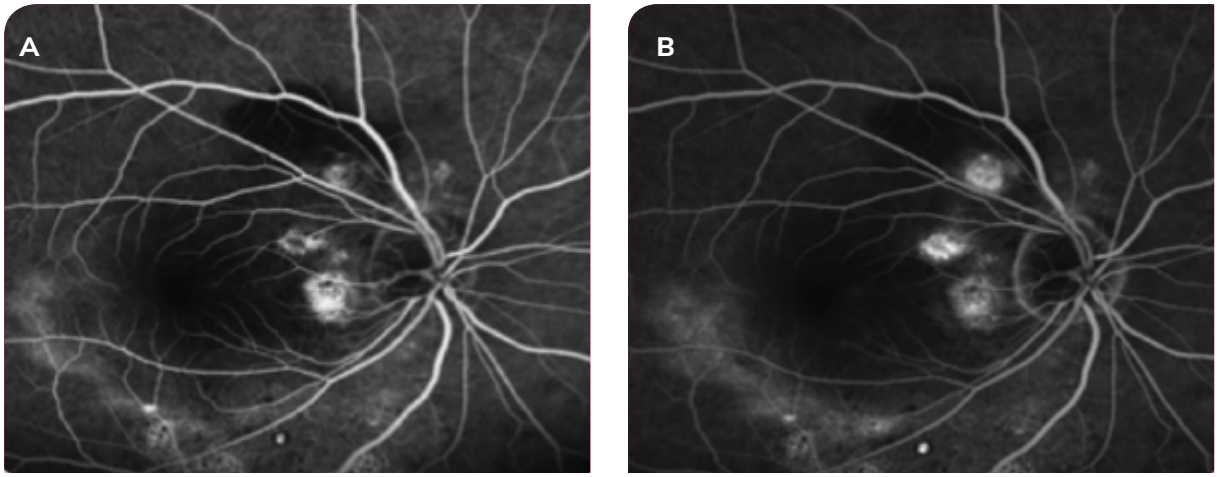

Fig. 3: Early-phase (A) and late-phase (B) fluorescein angiography.

Progressive hyperfluorescence of aneurysmal dilations, with little diffusion during the late phase and a hyperfluorescent branching vascular network that is difficult to differentiate from the polyps.

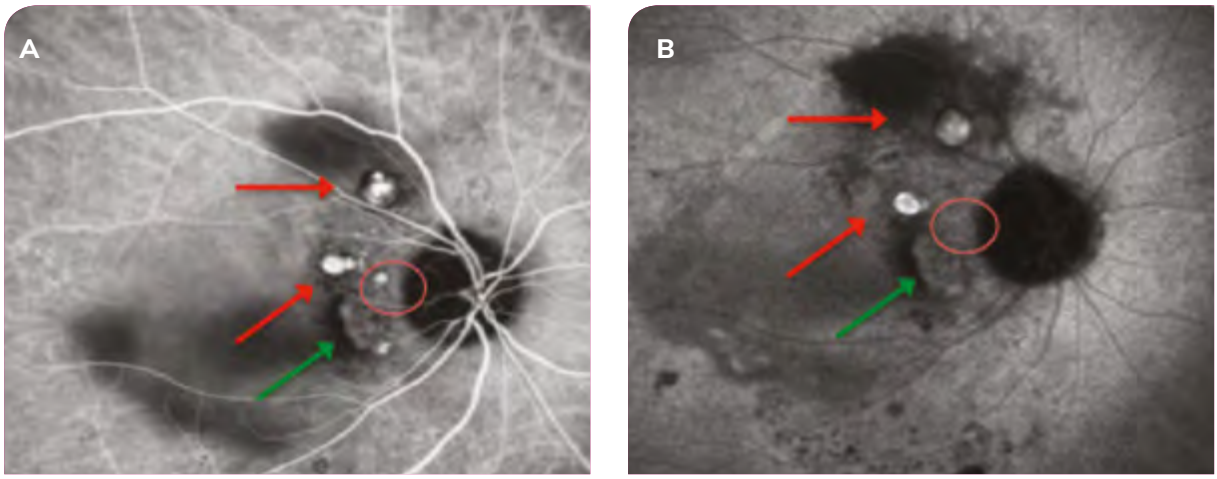

Fig. 4: Early-phase (A) and late-phase (B) ICG angiography.

The polyps appear as round, hyperfluorescent lesions (red arrows) in the early phases and may remain into the late phases or undergo “wash-out” (red circle). The polyps are accompanied by the BVN (green arrow), which is visible in the early phases with polyps located within the network or on its edge, resulting in a late hyperfluorescent lesion.

3) SD-OCT

A diagnosis of PCV can be strongly suspected based on OCT findings. Polyps appear as dome-shaped elevations in the RPE containing one or more hyperreflective rings associated with a hyporeflective centre. The BVN causes flat, irregular elevation of the RPE ("double layer sign"), visible as two highly reflective layers (the RPE and a layer beneath the RPE). If exudation is present, serous retinal detachment, intraretinal cystoid spaces or retinal thickening may be observed. Swept-source imaging or EDI usually reveals a pachychoroid (> 300 µm) associated with "pachyvessels"[2] (Figure 5).

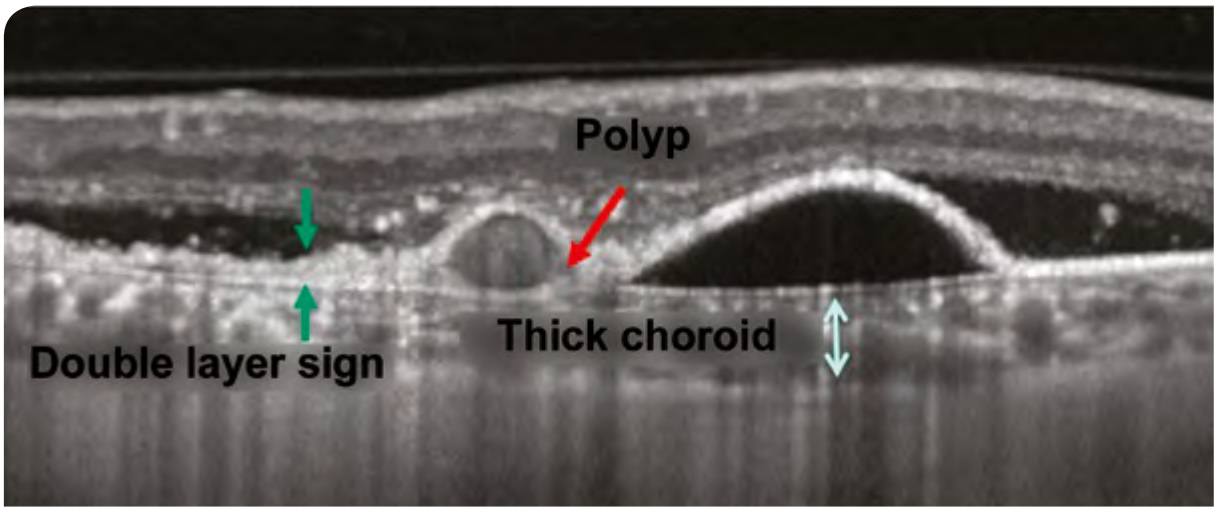

Fig. 5: Polypoidal choroidal vasculopathy as it appears in SD-OCT.

The polyps look like an ogival or "steep slope" PED, sometimes adjoining a serous PED. The double layer sign is also found, along with a thick choroid.

4) OCTA

OCTA is at present of little use when it comes to imaging polyps. However, the BVN, which is characterised by linear blood flow, is easily detected by OCTA. Polypoid lesions appear in most cases as hypodense round structures with no flow or hyperdense round structures with flow (between 17 and 45% of cases, depending on the series[4]), occasionally encircled by a hypodense halo. The lack of signal in the polyp does not mean that there is no blood flowing, rather that the characteristics of the blood flow do not meet the OCTA detection criteria (Figures 6 and 7). This failure to detect the blood flow may be caused by signal attenuation linked to the RPE, or by the flow characteristics being undetectable: the flow may be too weak or circulating only at the edges of the polyp, or there may be hyalinisation of the polyp, blocking out the light. As the technology currently stands, therefore, OCTA cannot be used in place of ICG to detect and assess PCV[4].

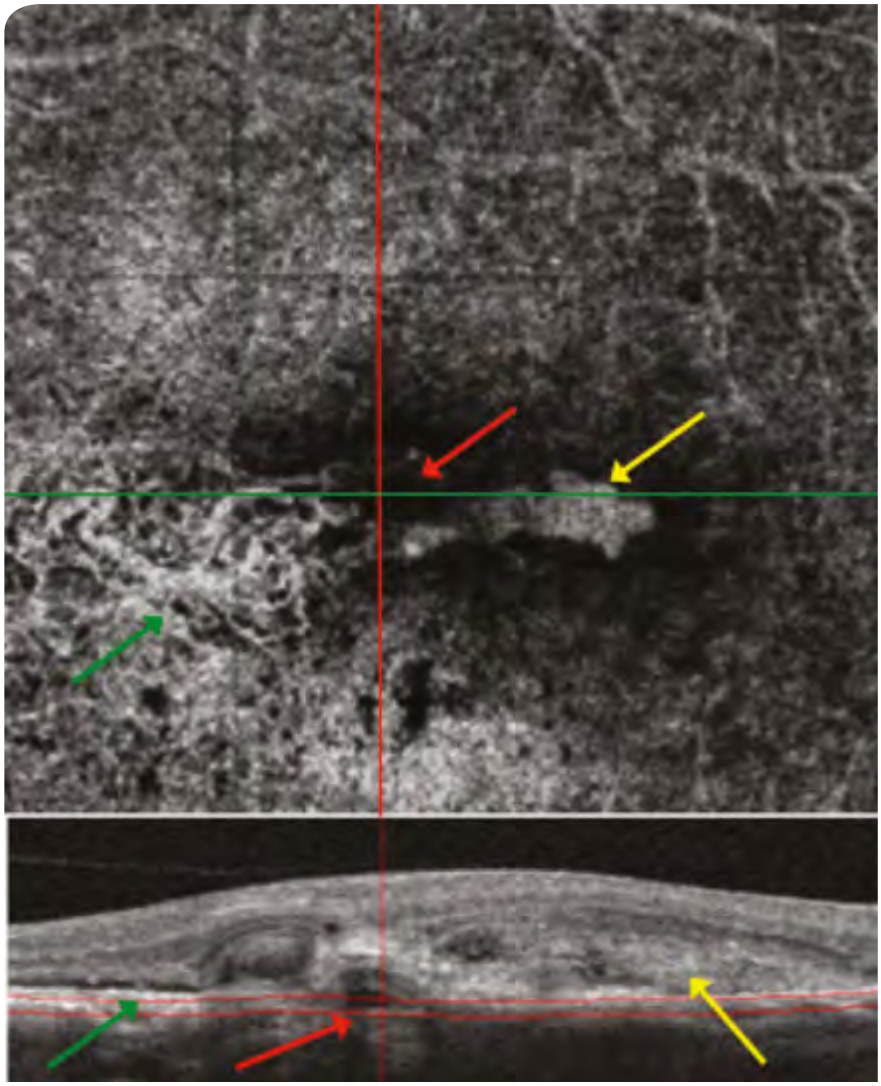

Fig. 6: PCV associated with type 2 choroidal neovascularisation in a treatment-naive male patient.

OCTA of the choriocapillaris shows the abnormal choroidal network in the form of a hyperdense lesion with flow (green arrow). The polypoid lesion appears as a hypodense, round structure with no flow (red arrow) and the neovascularisation as a hyperdense structure with flow (yellow arrow).

2. PCV classification

Certain authors have suggested categorising PCV into different subtypes[5-6] based on how it appears in ICG and OCT. Type 1 PCV, or "polypoidal neovascularisation", is distinguishable by its drainage network (the BVN) and feeder vessel, a thinner choroid with large lesions, and a positive response to anti-VEGF (Figure 7). Type 2 PCV, or "idiopathic PCV", features no BVN, or only a very faint one, a small lesion and a thicker choroid (Figure 8). Recently, an American team proposed a new term for PCV: "aneurysmal type 1 choroidal neovascularisation"[5]. However, there is no consensus around these subcategories and terms.

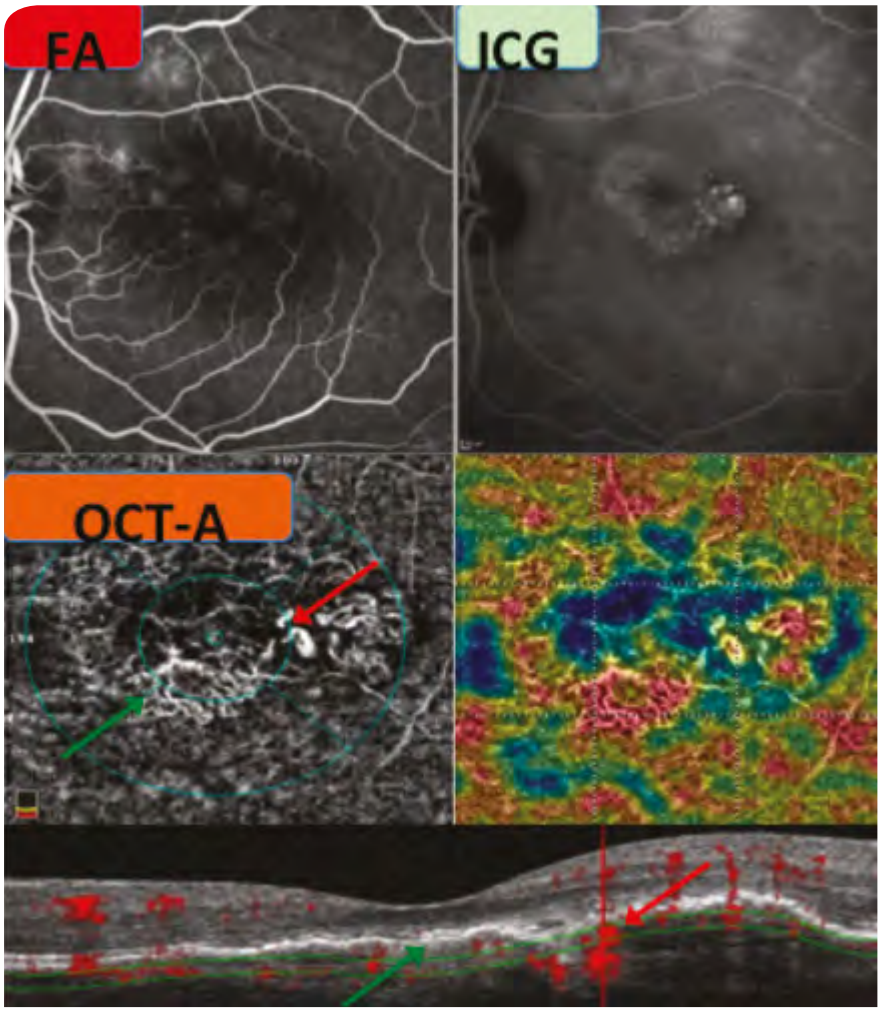

Fig. 7: PCV in a male patient undergoing treatment.

Top left and top right: fluorescein angiography and ICG images.
Middle left, middle right and bottom: OCTA with flow map (segmentation through the polyps and BVN). The polypoid lesion appears as a hyperdense, round structure with flow (red arrow) and the BVN as a hyperdense lesion with flow (green arrow).

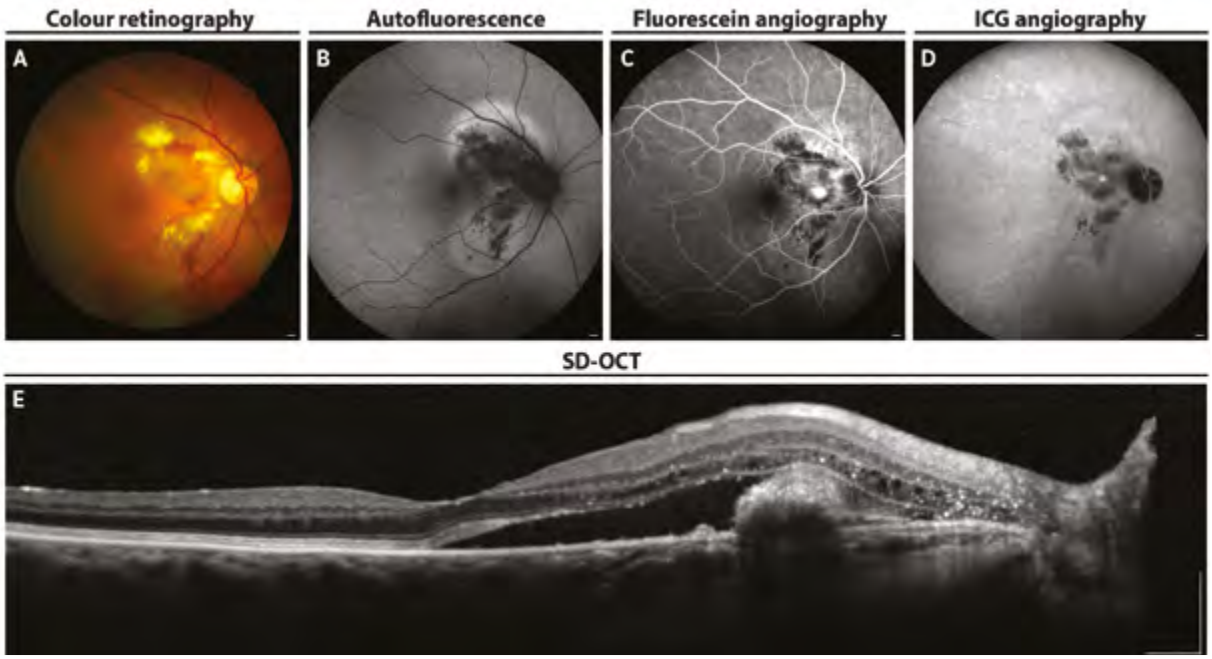

Fig. 8: Multimodal imaging of type 2 haemorrhagic polypoidal choroidal vasculopathy.

Colour fundus photograph (A) showing a haemorrhagic serous detachment between the optic disc and the macula. Autofluorescent photograph (B) showing hypoautofluorescent areas of serous retinal detachment (SRD). Fluorescein angiography (C) showing late-phase leakage from the polypoidal detachment. ICG angiography (D) showing late hypercyanescence of the polyp. SD-OCT (E) showing a hyperreflective polypoidal elevation, hyperreflective white dots and a macular SRD.

Conclusion

ICG remains the gold standard for diagnosing PCV and can be useful for monitoring it. OCT can provide highly characteristic images of PCV, while the current resolution of OCTA is insufficient for it to replace ICG in PCV. Finally, a diagnosis of AMD must be reassessed by ICG if the therapeutic response is insufficient, as PCV may be present. Angiography for PCV can also involve OCT B-scan, en-face OCT and OCTA, since they can distinguish between the BVN and polypoid lesions and display the neovascular activity, revealing the extent of intraretinal and subretinal exudation.

References

1. Yannuzzi LA. Idiopathic polypoidal choroidal vasculopathy. Macula Society Meeting 1982; Miami, Florida, USA.
2. Gallego-Pinazo R, Dolz-Marco R, Gómez-Ulla F *et al.* Pachychoroid Diseases of the Macula. Med Hypothesis Discov Innov Ophthalmol. 2014;3(4):111-5.
3. Dansingani KK, Gal-Or O, Sadda SR *et al.* Understanding aneurysmal Type 1 neovascularization (polypoidal choroidal vasculopathy): a lesson in the taxonomy of 'expanded spectra' - a review. Clin Exp Ophthalmol. 2018;46(2):189-200.
4. Srour M, Querques G, Semoun O, *et al.* Optical coherence tomography angiography characteristics of polypoidal choroidal vasculopathy. Br J Ophthalmol. 2016 ;100(11):1489-1493
5. Kawamura A, Yuzawa M, Mori R *et al.* Indocyanine green angiographic and optical coherence tomographic findings support classification of polypoidal choroidal vasculopathy into two types. Acta Ophthalmol. 2013;91:e474–e481.
6. Tanaka K, Nakayama T, Mori R *et al.* Associations of complement factor H (CFH) and age-related maculopathy susceptibility 2 (ARMS2) genotypes with subtypes of polypoidal choroidal vasculopathy. Invest Ophthalmol Vis Sci. 2011;52:7441–7444.

Type 1 neovascularisation

PART 7: Fibrous choroidal neovascularisation

Alexandra Miere, Manar Addou-Regnard, Eric Souied

1. Definition

Subretinal fibrosis is the result of complex tissue repair mechanisms, secondary to either the natural healing process[1] or treatment with vascular endothelial growth factor inhibitors (anti-VEGF therapy)[2]. Recent studies on animal models[3-6] have found that the key factors in the development of fibrosis are connective tissue growth factor (CTGF), platelet-activating factor (PAF), the platelet-activating factor receptor (PAF-R) and macrophage-rich peritoneal exudate cells (PEC). In addition, the extensive use of anti-VEGF therapy to treat exudative age-related macular degeneration (AMD) has been found to carry a risk of the treated choroidal neovascularisation developing into macular atrophy and/or subretinal fibrosis, both of which are associated with poor visual outcomes[7,8].

2. Diagnosis

During dilated fundus examination, subretinal fibrosis can be identified as a clearly defined accumulation of raised, yellowish tissue, often with concave edges (Figure 1). In fluorescein angiography (FA), fibrosis is characterised by impregnation of the lesion in the late phases, with no leakage of the dye[7,8] (Figure 2). In SD-OCT, fibrosis appears as a compact, hyperreflective subretinal lesion, possibly accompanied by loss or fragmentation of the adjacent retinal pigment epithelium (RPE) and ellipsoid zone (Figure 1).

OCT-angiography (OCTA) is an imaging technique that offers excellent resolution at defined depths[9,10], enabling detailed analysis of the fibrotic scar. OCTA images of subretinal fibrosis almost always reveal a perfused vascular network, along with collateral architectural changes in the outer retina and the choriocapillaris (Figures 2 and 3). However, this examination can be impossible to interpret in some cases, due to very poor visual acuity or an inability to hold the gaze and the need for a high level of patient cooperation.

The neovascular network inside the fibrotic scar can display several different patterns, the most common of which is the “pruned tree” or “dead tree” (Figures 2 and 3), defined by an absence of visible fine capillaries in the slab corresponding to the fibrosis (outer retina and/or choriocapillaris). The accumulation of fibrous tissue may cause a blocking effect, resulting in a flow/signal void (Figure 3). In OCTA, subretinal fibrosis associated with neovascular AMD can be identified as distinct abnormal vascular networks within the fibrotic scar, which were previously undetectable by FA or SD-OCT alone[11].

The development of a qualitative classification for these networks would prove particularly valuable from a clinical and physiopathological perspective.

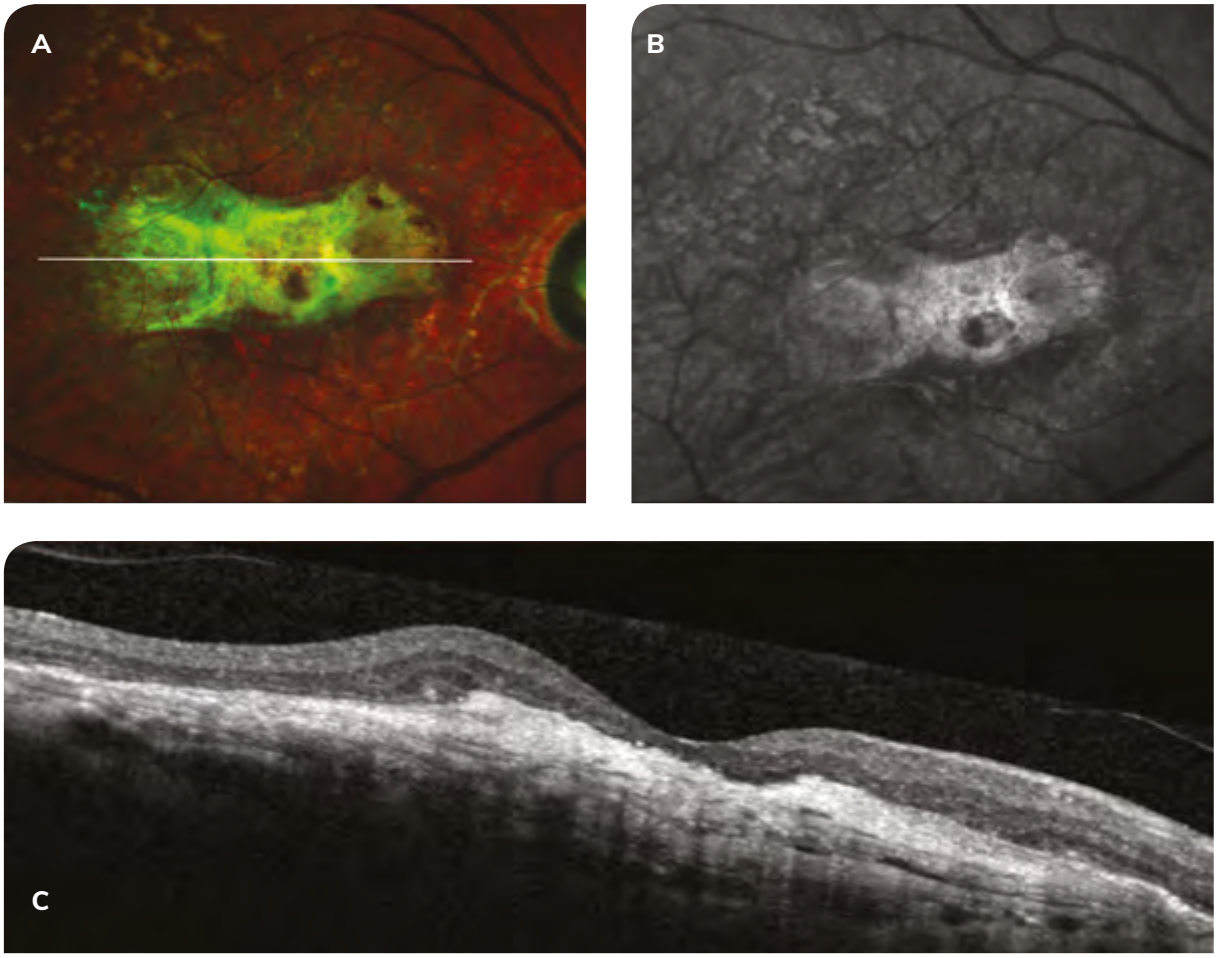

Fig. 1: Non-invasive multimodal imaging of the right eye of a male patient with a history of exudative AMD.

A: The Multicolor® image shows a clearly defined, yellowish lesion with concave edges.
B: In the infrared image, the lesion is well defined and hyperreflective.
C: The SD-OCT slice through the centre of the lesion shows a compact, uniform hyperreflective lesion. The retinal pigment epithelium is barely visible.

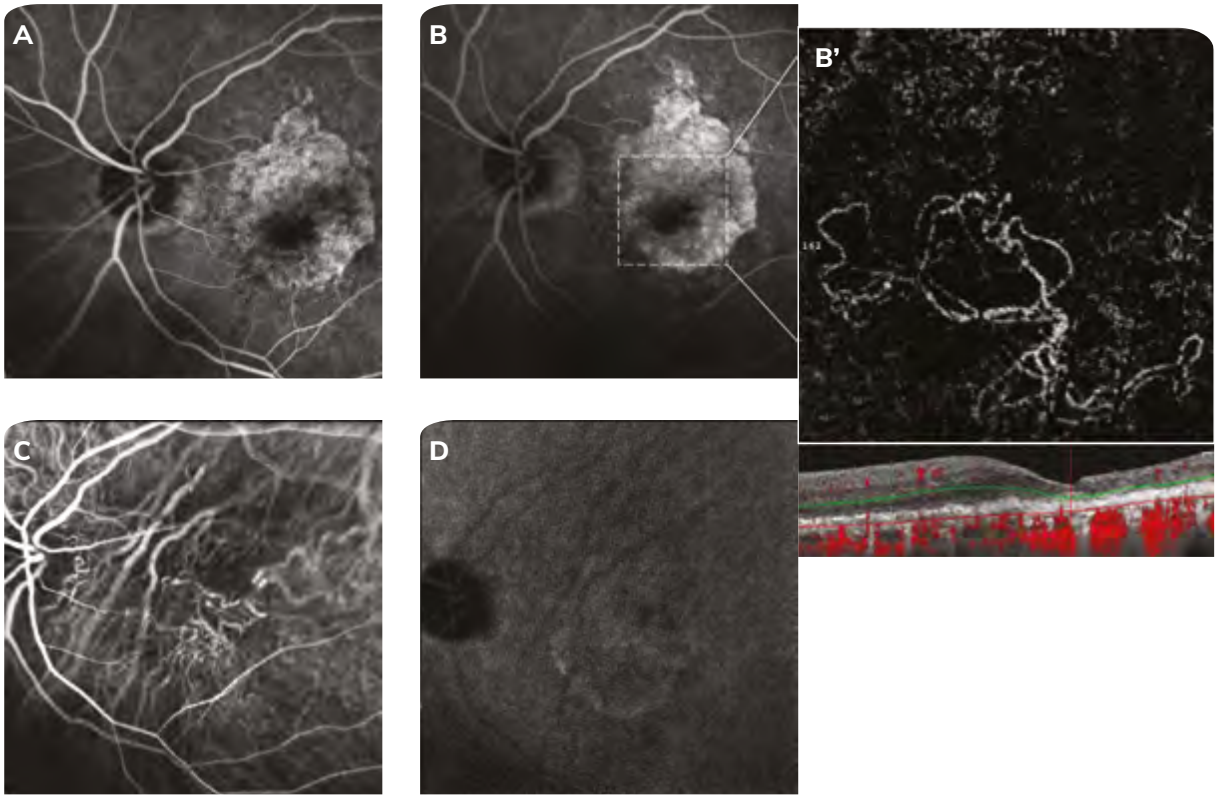

Fig. 2: Invasive and non-invasive multimodal imaging of the left eye of a female patient with a history of exudative AMD.

A and B: Fluorescein angiography in the early (A) and late (B) phases shows a hyperfluorescent subfoveal lesion, with no leakage of the dye in the late phases.
B': The OCTA flow image and the corresponding B-scan reveal, in the central 10° (3 x 3 mm acquisition window), the presence of a high-flow vascular network in the outer retina slab. Note that there are no fine capillaries, suggesting a "pruned tree" or "dead tree" pattern.
C and D: Indocyanine green angiography reveals the occult component of the fibrotic neovascular membrane.

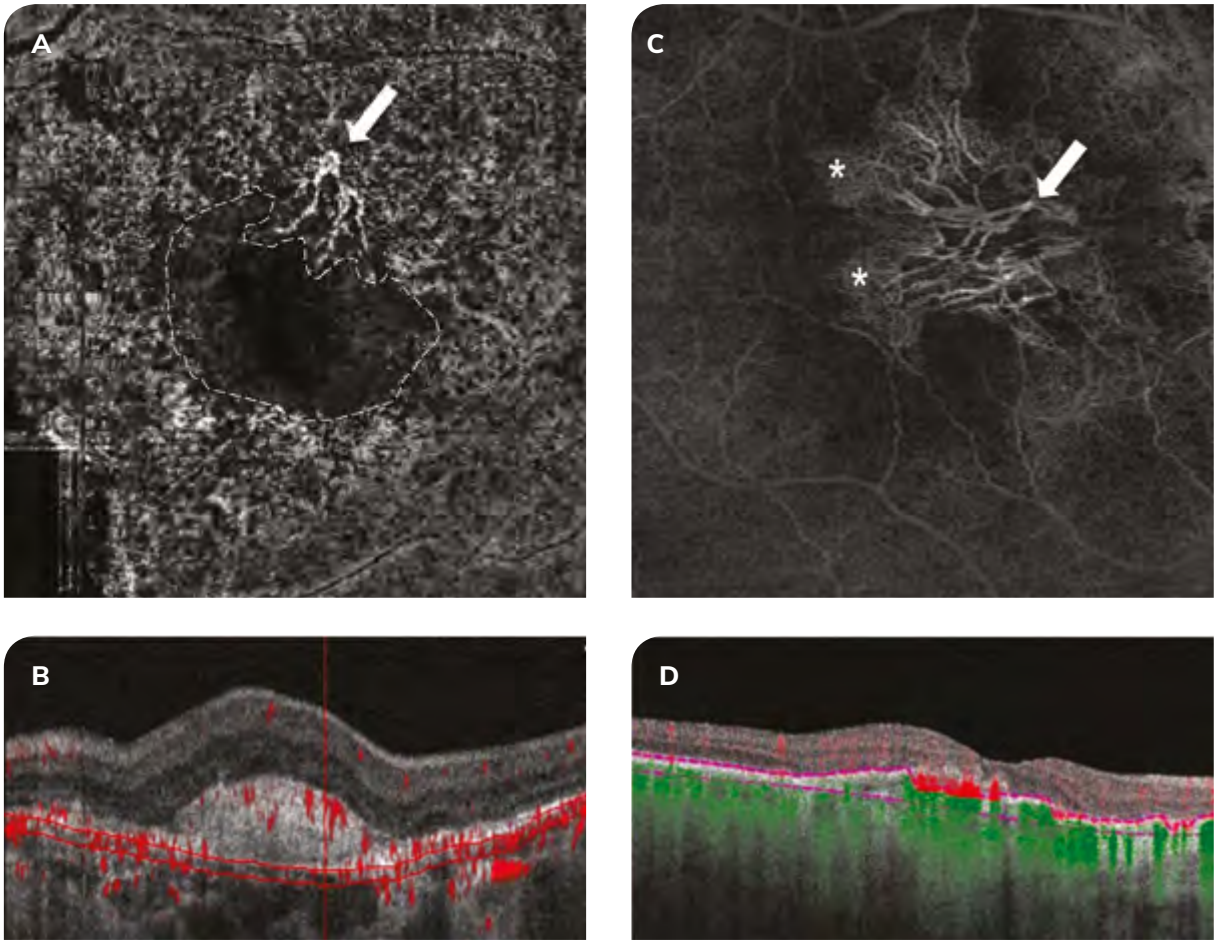

Fig. 3: Different OCTA images (6 x 6 mm) of high-flow networks inside fibrotic lesions.

A and B: Flow image (A) and corresponding B-scan (B) of a male patient with subretinal fibrosis secondary to AMD. In the flow image (A), a high-flow network can be seen in the choriocapillaris slab (white arrow), along with a flow/signal void caused by the fibrous tissue (dotted line).
C and D: Flow image (C) and corresponding B-scan (D) of a different male patient with subretinal fibrosis secondary to AMD. In the flow image (C), a high-flow "pruned tree" network can be seen in the slab including the fibrotic lesion, with the main vessels still visible (white arrow). Note that at either end of the lesion, there is nevertheless some capillary sprouting visible (asterisk).

References

1. Kumar V, Abbans K, Nelson F. Robbins and Cotran pathologic basis of disease. 9th ed. Philadelphia: Elsevier Saunders; 2014.

2. Hwang JC, Del Priore LV, Freund KB *et al.* Development of subretinal fibrosis after anti-VEGF treatment in neovascular age-related macular degeneration. Ophthalmic Surg Lasers Imaging 2011;42:6-11.

3. Moussad EE, Brigstock DR. Connective tissue growth factor. What's in a name? Mol. Genet. Metab. 2000; 71, 276–292.

4. Zhang H, Yang Y, Takeda A *et al.* ANovel Platelet-Activating Factor Receptor Antagonist Inhibits ChoroidalNeovascularization and Subretinal Fibrosis. PLoS One. 2013 27;8(6):e68173.

5. Jo YJ, Sonoda KH, Oshima Y *et al.* Establishment of a new animal model of focalsubretinal fibrosis that resembles disciform lesion in advanced age-related macular degeneration. Invest Ophthalmol Vis Sci 2011;52:6089-6095.

6. Cui W, Zhang H, Liu ZL. Interleukin-6 receptor blockade suppresses subretinal fibrosis in a mouse model. Int J Ophthalmol2014;7:194-197.

7. Bloch SB, Lund-Andersen H, Sander B, Larsen M. Subfoveal fibrosis in eyes withneovascular age-related macular degeneration treated with intravitrealranibizumab. Am J Ophthalmol 2013;156:116-124.

8. Channa R, Sophie R, Bagheri S *et al.* Regression of choroidal neovascularization results in macular atrophy in anti-vascular endothelial growth factor-treated eyes. Am J Ophthalmol 2015;159:9-19.

9. Jia Y1, Tan O, Tokayer J *et al.* Split-spectrum amplitude-decorrelation angiography with optical coherence tomography. Opt Express 2012; 20: 4710-4725.

10. Jia Y1, Bailey ST, Wilson DJ *et al.* Quantitative optical coherence tomography angiography of choroidal neovascularization in age-related macular degeneration. Ophthalmology 2014;121:1435-1444.

11. Miere A, Semoun O, Cohen SY *et al.* Optical coherence tomography angiography features of subretinal fibrosis in age-related macular degeneration. Retina. 2015; 35(11): 2275-84.

5

Type 2 neovascularization secondary to AMD

Al'a El Ameen

"Pre-epithelial" or "visible" type 2 choroidal neovascularisation (CNV) is the least common form of neovascularisation found in exudative age-related macular degeneration (AMD) (17.6% of cases)[1]. However, the visible characteristics of this form were the first to be described in the literature, since it can be seen directly in fluorescein angiography (FA). Like type 1 CNV, it is choroidal in origin, but expands below the retina after breaking through Bruch's membrane and the retinal pigment epithelium (RPE).

During **fundus examination**, it appears as a slightly raised yellowish macular lesion, sometimes accompanied by bleeding around the edges (Figure 1).

Studies of **infrared photographs** (820 nm) of type 2 CNV have revealed the presence of a whitish ring encircling a dark central core[2]. The edges of this ring correspond to the leakage zone in late-phase FA and the black halo encircling the neovascular membrane in the early phase (Figures 2 and 4).

Fluorescein angiography has long been the imaging gold standard for diagnosing type 2 CNV. It appears as a well defined area of hyperfluorescence corresponding to the neovascular membrane in the early phases, surrounded by a hypofluorescent area. The late phases are marked by gradual leakage of the dye from this lesion (Figures 2, 3, 4 and 5).

In **indocyanine green angiography**, type 2 CNV is often visible in the early phases as a hypercyanescent neovascular network that generally tends to disappear in the later phases (wash-out) (Figures 2, 3 and 4), but occasionally an area of hypercyanescence remains.

OCT shows both the neovascularisation and its exudative activity. In SD-OCT (spectral-domain OCT), type 2 neovascularisation is characterised by a pre-epithelial hyperreflective fusiform lesion accompanied by underlying hyporeflectivity (due to a shadow effect). Within this inhomogeneous hyperreflectivity, there is an area of abnormality in the appearance of the RPE, which can vary in size. If the neovascularisation is recent, the hyperreflectivity is not very dense or homogeneous, while older fibrovascular lesions result in more marked hyperreflectivity. As the neovascularisation progresses, slightly hyperreflective "grey" exudation gradually appears[3], resulting in an accumulation of hyporeflective subretinal fluid (serous retinal detachment [SRD]) at the edges or on top of the neovascularisation, along with intraretinal spaces (Figures 1 and 3).

OCT-angiography (OCTA) provides direct images of the neovascular network. The various types of neovascularisation that occur secondary to AMD are classified based on the slab in which the neovessels are visible and the presence or absence of flow in the corresponding B-scan. Type 2 neovascularisation is primarily visible in the outer retina slab, which is normally avascular[4] (Figures 2, 3 and 5). In certain cases, a feeder vessel can be identified. Numerous studies have attempted to assess the sensitivity of OCTA in detecting neovascularisation, with results ranging from 85 to 100%[5-7].

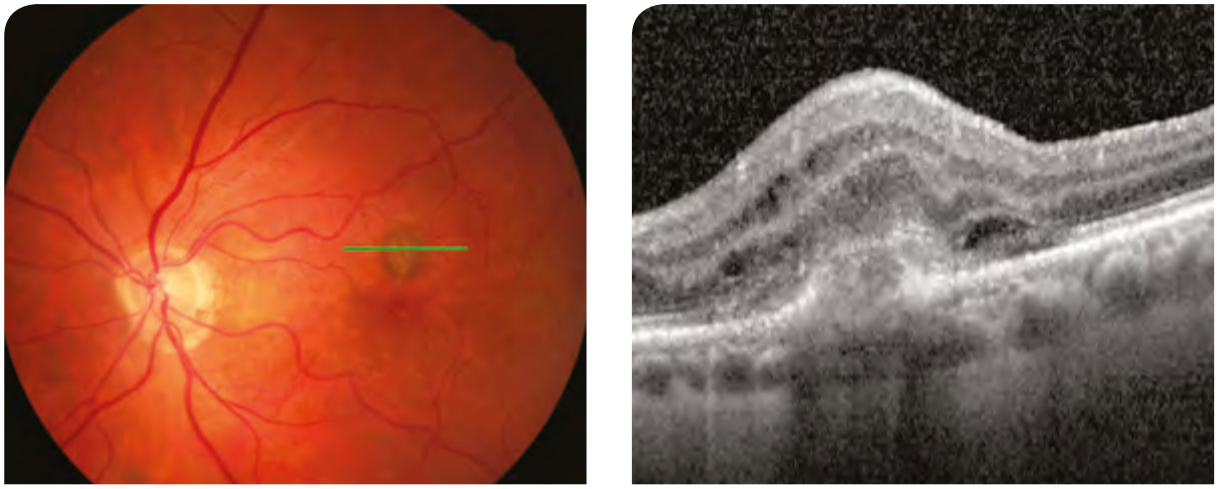

Fig. 1: Fundus photograph showing an oval, greyish superior macular lesion secondary to type 2 neovascularisation.

The SD-OCT slice through this lesion (green line) shows that it is hyperreflective, pre-epithelial and accompanied by SRD and exudative intraretinal spaces.

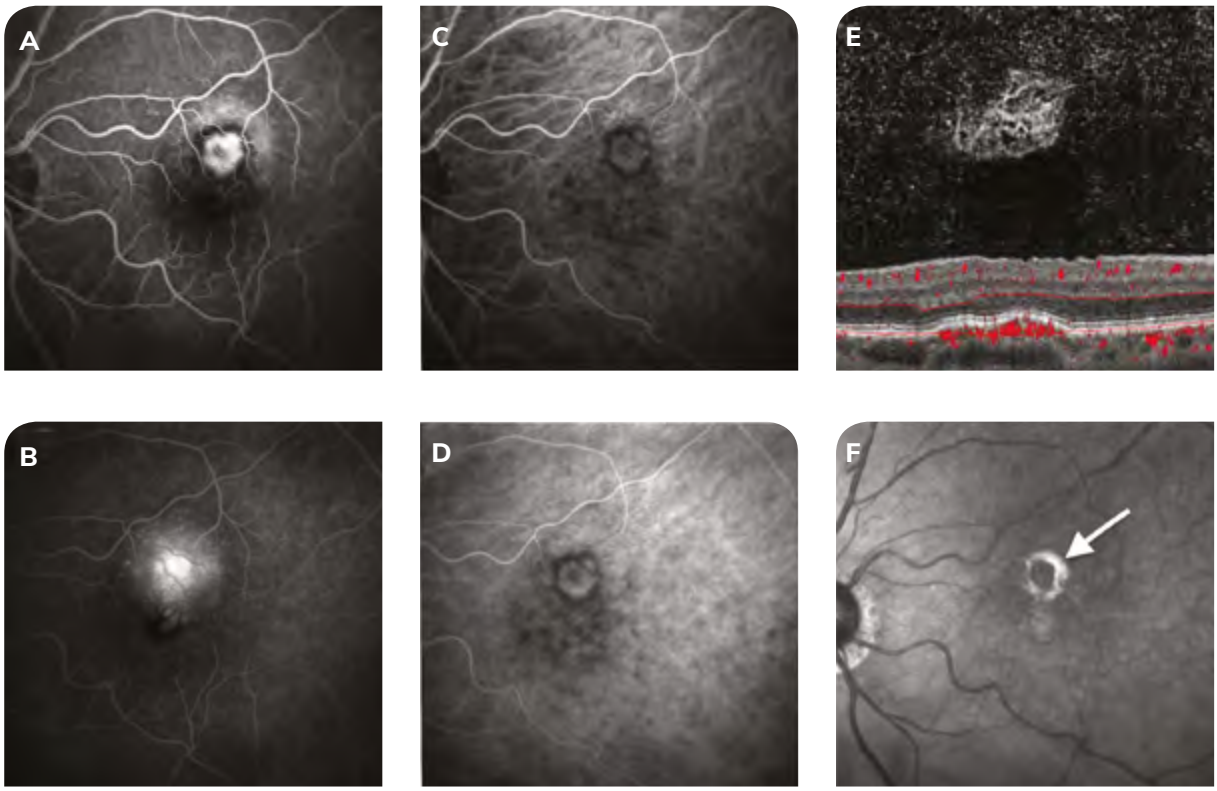

Fig. 2: Type 2 CNV in fluorescein angiography and ICG angiography.

A: The lesion from Figure 1 is hyperfluorescent in the early phase of fluorescein angiography and surrounded by a hypofluorescent ring.
B: The hyperfluorescence increases in intensity into the late phases of FA, with mild diffusion.
C: The early phase of ICGA reveals a hypercyanescent neovascular network.
D: The cyanescence increases slightly in the late phases, with no marked diffusion.
E: OCTA (Optovue®) clearly shows the type 2 CNV in the outer retina.
F: In infrared imaging, the neovascularisation appears as a whitish, hyperreflective ring (white arrow) encircling a dark central core.

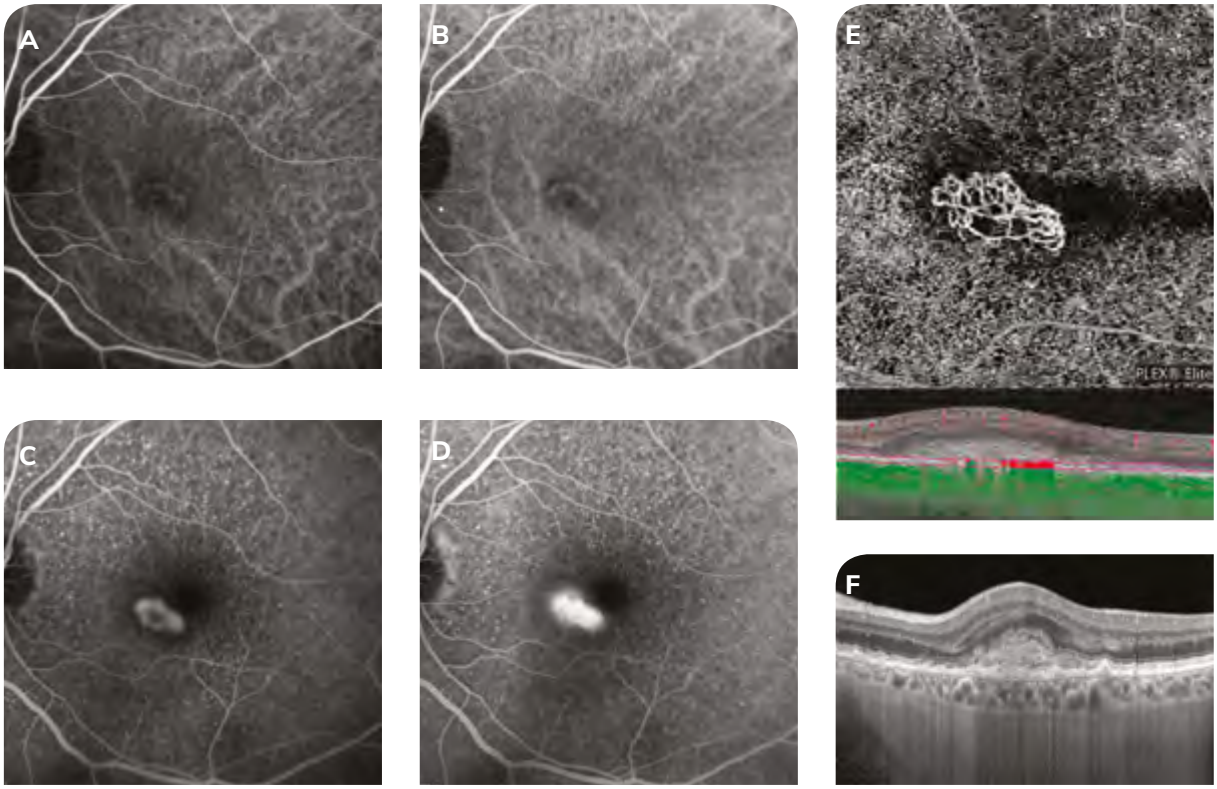

Fig. 3: Multimodal imaging of type 2 CNV.

A: Early-phase ICGA: well defined area of hypercyanescence corresponding to the neovascularisation.
B: Late-phase ICGA: the cyanescence increases slightly over time.
C: Early-phase fluorescein angiography: early hyperfluorescent image.
D: Late-phase fluorescein angiography: gradual leakage of the dye.
E: Hyperintense neovascular network clearly visible in OCTA (Zeiss® Plex Elite) in the outer retina slab.
F: The SD-OCT slice shows a pre-epithelial hyperreflective lesion causing an increase in retinal thickness.

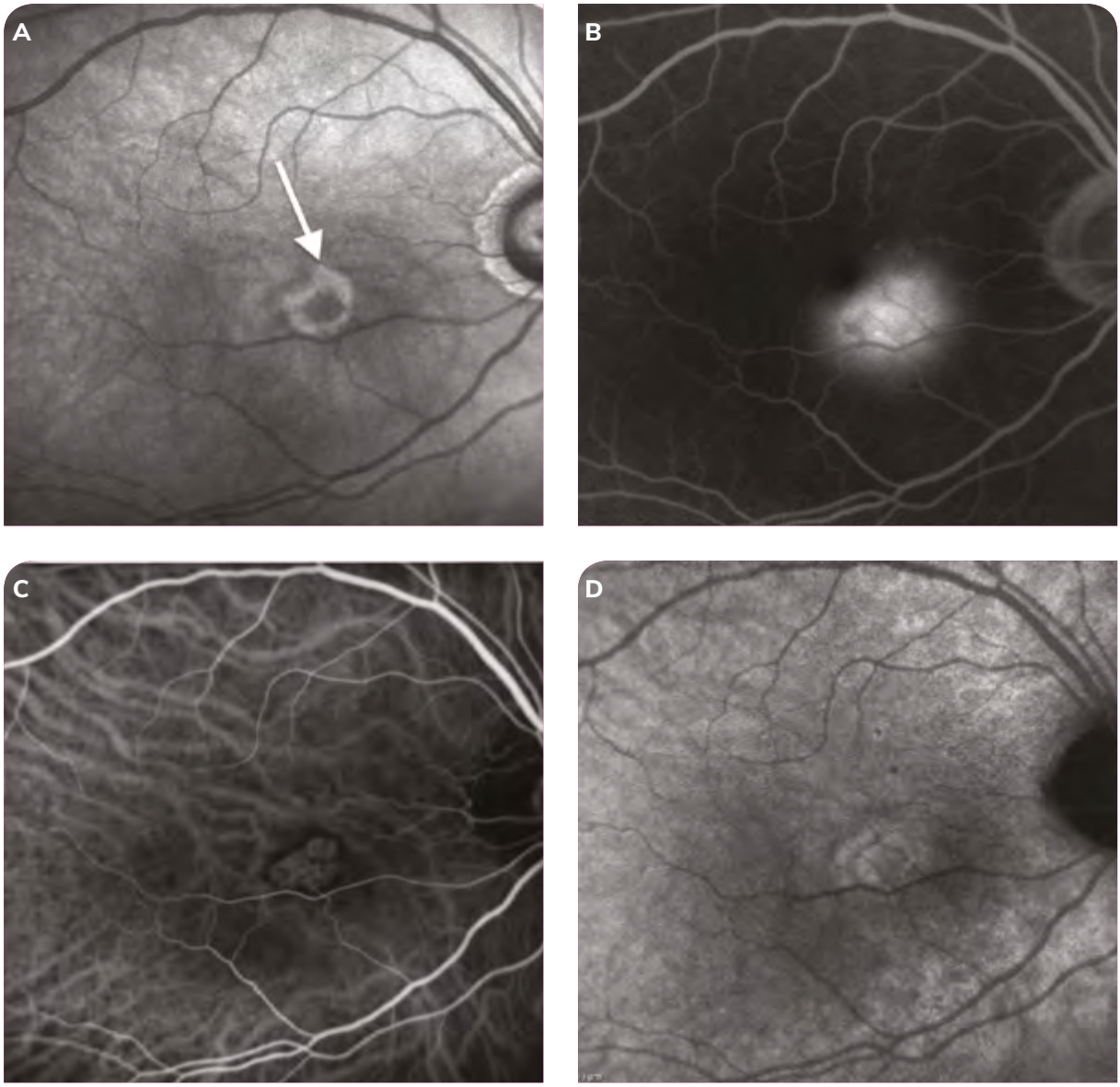

Fig. 4: Multimodal imaging of type 2 CNV.

A: Infrared photograph: the neovascularisation appears as a whitish, hyperreflective ring (white arrow) with a dark central core.
B: Late-phase fluorescein angiography: gradual leakage of the dye.
C: Early-phase ICGA: well defined area of hypercyanescence corresponding to the neovascularisation.
D: Late-phase ICGA: the cyanescence tends to decrease over time, due to wash-out.

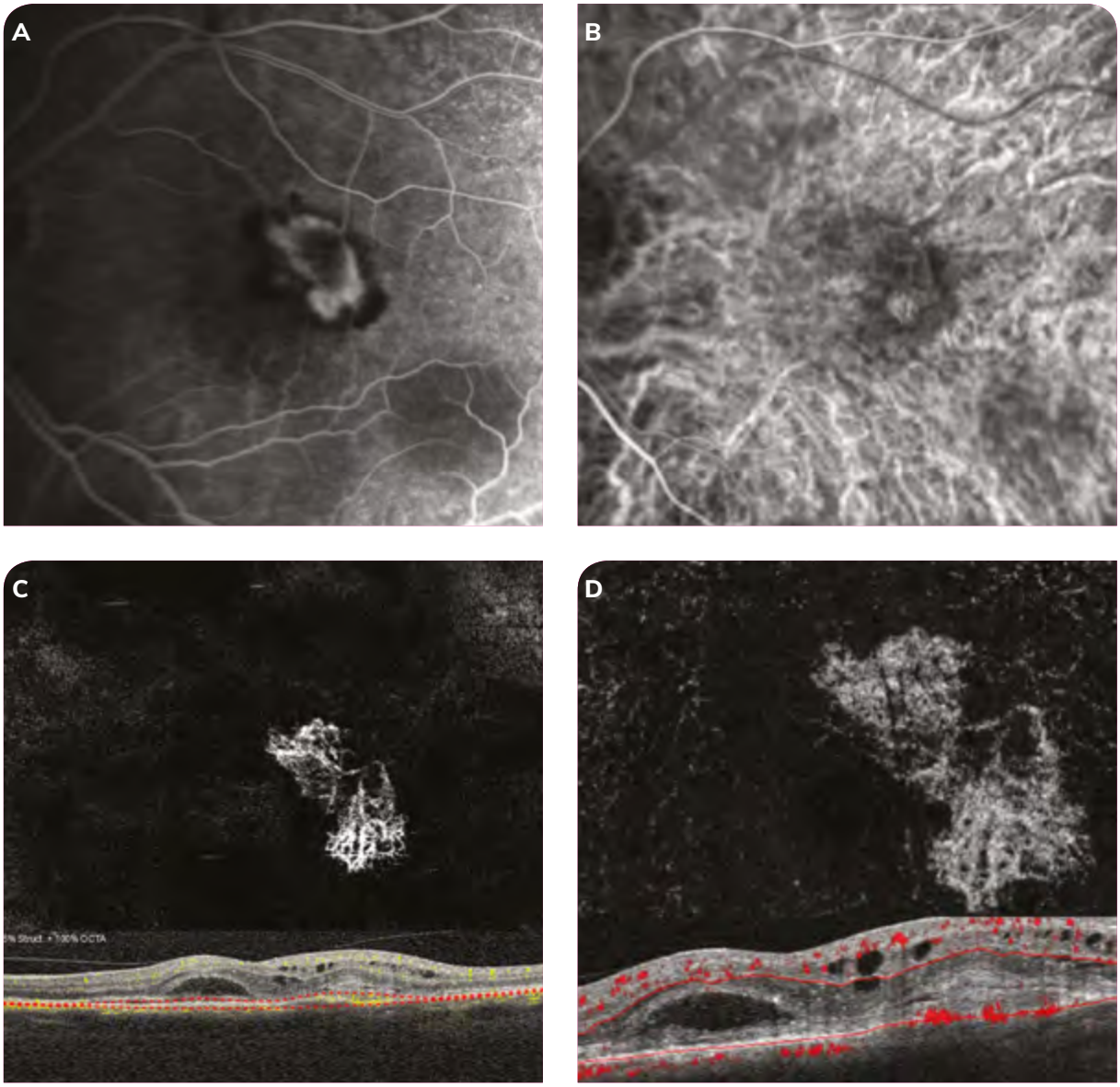

Fig. 5: Multimodal imaging of type 2 CNV.

A: Hyperfluorescent foveal lesion visible in the early phase of fluorescein angiography.
B: Neovascular network visible in early-phase ICGA.
C: OCTA (Spectralis-HRA®) and D: OCTA (Optovue®), both showing the hyperintense neovascularisation in the outer retina layer.

References

1. Cohen SY, Creuzot-Garcher C, Darmon J, *et al.* Types of choroidal neovascularisation in newly diagnosed exudative age-related macular degeneration. Br J Ophthalmol. sept 2007;91(9):1173-6.

2. Semoun O, Guigui B, Tick S *et al.* Infrared features of classic choroidal neovascularisation in exudative age-related macular degeneration. Br J Ophthalmol. févr 2009;93(2):182-5.

3. Ores R, Puche N, Querques G *et al.* Gray hyper-reflective subretinal exudative lesions in exudative age-related macular degeneration. Am J Ophthalmol. août 2014;158(2):354-61.

4. El Ameen A, Cohen SY, Semoun O et al. Type 2 neovascularization secondary to age-related macular degeneration imaged by optical coherence tomography angiography: retina. 2015;35(11):2212-8.

5. Inoue M, Jung JJ, Balaratnasingam C *et al.* A Comparison Between Optical Coherence Tomography Angiography and Fluorescein Angiography for the Imaging of Type 1 Neovascularization. Invest Ophthalmol Vis Sci.2016;57(9):314-323.

6. Faridi A, Jia Y, Gao SS *et al.* Sensitivity and Specificity of OCT Angiography to Detect Choroidal Neovascularization. Ophthalmol Retina. 2017;1(4):294-303.

7. Souedan V, Souied EH, Caillaux V *et al.* Sensitivity and specificity of optical coherence tomography angiography (OCT-A) for detection of choroidal neovascularization in real-life practice and varying retinal expertise level. Int Ophthalmol. 2018;38(3):1051-60.

6

Type 3 neovascularization

Alexandra Miere, Giuseppe Querques, Roxane Bunod, Eric H. Souied

Type 3 neovascularisation is a clinical form of neovascular AMD that preferentially affects the neurosensory retina and causes a compensatory telangiectasic neovascular response, associated with intraretinal proliferation[1].

1. History

In 1992, Hartnett described an angiomatous retinal lesion associated with drusen, which caused pigment epithelial detachment[2]. The origins of this form of neovascular AMD have been hotly contested over the years. Several different terms have been used to refer to this kind of lesion, including "chorioretinal anastomosis" (CRA) and "retinal angiomatous proliferation" (RAP).

In 2001, Yannuzzi described RAP as an angiomatous proliferation of retinal origin extending into the subretinal space. Several hypotheses were put forward to explain the formation of these lesions, which originate in the deep capillary plexus, including communication with (pre)existing choroidal neovascularisation[3,4].

Two years later, Gass described CRA as an intraretinal extension of type 1 neovascularisation[5]. It was Freund who eventually introduced the term "type 3 neovascularisation", as a logical extension of Gass' categorisation[5], to bring together the various different potential origins of this vascular complex. According to Freund, type 3 neovascularisation can cover all of the following[6]:

- Focal neovascular proliferation originating in the deep capillary plexus (essentially RAP)[1,6,7]
- Intraretinal neovascular extension of a type 1 choroidal neovascular membrane (occult choroidal neovascularisation) (essentially CRA)[1,5-7]
- De novo ruptures of Bruch's membrane, with neovascular infiltration of the retina[1,6,7].

2. Diagnosis

In **fundus examination**, type 3 neovascularisation is often characterised by small-scale haemorrhage near a vessel, often close to the fovea.

Type 3 lesion diagnosis and treatment response are determined using various imaging techniques: fluorescein angiography (FA), indocyanine green angiography (ICGA) and spectral-domain optical coherence tomography (SD-OCT)[3].

In **FA**, type 3 neovascularisation appears as a hyperfluorescent intraretinal vascular complex, typically located at the edge of the avascular foveal zone, resulting in late-phase leakage.

In **ICGA**, type 3 lesions are visible in the early phases in the form of a hyperfluorescent lesion, resulting in a "hot spot" in the late phases[3,8,9] (Figures 1 and 2).
SD-OCT plays a key role in type 3 neovascularisation. Typically, type 3 neovascularisation involves thinning of the choroid. The various stages in its development were recently categorised by Su *et al.*[10] as follows:

- Stage 1: intraretinal hyperreflective foci (HRF) associated with cystoid macular oedema, but no outer retinal disruption

- Stage 2: progression towards outer retinal disruption, with or without disruption of the retinal pigment epithelium

- Stage 3: posterior progression of the type 3 lesion, resulting in proliferation through the retinal pigment epithelium and serous pigment epithelial detachment (Figure 2).

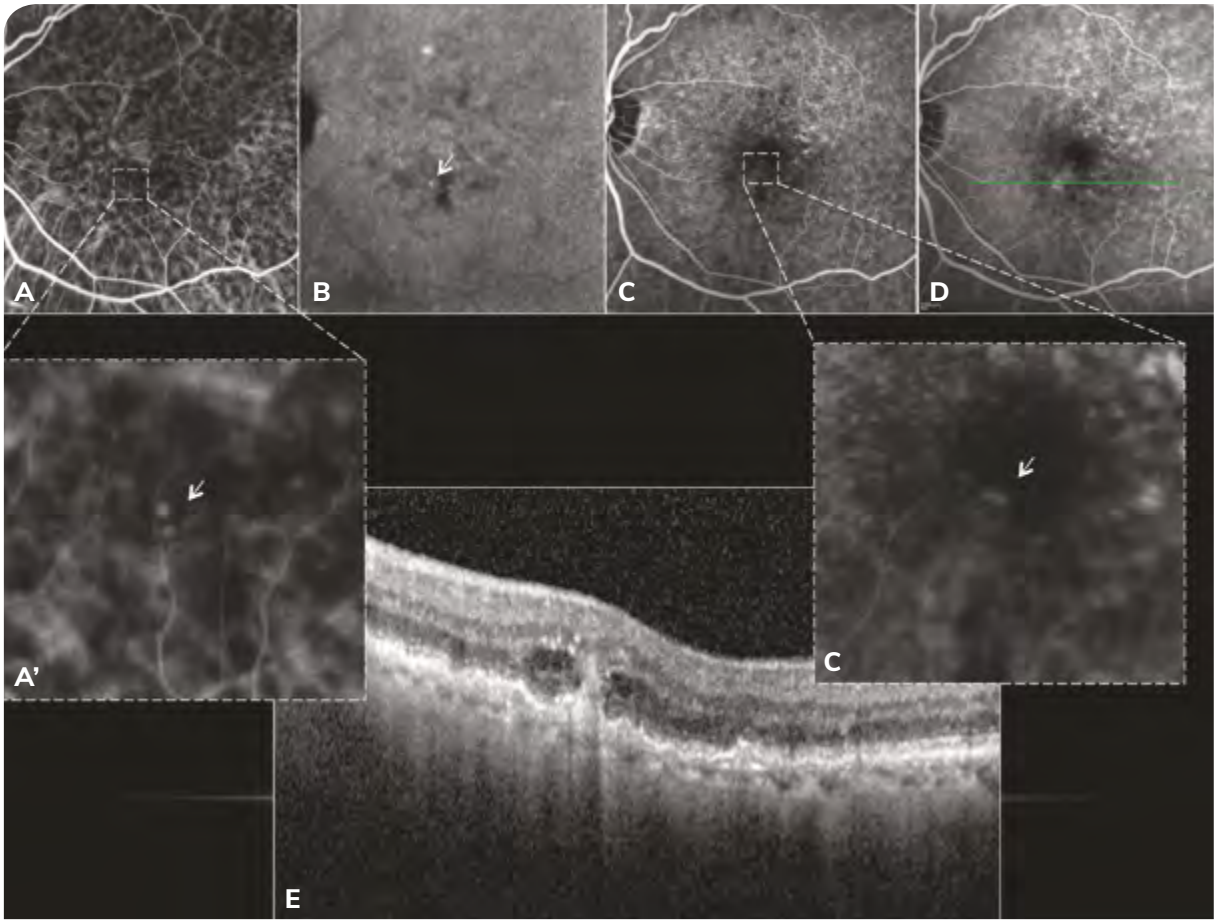

Fig. 1: Multimodal imaging of the left eye of an 83-year-old woman with type 3 neovascularisation.

A and B: Indocyanine green angiography reveals a hypercyanescent lesion in the early phases (A, white arrow on enlarged image A') and late phases ("hot spot") (B, white arrow).
C and D: Early-phase (C, white arrow on enlarged image C') and late-phase (D) fluorescein angiography shows a hyperfluorescent lesion below the avascular foveal zone, causing significant leakage.
E: Optical coherence tomography shows a funnel-shaped, hyperreflective intraretinal lesion accompanied by cystoid spaces.

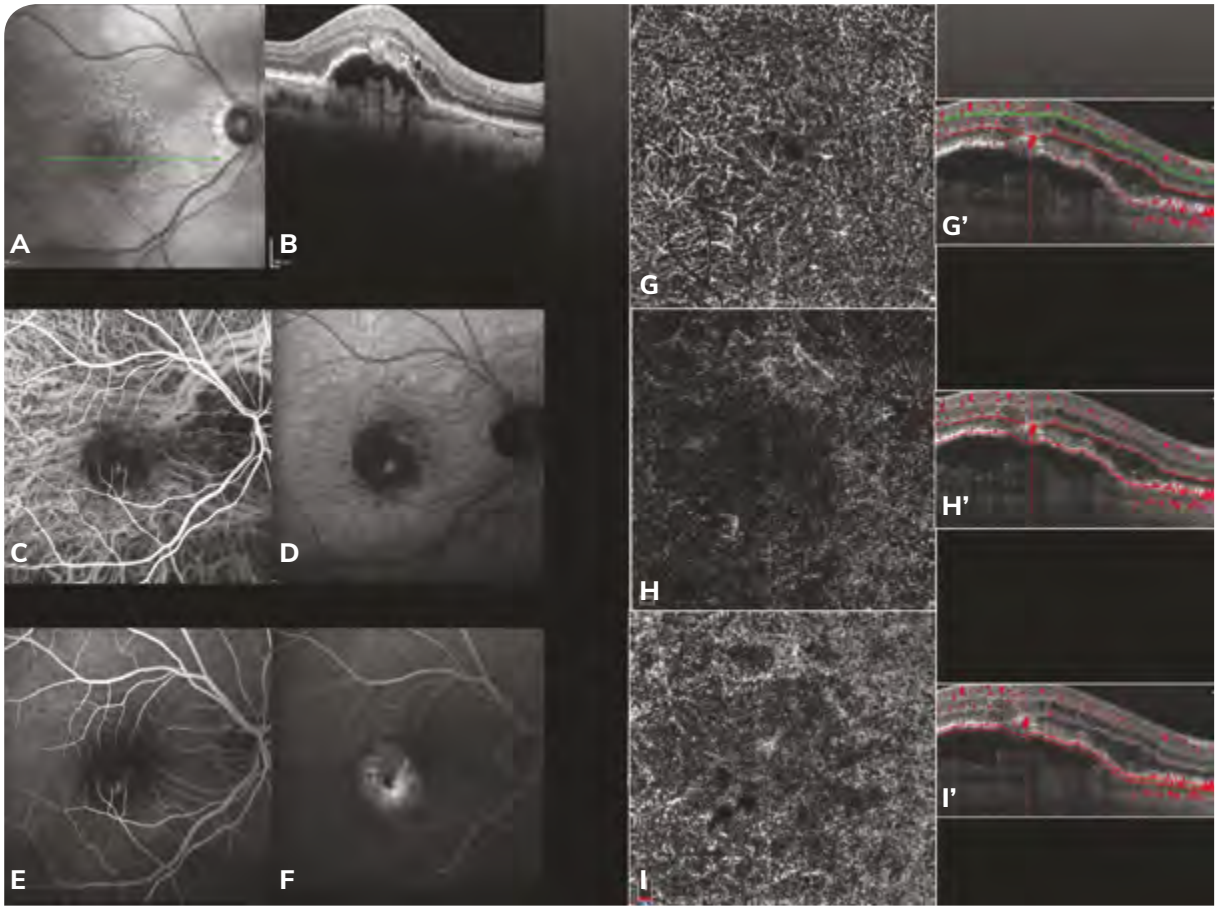

Fig. 2: Multimodal imaging of the right eye of a 78-year-old woman with type 3 neovascularisation.

A and B: The B-scan (B), guided by the infrared photograph (A), through the lesion below the avascular foveal zone reveals a hyporeflective pigment epithelial detachment, above which is a hyperreflective intraretinal vascular complex.
C and D: Indocyanine green angiography (C: early phase, D: late phase).
E and F: Fluorescein angiography (E: early phase, F: late phase) showing a hyperfluorescent lesion on the edge of the avascular foveal zone, causing a typical "hot spot" (D) in the late-phase ICGA images.
G and G': OCTA images: B-scan with flow superimposed (G') and en-face image of the deep capillary plexus (G) in 3 x 3 mm, revealing flow in the hyperreflective complex.
H and H': B-scan with flow superimposed (H') and en-face image of the outer retina (H) in 3 x 3 mm, revealing a tuft-shaped lesion.
I and I': B-scan with flow superimposed (I') and en-face image of the choriocapillaris (I) in 3 x 3 mm, showing no neovascular lesions in this area.

3. Benefits of OCT-angiography

OCT-angiography (OCTA) has been used for several years to precisely analyse the retinal and choroidal microcirculation.

Acquisition windows of 3 x 3 mm and correct segmentation of the deep capillary plexus, outer retinal layers (outer retina) and choriocapillaris provide valuable information on the physiopathology and progression of type 3 lesions.

In OCTA, type 3 neovascularisation is defined by retino-retinal anastomosis (Figure 3). From the deep capillary plexus (origin), high-flow vessels extend into the outer retina, forming a high-flow, tuft-shaped lesion (hatched) (Figures 2 and 3). This lesion may gradually extend further, into the area below the retinal pigment epithelium and/or the choriocapillaris: a small glomerular lesion ("clew-like" lesion) can be seen in the OCTA image[11].

OCTA provides additional evidence to confirm that, in the majority of cases, type 3 neovascularisation is characterised by an intraretinal vascular complex originating in the deep capillary plexus (Figures 2 and 3)[11,12].

4. Progression

Two distinct lesion progression profiles have been observed when monitoring patients undergoing anti-VEGF therapy: either progression to atrophy (characterised by the lesion disappearing from the outer retina slab) or progression into the space below the retinal pigment epithelium (characterised by the persistence or *de novo* appearance of the small glomerular lesion in the choriocapillaris layer)[13].

It is therefore essential to take good quality images at the first examination and during follow-up in order to determine the progression profile.

5. Nascent type 3

One of the early signs of type 3 neovascularisation described recently by Sacconi *et al.*[12] is hyperreflective intraretinal foci located above a drusenoid PED, which can be easily confused with pigment migration. OCTA evidences early flow in these foci, before the exudative type 3 neovascular lesion appears. A new entity, "nascent type 3 neovascularisation", has therefore been created to describe this progression from a preclinical stage (hyperreflective focus and no exudation) to a clinical stage (progression of the lesion from the deep capillary plexus into the retinal pigment epithelium and the space below it, accompanied by exudation)[12] (Figure 4).

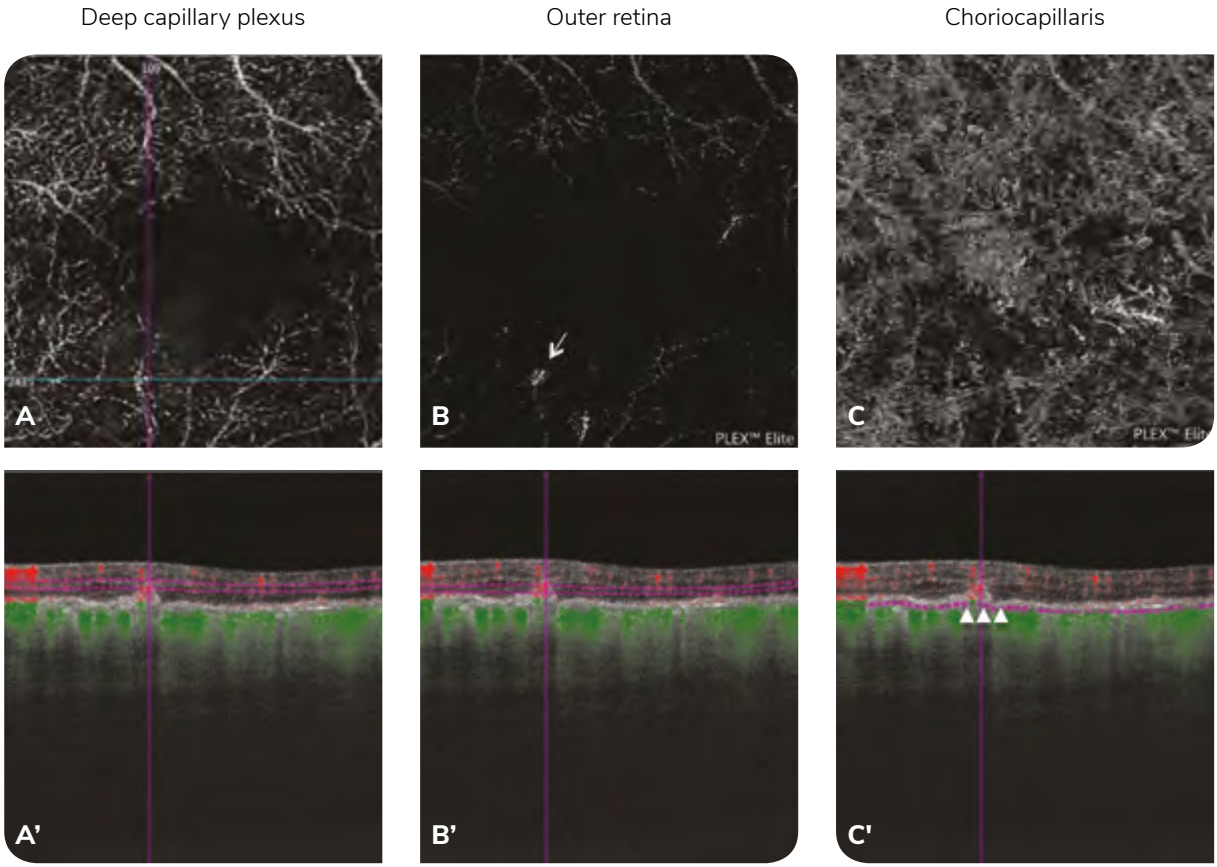

Fig. 3: OCTA of the left eye of the female patient in Figure 1.

A: En-face image of the deep capillary plexus slab, showing a high-flow vessel and a lesion at the intersection of the two navigation lines.
B: The outer retina slab reveals a high-flow, tuft-shaped lesion (white arrow).
C: Note that in the en-face image of the choriocapillaris slab, the lesion is not visible.
A', B' and C': B-scan with flow superimposed for each automatically segmented slab, showing the flow in this small, hyperreflective intraretinal complex. The flow is confined to the intraretinal zone (C', white arrowheads).

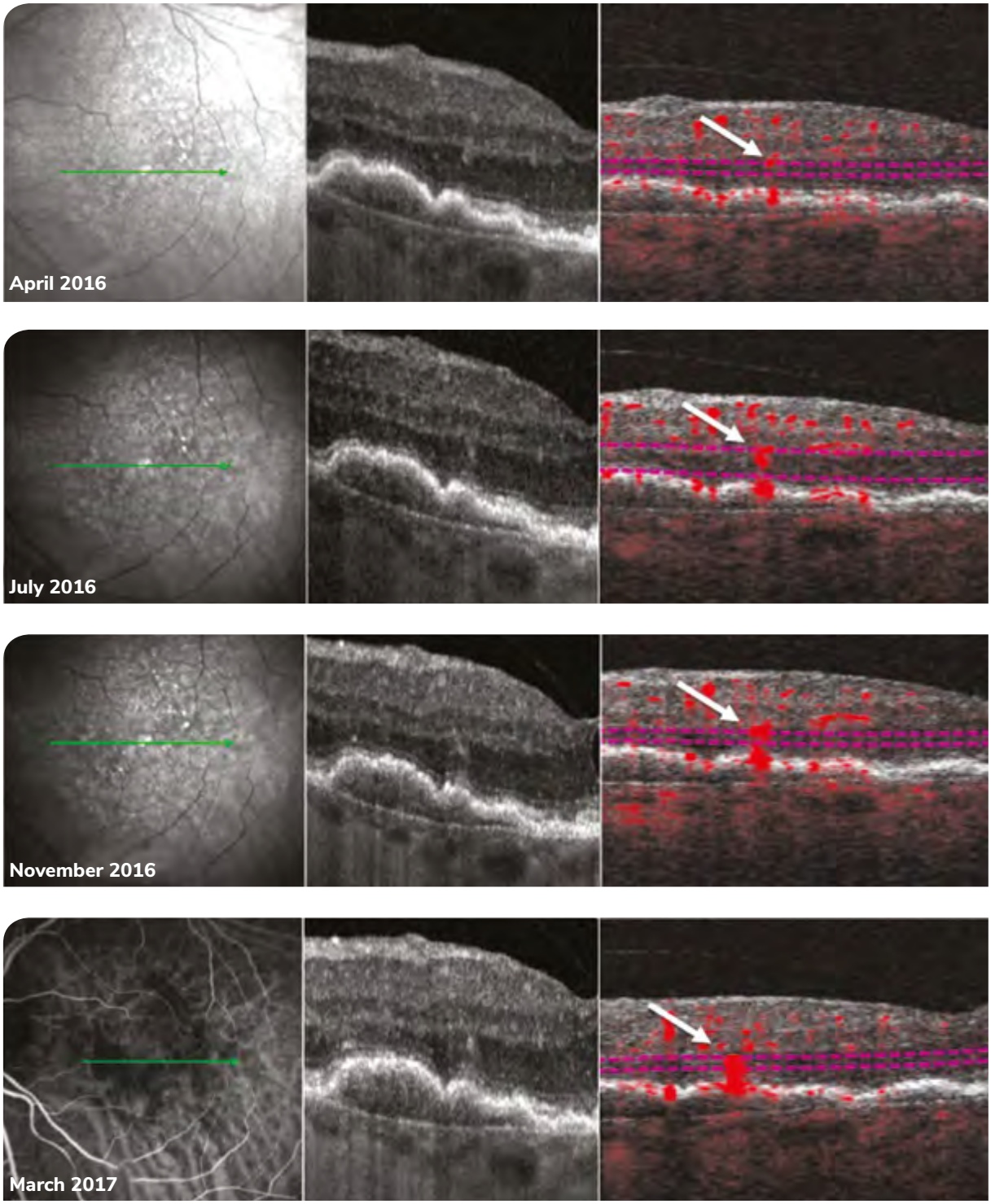

Fig. 4: Nascent type 3.

In April 2016, note the presence of a hyperreflective intraretinal lesion, located above a drusenoid PED, which could easily be confused with pigment migration. The OCTA B-scan shows that there is flow within it (arrow). Over time, the lesion gets closer to the PED, eventually taking the typical form of type 3 neovascularisation. This is therefore a case of nascent type 3 (images by Prof. Giuseppe Querques).

Conclusion

Both invasive (FA, ICGA) and non-invasive (SD-OCT, OCTA) multimodal imaging techniques are used to diagnose and monitor patients with type 3 neovascularisation. OCTA has confirmed the intraretinal origin of this neovascular lesion, which differs from type 1 and type 2 neovascularisation in that it originates in the deep capillary plexus.

References

1. Freund KB, Ho IV, Barbazetto IA, *et al.* Type 3 neovascularization: the expanded spectrum of retinal angiomatous proliferation. Retina 2008;28:201–211.
2. Hartnett ME, Weiter JJ, Garsd A, Jalkh AE. Classification of retinal pigment epithelial detachments associated with drusen. Graefes Arch Clin Exp Ophthalmol. 1992;230:11e19.
3. Querques G, Souied EH, Freund KB. How has high-resolution multimodal imaging refined our understanding of the vasogenic process in Type 3 neovascularization? Retina 2015;35:603-13.
4. Yannuzzi LA, Negrao S, Iida T, *et al.* Retinal angiomatous proliferation in age-related macular degeneration. Retina 2001;21:416–434.
5. Gass JD. Biomicroscopic and histopathologic considerations regarding the feasibility of surgical excision of subfoveal neovascular membranes. Am J Ophthalmol 1994;118:258–298.
6. Freund KB, Ho IV, Barbazetto IA, *et al.* Type 3 neovascularization: the expanded spectrum of retinal angiomatous proliferation. Retina. 2008;28:201–211.
7. Yannuzzi LA, Freund KB, Takahashi BS. Review of retinal angiomatous proliferation or Type 3 neovascularization. Retina 2008;28:375–384.
8. Kuhn D, Meunier I, Soubrane G, Coscas G. Imaging of chorioretinal anastomoses in vascularized retinal pigment epithelium detachments. Arch Ophthalmol 1995;113:1392–1398.
9. Jackson TL, Danis RP, Goldbaum M, *et al.* Retinal vascular abnormalities in neo-vascular age-related macular degeneration. Retina 2014;34:568–575.
10. Su D, Lin S, Phasukkijwatana N, *et al.* An updated staging system of type 3 neovascularization using spectral domain optical coherence tomography. Retina. 2016; 36 suppl 1: s40-s49.
11. Miere A, Querques G, Semoun O, *et al.* Optical coherence tomography angiography in early type 3 neovascu-larization. Retina. 2015 nov; 35(11): 2236-41.
12. Sacconi R, Sarraf D, Garrity S, *et al.* Nascent Type 3 Neovascularization in Age-Related Macular Degeneration. Ophthalmology Retina. (2018). 10.1016/j.oret. 2018.04.016.13. Miere A, Querques G, Semoun O, *et al.* Optical coherence tomography angiography changes in early type 3 neovascularization after anti-vascular endothelial growth factor treatment. Retina. 2017;37(10):1873-1879.

7

Adult-onset foveomacular vitelliform dystrophy (AFVD)

Jean-Louis Bacquet, Agnès Glacet-Bernard

1. Introduction

Adult-onset foveomacular vitelliform dystrophy (AFVD) is an eye disease found in middle aged to elderly patients. It is fairly common and there is disagreement as to the best way to diagnose and manage it (additional examinations, risk of complications, treatment).

It is commonly confused with other diseases, and certain aspects of its diagnosis and treatment are the same as for age-related macular degeneration. However, its natural history, clinical and paraclinical presentation and, in some cases, its genetic origin mark it out from AMD.

1) Definition: disease classification

AFVD is defined by a deposit of vitelliform ("resembling an egg yolk") material in the macula of a patient aged over 50 years.

a) Historic definition

The first description of AFVD is in a 1974 work by Donald Gass, in which he provides a clinicopathologic description of a "peculiar" macular dystrophy in nine patients. He links these clinical observations to the angiographic behaviour of the lesion and concludes that the macular dystrophy is presumably genetic in origin and autosomal dominant.

b) Contemporary definition

The precise, current definition of AFVD is summarised by Chowers *et al.*:

- It is a clinically and genetically heterogeneous disorder
- The term "dystrophy" is usually reserved for monogenic diseases and therefore should only be applied to genetic cases of AFVD, which are fairly rare
- The link with AMD and pattern dystrophy is not clear
- A similar-looking submacular deposit of foveal material can be observed in other pathological situations (toxicity, immune disease, infectious disease, injury etc.).

Today, AFVD is therefore considered to be a spectrum rather than a specific retinal disease.
The variety of different terms used to refer to AFVD contributes to the confusion:

- Adult vitelliform macular degeneration (according to Glacet-Bernard *et al.*, Epstein *et al.* and Greaves *et al.*)
- Pseudovitelliform macular degeneration (according to Sabates *et al.*)
- Adult-onset foveomacular pigment epithelial dystrophy (according to Vine *et al.*)
- Adult pseudovitelliform dystrophy (according to Burgess *et al.*)
- Adult vitelliform macular dystrophy (according to Bird *et al.*)

In 1997, Marmor *et al.* suggested that AFVD falls within the **pattern dystrophy** group, and it remains as such in several reference works (e.g. *Retinal Atlas*, Yannuzzi *et al.*) (Figure 1).

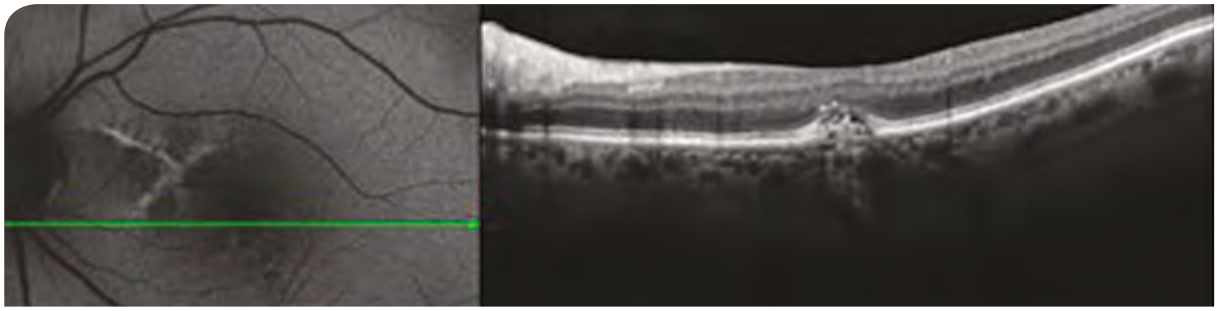

Fig. 1: Blue-light autofluorescence photograph and OCT slice.
AFVD in the vitelliruptive stage, associated with linear retinal pigment epithelium changes evocative of pattern dystrophy (Deutman's butterfly-shaped pattern dystrophy).

2) Physiopathology and genetics

There is no convincing definitive physiopathogenic theory to explain this accumulation of subfoveal material. The nature of the material has been established through *post-mortem* biochemical and histological examination. It primarily comprises debris resulting from phagocytosis of the photoreceptor outer segments (which are rich in opsins and vitamin A derivatives), as well as pigment from the RPE, lipofuscin, macrophages and pigment epithelial cells.

Numerous authors have focused on genetic AFVD, resulting in information on the mechanisms by which the material accumulates at molecular level. As with AMD, genetic research has given us a clearer idea of the cellular and molecular natural history of AFVD.

- AFVD linked to monoallelic *BEST1* mutation appears to be due to impaired **phagocytosis** of the photoreceptor outer segments.
- AFVD linked to monoallelic *PRPH2* mutation seems to be caused by **structural aberrations of the photoreceptor outer segments**, making it harder and slower for them to be internalised and broken down.
- More rarely, another gene, IMPG, described by Isabelle Meunier, Christian Hamel *et al.*, causes impairment of the **interphotoreceptor matrix** (IPM). This disturbs the cycle of internalisation/renewal by the RPE.

In "non-genetic" AFVD, the most likely causal mechanism is **local dysfunction of the RPE**. The natural history of AFVD is probably **less severe and slower** than that of AMD.

2. Clinical presentation

AFVD is described as typically bilateral in effect, but in practice is often asymmetrical. The functional signs reported by patients with AFVD are those found with AMD (though often not all are present). However, it is frequently discovered unexpectedly during a routine ophthalmology consultation after the age of 40 years. A diagnosis may be suspected in the presence of a yellowish deposit of subretinal material, without the patient reporting any issues, and visual acuity is frequently maintained (Figure 2).

1) Natural history and complications

The disease begins with a deposit of subretinal material in the macular zone. The main explanation for this location is increased retinoid metabolism in the macular zone, combined with lower resorption capacity, which is also commonly found in the physiopathogenesis of macular oedema (microglial and lymphatic system, cones predominant, system linked to Müller cells only). Another interesting hypothesis is a distinct visual cycle—at molecular level—between cones and rods.

This material is then subjected to as yet unknown factors and ends up breaking down and being reabsorbed, sometimes with no impact on the photoreceptors or visual acuity, sometimes affecting retinal function (atrophy). Neovascularisation may occur at any stage of the disease.

2) Material accumulation/resorption sequence

The accumulation of initially homogeneous subretinal material takes on a “foliated” appearance: often several distinct layers piled on top of one another like domes. The upper section of the material is then reabsorbed, indicated by two common OCT signs:

- A hyporeflective growth under the photoreceptors, with an elongated appearance (Figure 3)
- Hyperreflective intraretinal dots, not always accompanied by pigment in biomicroscopy (Figure 4).

3) Macular atrophy

One of the most severe complications is macular atrophy complicating the resorption of the material: visual acuity is often limited to 20/400 or less (Figure 5).

When it is the only observed ophthalmological sign, this atrophy makes **retrospective diagnosis** difficult, if not impossible. The peri-atrophic retina may be free of any kind of lesion associated with pattern dystrophy. A diagnosis must therefore be determined in the same way as with other causes of bilateral macular atrophy: AMD, late-onset Stargardt disease, central areolar choroidal dystrophy, cone dystrophy etc.

This outcome remains rare to our knowledge, but in the literature, geographic atrophy resulting from AFVD is not usually studied separately to other diagnoses.

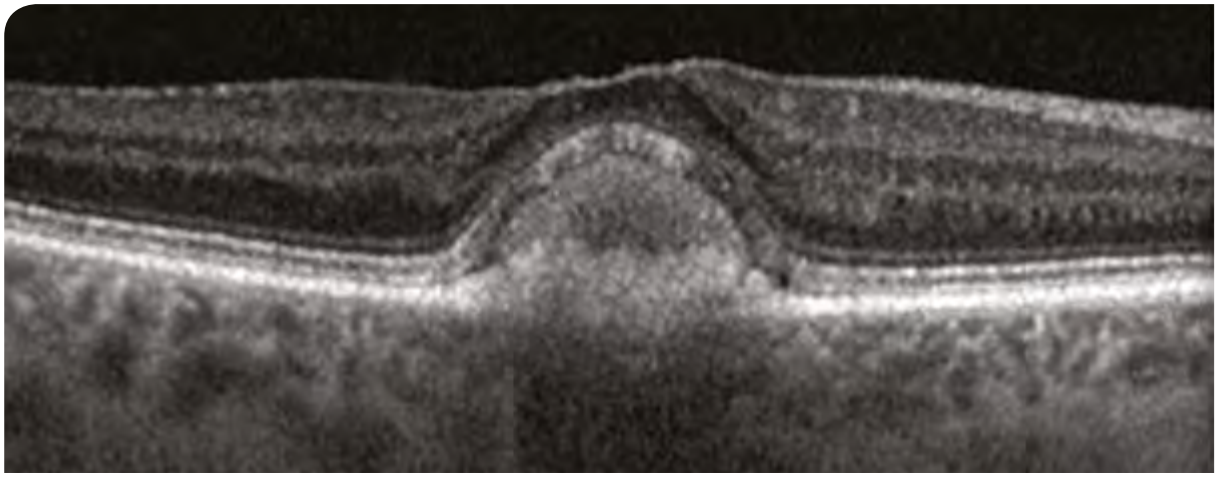

Fig. 2: Accumulation of subfoveal subretinal material in strata with intact retinal lamination and no visible atrophy. Vitelliform-stage AFVD.

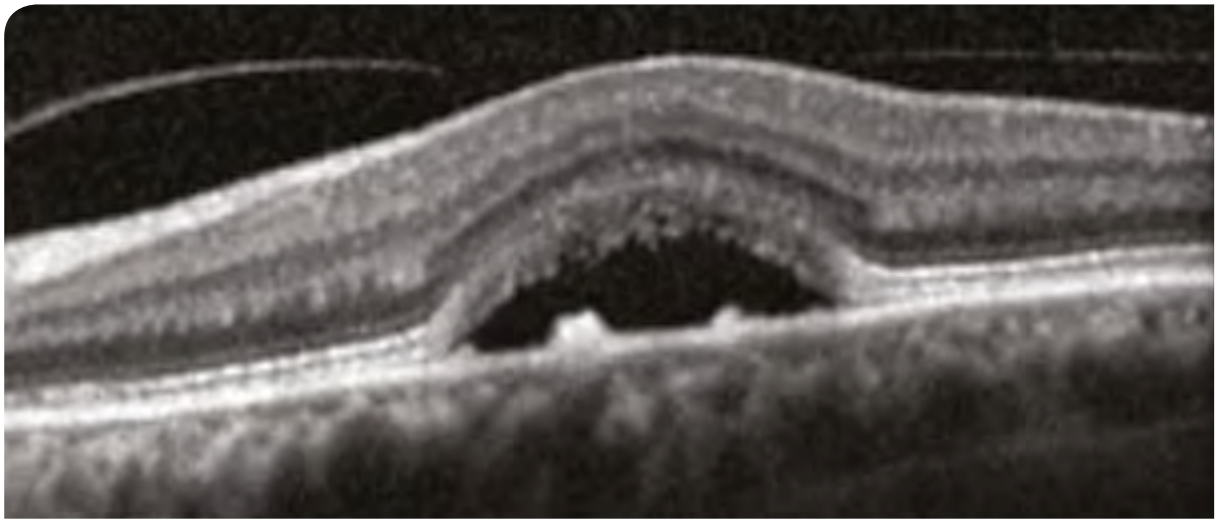

Fig. 3: Resorption-stage AFVD.
The photoreceptors are stretched mechanically, having lost their physiological interdigitation with the retinal pigment epithelium.

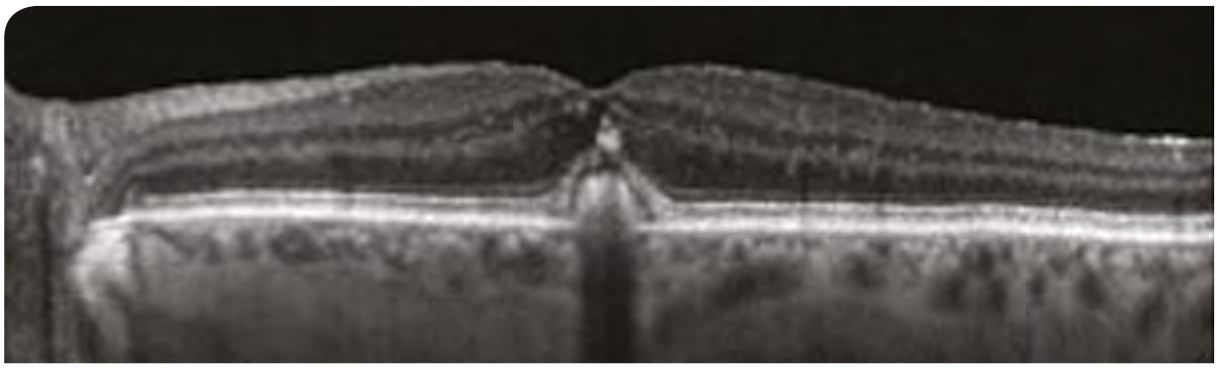

Fig. 4: Hyperreflective dots above the subretinal material in a 56-year-old male patient.
Visual acuity 20/20, no pigment migration observed.

4) Neovascular complications

As with atrophic progression, the frequency of choroidal neovascularisation (CNV) is difficult to quantify not only due to the difficulty of defining AFVD as a clinical entity, but because the literature often does not distinguish between neovascularisation and macular atrophy when discussing the complications of AFVD. Furthermore, imaging results can be misleading if an exudative lesion is present, as it may be mistaken for neovascularisation. According to the literature, CNV can complicate AFVD at any stage of the disease. Its prevalence is approximately 10%.

3. Imaging

1) Multimodal imaging (Figures 6, 7 and 8)

AFVD is diagnosed using multimodal imaging, as follows:

- Colour fundus photography showing monofocal or multifocal deposits of material, and any macular haemorrhage or angioid streaks
- Infrared imaging, which can be informative for at least two reasons: it can show very clear images of pattern dystrophy and the presence of reticular pseudodrusen, with their characteristic umbilicate appearance
- Blue-light autofluorescence imaging of the central 15 degrees, which can be used to measure the level of autofluorescence of the subretinal material and help rule out any differential diagnoses and associated lesions
- Spectral domain OCT: dense slices of the macula and a horizontal and vertical slice. This is important due to the sloped shape of the material during resorption. The nature of any associated drusen can be better determined using these macular slices than by examining the fundus.
- Enhanced depth imaging through the fovea, to assess **choroidal thickness**, which typically increases.

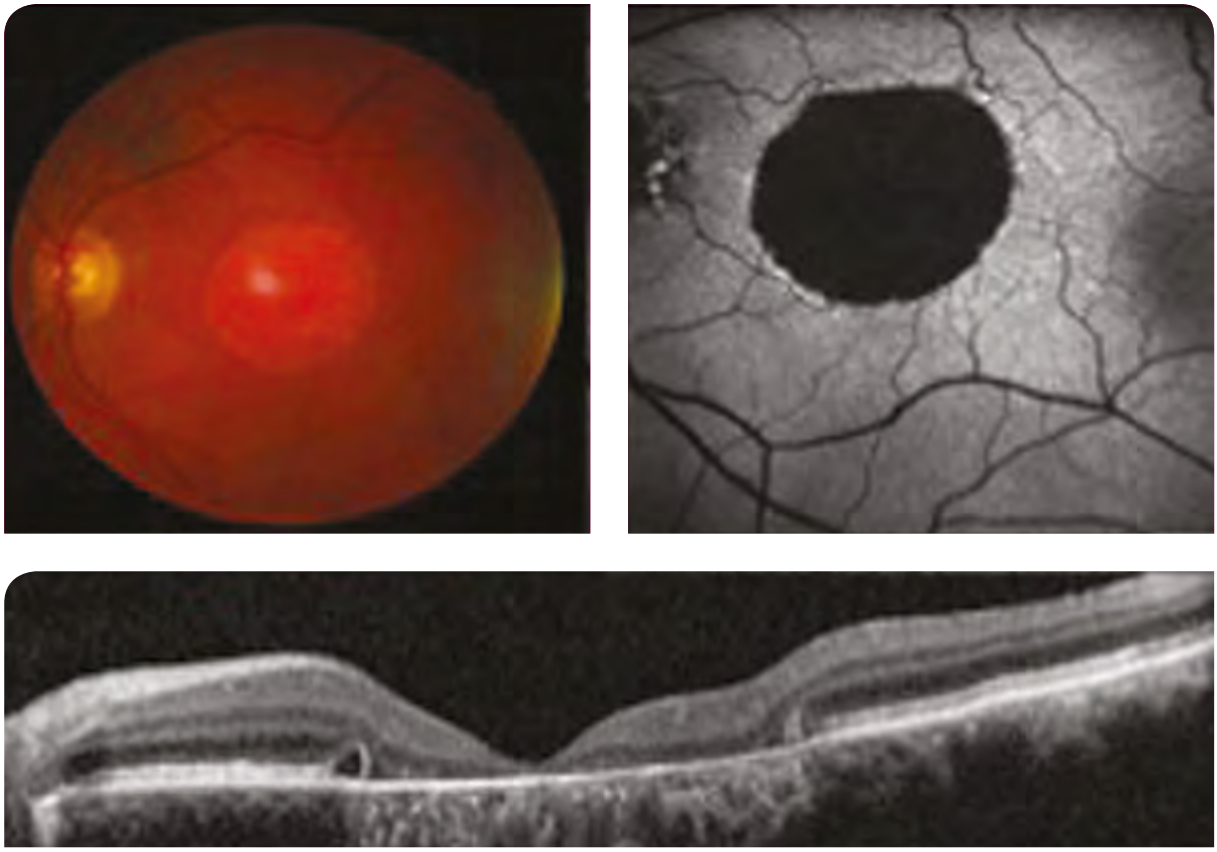

Fig. 5: Extensive molecular atrophy with distinct edges complicating AFVD in an 82-year-old female patient.
Visual acuity 20/250, Parinaud scale < P14. Peri-atrophic, hyperautofluorescent border; hyperautofluorescent peripapillary pigment epithelium changes linked to associated pattern dystrophy appearance. Note the disappearance of the subretinal material in the OCT image.

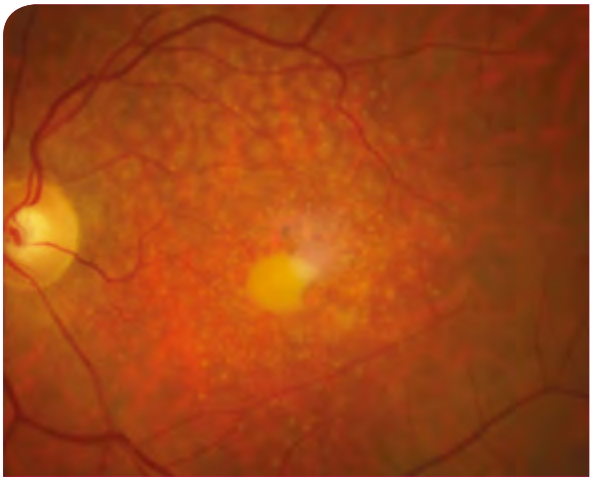

Fig. 6: Colour fundus photograph of AFVD showing the accumulation of yellowish material.

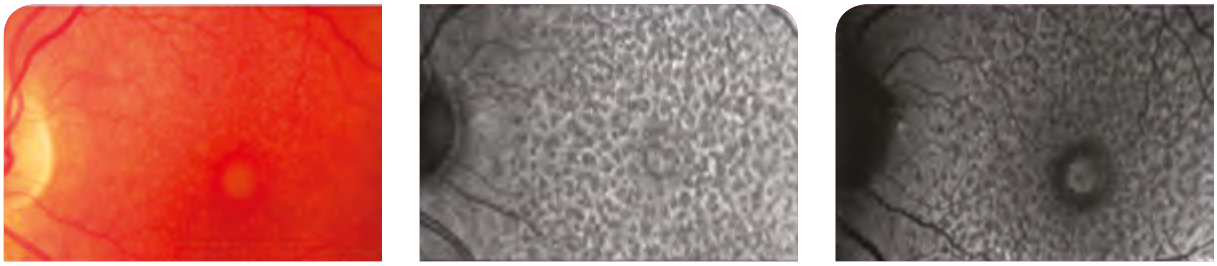

Fig. 7: Multimodal imaging of a 67-year-old female patient with both AFVD and reticular pseudodrusen.
Left: Colour fundus photograph showing the accumulation of yellowish material. Middle: Infrared (IR) photograph.
Right: Blue-light autofluorescence photograph.

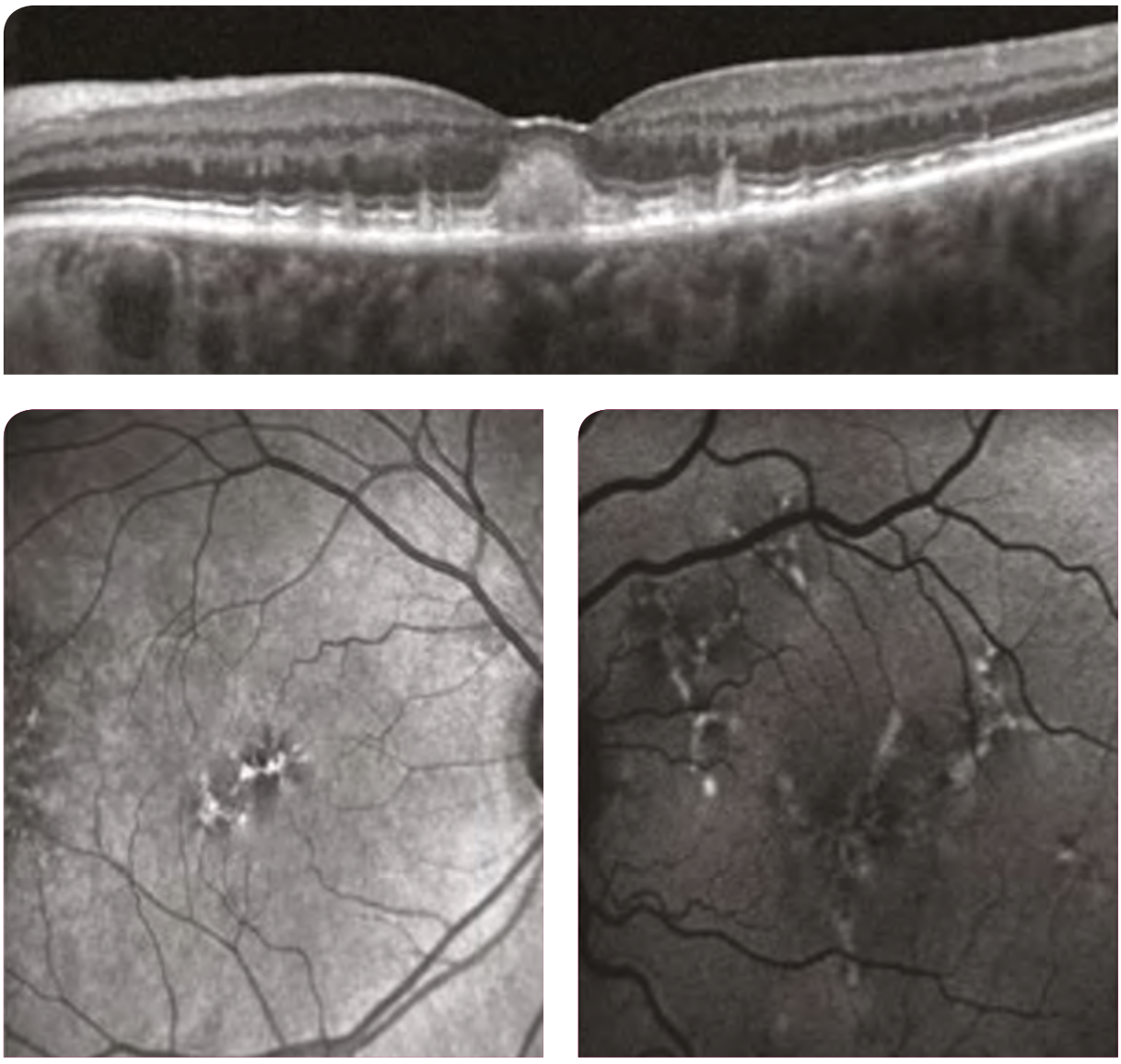

Fig. 8: Multimodal imaging of a 56-year-old male patient with AFVD and bilateral associated pattern dystrophy.
Top: SD-OCT showing the accumulation of material in the form of a regular, homogeneous, hyperreflective lesion above the retinal pigment epithelium. Bottom left: Infrared (IR) photograph. Bottom right: Autofluorescence photograph showing the accumulation of material and reticular lesions.

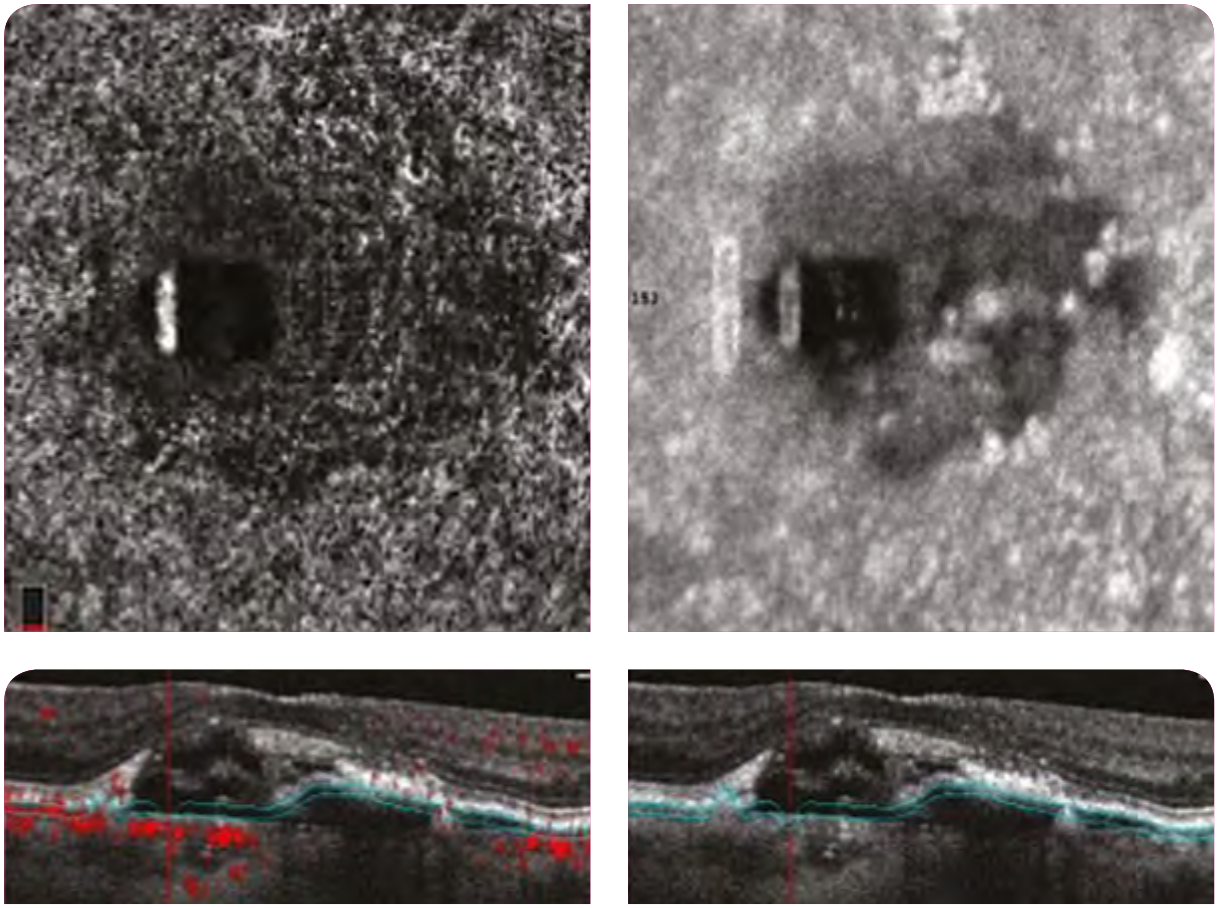

Fig. 9: AFVD in OCTA and en-face OCT.
Top left: En-face OCTA slice: Hyperreflective vertical line nasal to the fovea, caused by an artefact. The corresponding OCT B-scan (bottom left) does not find any flow here. It is the result of incorrect segmentation and there is no neovascular complication. Right: En-face structural OCT.

2) AFVD and OCT-angiography

In general, there are several types of artefacts that can impact on the quality of the images. Clinical experience and an analysis of the literature show that the following artefacts are most common in AFVD:

- Projection of the superficial capillary plexus
- Segmentation errors linked to the deposit of material, which disrupts the automatic recognition of the anatomy of the normal retinal layers
- Movement artefacts: certain patients with severe forms of the disease (in particular, those with neovascularisation and atrophy) may have difficulty holding their gaze, and image acquisition can therefore be difficult.

When diagnosing choroidal neovascularisation using OCTA, it is important to identify any false positives and false negatives linked to artefacts. For example, projection artefacts—caused by a hyperreflective retinal pigment epithelium—cause variations in the reflected light, which are then interpreted as movement by the OCTA device, leading to numerous false positives, such as for drusenoid PED. We have also observed this type of artefact within the subretinal material, associated with artefacts linked to incorrect automatic segmentation (Figure 9).

The scientific literature concerning imaging for CNV associated with AFVD can be summarised as follows:

- CNV can be assessed qualitatively: it is clearly visible in OCTA, with good sensitivity and specificity
- The sensitivity of OCTA is better than or equal to that of angiography when diagnosing CNV
- Quantitative changes in retinal perfusion can be visualised for all the examined vascular plexuses.

4. Treatment

There is currently no specific treatment that affects the progression of AFVD. Unlike AMD, no studies have found dietary supplements rich in antioxidants, omega-3, lutein or zeaxanthin to be therapeutically effective for this indication.

However, the efficacy of anti-VEGF drugs in treating neovascular complications is well demonstrated: In 2013, Mimoun *et al.* published a case series of 24 patients with AFVD treated with anti-VEGF therapy using a similar protocol to that used for AMD (three initial anti-VEGF injections in naive patients), with anatomical and functional success. To our knowledge, no therapeutic studies have compared the different anti-VEGF drugs in this indication. Dynamic phototherapy and laser treatment for AFVD have been found to carry a risk of iatrogenic atrophy and were therefore dropped in favour of anti-VEGF drugs.

AFVD can be distinguished from CNV-induced serous retinal detachment through careful examination of complementary images: numerous patients with AFVD are incorrectly treated with anti-VEGF drugs, with no clear effect on the subretinal material.

It is important here to point out the lack of data regarding:

- Differences in treatment response compared to AMD
- The proportion of patients who respond well (the happy few) vs those with a standard response vs those who do not respond to anti-VEGF treatment
- The impact of this treatment on the accumulation and resorption of the material, the retinal atrophy that can accompany this resorption, and the unknown iatrogenic effects.

In the future, gene function restoration protocols may be developed for AFVD with established genetic causes, in particular through viral vector-mediated gene therapy.

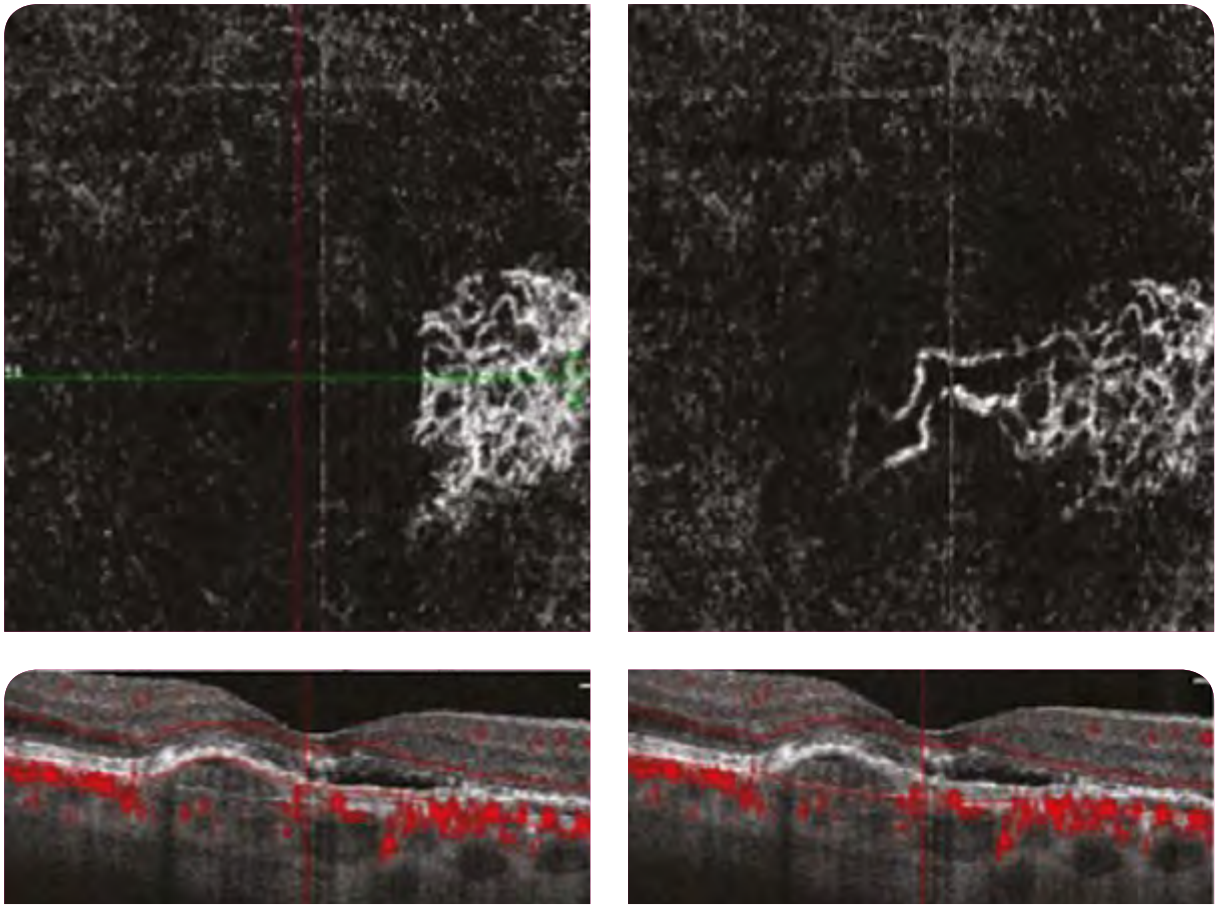

Fig. 10: Image of a neovascular network with automatic segmentation (left) and after manual re-segmentation (right). Note the clearer appearance of the whole neovascular membrane.

References

Chowers I., Tiosano L., Audo I. *et al.* Adult-onset foveomacular vitelliform dystrophy A fresh perspective. Progress in Retinal and Eye Research; 2015:47:64-85.

Gass J.D., A clinicopathologic study of a peculiar foveomacular dystrophy. Transactions of the American Ophthalmological Society, 1974 :72 :139-56

Renner AB, Tillack H, Kraus H, *et al.* Morphology and functional characteristics in adult vitelliform macular dystrophy. Retina Phila Pa. 2004;24(6):929-939.

Meunier I, Sénéchal A, Dhaenens C-M, *et al.* Systematic Screening of BEST1 and PRPH2 in Juvenile and Adult Vitelliform Macular Dystrophies: A Rationale for Molecular Analysis. Ophthalmology. 2011;118(6):1130-1136

Meunier I, Manes G, Bocquet B, *et al.* Frequency and Clinical Pattern of Vitelliform Macular Dystrophy Caused by Mutations of Interphotoreceptor Matrix IMPG1 and IMPG2 Genes. Ophthalmology. 2014;121(12):2406-2414. doi:10.1016/j.ophtha.2014.06.028

Lupidi M, Coscas G, Cagini C, Coscas F. Optical Coherence Tomography Angiography of a Choroidal Neovascularization in Adult Onset Foveomacular Vitelliform Dystrophy: Pearls and Pitfalls. Investig Opthalmology Vis Sci. 2015;56(13):7638

Mimoun G, Caillaux V, Querques G, Rothschild P-R, Puche N, Souied EH. Ranibizumab for choroidal neovascularization associated with adult-onset foveomacular vitelliform dystrophy: one-year results. Retina Phila Pa. 2013;33(3):513-521

Battaglia Parodi M, Rabiolo A, Cicinelli MV, Iacono P, Romano F, Bandello F. Quantitative analysis of Optical Coherence Tomography Angiography in Adult-Onset Foveomacular Vitelliform Dystrophy: Retina. January 2017:1.

8

Geographic atrophy: a new classification

Vittorio Capuano, Joel Uzzan

1. Definition

Geographic atrophy (GA) is the atrophic or "dry" form of age-related macular degeneration (AMD). It is characterised by atrophy of the outer layers of the retina (retinal pigment epithelium and photoreceptors), leading to more or less total loss of retinal sensitivity (scotoma)[1].

GA occurs in the late phase of age-related maculopathy (ARM), which is characterised by the presence of drusen and/or pseudodrusen associated with pigment epithelium changes (hypopigmentation or hyperpigmentation).

2. Risk factors

From what we currently understand, GA appears to be a multifactorial disease.

Several studies have highlighted a number of risk factors for the development and progression of atrophic AMD (other than age), including certain diets and smoking.

In terms of genetics, two loci associated with the disease have been identified in 1q32 and 10q26[2]. The first is a locus that also includes the gene coding for complement factor H (CFH), which is involved in the alternative complement pathway (an inflammation factor). The second locus includes "age-related maculopathy susceptibility 2" *(ARMS2)*[3]. However, genetic counselling is only called upon in exceptional cases.

3. Diagnosis

Diagnosis is clinical and paraclinical: a visual acuity test, patient interview and multimodal imaging are the three key stages. The use of the ETDRS score for visual acuity is strongly recommended, since it is better suited to poor vision. Family history and clinical history are very important in establishing a diagnosis—in particular, the patient's age and the age at which the first symptoms appeared (potentially in the form of nyctalopia). In terms of multimodal imaging, we are going to look at the three key examinations for diagnosing GA.

1) Fundus photography (traditional classification)

The traditional classification of GA is based on fundus photography.

The atrophic areas appear as round or polylobed **whitish lesions**, often multifocal, within which the large choroidal vessels are more visible than usual (Figure 1). The edges are distinct and sometimes marked by slight hyperpigmentation. These atrophic lesions vary greatly in position, number and size. A size of 0.05 mm^2 was defined as the lower limit for diagnosing GA by a team of researchers in 1995[4].

More recently, the 2013 AREDS study amended this limit: the atrophic lesion must be a minimum of 0.145 mm^2 (i.e. 1/4 of a disc diameter)[5].

At present, several “wide-field” and “ultra-wide-field” fundus cameras are available on the market. The value of this type of imaging lies in its ability to visualise lesions outside the arcades and more on the periphery. While atrophic AMD always spares the middle periphery and rarely extends beyond the arcades, the quality of wide-field images means they can usually be used to characterise macular lesions (Figure 2).

Nevertheless, fundus photography alone is insufficient, in particular where the edges of the GA are not easily visible. Pseudodrusen are often hard to see or not visible at all. In addition, the quality of fundus photographs can be affected by milieu opacity or mediocre dilatation, and remains very operator-dependent.

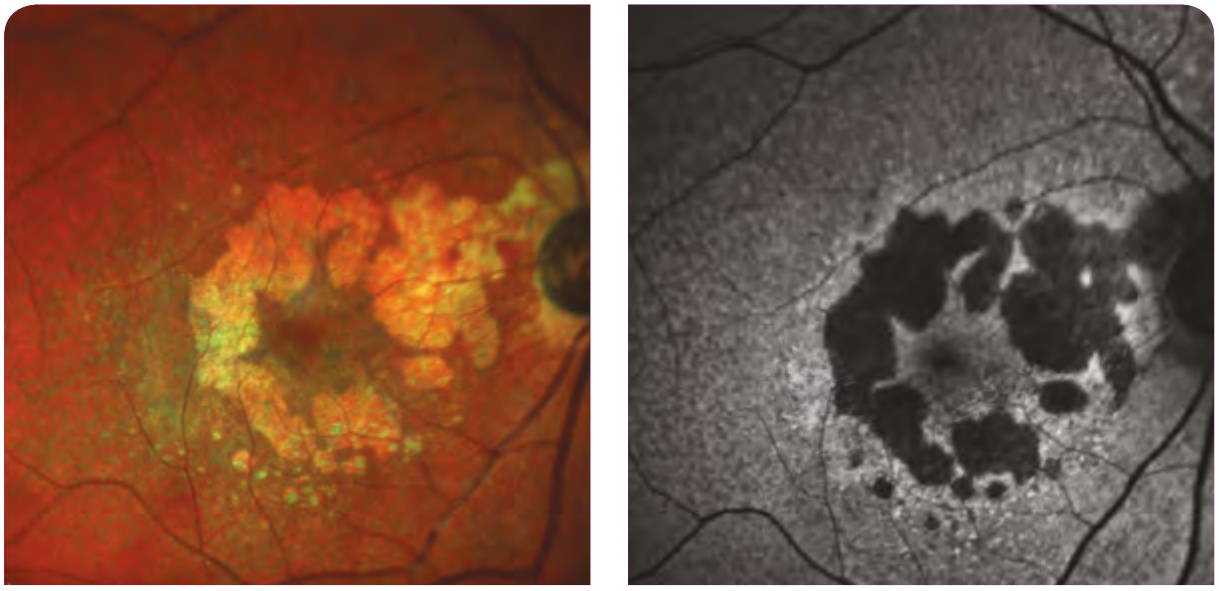

Fig. 1: Multicolor® and autofluorescence photographs of geographic atrophy.

Fig. 2: Wide-field image of geographic atrophy.

2) Optical coherence tomography (new classification)

In 2017, a group of international retinal imaging experts put forward a new classification for retinal atrophy based on OCT[6,7].

According to the authors, OCT is the best tool for this classification, which employs characteristics specific to this type of imaging:

- OCT displays every layer of the retina
- En-face reconstruction can highlight the cell loss in each layer
- OCT can detect areas of atrophy at an earlier stage
- "Eye tracker" mode allows a specific area of the retina to be monitored over time automatically
- OCT is the gold standard for diagnosing and monitoring exudative AMD and is a widely used tool
- OCT images are very similar to histological slice images
- OCT provides information on whether the fovea is affected by the disease.

The authors based their new terminology on the presence of complete or incomplete atrophy of two structures visible in OCT: the outer retina and the retinal pigment epithelium (RPE). The combinations thereof form four phenotypes:

- c-RORA (complete RPE and Outer Retinal Atrophy)
- i-RORA (incomplete RPE and Outer Retinal Atrophy)
- c-ORA (complete Outer Retinal Atrophy)
- i-ORA (incomplete Outer Retinal Atrophy).

This classification is based on the fact that outer retinal atrophy (in particular of the photoreceptors) is not necessarily associated with RPE atrophy. This is the case for atrophy due to pseudodrusen, where photoreceptor atrophy is observed without atrophy of the underlying RPE. However, RPE atrophy is always associated with atrophy of the overlying layer of photoreceptors. The concept of “complete” and “incomplete” atrophy is also introduced in this classification, due to the slow progression of retinal and RPE cell breakdown. Finally, “hypertransmission” of the OCT signal in the choroid is considered and, if found, described as either ''homogeneous” or “inhomogeneous” (used here as synonyms for “complete” and “incomplete”).

This OCT-based classification has been validated by histological examination of donor samples in a comparative *post mortem* study of OCT and histology; the OCT data and histology data were found to match exactly.

“**cRORA**” is defined by the presence of the following three characteristics (Figure 3):

a) A homogeneous area of hypertransmission measuring at least 250 µm

b) A missing section in the RPE line measuring at least 250 µm

c) A missing section in the overlying line of photoreceptors.

“**iRORA**” does not meet any of the three “cRORA” characteristics, instead displaying inhomogeneous hypertransmission and an irregular break in the RPE and photoreceptor lines (Figure 4).

“**cORA**” is defined by a complete absence of the photoreceptor line and the presence of an intact RPE line.

“**iORA**” is defined by a break in the photoreceptor layer, along with an intact RPE line, *and no hypertransmission* (Figure 5).

Other characteristic signs of GA are visible in OCT but are not used in this classification. The most well-known include ghost drusen[8], outer retinal corrugation[9], wedge-shaped subretinal hyporeflectivity[10] and quiescent neovascularisation[11].

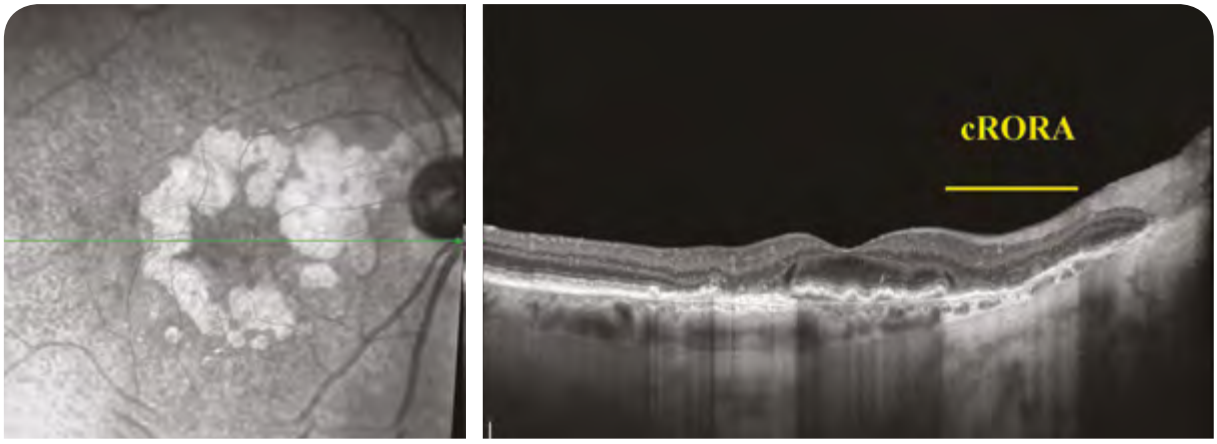

Fig. 3: SD-OCT of cRORA geographic atrophy.

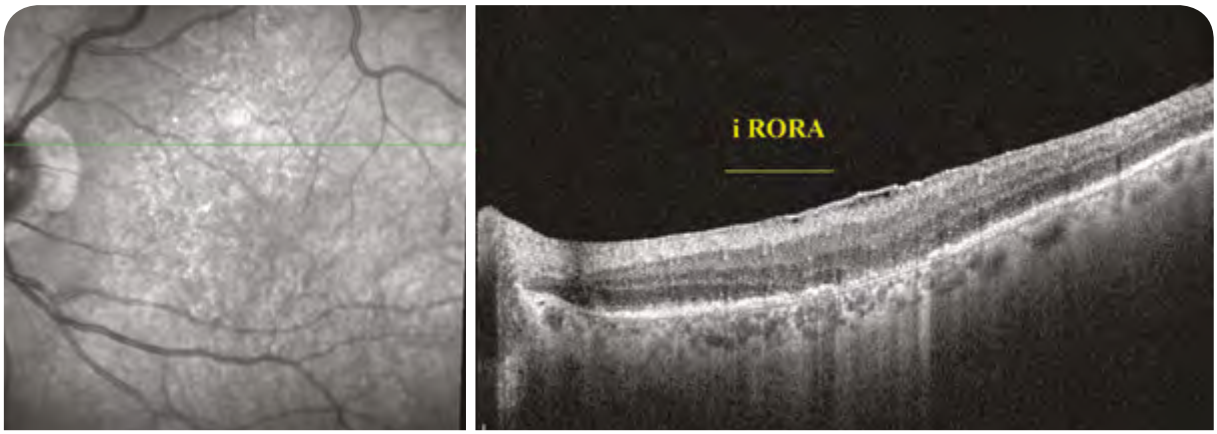

Fig. 4: SD-OCT of iRORA geographic atrophy.

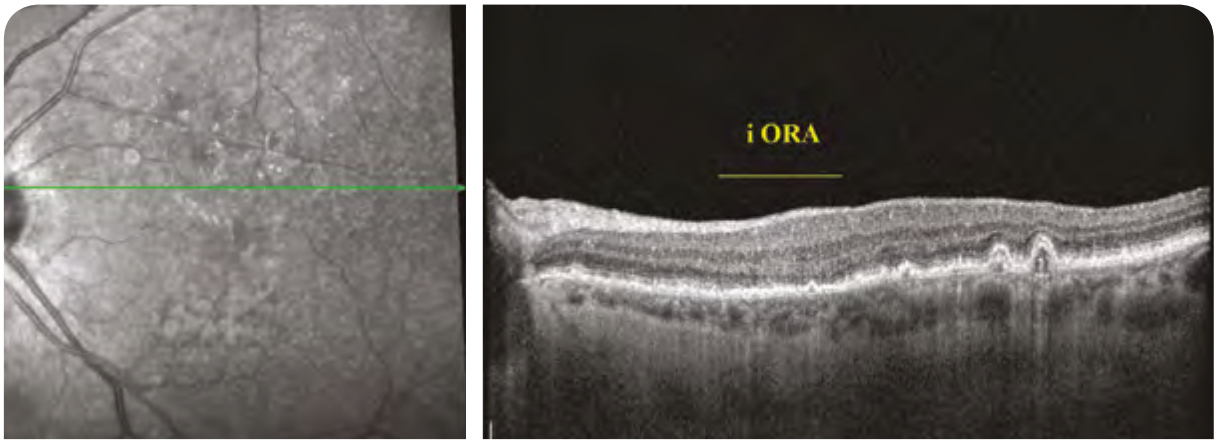

Fig. 5: SD-OCT of iORA geographic atrophy.

3) Other complementary examinations

a) Autofluorescence

Autofluorescence imaging of the fundus is the gold standard for measuring GA **progression** in multi-centre studies, using the semi-automatic surface quantification software "Region Finder", developed by Frank Holtz. It is also a very useful examination in everyday practice to confirm a diagnosis of GA and to quantify it.

Two types of autofluorescence device are currently available on the market: blue light and green light. Both work in similar ways.

When the RPE is stimulated by light, it responds by releasing its own physiological fluorescence. If the RPE is damaged, increased fluorescence is generally observed around the edges of the atrophy (hyperautofluorescence). In the case of severe damage, there is no fluorescence (hypoautofluorescence) (Figure 1).

The average speed of atrophic progression was measured at 1.85 mm^2/year by Shmitz-Valckenberg[12] (the speed of centrifugal progression is greater than that of centripetal progression) (Figure 6).

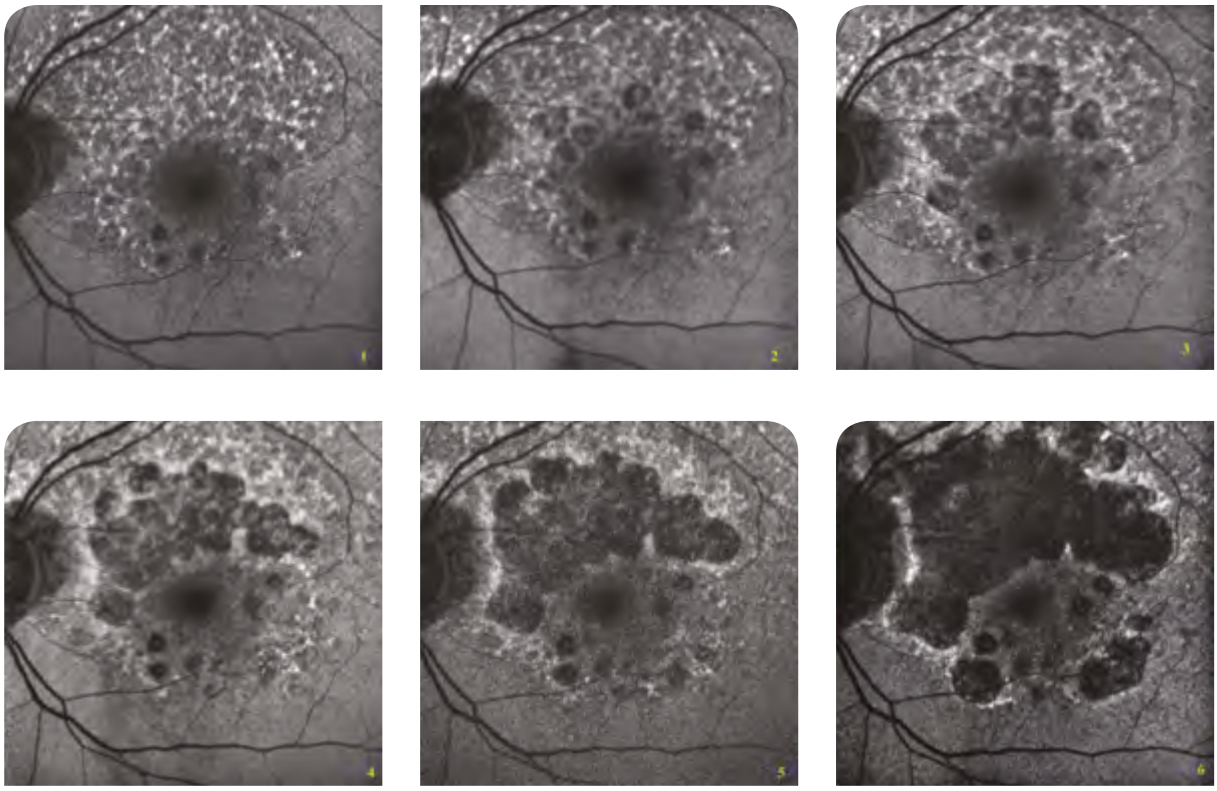

Fig. 6: Confluent progression of GA in autofluorescence images over six years: centrifugal progression is quicker that centripetal.

The main disadvantages of autofluorescence are significant glare for the patient and a lack of information on the condition of the other retinal layers. In addition, blue autofluorescence will not work effectively around the foveal zone due to blocking by xanthophyll pigment; near-infrared autofluorescence must be used instead.

b) Fluorescein and indocyanine green angiography

Although they provide fairly precise images of the signs of GA, invasive examinations such as fluorescein angiography and indocyanine green angiography are not currently indicated for the diagnosis of GA, unless atrophy secondary to exudative AMD or to lesions at high risk of exudation, such as quiescent neovascularisation, is suspected.

c) Optical coherence tomography angiography (OCT-angiography, OCTA)

OCTA is valuable primarily because it can detect neovascularisation (active, inactive and quiescent) without the need to inject a dye.

Reduced vascular density has been observed at the edges of the atrophy[13]. Measurements of atrophy size are reproducible with OCTA[14], but this method has not (yet) been validated for randomised, multi-centre studies.

d) Electrophysiology

Electrophysiology is not a routine complementary examination for diagnosing GA, but it is crucial in distinguishing between GA and cone dystrophy or cone-rod dystrophy in which the cones are primarily affected. It will primarily be of use in cases where the atrophy is not associated with hyperautofluorescent deposits.

Conclusion

GA is diagnosed based on a careful assessment of several different imaging findings, plus information gathered from the patient. A new, OCT-based classification has recently been put forward that includes histology findings for the first time. With no treatment available at this time, better description and classification of this form of AMD remains difficult but necessarily multimodal.

References

1. Freund KB, Sarraf D, Mieler W, *et al.* The Retinal Atlas. 2nd ed. Amsterdam: Elsevier; 2017.

2. Hageman GS, *et al.* A common haplotype in the complement regulatory gene factor H (HF1/CFH) predisposes individuals to age-related macular degeneration. Proc Natl Acad Sci U S A. 2005;102:7227– 7232.

3. Rivera A, *et al.* Hypothetical LOC387715 is a second major susceptibility gene for age-related macular degeneration, contributing independently of complement factor H to disease risk. Hum Mol Genet. 2005;14:3227– 3236.

4. Bird AC, Bressler NM, Bressler SB, *et al.* An International classification and grading system for age-related maculopathy and age-related macular degeneration. The International ARM Epidemiology Study Group. Surv Ophthalmol 1995;39:367–374.

5. Danis RP, Domalpally A, Chew EY, *et al.* Methods and reproducibility of grading optimized digital color fundus photographs in the Age-Related Eye Disease Study 2 (AREDS2 Report Number 2). Invest Ophthalmol Vis Sci 2013;54(7):4548–4554.

6. Sadda SR, Guymen R, Holz FG *et al.* Consensus Definition for Atrophy Associated with Age-Related Macular Degeneration on OCT: Classification of Atrophy Report 3. Ophthalmology 2018.

7. Garrity ST, Sarraf D, Freund KB *et al.* Multimodal imaging of nonneovascular age-related macular degeneration. Invest Ophthalmol Vis Sci. 2018; 59:AMD48–AMD64.

8. Bonnet C, Querques G, Zerbib J. *et al.* Hyperreflective pyramidal structures on optical coherence tomography in geographic atrophy areas. Retina. 2014.

9. Ooto S, Vongulkariti S, Sato T. *et al.* Outer retinal corrugations in age-related macular degeneration. JAMA Ophthalmol. 2014;132:806–813.

10. Querques G. Capuano V, Bandello F. *et al.* WEDGE-SHAPED SUBRETINAL HYPOREFLECTIVITY IN GEOGRAPHIC ATROPHY. Retina, 2015.

11. Capuano V. Miere A, Querques L, *et al.* Treatment-Naïve Quiescent Choroidal Neovascularization in Geographic Atrophy Secondary to Nonexudative Age-Related Macular Degeneration. Am J Ophthalmol. 2017 Oct;182:45-55.

12. Schmitz-Valckenberg S, Sahle JA, Danis R. *et al.* Natural history of geographic atrophy progression secondary to age-related macular degeneration (greographic atrophy progression study). Ophthalmology 2016.

13. Sacconi R, Corbelli E, Carnevali A. *et al.* OPTICAL COHERENCE TOMOGRAPHY ANGIOGRAPHY IN GEOGRAPHIC ATROPHY. Retina. 2017.

14. Corbelli E, Sacconi R, Rabiolo A. *et al.* Optical Coherence Tomography Angiography in the Evaluation of Geographic Atrophy Area Extension. Invest Ophthalmol Vis Sci. 2017.

9

Differential diagnoses for AMD

Polina Astroz, Olivia Zambrowski

AMD is the most common cause of visual impairment in the developed world. However, it is important to be aware of several other more rare diagnoses that have their own specific characteristics but can be complicated by atrophy or macular neovascularisation. There are many causes of macular atrophy. Some of these diseases can also be complicated by neovascularisation. These are often found in younger patients than those affected by AMD, but late-onset forms are not uncommon, and patients may present at consultations in the scarring stage.

Patient interviews, family history, clinical examination and conventional multimodal imaging (MMI) combined with OCTA are essential for both diagnosis and treatment.

1. Pachychoroid

This new entity was proposed in 2013 and covers a spectrum of clinical presentations with shared characteristics: reduced visibility of the choroidal vessels in the fundus, focal or diffuse thickening of the choroid, dilation of the "pachyvessels" in Haller's layer with thinning of Sattler's layer and the choriocapillaris, and choroidal hyperpermeability visible in the late phase of indocyanine green (ICG) angiography.

1) Central serous chorioretinopathy

This primarily affects young men (72–88% of cases). Several risk factors have been described, including endogenous or exogenous corticosteroid therapy and type A personality, among others.

MMI is essential to both diagnosis and monitoring. In autofluorescence imaging, RPE defects are typically visible, associated with gravitational tracks. SD-OCT shows SRD, small PEDs corresponding to leakage points, extension of the photoreceptor outer segments and—in chronic forms—a flat, irregular PED, fibrin, degenerative macular oedema and outer retinal tubulation. Flat, irregular pigment epithelial detachment (FIPED) in chronic CSCR is associated in 19–29% of cases with type 1 CNV in conventional MMI. However, due to the RPE changes that occur in chronic forms, it is often difficult to identify this type 1 CNV. OCT-angiography (OCTA) is extremely useful in CSCR. In the literature, OCTA detects type 1 CNV in 35–95% of cases *versus*19–29% of cases for conventional multimodal imaging (Figure 1). CSCR with or without neovascularisation can be mistaken for exudative AMD.

2) Pachychoroid neovasculopathy

Type 1 CNV associated with a pachychoroid and with no other cause of CNV (AMD, myopia, inflammatory diseases etc.) has been termed "pachychoroid neovasculopathy".

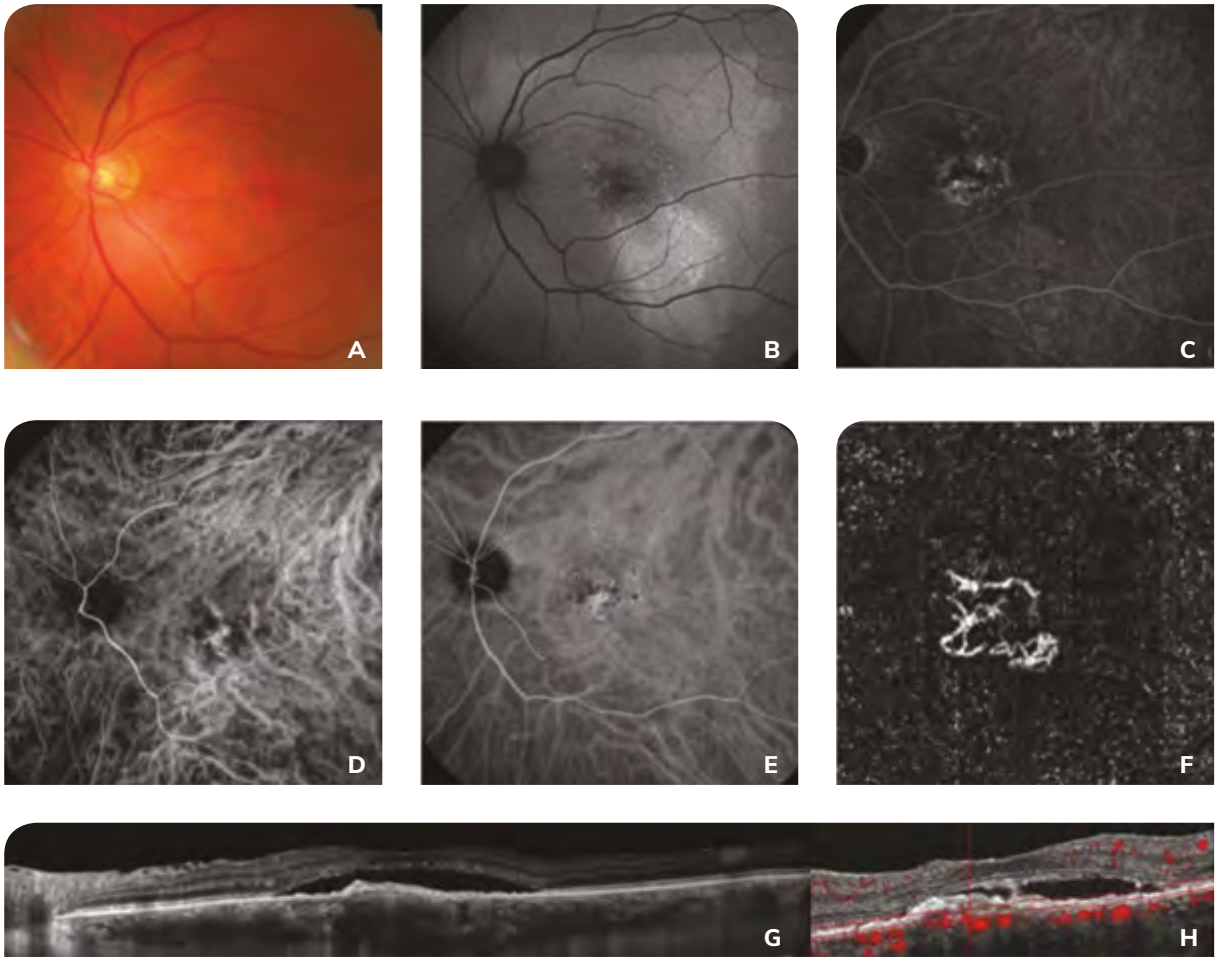

Fig. 1: Multimodal imaging and OCTA of the left eye of a male patient with central serous chorioretinopathy complicated by type 1 choroidal neovascularisation.
Colour fundus photographs (A). Autofluorescence image showing retinal pigment epithelium changes and gravitational tracks (B). Late-phase fluorescein angiography showing macular pinpoints (C). Pachyvessels are visible in the early phase of ICG angiography (D), along with late hyperpermeability (E). OCTA with manual segmentation, showing an area between the retinal pigment epithelium (RPE) and 30 microns below it with neovascular flow (F). The flow is also visible in the corresponding B-scan (H). EDI-OCT shows a FIPED associated with a SRD and a thick choroid measuring 460 microns (G).

3) Polypoidal choroidal vasculopathy (PCV)

Pachychoroid neovasculopathy and CSCR with type 1 CNV can be complicated by polyps in 36% of cases. Type 1 CNV is the equivalent of the branching vascular network. Recently, a new term has been put forward for PCV: “aneurysmal type 1 CNV”, but this remains controversial.

2. EMAP (extensive macular atrophy with pseudodrusen-like appearance)

EMAP was described in 2009 by Prof. Hamel's team in Montpellier and is characterised by an atrophic macular lesion associated with reticular pseudodrusen. It generally affects younger patients than atrophic AMD (around 50 years old). It progresses more quickly and the symptoms are central scotoma associated with nyctalopia, which must be identified by interviewing the patient.

The macular lesions are bilateral and symmetrical, with a vertical main axis. Diffuse squamous lesions can be seen in the peripheral areas. The lesions may be complicated by macular neovascularisation, which responds fairly well to anti-VEGF intravitreal injections.

A full-field electroretinogram (ERG) will confirm a change in the rod system response consistent with nyctalopia, but a normal ERG does not rule out the diagnosis.

No predisposing genetic factors have been identified, but within a large national French cohort, patients seemed more likely to be female, with no particular history, and of menopausal age (Figure 2).

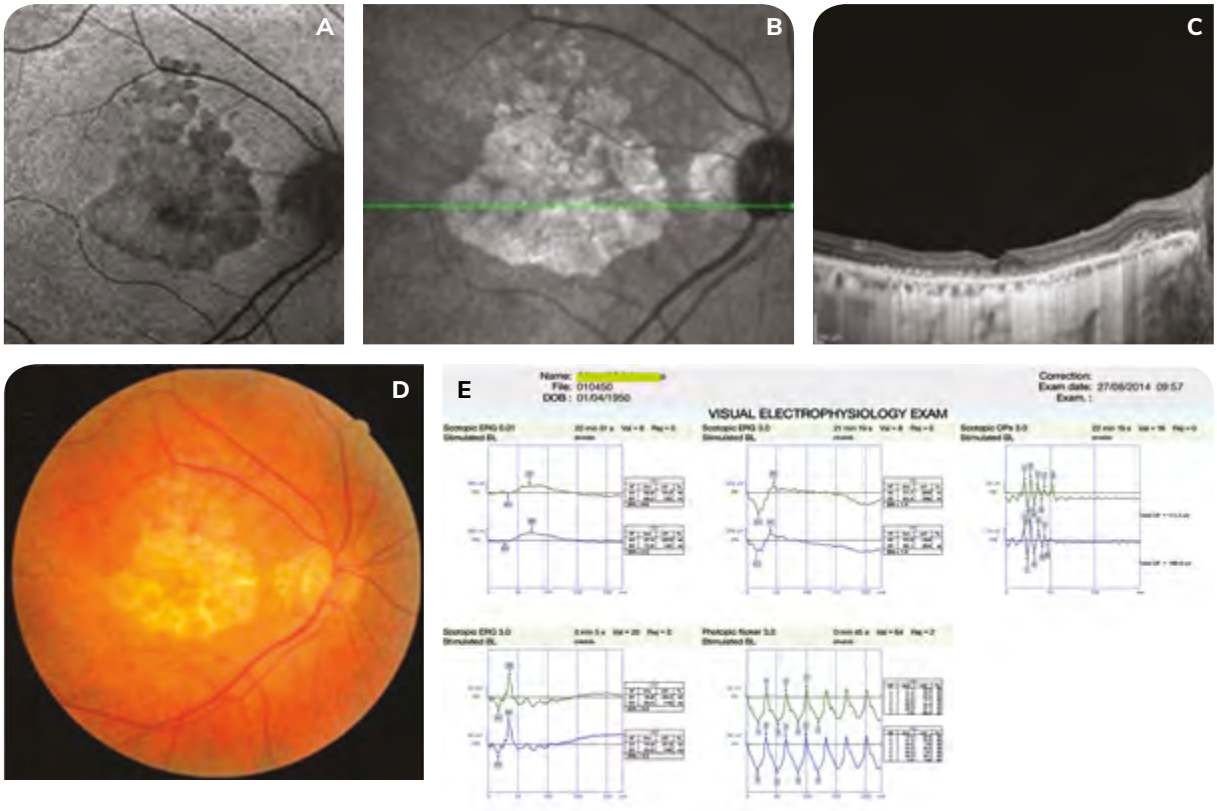

Fig. 2: Multimodal imaging of a 65-year-old female patient with progressive loss of visual acuity and a central scotoma, associated with disabling night vision impairment.
(A) In the autofluorescence photo, the area of atrophy is not particularly dense at this stage, and contrasts with the extent of the impairment. The vertical appearance of the lesions also suggests a possible diagnosis of EMAP. (B) In the infrared photograph and SD-OCT (C), the reticular pseudodrusen and macular atrophy with complete restructuring of the ellipsoid zone are also supportive of this diagnosis. (D) The atrophy in the fundus has no specific appearance, but the peripheral areas should be checked for squamous lesions. (E) Finally, full-field ERG reveals highly altered responses, with significant dysfunction of both the rod and cone systems. The diagnosis of EMAP is confirmed.

3. Idiopathic macular telangiectasia

Macular telangiectasia is a morphological abnormality of the macular capillaries. It was initially described in the juxtafoveal zone by Gass in 1968, but the currently used classification is slightly more recent.

The classification is as follows:

Type 1: Men aged over 55 years, unilateral lesion, sometimes associated with peripheral vascular abnormalities. Cystoid macular oedema (CMO) and exudates are common

Type 2: Men or women aged under 60 years, slight bilateral juxtafoveal capillary dilatation, generally in the temporal area within the median raphe. Risk of neovascularisation

Type 3: Men aged 50 years, bilateral occlusive vascular capillary lesion with no peripheral vascular abnormalities.

Type 2 or "mac tel" lesions can be quite easily mistaken for neovascular AMD. These lesions are characterised by acute bilateral macular disease, visible in SD-OCT as intraretinal spaces (with no systematic thickening of the macula) in the juxtafoveal zone, associated in fluorescein angiography with moderate leakage in the late phase. These cavitation-type spaces initially appear in the inner layers of the retina, then progress towards the outer layers, with the development of secondary atrophy or, in rare cases, subretinal neovascularisation. OCTA is a new tool that can be used to diagnose the condition by displaying vascular abnormalities in several different retinal layers. In the early stages, rarefaction of the deep and superficial capillary networks is observed, with focal capillary dilatations associated with a right-angle drainage vein. Next, the retinal capillaries in the outer retina are affected as a result of the changes in the superficial and deep capillary plexus. If subretinal neovascularisation has occurred, OCTA can be used to diagnose the neovascularisation without fluorescein diffusion getting in the way (Figure 3).

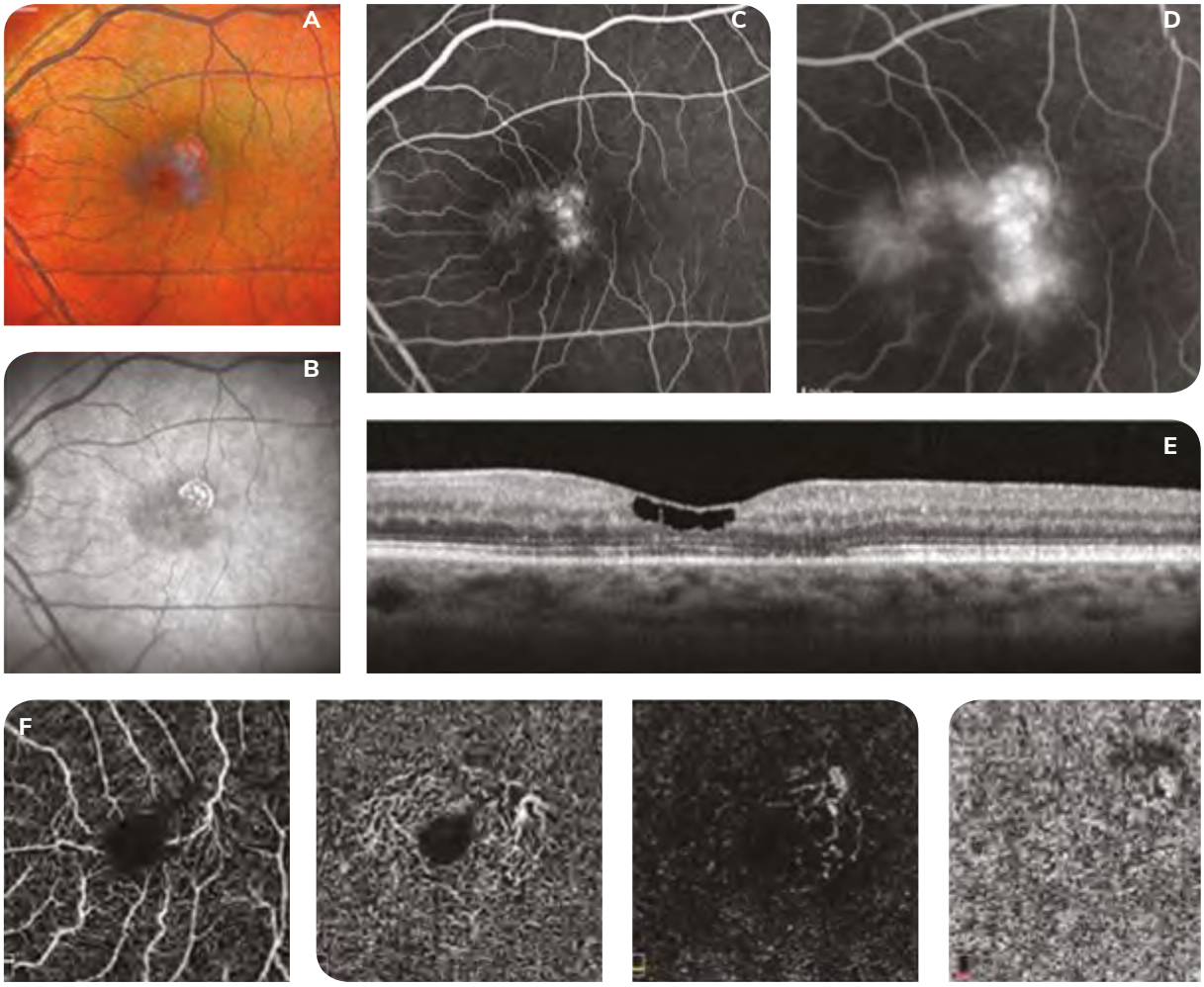

Fig. 3: A 55-year-old man with decreased visual acuity and recent metamorphopsia in the left eye.
(A) The Multicolor® photograph reveals a non-haemorrhagic superior parafoveal lesion, (B) also visible in the infrared image. (C and D) Leakage is visible around the lesion in fluorescein angiography, increasing over the course of the sequence, but the SD-OCT image (E) shows cavitation in the inner layers of the macular with no overall increase in macular thickness, associated with changes to the ellipsoid line, which is not typical of exudative AMD. (F) The OCTA image confirms the diagnosis of type 2 macular telangiectasia ("mac tel"). The lesion is present in all the retinal slices, with rarefaction of the surrounding capillaries and, crucially, a right-angle drainage vein.

4. Inherited retinal degeneration

1) Macular dystrophy

a) Pattern dystrophy

Pattern dystrophy (or reticular, butterfly-shaped or Deutman's dystrophy) covers heterogeneous bilateral autosomal-dominant dystrophies characterised by yellowish macular deposits and pigment migration. In general, the visual prognosis is good, with a slight decrease in central vision in the elderly.

b) Maternally inherited diabetes and deafness (MIDD) and MELAS

MIDD (Maternally Inherited Diabetes and Deafness) combines diabetes, sensorineural hearing loss and pattern dystrophy. It is linked to the A3243G mitochondrial DNA mutation. Its impact on the eye manifests as retinal pigment epithelium changes associated with areas of macular atrophy and typical pattern dystrophy in autofluorescence imaging.

MELAS syndrome (Mitochondrial Encephalopathy with Lactic Acidosis and Stroke-like episodes) combines mitochondrial myopathy, lactic acidosis, encephalopathy and acute stroke-like neurological symptoms. It is caused by mitochondrial DNA mutations. Its impact on the eye manifests as deposits in the posterior pole and peripapillary zone, pattern dystrophy and areas of perifoveal atrophy.

c) Central areolar choroidal dystrophy (CACD)

CACD is a rare hereditary bilateral dystrophy characterised by retinal pigment epithelium changes, followed by atrophy of the RPE and choriocapillaris. Full-field ERG and EOG are normal, while multifocal ERG, pattern ERG and colour vision can be abnormal. Mutations in the peripherin/RDS gene are very commonly associated with this disease.

d) Stargardt disease

This disease is genetically and phenotypically heterogeneous. It particularly affects young people, but can sometimes be discovered later, making differential diagnosis with AMD more difficult. The most commonly mutated gene is ABCA4 and transmission is autosomal recessive. It is characterised by flecking in the posterior pole, no peripapillary involvement and a dark choroid in fluorescein angiography, progressing to complete macular atrophy (Figure 4). Fundus flavimaculatus is characterised by a later onset and slower progression. Rare cases of neovascularisation have been described in the literature.

e) Best disease

Best disease is autosomal dominant and of variable penetrance. It is characterised by the appearance of a vitelliform macular deposit in young adults or children, and progresses through five stages: previtelliform, vitelliform, pseudohypopyon, vitelliruptive and atrophy (Figure 5). Rare cases of neovascularisation have been described. Differential diagnosis with AMD becomes difficult at the atrophic stage. The diagnosis can be confirmed by examining the patient's family history and identifying any changes in EOG response or vitelliform material in the contralateral eye.

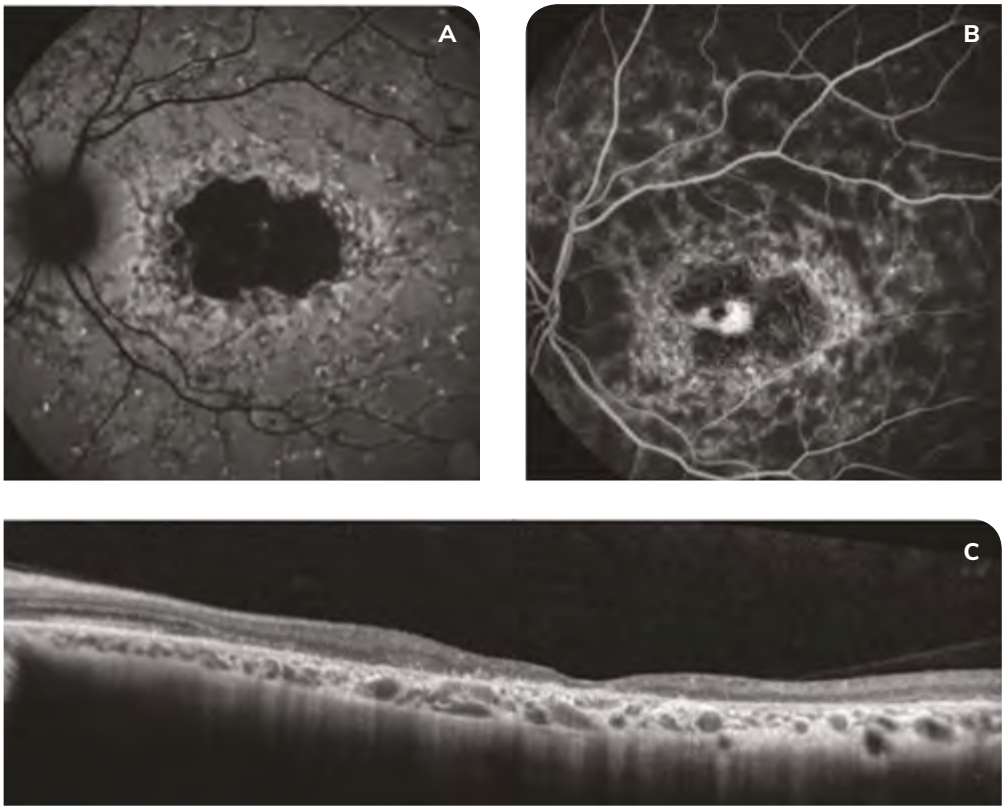

Fig. 4: Multimodal imaging of Stargardt disease in a 55-year-old female patient.
The autofluorescence image of the left eye shows macular atrophy associated with pisciform hyperautofluorescent flecks, plus a few hypoautofluorescent flecks (A). Fluorescein angiography shows a dark choroid (B). Note the peripapillary zone is not affected. SD-OCT shows outer retinal atrophy and foveal and perifoveal retinal pigment epithelial atrophy.

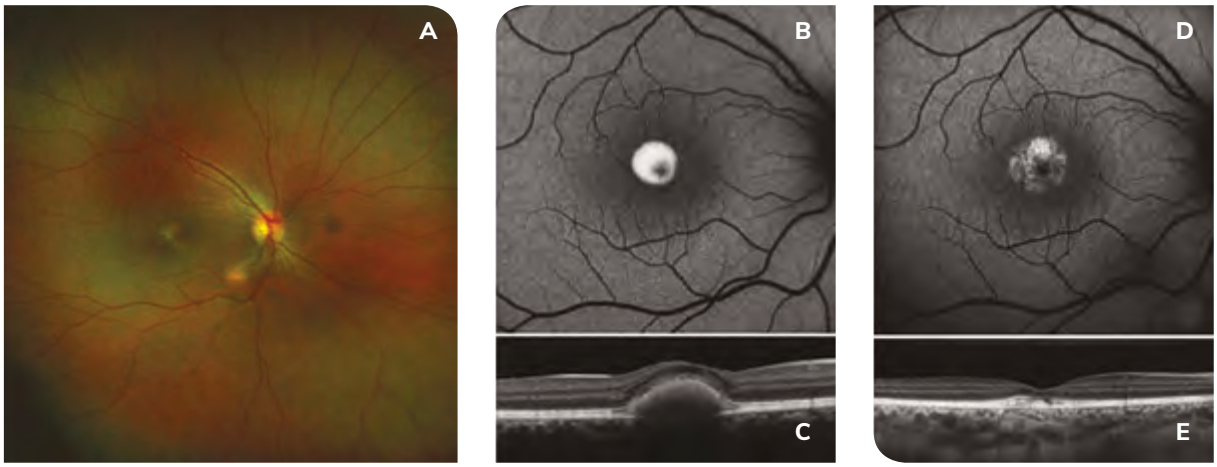

Fig. 5: Multimodal imaging of Best disease in a 34-year-old female patient.
The ultra-wide-field colour fundus photo (Optos®) of the right eye shows a single deposit of foveal vitelliform material (A). The initial autofluorescence photo shows that the material is round and hyperautofluorescent (B). It is located in the subretinal space in SD-OCT (C). Ten years later, the material is fragmented in the autofluorescence image (D), with regression of the material in SD-OCT (E), triggering off the beginnings of foveal atrophy.

2) Retinal dystrophy beyond the macula: cone and cone-rod dystrophy

Genetic cases of retinal dystrophy can be discovered very late. If a patient presents with an atrophic or exudative macular lesion, it can be easily confused with AMD, particularly in the presence of macular oedema and, in rarer cases, neovascular complications.

If the retinal imaging (OCT, autofluorescence) or patient history are atypical, it is important to look for photophobia, nyctalopia or a family history of retinal disease, as well as associated signs in the fundus, particularly in the retinal periphery (e.g. osteoblasts or white spots). Electrophysiological examination should also be considered (full-field ERG, electro-oculogram, multifocal ERG). If there are any functional abnormalities in the cone and/or rod system as a whole, it cannot simply be a case of AMD, since the functional impairment in this case spreads far beyond the limits of the posterior pole.

In order to distinguish between macular dystrophy, cone dystrophy and cone-rod (or rod-cone) dystrophy, it is useful to examine the initial symptoms (nyctalopia or photophobia), family history, associated signs in the fundus and the percentage reduction in the cone and rod system response ranges in full-field ERG (Figure 6).

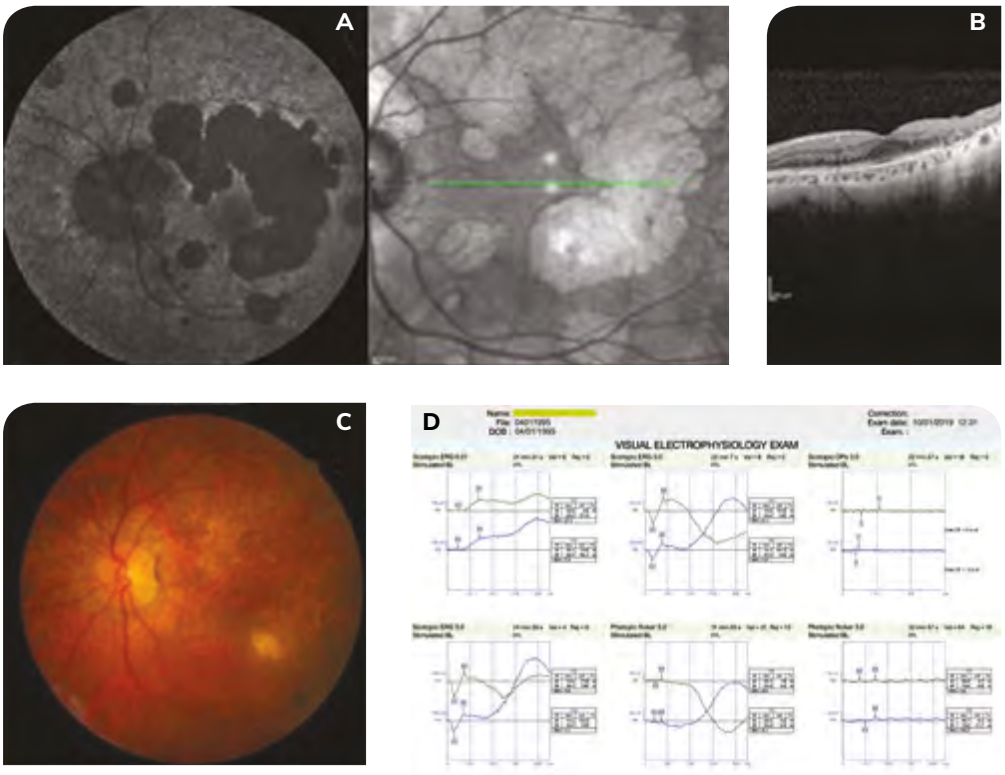

Fig. 6: 82-year-old woman monitored for several years for atrophic AMD.
The atrophic lesions in the fundus (C) are extensive and the patient reports a considerable loss of independence, although the fovea remains unaffected (A and B). Further discussion with the patient reveals consanguinity, photophobia dating back several years and, recently, nyctalopia: a full-field ERG is therefore performed. (D) The ERG responses confirm cone-rod dysfunction, compatible with a diagnosis of cone-rod dystrophy, probably of genetic origin and autosomal recessive.

5. Drug toxicity

1) Synthetic antimalarials

Synthetic antimalarials (SAMs) are widely used to treat chronic inflammatory diseases.

Their toxic effects on the retina have been known for a long time, but the mechanism by which this occurs remains poorly understood. Prevalence varies depending on the dose and treatment duration: the main risk factor is the daily dose, correlated with actual weight.

In the early stages, the effects of SAM toxicity cannot be confused with AMD: it is characterised by thinning of the ellipsoid zone and the outer nuclear layer, which has a "flying saucer" appearance. In the late stages, the RPE atrophy begins to look like a bull's-eye, but can sometimes extend across a large area of the posterior pole. It is in these later forms that differential diagnosis can become difficult, particularly if the treatment was discontinued a long time ago, if the disease developed slowly and if the patient presents at the age of around 60 years complaining of unexplained reduced visual acuity with significant macular atrophy.

The diagnosis can be confirmed through targeted questioning of the patient and if there is no or only partial foveal involvement, no neovascularisation, highly symmetrical atrophy, and, in general, changes in the cone and rod system responses in full-field ERG (Figure 7).

2) Tamoxifen

Tamoxifen is an oestrogen blocker primarily used as an adjuvant therapy for hormone-dependent breast cancer. Maculopathy was first identified as a side effect in 1978, and is characterised by yellowish perifoveal deposits associated with pigment migration and angiographic leakage.

Maculopathy is also found with lower doses of tamoxifen, involving macular thinning, cavitations that appear atrophic and, in some cases, pseudoholes. Some patients may display changes in the ellipsoid zone and foveal photoreceptors. In these cases, the patient should be asked whether they have used this medicine—particularly over the long term—before a diagnosis of atrophic AMD or macular telangiectasia is made. Atrophic lesions, pigment migration and pseudocystic cavities do not appear to be reversible upon treatment discontinuation, unlike other potential signs, such as corneal deposits and macular oedema (Figure 8).

3) Deferoxamine

Deferoxamine is an iron and aluminium chelator used in the treatment of haemochromatosis and in patients who receive multiple blood transfusions. Maculopathy is just one of its many side effects, and was first identified as such in the 1980s. It primarily affects the retinal pigment epithelium, with a direct toxic effect on the cells of the RPE and/or Bruch's membrane, with pigment epithelium changes in the fundus, visible more clearly in autofluorescence images. In the foveal zone, SD-OCT reveals thinning of the RPE, with deposits, irregularities or atrophy; breaks in the ellipsoid line; photoreceptor attenuation; and, in some cases, tubulation around the areas of atrophy. In the early stages of intoxication, OCT may reveal a serous retinal detachment with extension of the outer segments, which resolves upon treatment discontinuation.

4) Ritonavir

Macular atrophy secondary to treatment with ritonavir, an HIV protease inhibitor, has never been described in clinical studies, but has been found in numerous patients after many years of treatment (patients may be over 55 years old before the lesions are discovered). Areas of retinal pigment epithelium and photoreceptor atrophy are surrounded by areas of irregularity in the outer segments, interdigitation areas and the ellipsoid zone, associated with accumulations of pigment on the retinal side of the RPE. Crystalline deposits are less commonly seen in OCT due to their small size. It is important to contact the prescribing doctor if this side effect is observed, as it can often go unrecognised.

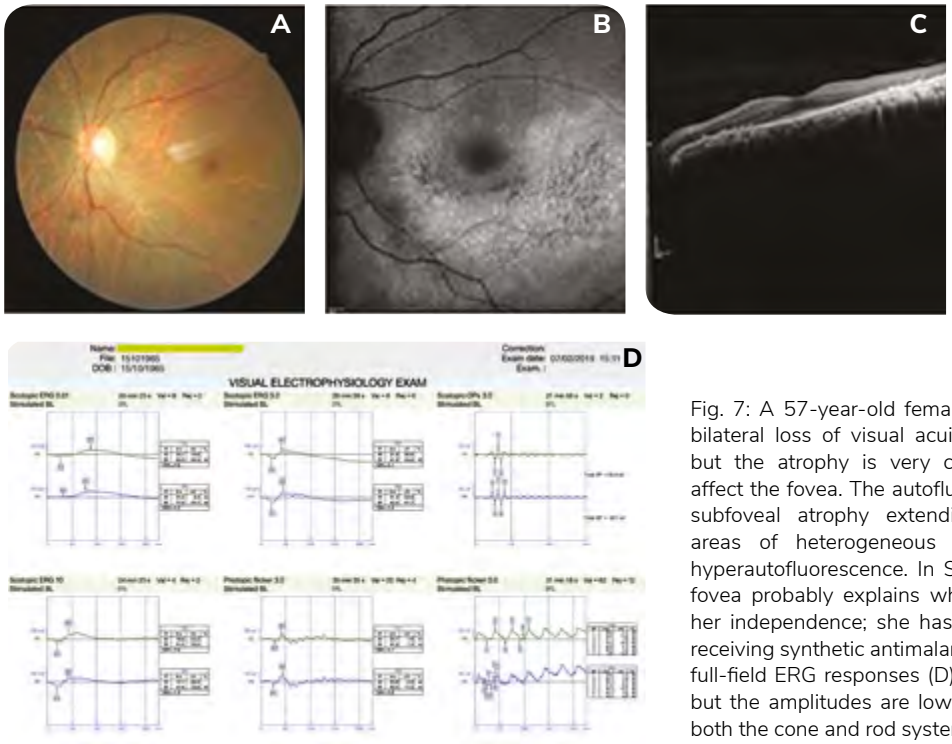

Fig. 7: A 57-year-old female patient with progressive, bilateral loss of visual acuity. The fundus (A) is pale, but the atrophy is very clear, although it does not affect the fovea. The autofluorescence photo (B) shows subfoveal atrophy extending to the arcades, with areas of heterogeneous hypoautofluorescence and hyperautofluorescence. In SD-OCT (C), the unaffected fovea probably explains why the patient has retained her independence; she has not seen a doctor despite receiving synthetic antimalarials for 15 years. Finally, the full-field ERG responses (D) are of normal morphology, but the amplitudes are lower, confirming a disorder of both the cone and rod systems.

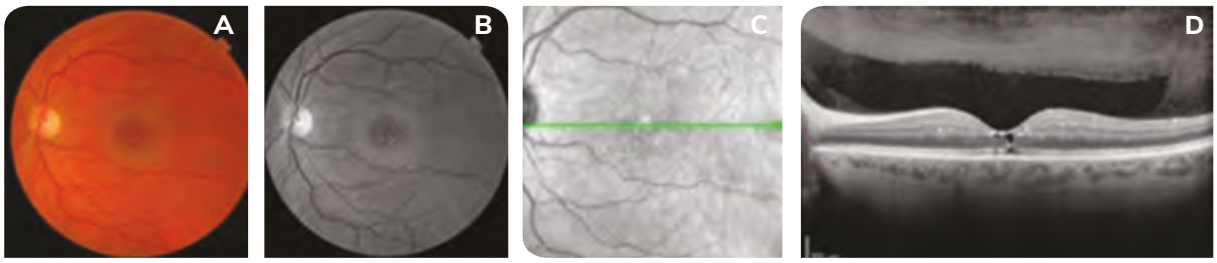

Fig. 8: A female patient presenting with decreased visual acuity during selective oestrogen receptor modulator therapy for breast cancer.
The presence of a crystalline deposit in the fundus (A) in this context suggests this is the most likely diagnosis. The crystals are easily visible in the infrared (C) and autofluorescence (B) images. In SD-OCT (D), the pseudo-telangiectasia, with intraretinal cavitations associated with ellipsoid line changes also confirms the diagnosis.

6. CAR syndrome (cancer-associated retinopathy)

If an atypical atrophic lesion is discovered, a paraneoplastic syndrome should be suspected. This applies, for example, if the lesions and visual acuity loss develop too quickly, if the small size of the lesions is inconsistent with the presence of major functional impairment or if nyctalopia and/or photophobia are described when interviewing the patient. In these cases, wider-field images should be taken (55° and over) and angiography and full-field ERG (and/or EOG) should be conducted. If atypia is confirmed, a full assessment should be conducted to identify any unknown cancerous lesions—including blood tests, a PET scan and mammography—unless the patient is already known to have a tumour.

If any doubt remains as to the cause of the lesion, tests can be conducted to look for serum antibodies specific to paraneoplastic syndromes.

The treatment is of course cancer treatment, but the prognosis for visual function often remains poor regardless (Figure 9).

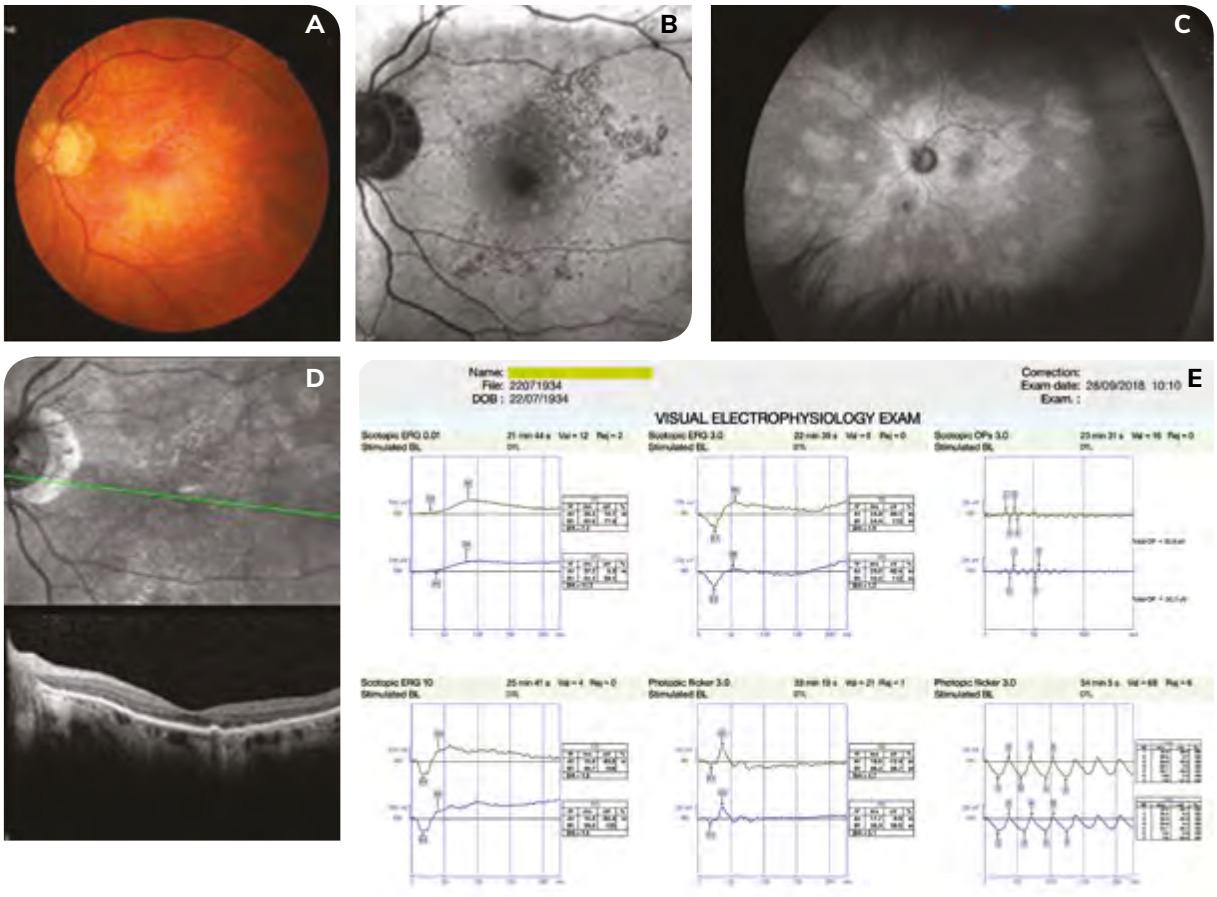

Fig. 9: An 85-year-old female patient seeking a second opinion for atrophic AMD, since she has experienced a significant loss of independence in recent months.
In the fundus (A), the atrophic lesion is aspecific, with several small pigmented spots superior to the fovea. The atrophy around the fovea has a "bunch of grapes" appearance, which calls the diagnosis into question (B). In the ultra-wide-field photos (C), there are highly heterogeneous areas of hypoautofluorescence and hyperautofluorescence, with no obvious distribution pattern. Fluorescein and indocyanine green angiography rule out an inflammatory disease (white dot syndrome). SD-OCT (D) does not provide any further information on the origin of these lesions. Full-field ERG (E) confirms moderate overall retinal dysfunction which—in this patient with recent, rapid loss of visual acuity—is suggestive of a paraneoplastic syndrome. Further aetiological investigation confirmed the presence of colon cancer, which no doubt caused the paraneoplastic syndrome.

7. Chorioretinal inflammatory diseases

Chorioretinal inflammatory diseases particularly affect young, active people. They can cause macular atrophy and, in rare cases, are complicated by choroidal neovascularisation (CNV), which can make the condition difficult to differentiate from AMD in older patients or those in the scarring stage.

1) Multifocal choroiditis (MFC) and punctate inner choroidopathy

At present, some authors believe these two clinical presentations are distinct, while others believe they lie on a continuum of the same disease. The visual prognosis for these patients depends on the level of macular complication: active and/or atrophic inflammatory macular lesions; CNV (6.7–76.9%), usually type 2; macular oedema (0–37.5%); and epiretinal membrane (0–11%). Fundus examination reveals white-to-yellowish macular and/or peripheral patches progressing towards atrophy, potentially complicated by CNV. It can be difficult to differentiate the active patches from CNV using conventional MMI. Only 66.7% of CNV presents exudative signs in SD-OCT. OCTA has proven highly useful in this disease due to its ability to diagnose CNV at an early stage (Figure 10). In the literature, 6–14% of lesions thought to be active inflammatory patches in conventional MMI were found to have neovascular flow in OCTA.

2) Multiple evanescent white dot syndrome (MEWDS)

MEWDS is an acute unilateral disease characterised by multiple white-to-yellowish retinal spots. It particularly affects young short-sighted women. Rare bilateral cases have been described. Upon clinical examination, these spots are associated with foveal granularity. In indocyanine green angiography, they are more numerous and hypofluorescent in the late phase. In SD-OCT, a break in the ellipsoid line and interdigitations may be visible near the spots, with foveal subretinal hyperreflectivity in certain cases. In OCTA, there are no abnormalities of the choriocapillaris in conjunction with the spots, which confirms that the lesions are located in the outer retina. In most cases, the lesions heal spontaneously within four to eight weeks. In rare cases, this disease can be complicated by CNV, usually type 2.

3) Acute posterior multifocal placoid pigment epitheliopathy (APMPPE)

APMPPE has been described as a disease of the retinal pigment epithelium. It is characterised by the appearance of whitish polycyclic plaques in the posterior pole, which heal spontaneously in the majority of cases. However, relapse is possible, sometimes with atrophic macular complications or, more rarely, CNV. The observed abnormalities may be caused by ischaemia of the choriocapillaris.

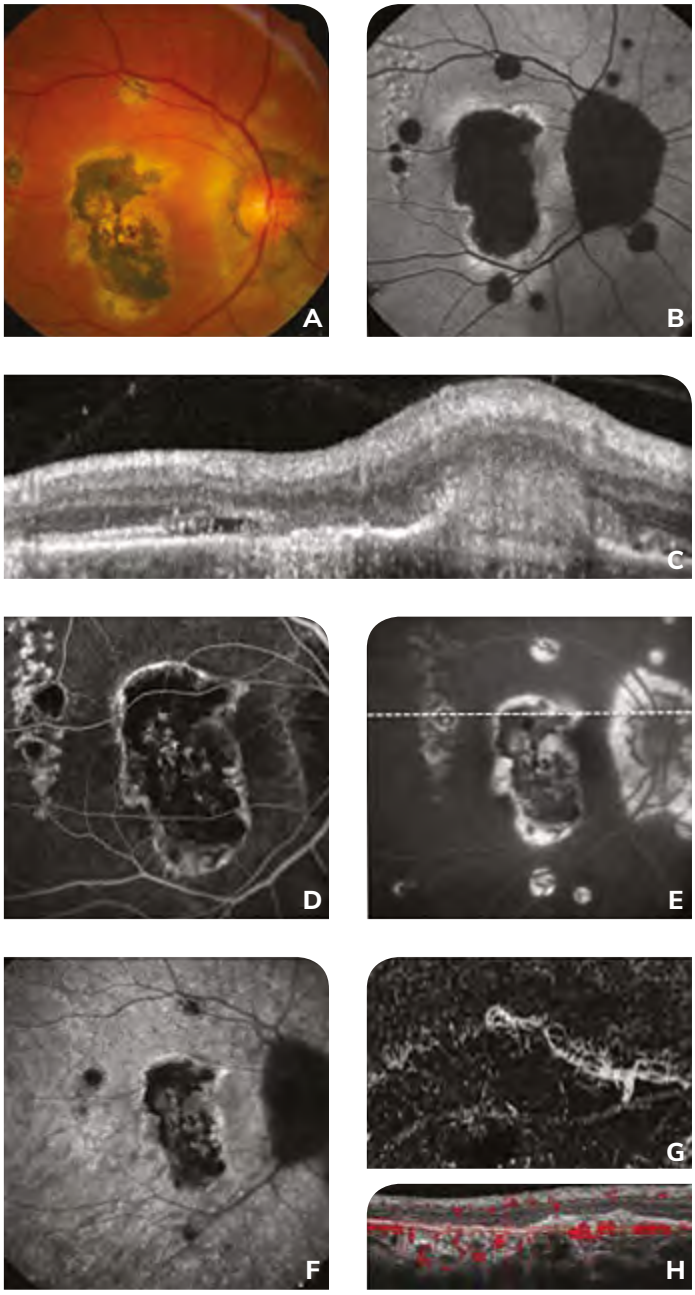

Fig. 10: Multimodal imaging of a 57-year-old female patient with multifocal choroiditis complicated by type 2 choroidal neovascularisation along the edges of an area of macular atrophy in the right eye.
The colour fundus photo (A) shows several atrophic patches that are hypoautofluorescent (B). The SD-OCT slice (C) through the superior section of the macular atrophy (dotted line in image E) shows subretinal hyperreflectivity associated with a SRD compatible with active type 2 CNV. Fluorescein angiography shows early hyperfluorescence (D) with late leakage from the lesion (E) and a late-phase plaque in ICG (F). Finally, OCTA shows the neovascular flow in the manually segmented slab, between the retinal pigment epithelium and 30 microns below it (G), with flow in the corresponding B-scan slice (H), confirming the neovascular complication.

4) Serpiginous choroiditis

Serpiginous choroiditis is a chronic, recurrent, often bilateral disease with—typically—finger-like peripapillary lesions and centrifugal progression. It is a disease of the choriocapillaris. Patients with this disease should be assessed for TB infection. ICG angiography shows hypoautofluorescent lesions corresponding to ischaemia of the choriocapillaris. Hypoperfusion of the choriocapillaris has therefore been found in OCTA regardless of the disease stage. This disease is complicated by CNV in 35% of cases.

5) Persistent placoid maculopathy (PPM)

This disease was described by Golchet *et al.* in 2005 as being similar to serpiginous choroiditis, with chronic macular lesions that spare the peripapillary zone but are associated with normal or subnormal visual acuity. In OCTA, hypoperfusion of the choriocapillaris has been found around the lesions, suggesting that the disease could be secondary to this hypoperfusion. CNV develops in 92% of cases.

6) Birdshot chorioretinopathy

This is a rare, bilateral chorioretinopathy with an understated inflammatory reaction in the anterior chamber, vitritis, vasculitis and whitish spots. It is strongly associated with HLA-A29. Its complications are macular oedema (100%), epiretinal membrane, CNV (11%), atrophy and vasculitis.

7) Acute zonal occult outer retinopathy (AZOOR)

This rare retinopathy is characterised by a delineating line marking the edge of the disease progression area; a "trizonal" pattern defined by normal autofluorescence outside the delineating line (zone 1), heterogeneous granular hyperfluorescence of the AZOOR lesion (zone 2) and hypoautofluoresence corresponding to the choroidal atrophy (zone 3); and multizonal progressive abnormalities. The lesions are typically peripapillary, with centrifugal progression, but cases with centripetal progression have been described.

Conclusion

The most common cause of atrophy and neovascularisation in patients aged over 55 years is AMD. However, several differential diagnoses must be considered, particularly in the absence of drusen. A carefully conducted patient interview (disease history, family history, medication), clinical examination with MMI plus OCTA and, in some cases, additional examinations (ERG, EOG) are essential to making the correct diagnosis and adapting treatment and monitoring accordingly.

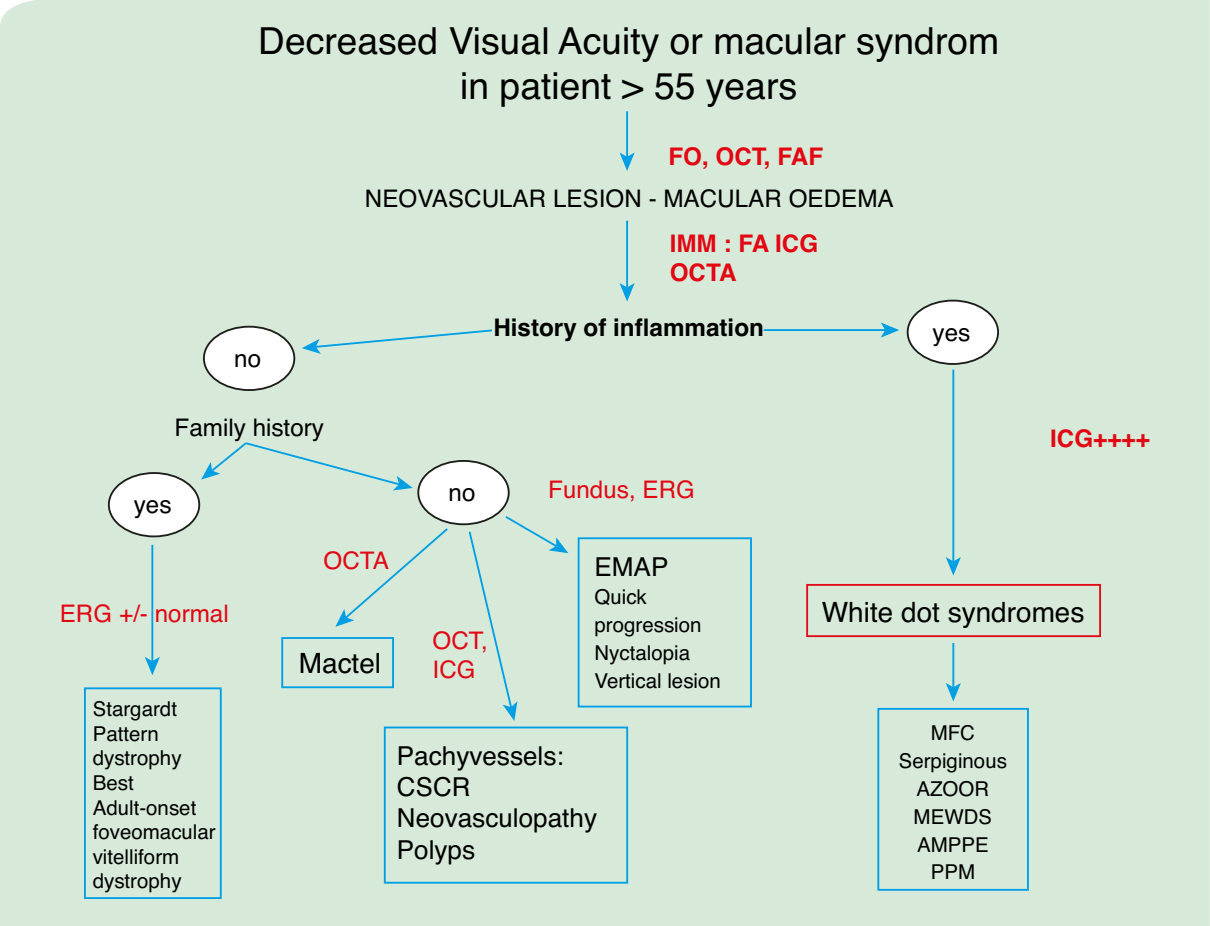

DVA: decreased visual acuity; F: fundus; FAF: fundus autofluorescence; MMI: multimodal imaging; FA: fluorescein angiography.

Main differential diagnoses for AMD

- Pachychoroid (central serous chorioretinopathy, pachychoroid neovasculopathy, polypoidal choroidal vasculopathy)
- EMAP
- Idiopathic macular telangiectasia
- Inherited retinal degeneration: pattern dystrophy, MIDD and MELAS, central areolar choroidal dystrophy, Stargardt disease, Best disease, cone or cone-rod dystrophy
- Drug toxicity
- CAR syndrome
- Chorioretinal inflammatory diseases (MFC, MEWDS, APMPPE, PPM, birdshot, serpiginous choroiditis, AZOOR)

References

- Pachychoroid:
Warrow DJ, Hoang QV, Freund KB. Pachychoroid pigment epitheliopathy. Retina 2013;33:1659-72.
Pang CE, Freund KB. Pachychoroid neovasculopathy. Retina 2015;35:1-9.
Astroz P, Balaratnasingam C, Yannuzzi LA. Cystoid Macular Edema and Cystoid Macular Degeneration as a Result of Multiple Pathogenic Factors in the Setting of Central Serous Chorioretinopathy. Retin Cases Brief Rep 2017;11 Suppl 1:S197-S201.
Dansingani KK, Balaratnasingam C, Klufas MA, *et al.* Optical Coherence Tomography Angiography of Shallow Irregular Pigment Epithelial Detachments In Pachychoroid Spectrum Disease. Am J Ophthalmol 2015;160:1243-54 e2.
Costanzo E, Cohen SY, Miere A, *et al.* Optical Coherence Tomography Angiography in Central Serous Chorioretinopathy. J Ophthalmol 2015;2015:134783.
Bousquet E, Bonnin S, Mrejen S, *et al.*. Optical Coherence Tomography Angiography of Flat Irregular Pigment Epithelium Detachment in Chronic Central Serous Chorioretinopathy. Retina 2018;38:629-38.
Dansingani KK, Gal-Or O, Sadda SR, *et al.* Understanding aneurysmal Type 1 neovascularization (polypoidal choroidal vasculopathy): a lesson in the taxonomy of 'expanded spectra' - a review. Clin Exp Ophthalmol 2018;46:189-200.

- EMAP:
Hamel, CP, Meunier I, Arndt I, *et al.* Extensive Macular Atrophy with Pseudo-drusen-like Appearance: A New Clinical Entity. American Journal of Ophthalmology ; 2009: 609 20.
Douillard A Picot MC, Delcourt C, *et al.* Dietary, Environmental, and Genetic Risk Factors of Extensive Macular Atrophy with Pseudo-drusen, a Severe Bilateral Macular Atrophy of Middle-Aged Patients. Scientific Reports ; 2018: 6840

- Macular telangiectasia:
Gass JD, Blodi BA. Idiopathic juxtafoveolar retinal telangiectasis. Update of classification and follow up study. Ophthalmology ; 1993 :1536-1546
Yannuzzi LA., Bardal AM, Freund KB *et al.* Idiopathic Macular Telangiectasia. Retina 2006 450 60.
Toto, L, Di Antonio L, Mastropasqua R, *et al.* Multimodal Imaging of Macular Telangiectasia Type 2: Focus on Vascular Changes Using Optical Coherence Tomography Angiography. Investigative Ophthalmology & Visual Science ; 2016 : 268-276.
Capuano, V, Miere A, Amoroso F, *et al.* Uncommon retinal vascular diseases. 2016 ; 453-73.
Spaide RF, Yannuzzi LA, Maloca PM. Retinal-choroidal anastomosis in macular telangiectasia Type 2 . Retina ; 2018 : 1920 29.

- Inherited retinal degeneration:
Van den Ouweland JM, Lemkes HH, Ruitenbeek W, *et al.* Mutation in mitochondrial tRNA(Leu)(UUR) gene in a large pedigree with maternally transmitted type II diabetes mellitus and deafness. Nat Genet 1992;1:368-71.
Massin P, Guillausseau PJ, Vialettes B, *et al.* Macular pattern dystrophy associated with a mutation of mitochondrial DNA. Am J Ophthalmol 1995;120:247-8.
Gerber S, Rozet JM, van de Pol TJ, *et al.* Complete exon-intron structure of the retina-specific ATP binding transporter gene (ABCR) allows the identification of novel mutations underlying Stargardt disease. Genomics 1998;48:139-42.
Querques G, Bocco MC, Soubrane G, Souied EH. Intravitreal ranibizumab for choroidal neovascularization associated with Stargardt's disease. Graefes Arch Clin Exp Ophthalmol 2008;246:319-21.
Hamel C, *et al.* Retinitis Pigmentosa, Orphanet J Rare Dis, 2006, :40
Berger W *et al* : The molecular basis of human retinal and vitreoretinal diseases ; Prog Retin Eye Res, 2010, 29 :335-375.
Lima *et al*, Structural assesment of hyperautofluorescent ring in patients with retinitis pigmentosa, Retina, 2009, 1025-1031.
Hajali *et al.* The prevalence of cystoids macular oedema in retinitis pimentosa patients determined by OCT, Br J Ophthalmol, 2008, 92, 1065-1068.
Sayadi J, Miere A, Souied EH, *et al.* Type 3 Neovascularization Associated with Retinitis Pigmentosa. Case Reports in Ophthalmology ; 2017: 245 49.

- Drug toxicity:
Marmor MF, Kellner U, Lai TYY, *et al.* American Academy of Ophthalmology. Recommendations on screening for chloroquine and hydroxychloroquine retinopathy (2016 Revision). Ophthalmology 2016:1386-94.
Nair AA, Marmor MF. ERG and other discriminators between advanced hydroxychloroquine retinopathy and retinitis pigmentosa. Documenta Ophthalmologica. 2017: 175-183
Koinzer S, Klettner A, Treumer F, *et al.* Correlation of fundus autofluorescence, spectral-domain optical coherence tomography, and microperimetry in late deferoxamine maculopathy. Retinal Cases Brief Report 2012:50-5.
Kaiser-Kupfer MI, Lippman ME. Tamoxifen retinopathy. Cancer Treat Rep 1978:315-20.
Kaiser-Kupfer MI, Kupfer C, Rodrigues MM. Tamoxifen Retinopathy: A Clinicopathologic Report. Ophthalmology 1981:89-93.
Faure C, Paques M, Audo I. Electrophysiological features and multimodal imaging in ritonavir-related maculopathy. Documenta Ophthalmologica. 2017:241-8.

- CAR syndrome:
Sadowski, B., Kriegbaum C, Apfelstedt-Sylla E. Tamoxifen Side Effects, Age-Related Macular Degeneration (AMD) or Cancer Associated Retinopathy (CAR)? European Journal of Ophthalmology. 2001: 309 12.

- Chorioretinal inflammatory diseases:
Spaide RF, Goldberg N, Freund KB. Redefining multifocal choroiditis and panuveitis and punctate inner choroidopathy through multimodal imaging. Retina 2013;33:1315-24.
Astroz P, Miere A, Mrejen S, *et al.* Optical Coherence Tomography Angiography to Distinguish Choroidal Neovascularization from Macular Inflammatory Lesions in Multifocal Choroiditis. Retina 2017.
Jampol LM, Sieving PA, Pugh D, *et al.* Multiple evanescent white dot syndrome. I. Clinical findings. Arch Ophthalmol 1984;102:671-4.
Yannuzzi NA, Swaminathan SS, Zheng F, *et al.* Swept-Source OCT Angiography Shows Sparing of the Choriocapillaris in Multiple Evanescent White Dot Syndrome. Ophthalmic Surg Lasers Imaging Retina 2017;48:69-74.
Gass JD. Acute posterior multifocal placoid pigment epitheliopathy. Arch Ophthalmol 1968;80:177-85.
Bowie EM, Sletten KR, Kayser DL, Folk JC. Acute posterior multifocal placoid pigment epitheliopathy and choroidal neovascularization. Retina 2005;25:362-4.
Golchet PR, Jampol LM, Wilson D, *et al.* Persistent placoid maculopathy: a new clinical entity. Trans Am Ophthalmol Soc 2006;104:108-20.
Puche N, Hera R, Terrada C, Souied EH. Persistent Placoid Maculopathy Imaged by Optical Coherence Tomography Angiography. Retin Cases Brief Rep 2016;10:297-301.
Mrejen S, Khan S, Gallego-Pinazo R, *et al.* Acute zonal occult outer retinopathy: a classification based on multimodal imaging. JAMA Ophthalmol 2014;132:1089-98.

10

Micronutrition and age-related macular degeneration

Sergio Piscitello, Pierre Sustronck

AMD is a complex, multifactorial disease. Genetics has been shown to play a major role in predisposition to AMD, but environmental factors—both protective and aggravating—are also fundamental. Several genetic polymorphisms have been identified to date, notably genes involved in the complement system (CFH, C3, C2, CFI, CFB), cholesterol metabolism (CETP, LIPC, ABCA1, APOE), extracellular matrix remodelling (TIMP3 and COL8A1) and oxidative stress (ARMS2). While genetics, the presence of these polymorphisms and patient age are non-modifiable risk factors, there are other modifiable factors. The main ones are smoking, excess weight and a diet lacking in certain micronutrients. There are three major types of micronutrients that appear to play a protective role in AMD: antioxidant vitamins and minerals, macular pigments and omega-3 polyunsaturated fatty acids.

1. Vitamins and minerals

AREDS Report No. 8[1], published in 2001, provided the initial evidence for the protective role of vitamins and minerals in AMD. AREDS was a randomised, multi-centre, double-blind study of 3640 patients monitored for an average period of 6.3 years, in which the patients were divided into four categories based on the severity of their AMD (Table 1). The patients received one of the following four treatments: placebo (933 patients), zinc (945 patients), antioxidants (904 patients) and zinc + antioxidants (833 patients). The administered doses of vitamin E, vitamin C and zinc were well above the recommended daily allowances (Table 2). At five years, the probability of progression to severe AMD in the category 3 and 4 patients was 28% for the placebo group. The risk was lower—to a statistically significant extent—in the groups supplemented with zinc (21%) and zinc + antioxidants (20%) (Figure 1). This was the first prospective, randomised, interventional study to demonstrate a 25% reduction in the risk of progression to severe forms of AMD in category 3 and 4 patients supplemented with zinc + antioxidants.

In terms of five-year visual acuity, the probability of vision loss of at least 15 letters in category 3 and 4 patients was 29% for the placebo group and 23% for those treated with zinc + antioxidants. One of the limitations of the study was that it was not designed to identify whether dietary supplements reduce disease progression in patients who already have severe AMD in both eyes.

Category 1	Several small drusen (< 63 µm in diameter) or no drusen
Category 2	Numerous small drusen, pigment abnormalities or at least one intermediate drusen (> 63 µm in diameter)
Category 3	Numerous intermediate drusen or geographic atrophy not involving the central macula, or at least one large drusen (> 125 µm in diameter)
Category 4	Severe AMD in one eye or visual acuity of less than 20/32 in one eye due to non-severe AMD

Table 1

Antioxidants	• Vitamin C 500 mg/day • Vitamin E 400 IU/day • Beta-carotene 15 mg/day (only if patient a non-smoker)
Zinc and copper	• Zinc oxide 80 mg/day • Copper oxide 2 mg/day (to prevent anaemia)

Table 2

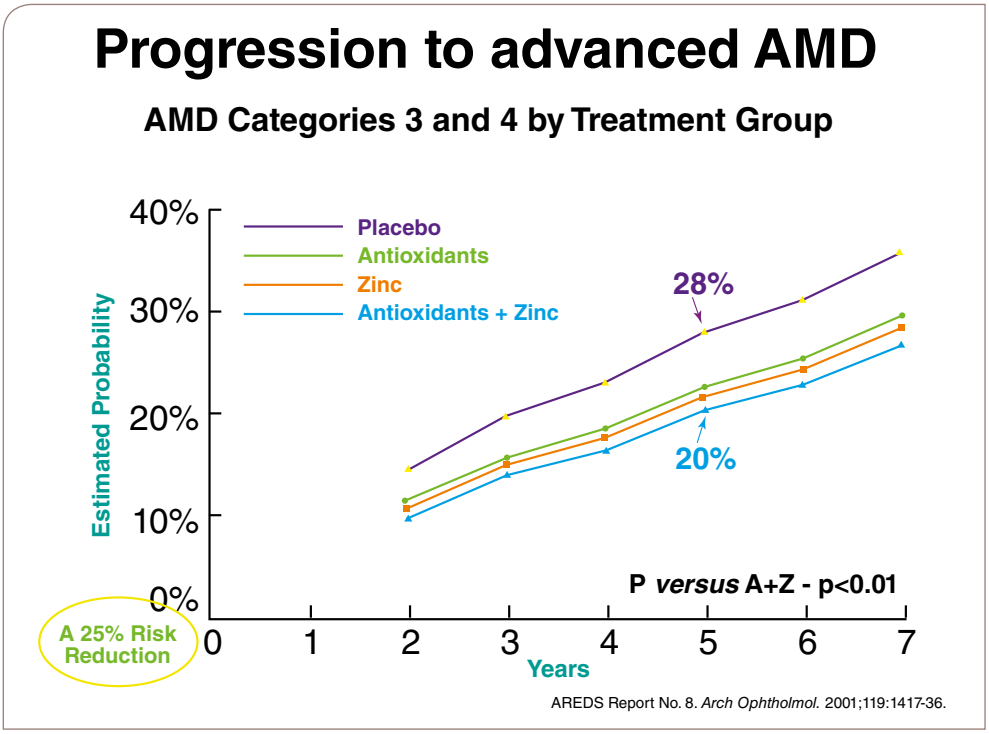

Fig. 1: Probability of developing advanced AMD over time (AREDS)

2. Macular pigment

1) Definition

There are over 600 carotenoids in the natural world, 140 of which are edible. Three of these are the main components of the yellow macular pigment. The three isomers in macular pigment are lutein (structurally related to alpha-carotene), zeaxanthin (related to beta-carotene) and, to a lesser extent, meso-zeaxanthin (an isomer of zeaxanthin). They belong to a subcategory of carotenoids known as xanthophyll pigment. There are twenty or so carotenoids found in human serum, the five main ones being lycopene, alpha-carotene, beta-carotene, lutein and zeaxanthin. Only lutein, zeaxanthin and meso-zeaxanthin are found in the macula, at concentrations around 10,000 times those found in serum.

The maximum concentrations are found in the centre of the fovea, where zeaxanthin predominates. However, lutein is found in greater concentrations than zeaxanthin in the periphery area. All three are primarily concentrated in the Henle fibre layer (zeaxanthin mainly in the cones and lutein in the rods), but are also found in the retinal pigment epithelium and photoreceptor outer segments.

2) Protective role of supplementation

Macular pigment improves the visual performance of the macula by reducing chromatic aberrations and glare. It also has antioxidant properties, both direct (as an antioxidant agent) and indirect (by filtering out short wavelengths, which provides photochemical protection via lipofuscin), as well as anti-inflammatory properties. Zeaxanthin and lutein are not synthesised by the body and must be sourced entirely from food. Numerous studies have highlighted the protective properties of a diet rich in carotenoids vis-à-vis the risk of AMD.

In the 1990s, Seddon *et al.* were the first to demonstrate that increasing one's consumption of foods rich in certain carotenoids—in particularly certain dark green leafy vegetables—can reduce the risk of developing advanced or exudative AMD[3]. The prospective POLA[2] study, conducted on 2584 patients, proved that the risk of AMD (early or severe) reduces by 79% in subjects with high plasma concentrations of zeaxanthin and lutein. In the Eye Disease Case Control Study Group[5], subjects with higher carotenoid serum concentrations had a markedly reduced risk of neovascular AMD. In 2003, a study by Gale[4] *et al.* found that this risk was significantly higher in people with lower plasma concentrations of zeaxanthin. In 2006, the CAREDS[6] study found that diets rich in zeaxanthin and lutein can protect healthy women under the age of 75 from developing intermediate AMD. Other epidemiological studies have had similar findings[22]. The AREDS2 study also looked at omega-3 supplementation, comparing this to the supplementation considered in the first AREDS study[23].

3) Effect on quality of life

The randomised, double-blind, interventional, prospective LAST[7] study, of sound methodology, assessed 90 patients with atrophic AMD over 12 months.

The authors evaluated the effects of supplementation with lutein alone or in combination with other carotenoids and antioxidants on macular pigment optical density (MPOD), measured using heterochromatic flicker photometry (MacularMetrics® device) and in objective vision tests. MPOD increased by 36% in the lutein group (L) and by 43% in the lutein plus antioxidants, vitamins and minerals group (L/A) (Figure 2). In addition, visual acuity increased by 5.4 letters in the L group and 3.5 in the L/A group. Contrast sensitivity improved in both groups, and quality of life (measured by a VF-14 questionnaire relating to subjective recovery after glare) improved in the L/A group.

These results suggest that xanthophyll pigments play a protective role in the prevention of AMD.

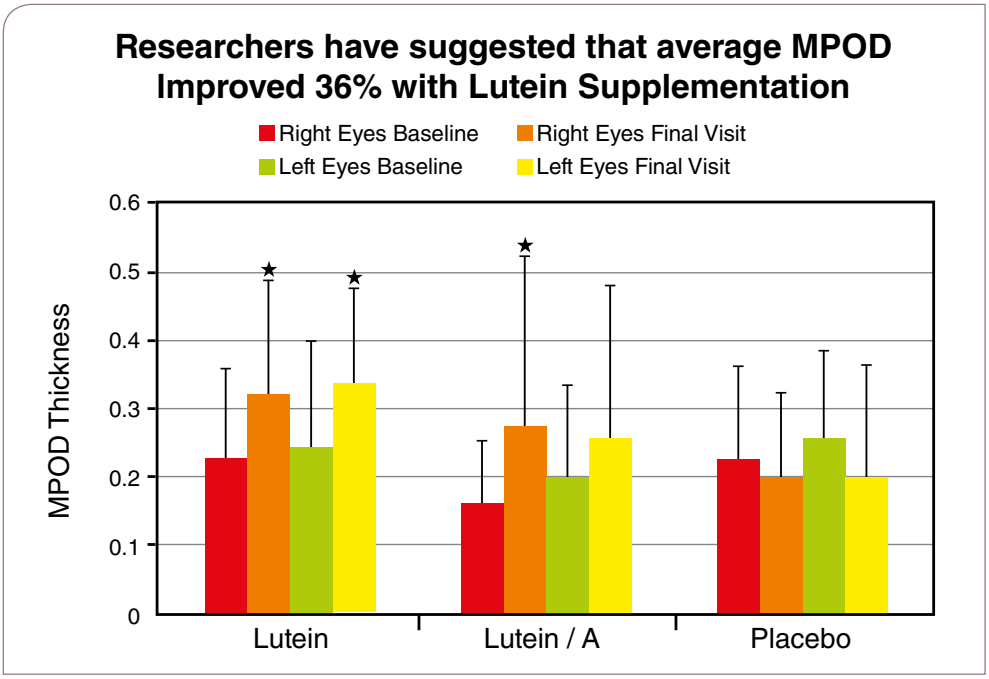

Fig. 2: Probability of developing advanced AMD over time (AREDS)

3. Omega-3 unsaturated fatty acids (vitamin F)

1) Definition

Fatty acids are referred to as "unsaturated" when they contain at least one double covalent bond between the carbon atoms (C=C). Some of these fatty acids (such as omega-3 and omega-6) cannot be synthesized by the body and must be provided through the diet.

2) DHA

Eicosapentaenoic acid (EPA) is partially converted into docosahexaenoic acid (DHA) and omega-3 after being absorbed through the intestines. Omega-3 has numerous biological effects on the blood vessels and tissues, acting through signal transduction, gene expression regulation and cell membrane remodelling. DHA is a key lipid component of the photoreceptor membranes, where it plays a crucial role in maintaining their structural and functional integrity. In the retina, DHA increases mitochondrial activity and has antioxidant, anti-inflammatory, antiapoptotic and antiangiogenic effects. The continual renewal of the retinal membranes requires a constant source of omega-3. This is why diets rich in DHA and EPA can improve retinal function and delay the development of AMD.

3) Assumed protective role

In the 2000s, numerous scientific studies found a relationship between diets rich in DHA and low in saturated fats and a reduction in the risk of neovascular AMD.

Seddon *et al.* showed that increased omega-3 intake is associated with a lower risk of AMD in people with diets low in linoleic acid (an omega-6)[8]. Studies by Smith W[9], Augood[10] and Merle[11], the US Twin Study[12] and the POLANUT[13] study found that more frequent consumption of omega-3-rich fish is associated with a reduced risk of neovascular AMD. The findings of these studies show that the role of different types of dietary lipids is complex, in particular the relationship between saturated fats, omega-3, omega-6 and cholesterol.

In the Blue Mountains Eye Study, a clear association was observed between more frequent consumption of fish and a reduced risk of severe AMD[14]. Another study, conducted by Augood *et al.*, specifically examined the protective effect of EPA and DHA in elderly subjects and found that consuming fish oil at least once a week protected against neovascular AMD, as did a high dietary intake of DHA and EPA[15]. In 2009, the pilot study NAT1 found that omega-3 supplementation (DHA 480 mg/day; EPA 720 mg/day) was well tolerated and omega-3 concentration increased considerably in serum and red blood cell membranes[16].

Based on all these studies, it has long been assumed that dietary supplements rich in omega-3 would reduce the incidence and progression of AMD. However, in 2013, the AREDS2[17,23] and NAT2[18] studies called into question the preventive effects of omega-3 supplementation.

NAT2 was a randomised, double-blind, prospective, comparative study conducted in patients with unilateral neovascular AMD (CNV) receiving DHA (840 mg/day) and EPA (270 mg/day) or a placebo orally for a period of three years. The time to bilateral involvement was not significantly different between the treated group (19.5 ±10.9 months) and the placebo group (18.7 ±10.6 months). Similarly, there was no significant difference in the incidence of CNV between the two groups (28.4% *vs* 25.6%, respectively). However, an analysis of fatty acid levels in the red blood cell membranes identified a subgroup (the upper tertile) of patients receiving the supplement who regularly had high levels of DHA+EPA in these membranes. This subgroup had an almost 70% lower risk of developing CNV in the second eye than those in the lower tertile ($p = 0.047$).

The results of the AREDS2 study (multi-centre, randomised, double-blind over five years) were unexpected. In this study, 507 patients supplemented with EPA+DHA (650 mg/day + 350 mg/day) developed severe AMD compared to 493 in the control group treated with the AREDS formula (HR 0.97; 95% CI 0.82–1.16, $p = 0.7$), which suggests that omega-3 does not provide significant additional protection. However, it may be that the study design prevented any potential prophylactic effect of omega-3 from being demonstrated, given the low DHA intake during the study, the use of DHA ethyl ester and the failure to check actual capsule consumption by measuring membrane fatty acids.

It should be noted that there are several factors that could affect the reliability of these studies, including patient consumption of relevant functional foods, additional unreported self-supplementation in the control group, and treatment noncompliance in the treated group. The only way to truly identify the benefits of omega-3 on a slowly progressing disease such as AMD is to measure membrane fatty acids.

4) Interactions with the genotype

Complex interactions between genotype and diet should not be underestimated. A study by Reynolds *et al.*[19] found that subjects who are homozygous for the genotype ARMS2/HTRA1, which confers a high risk of AMD, can be protected from geographic atrophy by increased DHA intake. Those who do not have the genotype for this risk are not protected. Similarly, Merle BM *et al.* suggest that a genetic predisposition to AMD resulting from the CFH Y402H variant limits the benefits of DHA supplementation[20]. Regardless, it appears that people with a genetic predisposition to AMD can potentially benefit from taking omega-3 supplements. Pragmatically speaking, since the risk of taking omega-3 is low[16], the potential benefits can be considered greater than the risks, and the consumption of omega-3-rich supplements can therefore be recommended.

4. Dietary advice

A healthy, varied and nutritionally balanced diet can complement standard medical treatments. Patients can be advised to follow a diet rich in certain vitamins, minerals and omega-3.

Lutein and zeaxanthin are found in cabbage, broccoli, spinach, turnips, lettuce, peas, sweetcorn, green beans, carrots and celery. These can be recommended for consumption four times a week.

Vitamin E can be found in vegetable oils, nuts and seeds (walnuts, hazelnuts, almonds, pecans, pine nuts and sunflower seeds) and fresh fruit and vegetables (fennel, peas, salsify, avocado, spinach, parsley, cabbage, kiwi, blueberries, mango and chestnuts). Two tablespoons of a variety of vegetable oils should be consumed daily, along with plenty of the aforementioned fresh fruit and vegetables.

Foods rich in vitamin C include fresh vegetables such as peppers, broccoli, cauliflower, cabbage, fennel and spinach—particularly when eaten raw—and fruit such as kiwi, citrus fruit, blackcurrants, strawberries, mango, blackberries, redcurrants, passion fruit, raspberries and melon. One raw vegetable and one fruit is recommended at every meal. High concentrations of omega-3 are found in oily fish (salmon, herring, trout, mackerel, sardines and tuna), nuts, and rapeseed, walnut and soya oil. Oily fish should be consumed at least twice a week. The main zinc-rich foods are meat, vegetables, eggs, wholegrain cereals, fish and dark chocolate.

After discussing diet and lifestyle, vitamin supplements can be offered to patients with advanced, unilateral AMD, since these seem to have a protective effect, reducing the risk of bilateral involvement at five years by 25%, according to the AREDS study[1,21].

References

1. Age-Related Eye Disease Study Research Group: A randomized, placebo-controlled, clinical trial of high-dose supplementation with vitamins C and E, beta carotene, and zinc for age-related macular degeneration and vision loss: AREDS report no.8. Arch Ophthalmol 2001;119:1417–1436.
2. Delcourt C, Carrière C, Delage M *et al.* Plasma Lutein and Zeaxanthin and other carotenoids as modifiable risk factors for age-related maculopathy and cataract: the POLA study. Invest Ophthalmol Vis Sci, 2006;47(6):2329-35.
3. Seddon JM, Ajani UA, Sperduto RD, *et al.* for the Eye Disease Case-Control Study Group. Dietary carotenoids, Vitamins A, C and E, and advanced age-related macular degeneration. JAMA, 1994;272:1413-21.
4. Gale CR, Hall NF, Phillips DI *et al.* Lutein and Zeaxanthin status and risk of AMD. Invest Ophthalmol Vis Sci, 2003;44: 2461-5.
5. Eye disease case-control study group. Antioxydant status and neovascular AMD. Arch Ophthalmol, 1993;111:104-9.
6. Moeller SM, Parekh N, Tinker L *et al.* Associations between intermediate age-related macular degeneration and Lutein and Zeaxanthin in the Carotenoids in age-related eye disease study (CAREDS). Arch Ophthalmol, 2006;124:1151-62.
7. S Richer, W Stiles, L Statkute *et al.* Double-masked, placebo-controlled, randomized trial of lutein and antioxidant supplementation in the intervention of atrophic age-related macular degeneration: the Veterans LAST study (Lutein Antioxidant Supplementation Trial). Optometry. 2004;75(4):216-30.
8. Seddon JM, Rosner B, Sperduto R *et al.* Dietary fat and risk for advanced AMD. Arch Ophthalmol 2001;119:1191–9.
9. Smith W, Mitchell P, Leeder SR. *et al.* Dietary fat and fish intake and age-related maculopathy. Arch Ophthalmol 2000;118: 401– 4.
10. Augood C, Chakravarthy U, Young I, *et al.* Oily fish consumption, dietary docosahexaenoic acid and eicosapentaenoic acid intakes and associations with neovascular age-related macular degeneration. Am J Clin Nutr 2008;88:398–406.
11. Merle B, Delyfer MN, Korobelnik JF, *et al.* Dietary omega-3 fatty acids and the risk for age-related maculopathy: the Alienor Study. Invest Ophthalmol Vis Sci 2011; 52:6004–11.
12. Seddon JM, George S, Rosner B. *et al.* Cigarette smoking, fish consumption, omega-3 fatty acid intake, and associations with AMD: the US Twin Study of AMD. Arch Ophthalmol 2006;124: 995–1001.
13. Delcourt C, Carrière I, Cristol JP, *et al.* Dietary fat and the risk of age-related maculopathy: the POLANUT study. Eur J Clin Nutr 2007;61:1341–4.
14. Tan JS, Wang JJ, Flood V *et al.* Dietary fatty acids and the 10-year incidence of age- related macular degeneration: the Blue Mountains Eye Study. Arch Ophthalmol 2009;127:656–665.
15. Augood C, Chakravarthy U, Young I *et al.* Oily fish consumption, dietary DHA and EPA intakes, and associations with neovascular AMD. Am J Clin Nutr 2008;88:398– 406.
16. Querques G, Benlian P, Chanu B *et al.* Nutritional AMD treatment phase I (NAT-1): feasibility of oral DHA supplementation in age-related macular degeneration. Eur J Ophthalmol 2009;19:100–106.
17. AREDS2 Research Group. Lutein + zeaxanthin and omega-3 fatty acids for AMD: the Age-Related Eye Disease Study 2 (AREDS2) randomized clinical trial. JAMA 2013;309:2005–2015.
18. Souied EH, Delcourt C, Querques G *et al.* Oral DHA in the prevention of exudative AMD: the Nutritional AMD Treatment 2 study (NAT2). Ophthalmology 2013;120:1619–1631.
19. Reynolds R, Rosner B, and Seddon M. Dietary omega-3 fatty acids, other fat intake, genetic susceptibility and progression to geographic atrophy. Ophthalmology. 2013; 120(5): 1020–1028.
20. Merle BM, Richard, Benlian *et al.* CFH Y402H and ARMS2 A69S Polymorphisms and Oral Supplementation with Docosahexaenoic Acid in Neovascular AMD Patients: The NAT2 Study. PLoS One. 2015 1;10(7):e0130816.
21. https://www.has-sante.fr/portail/upload/docs/application/pdf/201212/reco2clics_degenerescence_maculaire_liee_a_lage_prise_en_charge_diagnostique_et_therapeutique_2012-12-10_15-25-41_878.pdf
22. Age-Related Eye Disease Study Research Group, SanGiovanni JP, Chew EY, Clemons TE, *et al.* The relationship of dietary carotenoid and vitamin A, E, and C intake with age-related macular degeneration in a case-control study: AREDS Report No. 22. Arch Ophthalmol. 2007;125(9):1225-32.
23. AREDS2 Research Group, Chew EY, Clemons T, SanGiovanni JP, *et al.* The Age-Related Eye Disease Study 2 (AREDS2): study design and baseline characteristics (AREDS2 report number 1). Ophthalmology. 2012;119(11):2282-9.

11

Treatment protocols for exudative AMD

Hassiba Oubraham

Anti-VEGF intravitreal injections are the first-line treatment for sight-threatening exudative AMD. Three anti-VEGF drugs have been proven effective for this indication: ranibizumab, aflibercept and bevacizumab. The first two have an MA in France, while the third has a "temporary recommendation for [off-label] use" ("RTU") in hospitals.

The treatment regimens can be subdivided into two broad categories: a "reactive" regimen, which delivers the treatment after a relapse has occurred, and a "proactive" regimen, which treats the condition "a priori" before a relapse happens.

1. Reactive regimens

1) Simple PRN ("pro re nata" or "as needed")

After an induction phase of three injections each administered one month apart, the patient is monitored on a strict monthly basis. One or more further anti-VEGF injections are given if the disease is reactivated of if there are still signs of disease activity (Figure 1). The standard activity criteria for neovascular AMD are:

- A reduction in visual acuity of more than five letters (on the ETDRS scale) compared to the previous examination, attributable to choroidal neovascularisation
- The recent appearance of subretinal haemorrhage
- The presence of a macular serous retinal detachment
- The presence of intraretinal oedema spaces
- Significant expansion of a vascularised pigment epithelial detachment or signs of disease activity revealed by fluorescein angiography[1] or indocyanine green angiography
- Hyperreflective subretinal lesions in OCT[2], which are also considered to be signs of neovascular activity.

Practitioners must be aware of these signs and take them into account when making treatment decisions[1,2].

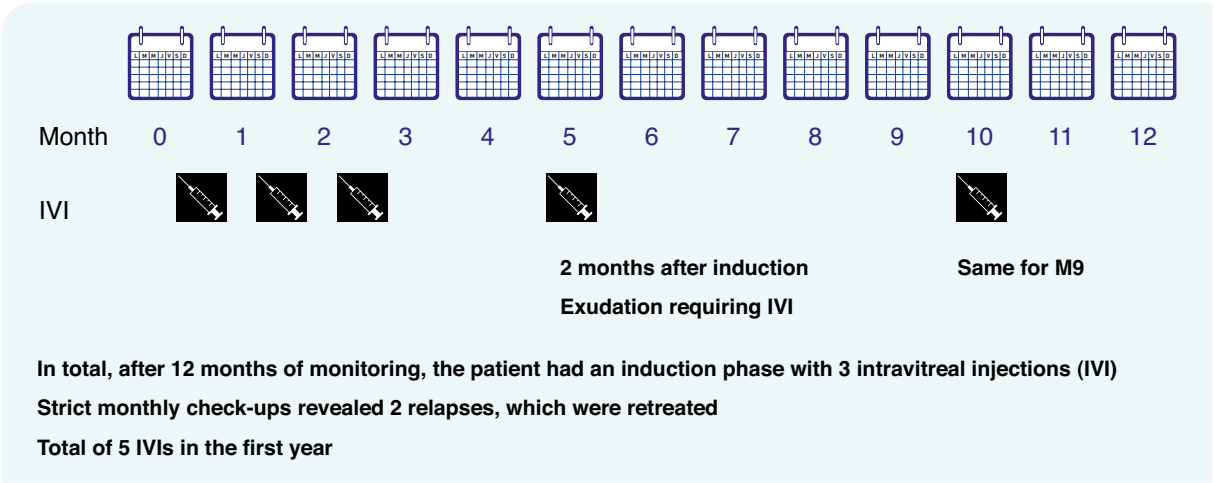

Fig. 1: Diagram of PRN protocol.

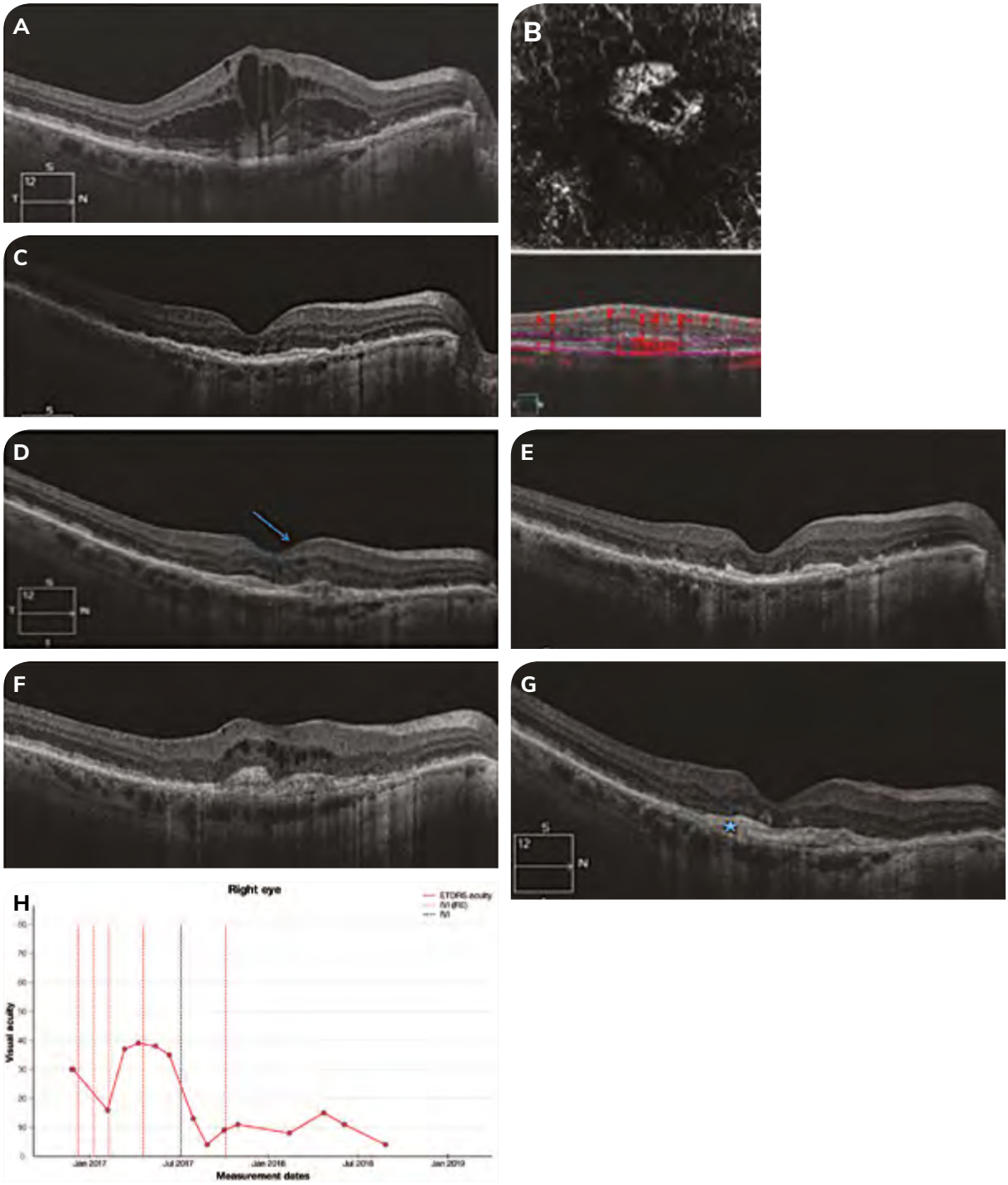

Fig. 2: Example of type 2 neovascularisation treated with anti-VEGF and monitored based on the PRN regimen, with two relapses and visual loss due to subretinal fibrous scarring.
A: Initial presentation: exudative lesion in the central macula, with pre-epithelial hyperreflective material, intraretinal fluid and intraretinal cysts in the central fovea. B: En-face OCTA shows the presence of flow, with a characteristic jellyfish appearance. C: One month after the induction phase with three anti-VEGF intravitreal injections (IVI): the intraretinal and subretinal fluid has disappeared, as have the intraretinal cysts. Anatomical response is good. D: First relapse two months after the last IVI: reappearance of intraretinal fluid with thickening of the pre-epithelial hyperreflective structure (CNV) and diffuse, very mild retinal thickening (arrow). An injection is given. E: Anatomical improvement after the fourth IVI. F, G: Major relapse despite regular monthly monitoring, causing a major, irreversible loss of visual acuity due to fibrous scarring of the central fovea (star). H: Visual acuity curve (based on ETDRS letter score) during the monitoring period. The irreversible drop in visual acuity after the second major neovascular relapse can be seen, caused by subretinal fibrous scarring (the vertical dotted lines represent the anti-VEGF IVIs).

The PRN regimen was found to be highly effective in the PrONTO[1] uncontrolled pilot study in terms of improving and maintaining visual acuity over 24 months. Randomised, controlled trials have proven its non-inferiority compared to strict monthly treatment (the treatment method used in the pivotal MARINA[3] and ANCHOR[4] studies): see the HARBOR[5] study and CATT[6] study for ranibizumab.

However, its transposition into clinical practice (real-life studies) has been a resounding failure, both in France[7-10] and worldwide[11,12]. There are many reasons for this failure, but the two main ones are doctors' inability to impose strict monthly monitoring, and a lack of patient compliance with this schedule due to comorbidities and transport problems[13].

Not being able to treat patients in a timely fashion and waiting for relapse can result in fibrotic lesions and irreversible loss of visual acuity[14] (Figure 2).

2) "Reinforced" and "capped" PRN

In 2009, Lala *et al.*[15] introduced the concept of a "relapse treatment" involving three injections at one-month intervals (instead of the single injection recommended in the PrONTO study). Their retrospective, single-centre study of 316 patients used a treatment protocol comprising a 3-injection induction phase followed by monthly check-ups with repeat treatment as needed. Relapses were treated with three monthly injections, while stable patients were treated every three months as standard. The average visual improvement after 3 years of follow-up was 8 letters for an average of 17 injections over a 3-year period.

This "reinforced" protocol was also used in the IVAN[16] study (a prospective, multi-centre, randomised study of 610 patients), which found that "reinforced" PRN was as effective as monthly treatment, but with an average of 7 injections per year (*versus* 12 for the monthly protocol).

2. Proactive regimens (before relapse)

1) "Treat and extend" or "inject and extend"

This regimen involves administering treatment at variable intervals depending on whether or not the retina appears dry during the patient's check-up. At each check-up, the patient is automatically retreated with an anti-VEGF injection, and the "dry" or "not dry" status of the retina determines not whether retreatment is required, but how long it will be until the patient's next check-up and treatment. Hence the name "treat and extend".

What does this look like in practice? (Figures 3 and 4)
Patients are treated monthly during the induction period, until the exudation completely disappears in OCT. Once no exudation remains, the time to the next visit and treatment is increased by two weeks (check-up and treatment at six weeks). If at six weeks, the ophthalmologist does not detect any signs of relapse, the patient is given an injection ("treat") and the time to the next visit and treatment is increased

("extend") by two weeks (check-up at eight weeks). If at eight weeks, there are still no signs of relapse, the patient is given an injection and the time to the next visit and treatment is extended by another two weeks (check-up at ten weeks). This "treat and extend" interval for simultaneous visits and treatments can be extended up to 12 weeks[17] and even 16 weeks. However, if during a visit, the examination reveals disease activity, the patient is retreated and the time to the next check-up and treatment is reduced by two weeks[18-20].

For as long as the retina remains wet, the check-up and retreatment interval will be reduced by two weeks each time, down to a minimum of four weeks between two injections (based on the recommendations for the use of anti-VEGF drugs).

The "treat and extend" strategy therefore meets the need for personalised treatment insofar as it seeks to determine for each patient the longest duration for which the treatment will remain effective before relapse occurs.

Once this interval has been determined, the strategy requires reinjection just before relapse in order to reliably maintain a dry retina (unlike the PRN strategy, which reinjects after relapse occurs).

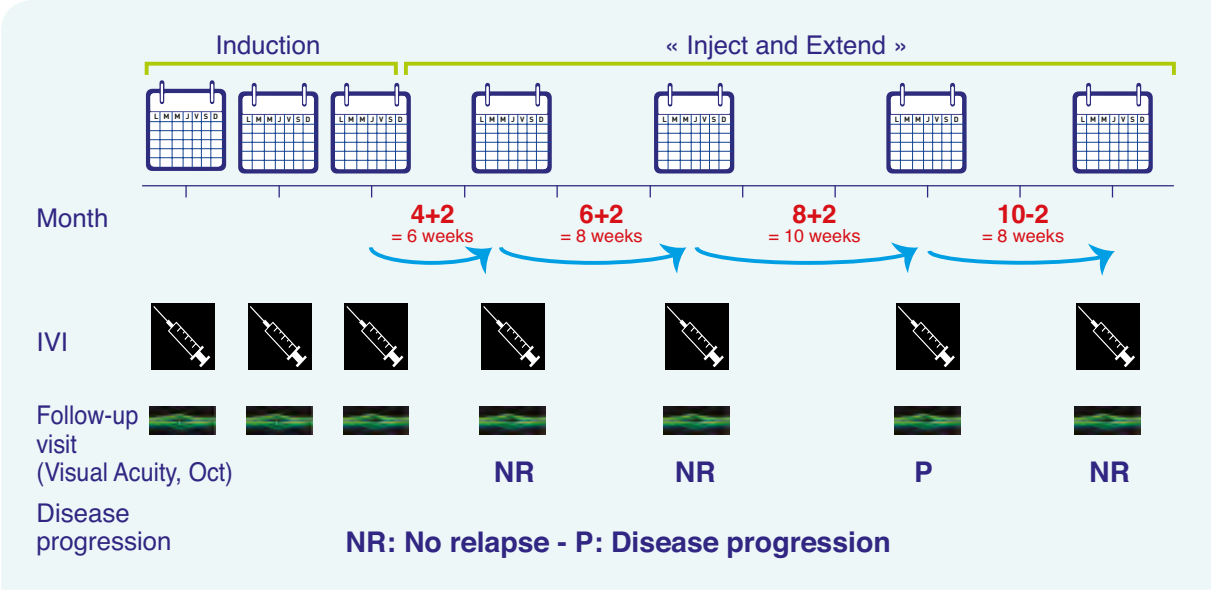

Fig. 3: Diagram of the "treat and extend" (or "inject and extend") protocol

The first check-up after the three induction phase IVIs takes place at six weeks (it could also take place at four weeks). If the patient is dry, another IVI is given and the time until the next check-up and IVI is extended by two weeks, i.e. to eight weeks. However, if the lesion is active, the IVI is given and the time to the next check-up is shortened to four weeks (or maintained at four weeks) and will remain at this length until the retina dries out.

2) Bimonthly fixed-interval treatment

This is the treatment regimen required by the 2014 European MA for aflibercept, based on the results of the VIEW[21] studies, which compared aflibercept 2 mg administered every two months after an induction phase of three monthly injections to ranibizumab 0.5 mg/0.05 ml administered every month. The study demonstrated the non-inferiority of aflibercept. The administration guidelines for aflibercept 40 mg/ml were amended in 2018, and fixed bimonthly treatment can now be replaced with a "treat and extend" regimen after the induction phase of three monthly injections.

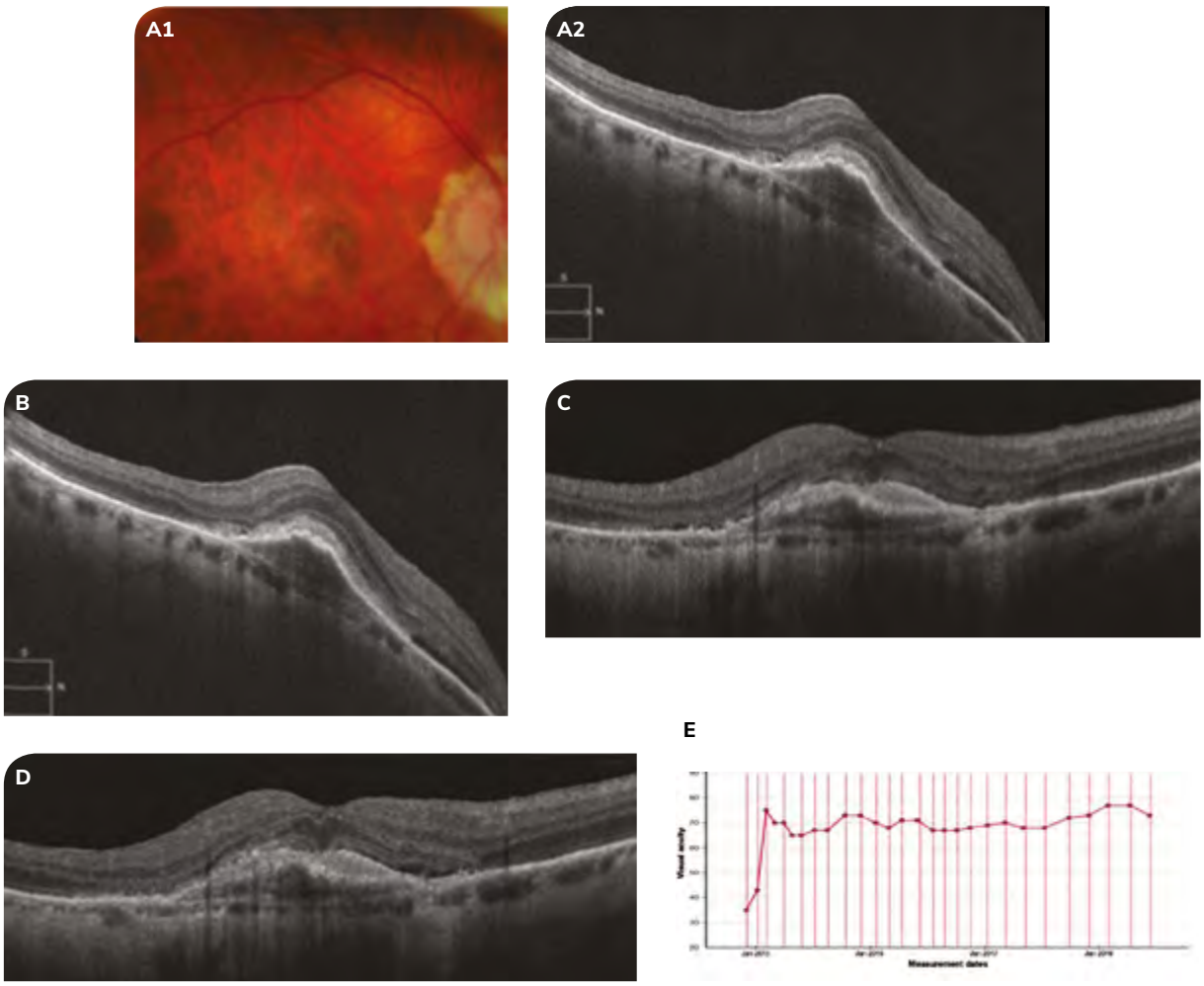

Fig. 4: Example of a "treat and extend" protocol

A1: Fundus photograph: initial presentation of type 1 neovascularisation.
A2: HD-OCT: a vascularised pigment epithelial detachment, a major serous retinal detachment and a pre-epithelial hyperreflective structure (grey). Treatment begins with an induction phase of three anti-VEGF IVIs.
B: OCT six weeks after the induction phase: the PED has reduced in height and the SRD and pre-epithelial grey area have disappeared. An injection is given and the patient is scheduled to return six weeks later for a check-up and another IVI.
C: No signs of relapse. The interval between treatments is extended to eight weeks.
D: After eight weeks, there are signs of neovascular relapse, with retinal thickening, a SRD and hyperreflective intraretinal dots. The IVI is given and the time to the next check-up and IVI is shortened to six weeks.
E: VA progression curve (based on ETDRS score) during the "treat and extend" period for this patient. Patient monitored for a total of 40 months, with an increase in VA of 37 letters, 26 IVIs (9 the first year, 8 the second and 6 the third).

3. Progressive regimens

The France Macula federation has developed a progressive regimen called IOI (Induction, Observation, Individualisation), which—after an induction phase of three monthly injections—involves monitoring progression every month for around six months and treating reactively (observation). A relapse pattern is established for the treated eye and the maintenance treatments are administered based on this pattern (individualisation)[22] (Figure 5).

For example: a patient is treated with three induction injections then is seen monthly. The first relapse is observed between four and eight weeks after the third injection. The patient is treated and their next injections scheduled for six weeks' away. Treatments with two or three injections—carried out with or sometimes without a prior OCT examination—are therefore possible. As a result, the treatment becomes less of a burden for both patients and medical teams, with less of an impact on patient quality of life. This concept of a relatively fixed relapse pattern, individual to each patient, is demonstrated in Mantel *et al.*[23].

After each round of treatment (two or three injections) based on the identified relapse pattern, a full functional and anatomical assessment needs to be carried out to check whether the relapse pattern has changed. If the retina has dried out, the period between treatments can be extended by two weeks. Conversely, if fluid is found, the reinjection period must be shortened by two weeks. It is important to check the condition of the contralateral eye at least once every four to six months, and as a matter of urgency if the patient reports problems.

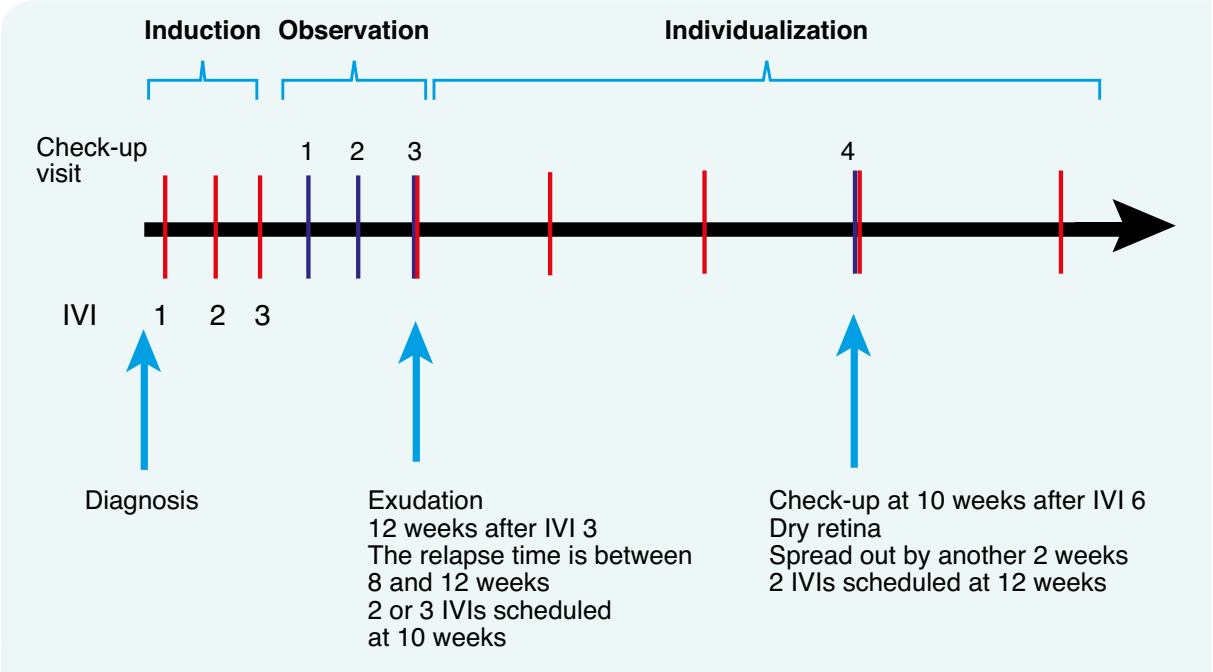

Fig. 5: Diagram of IOI protocol (injection, observation, individualisation)

After the first three induction IVIs, an observation phase begins, where the patient is checked monthly, with treatment as needed if relapse occurs (PRN). This phase lasts six to nine months, during which the patient's relapse profile is established. At the end of this observation period, the treatment is individualised based on the patient relapse profile, in anticipation of further relapses.

4. Combined anti-VEGF and photodynamic therapy

Combined anti-VEGF (ranibizumab) and verteporfin photodynamic therapy (vPDT) has proven effective at improving visual acuity and reducing the size of polypoidal lesions[24]. However, the EVEREST study—a randomised study of 61 patients comparing ranibizumab as monotherapy with combined ranibizumab-vPDT therapy—was not able to prove the superiority of the combined therapy in terms of improving visual acuity beyond six months[25].

The EVEREST II study—a large, randomised, controlled, multi-centre study conducted in 322 Asian patients and lasting 24 months—compared the long-term effects of the combined therapy to ranibizumab as monotherapy in polypoidal choroidal vasculopathy[26].

All the patients received three initial monthly injections of ranibizumab and were then monitored as per the PRN regimen. The patients were randomised to also receive either vPDT or no vPDT (sham-PDT group). At 12 months, the combined therapy group had an improvement in VA of 8.3 letters *versus* 5.1 letters for the monotherapy group ($p = 0.01$), with 4 IVIs *versus* 7 for the monotherapy group. It would therefore appear that for polypoidal choroidal vasculopathy which remains active after induction with three anti-VEGF IVIs, combined therapy is superior to monotherapy[26].

References

1. Lalwani GA, Rosenfeld PJ, Fung AE, *et al.* A variable-dosing regimen with intravitreal ranibizumab for neovascular age-related macular degeneration: year 2 of the PrONTO Study. Am J Ophthalmol 2009;148:43-58.
2. Ores R, Puche N, Querques G, *et al.* Gray hyper-reflective subretinal exsudative lesions in exsudative age-related macular degeneration. Am J Ophthalmol. 2014;158 (2):354-61.
3. Rosenfeld PJ, Brown DM, Heier JS *et al.* MARINA Study Group. Ranibizumab for neovascular age-related macular degeneration. N Engl J Med. 2006 5;355(14):1419-31.
4. Brown DM, Michels M, Kaiser PK, *et al.* ANCHOR Study Group. Ranibizumab versus verteporfin photodynamic therapy for neovascular age-related macular degeneration: Two-year results of the ANCHOR study. Ophthalmology. 2009;116(1):57-65.
5. Busbee BG, Ho AC, Brown DM, *et al.* HARBOR STUDY GROUP; Twelve-month efficacy and safety of 0.5 mg or 2.0 mg ranibizumab in patients with subfoveal neovascular age-related macular degeneration. Ophthalmology 2013;120(5):1046-56.
6. Martin DF, Maguire MG, Fine SL, *et al.* Comparison of Age-related Macular Degeneration Treatments Trials (CATT) Research Group Ranibizumab and bevacizumab for treatment of neovascular age-related macular degeneration: two-year results. Ophthalmology 2012;119(7):1388-98.
7. Cohen SY, Dubois L, Tadayoni R, *et al.* Results of one-year's treatment with ranibizumab for exudative age-related macular in a clinical setting. Am J Ophthalmol 2009;148(3): 409-13.
8. Cohen SY, Dubois L, Ayrault S, *et al.* Ranibizumab for exudative AMD in a clinical setting: differences between 2007 and 2010. Graefes Arch Clin Exp Ophthalmol 2013;251(11):2499-503.
9. Cohen SY, Mimoun G, Oubraham H, *et al.* LUMIERE Study Group. Changes in visual acuity in patients with wet age-related macular degeneration treated with intravitreal ranibizumab in daily clinical practice: the LUMIERE study. Retina 2013;33(3):474-81.
10. Souied EH, Oubraham H, Mimoun G, *et al.* TWIN Study Group. Changes un visual acuity in patients with age-related macular degeneration treated wih intravitreal ranibizulab in daily clinical practice: The TWIN Study. Retina 2015;35(9):1743-9.
11. Holz FG, Amoaku W, Donate J, *et al.* SUSTAIN Study Group Safety and efficacy of a flexible dosing regimen of ranibizumab in neovascular age-related macular degeneration: the SUSTAIN study. OPHTHALMOL. 2011;118(4):663-71.
12. Holz FG, Tadayoni R, Beatty S, *et al.* Determinants of visual acuity outcomes in eyes with neovascular AMD treated with anti VEGF agents: an instrumental variable analysis of the AURA study : Eye. 2016 Aug ; 30(8):1063-71.
13. Boulanger-Scemama E, Querques G, About F, *et al.* Ranibizumab for exudative age-related macular degeneration: A five year study of adherence to follow-up in a real-life setting. J Fr Ophtalmol. 2015;38(7):620-7.
14. Rosenfeld PJ, Shapiro H, Tuomi L, *et al.* MARINA and ANCHOR Study Groups. Characteristics of patients losing vision after 2 years of monthly dosing in the phase III ranibizumab clinical trials. Ophthalmology. 2011;118(3):523-30.
15. Lala C, Framme C, Wolf-Schnurrbusch UE, Wolf S. Three-year results of visual outcome with disease activity-guided ranibizumab algorithm for the treatment of exudative age-related macular degeneration. Acta Ophthalmol 2013;91(6):526-30.
16. Chakravarthy U, Harding SP, Rogers *et al.* IVAN Study Investigators; Ranibizumab versus bevacizumab to treat neovascular age-related macular degeneration: one-year findings from the IVAN randomized trial. Ophthalmology 2012 ; 119(7):1399-411.
17. Wykoff CC, Croft DE, Brown DM, Wang R, Payne JF, Clark L, *et al.* Prospective trial of treat-and-extend versus monthly dosing for neovascular age-related macular degeneration: TREX-AMD 1-Year Results. Ophthalmology 2015; 122 : 2514-22.
18. Barthelmes D, Nguyen V, Daien V, *et al.* Fight Retinal Blindness Study Group. Two years outcomes of « Treat and Extend » intravitreal therapy using aflibercept preferentially for neovascukar age-related macular. Retina. 2018;38(1):20-28.
19. Oubraham H, Cohen SY, Samimi S, *et al.* Inject and extend dosing versus dosing as needed: a comparative retrospective study of ranibizumab in exudative age-related macular degeneration. Retina 2011;31:26-30.
20. Freund KB, Korobelnik JF, Devenyi R, *et al.* Treat-and-extend regimens with anti-VEGF agents in retinal diseases: a literature review and consensus recom- mendations. Retina 2015;35:1489-506.
21. Heier JS, Brown DM, Chong V, *et al.* VIEW 1 and VIEW 2 Study Groups. Intravitreal aflibercept (VEGF trap-eye) in wet age-related macular degeneration. Ophthalmology 2012 ; 119(12) : 2537-48.
22. Semoun O, Cohen SY, Srour M, Creuzot-Garchet C, Oubraham H, Kodjikian L, *et al.* Comité scientifique de la Fédération France Macula. Individualized mana- gement of patients with exudative AMD, IOI Protocol: Injection-observational-individualization. J Fr Ophtalmol 2017;40:169-76.
23. Mantel I, Deli A, Iglesias K, Ambrezin A. Prospective study evaluating the predictibility of need for retreatment with intravitreal ranibizumab for age-related macular Graefes Arch Clin Exp Ophthalmol. 2013;251:697-704.
24. Koh AH, Chen LJ, Chen SJ, *et al.* Expert PCV Panel. Polypoidal choroidal vasculopathy: evidence-based guidelines for clinical diagnosis and treatment. Retina. 2013;33(4):686-716.
25. Koh A,Lee WK,Chen LJ, *et al.* EVERESTstudy: efficacy and safety of verteporfin photodynamic therapy in combination with ranibizumab or alone versus ranibizumab monotherapy in patients with symptomatic macular polypoidal choroidal vasculopathy. Retina. 2012;32(8):1453-1464.
26. Koh A, Lai TYY, *et al.* for the EVEREST II study group. Efficacy and Safety of Ranibizumab With or Without Verteporfin Photodynamic Therapyfor Polypoidal Choroidal Vasculopathy. A Randomized Clinical Trial. JAMA OPHTHALMOL. 2017;135(11):1206-1213.

12

Artificial intelligence and AMD

Daniel Seknazi, Oudy Semoun

1. Definition

Artificial intelligence (AI) is currently one of the most promising and dynamic fields of research in the medical world. It is a new area of medicine and it is important to understand the new vocabulary and concepts that come with it.

1) Artificial intelligence

AI refers to all the theories and techniques used to develop programs capable of simulating certain aspects of human intelligence.

2) Artificial neural networks

An artificial neural network (Figure 1) is an information system based on a network of units known as artificial neurons, which are organised in layers. Each neuron receives information through its dendrites and then activates or inhibits one of the neurons in the next layer via its axon. The message is thus sent down from the first neural layer into the last.

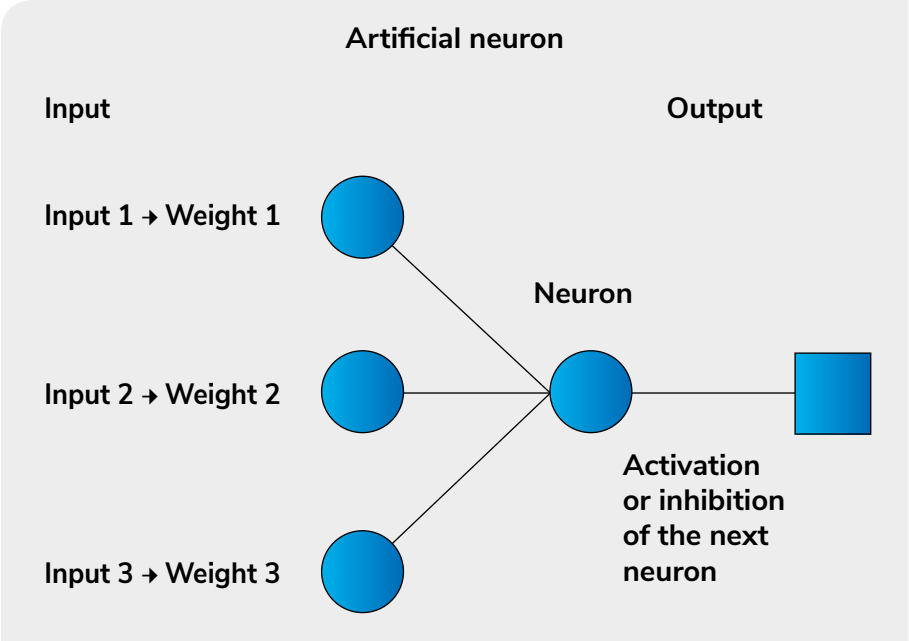

Fig. 1: Representation of an artificial neuron.

3) Machine learning

Machine learning (ML) is one of the techniques used in AI. It involves analysing a set of markers or characteristics by means of data (e.g. retinal thickness in an OCT image or number of haemorrhages). The AI algorithms learn to identify and categorise these characteristics based on a set of examples provided in advance. The efficacy of these traditional models of automatic learning depends primarily on how easy it is to distinguish between the selected characteristics. In traditional machine learning, the task of the engineer (or doctor) is therefore to manually define the characteristics specific to the field in question.

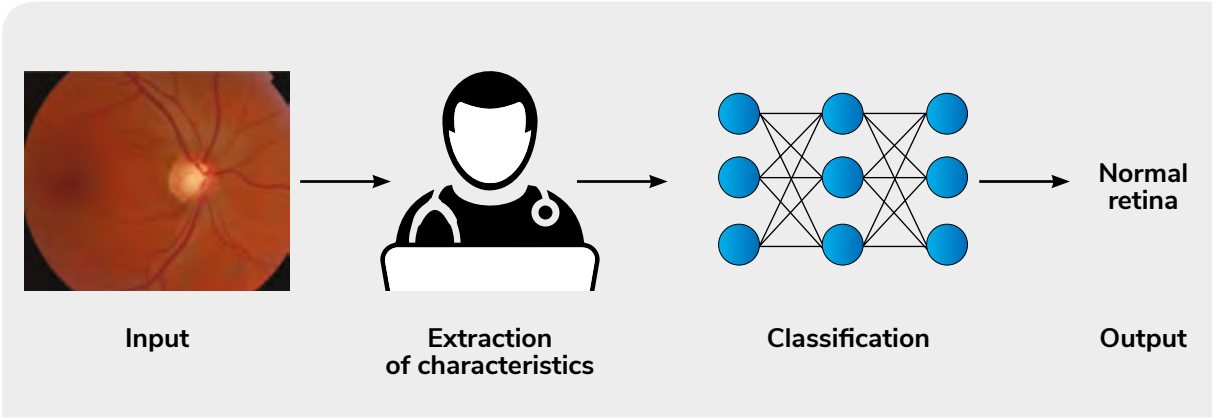

Fig. 2: Principle of machine learning.

4) Deep learning

Deep learning (DL) is a type of machine learning. DL involves a series of different neural layers. Each neural layer breaks down the input signal into increasingly abstract data and transfers the information via its synapse to the next neural layer. The message thus descends through the layers until it reaches the final neural layer. The network cannot only find and classify data as instructed: it can also decide for itself what it is looking for and how it wishes to classify the data.

The value of DL lies in its capacity for feedback, which enables it to learn from its mistakes and improve the sensitivity and specificity of a diagnosis. This feedback mechanism is known as “back propagation”. The main advantage of DL is therefore that its performance continually improves (Figure 3).

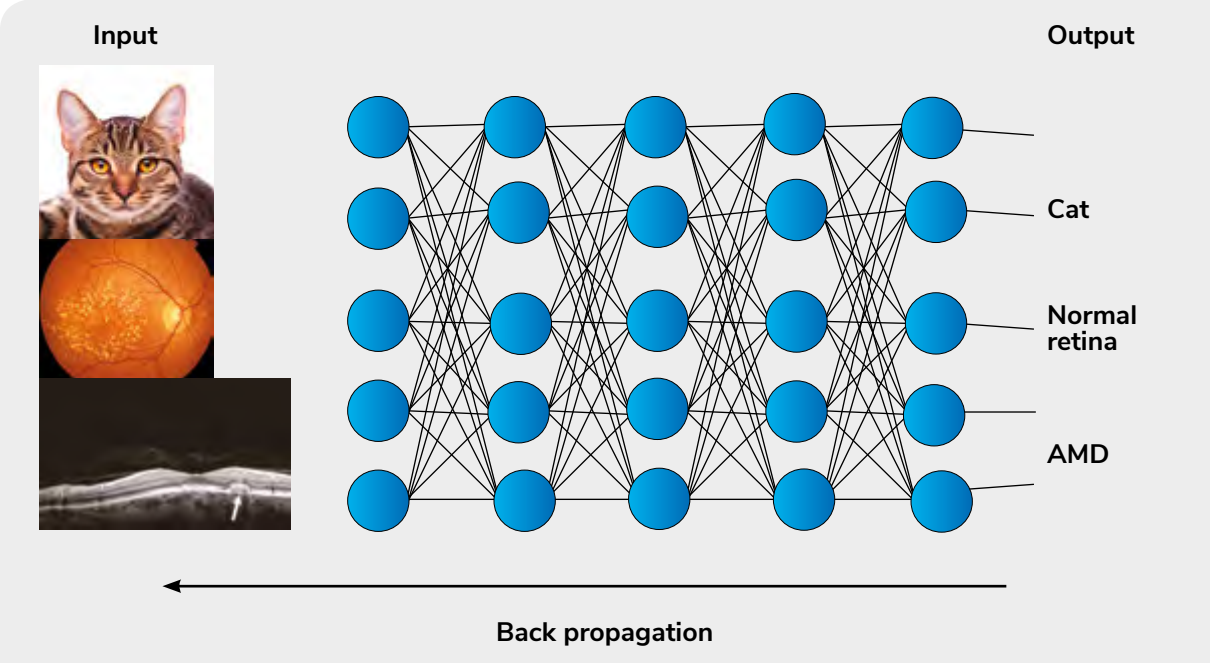

Fig. 3: Principle of deep learning.

2. Application to AMD

1) Diagnosis

- Screening

One of the main uses of AI in a disease such as AMD is to screen for at-risk and affected patients.

Burlina *et al.*[1] compared deep learning with "human" diagnosis using fundus photographs to determine the presence of AMD. They achieved a sensitivity of 88%, a specificity of 93% and a precision of 90% (in artificial intelligence, the term "precision" refers to the percentage of correctly categorised images). The results in the DL group were similar to those obtained in the human group. However, fundus photography is clearly not the best examination for diagnosing AMD.

- Drusen

One of the first studies to use AI in AMD was conducted by Van Grinsven *et al.*[2,3]. The authors used ML capabilities to identify drusen and reticular pseudodrusen. In their study, ML performed similarly to humans when detecting drusen. The area under the ROC curve was 0.95 for drusen and 0.94 for pseudodrusen.

- Diagnosing AMD

Several papers look at ML performance in AMD diagnosis. One of the first papers published was by Srinivasan *et al.*[4], who obtained a sensitivity of 100% for AMD and diabetic oedema in 45 patients (15 with AMD, 15 with diabetic macular oedema and 15 normal).

Treder *et al.*[5] used DL software (TensorFlow™, Google Inc., Mountain View, CA, USA) to diagnose exudative AMD from an OCT slice. After a training phase, they obtained a sensitivity of 100% and a specificity of 92% (precision 96%) across 100 patients (50 healthy, 50 diseased).

The same team[6] also studied DL in the diagnosis of geographic atrophy (GA) using autofluorescence imaging. The authors compared images of patients with GA to normal patients and patients with other retinal diseases. They obtained a sensitivity and specificity of 100%.

In addition to diagnosing AMD, AI can be used to categorise patients with AMD. Venhuizen *et al.*[7] used ML to separate patients into five grades (no AMD, early AMD, intermediate AMD, advanced AMD and GA). They achieved a sensitivity of 98% and a specificity of 91%.

Finally, once a diagnosis of AMD has been made, DL can be used to select a treatment. Prahs *et al.*[8] attempted to identify anti-VEGF requirements among patients with exudative AMD. They obtained a precision of 94.5% (sensitivity of 90.1% and specificity of 96.2%).

2) Prognosis

- Prediction of visual acuity

Schmidt-Erfurth *et al.*[9] tried to find a model to predict visual acuity at one year in patients presenting with exudative AMD.

- Prediction of IVI requirements

Bogunovic *et al.*[10] predicted the IVI requirements for a patient over the first two years of treatment. The authors used the HARBOR study cohort to determine whether it is possible to identify if a patient will require a large number of IVIs (>16 injections over 21 months) or a low number of IVIs (<5 injections over 21 months) after the induction period. The predictive model detected patients with “low IVI requirements” to a specificity of 71% and a sensitivity of 58%, and patients with “high IVI requirements” to a specificity of 71% and a sensitivity of 70%. The “human” prediction achieved sensitivities of just 41% and 37% and specificities of 84% and 84%.

- Risk of conversion to AMD

Schmidt-Erfurth *et al.*[11] studied the risk of a patient presenting with ARM converting to atrophic or exudative AMD after two years. They used morphological as well as demographic and genetic characteristics to determine this risk. In their model, the area under the ROC curve for conversion to exudative AMD was 0.68 (for a sensitivity of 0.80, the specificity was just 0.46). For conversion to atrophic AMD, the area under the curve was 0.80 (for a sensitivity of 0.80 and a specificity of 0.69).

3. Future perspectives

AI is a powerful tool that offers infinite possibilities. The role of doctors in the future has been firmly called into question.

With regard to AMD specifically, the potential usefulness of patient self-monitoring is already being considered. Devices already exist that allow OCT images to be taken at home[12].

Fundus camera software is also available for smartphones[13,14].

Combined with intelligence capable of making diagnoses and suggesting treatment, this recent progress will undoubtedly improve patient care and lead to a new role for the healthcare provider—one that has yet to be defined.

References

1. Burlina PM, Joshi N, Pekala M, *et al.* Automated Grading of Age-Related Macular Degeneration From Color Fundus Images Using Deep Convolutional Neural Networks. JAMA Ophthalmol. 1 nov 2017;135(11):1170.

2. Grinsven MJJP van, Lechanteur YTE, Ven JPH van de, *et al.* Automatic Drusen Quantification and Risk Assessment of Age-Related Macular Degeneration on Color Fundus Images. Invest Ophthalmol Vis Sci. 2013;54(4):3019-27.

3. Van Grinsven MJJP, Buitendijk GHS, Brussee C, *et al.* Automatic Identification of Reticular Pseudo-drusen Using Multimodal Retinal Image Analysis. Invest Ophthalmol Vis Sci. 2015;56(1):633-9.

4. Srinivasan PP, Kim LA, Mettu PS, *et al.* Fully automated detection of diabetic macular edema and dry age-related macular degeneration from optical coherence tomography images. Biomed Opt Express. 2014;5(10):3568.

5. Treder M, Lauermann JL, Eter N. Automated detection of exudative age-related macular degeneration in spectral domain optical coherence tomography using deep learning. Graefes Arch Clin Exp Ophthalmol. 2018;256(2):259-65.

6. Treder M, Lauermann JL, Eter N. Deep learning-based detection and classification of geographic atrophy using a deep convolutional neural network classifier. Graefes Arch Clin Exp Ophthalmol. 2018;256(11):2053-60.

7. Venhuizen FG, van Ginneken B, van Asten F, *et al.* Automated Staging of Age-Related Macular Degeneration Using Optical Coherence Tomography. Invest Ophthalmol Vis Sci. 2017;58(4):2318-28.

8. Prahs P, Radeck V, Mayer C, *et al.* OCT-based deep learning algorithm for the evaluation of treatment indication with anti-vascular endothelial growth factor medications. Graefes Arch Clin Exp Ophthalmol. 2018;256(1):91-8.

9. Schmidt-Erfurth U, Bogunovic H, Sadeghipour A, *et al.* Machine Learning to Analyze the Prognostic Value of Current Imaging Biomarkers in Neovascular Age-Related Macular Degeneration. Ophthalmol Retina. 2018;2(1):24-30.

10. Bogunovic H, Waldstein SM, Schlegl T, *et al.* Prediction of Anti-VEGF Treatment Requirements in Neovascular AMD Using a Machine Learning Approach. Investig Opthalmology Vis Sci. 2017;58(7):3240.

11. Schmidt-Erfurth U, Waldstein SM, Klimscha S, *et al.* Prediction of Individual Disease Conversion in Early AMD Using Artificial Intelligence. Investig Opthalmology Vis Sci. 2018;59(8):3199.

12. Chew EY, Clemons TE, Bressler SB, *et al.* Randomized Trial of a Home Monitoring System for Early Detection of Choroidal Neovascularization Home Monitoring of the Eye (HOME) Study. Ophthalmology. 2014;121(2):535-44.

13. Nazari Khanamiri H, Nakatsuka A, El-Annan J. Smartphone Fundus Photography. J Vis Exp JoVE. 2017;(125).

14. Sharma A, Subramaniam SD, Ramachandran KI. Smartphone-based fundus camera device (MII Ret Cam) and technique with ability to image peripheral retina. Eur J Ophthalmol. 2016;26(2):142-4.

Publication

Published by:

Théa Pharma
12 Rue Louis-Blériot - Z.I. du Brézet
63100 Clermont Ferrand
France
Tel. +33 (0)4 73 74 95 00

Théa Medical Bookshop Collection

Théa Pharma
12 Rue Louis-Blériot
63100 Clermont-Ferrand - France
Tel. +33 (0)4 73 74 95 00 - Fax +33 (0)4 73 98 28 52
www.theapharma.com

THE DMLA 0419